Math-for-industry
Education & Research Hub

ISSN2188-1200

Proceedings of Forum "Math-for-Industry" 2021 -Mathematics for Digital Economy-

Chief Editors: Osamu Saeki, Ho Tu Bao

Editors: Shizuo Kaji, Kenji Kajiwara,Nguyen Ha Nam, Ta Hai Tung,
Melanie Roberts, Masato Wakayama, Le Minh Ha,
Philip Broadbridge

九州大学マス·フォア·インダストリ研究所

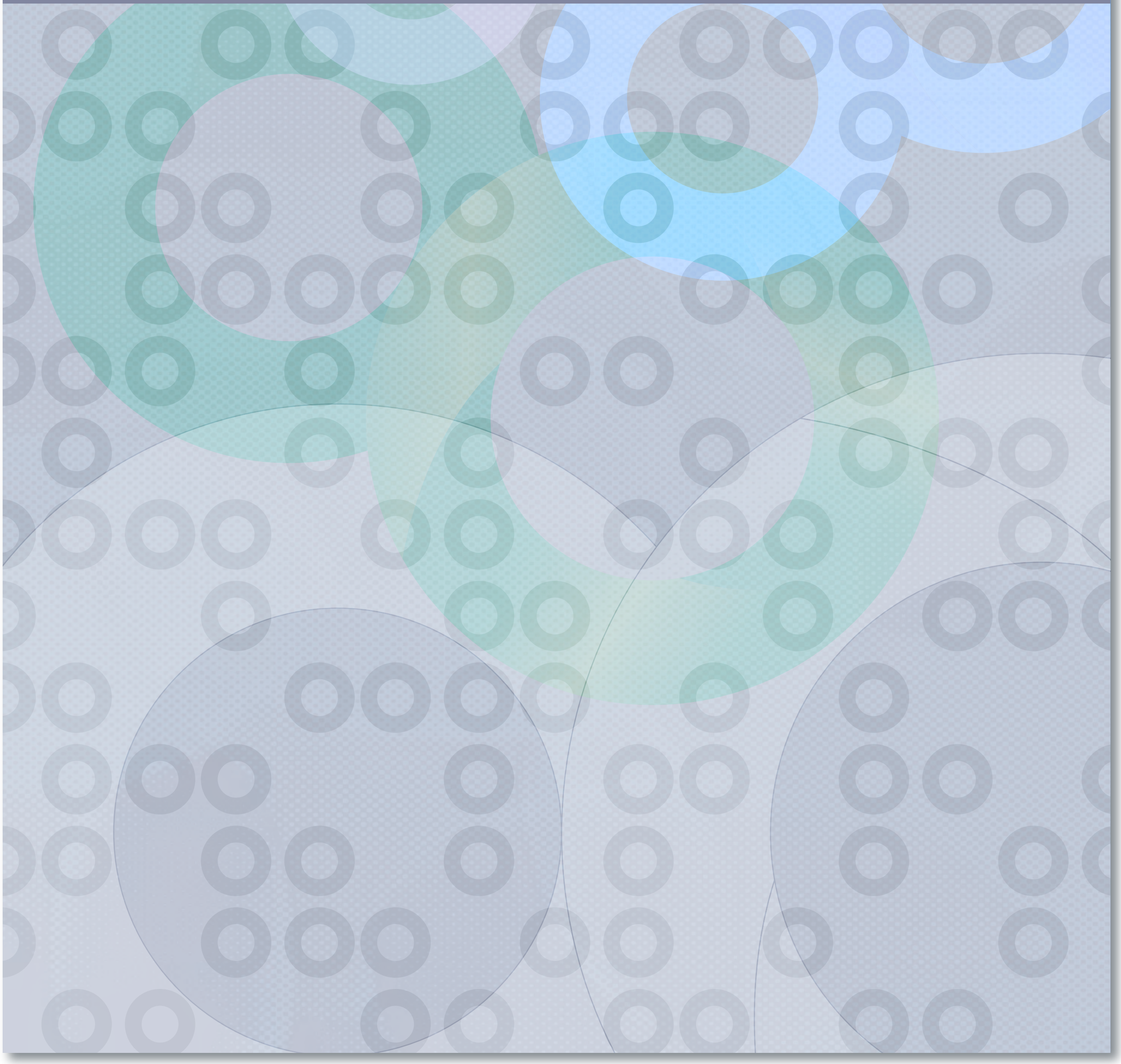

MI Lecture Note Vol.87 : Kyushu University

Proceedings of Forum “Math-for-Industry” 2021
-Mathematics for Digital Economy-

■Chief Editors:

Osamu Saeki (Kyushu University, Japan)

Ho Tu Bao (Vietnam Institute for Advanced Study in Mathematics, Vietnam)

Editors:

Shizuo Kaji (Kyushu University, Japan)

Kenji Kajiwara (Kyushu University, Japan)

Nguyen Ha Nam (Vietnam Institute for Advanced Study in Mathematics,
Vietnam)

Ta Hai Tung (Hanoi University of Science and Technology, Vietnam)

Melanie Roberts (Griffith University in Brisbane, Australia)

Masato Wakayama (Institute for Fundamental Mathematics, NTT, Japan)

Le Minh Ha (Vietnam Institute for Advanced Study in Mathematics, Vietnam)

Philip Broadbridge (La Trobe University, Australia)

About MI Lecture Note Series

The Math-for-Industry (MI) Lecture Note Series is the successor to the COE Lecture Notes, which were published for the 21st COE Program "Development of Dynamic Mathematics with High Functionality," sponsored by Japan's Ministry of Education, Culture, Sports, Science and Technology (MEXT) from 2003 to 2007. The MI Lecture Note Series has published the notes of lectures organized under the following two programs: "Training Program for Ph.D. and New Master's Degree in Mathematics as Required by Industry," adopted as a Support Program for Improving Graduate School Education by MEXT from 2007 to 2009; and "Education-and-Research Hub for Mathematics-for-Industry," adopted as a Global COE Program by MEXT from 2008 to 2012.

In accordance with the establishment of the Institute of Mathematics for Industry (IMI) in April 2011 and the authorization of IMI's Joint Research Center for Advanced and Fundamental Mathematics-for-Industry as a MEXT Joint Usage / Research Center in April 2013, hereafter the MI Lecture Notes Series will publish lecture notes and proceedings by worldwide researchers of MI to contribute to the development of MI.

October 2018
Osamu Saeki
Director
Institute of Mathematics for Industry

Proceedings of Forum "Math-for-Industry" 2021

-Mathematics for Digital Economy-

MI Lecture Note Vol.87, Institute of Mathematics for Industry, Kyushu University
ISSN 2188-1200
Date of issue: March 28, 2022
Chief Editors: Osamu Saeki, Ho Tu Bao
Editors: Shizuo Kaji, Kenji Kajiwara, Nguyen Ha Nam, Ta Hai Tung,
Melanie Roberts, Masato Wakayama, Le Minh Ha, Philip Broadbridge
Publisher:
Institute of Mathematics for Industry, Kyushu University
Graduate School of Mathematics, Kyushu University
Motooka 744, Nishi-ku, Fukuoka, 819-0395, JAPAN
Tel +81-(0)92-802-4402, Fax +81-(0)92-802-4405
URL https://www.imi.kyushu-u.ac.jp/

Preface

The FMfI2021 has been organized by the Vietnam Institute for Advanced Study in Mathematics, the Institute of Mathematics for Industry, and the Asia Pacific Consortium of Mathematics for Industry. This is the first time that the Forum was held in Hanoi, Vietnam - December 13-16, 2021.

The dramatic acceleration of digital transformation and the increasing role of applied mathematics across the world inspired us to run the FMfI2021 theme “Mathematics for Digital Economy”. It converged about 30 prominent scholars and industry experts to deliver excellent lectures in a comprehensive program.

A special session named ‘Mathematics of Covid-19’ was also included in response to the pandemic, with various modelling insights into the fight against it. There were further 28 posters selected to present at the Forum, covering a wide range of topics in many branches of mathematics. Their presentations, though short, were delivered in an unexpectedly interactive and interesting manner.

FMfI2021 was attended by more than 200 participants both in person and online, many attending it for the first time. I do believe the participants have gained fruitful and unforgettable experience at the FMfI2021.

I would like to acknowledge each and every person in the organizing staff, the organizing committee, invited speakers committee, and poster prize committee for their cooperative spirit and tremendous support. They worked very hard to make FMfI2021 a continued success in the history of the 11-year Institute. FMfI2021 indeed met its intended goals and reached broad participation. I would also like to express my gratitude to the FMfI2021 speakers for contributing their research results to the conference. Without their commitment and dedication, the proceedings could not have been produced.

I once again sincerely thank you all for making it all happen. It was with great pleasure that my colleagues and I had this opportunity to host a conference of this magnitude.

Le Minh Ha
Managing Director
Vietnam Institute for Advanced Study in Mathematics (VIASM)

FORUM

2021

Math for Industry

Mathematics for Digital Economy

DECEMBER 12-16
HANOI, VIETNAM

VIASM
VIETNAM INSTITUTE FOR
ADVANCED STUDY IN MATHEMATICS

Institute of Mathematics for Industry
Kyushu University

Asia Pacific Consortium of
Mathematics for Industry

The Asia-Pacific Consortium of Mathematics for Industry (APCMfI)

Mathematics for Industry (MfI) aims at the development of mathematics and its applications to enhance the quality of life on the planet by creating new technologies, improve industrial mathematical research and stimulate the two-way interaction between mathematics and industry. In Industrial Mathematics, it is the questions spawned by real world applications that drive the resulting two-way interaction between a particular application and the associated mathematics that is utilized and developed, and that sometimes involves, quite unexpectedly, deeper aspects and new areas of mathematics than initially anticipated.

Though its significance has often been overlooked, industrial mathematics has always been an essential aspect of the history, culture, traditions and development of mathematics, including much of modern theoretical mathematics. Directly and indirectly, developments in mathematics can be traced to the initial attempts to answer quite practical questions. The development of Galileo's telescope and the design of clocks represent early stimuli. Harmonic analysis and Fourier analysis have their origins in the study of heat transfer in metals. The conservation and minimization of energy engendered in the study of thermodynamics and fluid motion underlie much of the foundations of modern theoretical mathematics, as well as applied and industrial mathematics.

The increasing sophistication of modern industry, reflected in, for example, medical measurements, game theory applications in economics, psychology, behavioral science and biology, computer-controlled instrumentation, the efficient development of geothermal energy, the microbial treatment of waste water, Ito calculus in finance, etc., has generated a need and demand for mathematical expertise to stimulate, foster and implement the associated innovations. Even the theoretical areas of algebraic geometry, abstract algebra, topology, differential geometry and group theory are playing an increasingly important role in industrial endeavors connected with entertainment (such as games and movies), architecture, analysis of protein structure and error-correcting codes.

There is general agreement and support in the Asia-Pacific region to have regular industrial mathematics exchanges, conferences, internships, etc., which build on the activities already occurring. In fact, over the years since the concept of an Asian Consortium of Mathematics for Industry was first proposed and more recently when planning to formalize possibilities, there has been strong support and encouragement from colleagues in China, Hawaii, Korea, Malaysia and Singapore as well as Australia, New Zealand and Japan.

A small group, with the encouragement of various colleagues throughout the Asia-Pacific region, met in Canberra, March 31 to April 2, 2014, to do the initial planning for the formation and launch of APCMfI, with the emphasis being fundamentally Mathematics-for-Industry. Those directly involved in the discussions in Canberra were Bob Anderssen (Australia), Zainal Aziz (Malaysia), Frank de Hoog (Australia), Yasuhide Fukumoto (Japan), Alexandra Hogan (Australia), Geoff Mercer (Australia), Masato Wakayama (Japan) and Graeme Wake (New Zealand).

In any endeavours that involve the initiation and implementation of a new opportunity, the situation is similar to planting and nurturing a seed which will grow into a strong and robust tree. The meeting and deliberations of this group represented the preparation of the ground for the planting of the seed. The subsequent planting and nurturing involves the wide distribution of this initiative throughout the Asia-Pacific region; the seeking of seed funding from various mathematics departments, societies, agencies and industry; the establishment of a website; the launch of APCMfI under the MfI banner.

In 2021 the APCMfI turned into its second generation and reorganized the administration; the Council is chaired by Zainal Aziz (President) and driven by the Steering Committee, Philip Broadbridge(Australia, Vice President), Kenji Kajiwara (Japan, Secretary), Shizuo Kaji (Japan, Treasurer), and Melanie

Roberts (Australia, Communications). Other eight Council Members are from Australia, China, Korea, New Zealand, and Thailand. Among thirteen Council Members there are five female Members. The APCMfI will expand its activities to form a platform of collaborations of industrial and applied mathematics in the Asia Pacific region.

Planned Activities for APCMfI

An important component of the plans for APCMfI is a number of activities through which it interacts directly with the Asia-Pacific MfI communities and indirectly with the various international industrial mathematics consortia, organizations and individuals.

The underling goal is to stimulate the development of mathematics and its applications to enhance the quality of life on the planet by creating new technologies, improve industrial mathematical research and stimulate the two-way interaction between mathematics and industry.

The planned activities include:

a. facilitating the creation of internships for graduate students to work on industrial and governmental research projects in the Asia Pacific region; in principle, interns will spend several months working at their home institution and several months working with an industrial partner.

b. the promotion of regular Mathematics-for-Industry Study Groups (MfISG) having a strong Asia Pacific component with respect to both the problems to be studied and participation, taking advantage of study groups already operating in Australia, New Zealand, Japan and Malaysia,

c. the development within APCMfI of similar events e.g. “year projects” to the regular Mathematics-for-Industry Forums and Workshops, building on the successful annual Forums organized by the Institute of Mathematics for Industry (“IMI”) at Kyushu University,

d. the utilization of APCMfI for the exchange of information and publicity materials about industrial mathematics activities in the Asia Pacific region, such as electronic newsletters, publications, websites, etc.,

e. the organization of lectures and programs, either live or by video conference, that foster student participation by taking advantage of the similar time zones in the Asia Pacific region,

f. the fostering of a strong two-way interaction between (i) individuals and institutions engaged in mathematical and statistical research, and (ii) the needs and opportunities of industrial mathematics,

g. the development of synergetic links with other similar or relevant organizations, and

h. the identification of an international project that several governments might value and support.

History of the Forums "Math-for-Industry"

The Forums now have a decade-long history. Initiated by the Institute of Mathematics for Industry (IMI) at Kyushu University in Japan in 2010, the Forums have provided a meeting place for mathematical minds, and also to provide insights that enable the endeavors of industry-focused researchers to be shared within the region.

2010 Oct 21–23	Fukuoka, Japan Information Security, Visualization, and Inverse Problems, on the basis of Optimization Techniques
2011 Oct 24–28	Honolulu, US TSUNAMI - Mathematical Modelling Using Mathematics for Natural Disaster: Prediction, Recovery and Provision for the Future
2012 Oct 22–26	Fukuoka, Japan

	Information Recovery and Discovery
2013 Nov 4–8	Fukuoka, Japan The Impact of Applications on Mathematics
2014 Oct 27–31	Fukuoka, Japan Applications + Practical Conceptualization + Mathematics = Fruitful Innovation

In 2014, the Asia-Pacific Consortium of Mathematics for Industry (APCMfI) was formed, and the forums started to move around the Consortium's member countries, with themes that reflected each country's interests.

2015 Oct. 26–30	Fukuoka, Japan The Role and Importance of Mathematics in Innovation
2016 Nov. 21–23	Brisbane, AU Agriculture as a Metaphor for Creativity in all Human Endeavors
2017 Oct. 23–26	Honolulu, US Responding to the Challenges of Climate Change: Exploiting, Harnessing and Enhancing the Opportunities of Clean Energy
2018 Nov. 17-21	Shanghai, PRC Big Data Analysis, AI, Fintech, Math in Finance and Economics
2019 Nov. 18–21	Auckland, NZ Mathematics for the Primary Industries and the Environment
2021 Dec 13-16	Hanoi, Vietnam Mathematics for Digital Economy

FMfI2022 will be held in late November or mid-December in Melbourne, Australia, hosted by La Trobe University. FMfI2023 will be hosted by the IMI, Kyushu University, Japan. It is planned to be a satellite meeting of the International Congress of Industrial and Applied Mathematics in Tokyo

(ICIAM2023). It will be held one week prior to or after ICIAM2023 which is scheduled during 20-26 August 2023.

It is clear that the Forums traverse a wide range of topics, and that the abilities of mathematicians to address these affirm the importance of such specialists in the increasingly-complex ways in which society operates. The value that quantitative scientists and engineers provide to all communities cannot be underestimated. While most people appreciate effective and efficiently-operating systems, they often do not realize how these come about, and who is providing the sophisticated processes that underlie their efficiency.

While the speakers are experienced in their fields, the students who present posters and give talks about their work are the future leaders in APCMfI; they are valuable members of the "Math-for-Industry" community, and are particularly welcome at this Forum.

Information about the APCMfI and FMfI is extracted from the APCMfI website and the FMfI2019

The Vietnam Institute for Advanced Study in Mathematics

The Vietnam Institute for Advanced Study in Mathematics (VIASM) was established in late 2010 and officially came into operation on June 1st, 2011. The scientific director of the Institute is Professor Ngo Bao Chau, the 2010 Field Medalist.

Since then, our institute has become the meeting point for international and Vietnamese mathematicians, exchanging ideas, initiating new research projects, collaborating and connecting with young Vietnamese researchers and students.

We aim to promote and initiate basic research activities in mathematics and mathematical education in Vietnam, collaborating with other academic and research institutes around the world to strengthen the research and education ecosystem.

The main activity of the Institute is organizing research groups to conduct research programs and projects of high quality. Scientists in the same field will gather and work together at the Institute on a short-term basis. It aims to attract Vietnamese mathematicians from abroad and international mathematicians to Vietnam to participate in research and training together with their colleagues in Vietnam. This activity will strengthen the research branches which have taken root in Vietnam, and will incubate the formation of new branches of Mathematics.

Every year, the institute offers up to 5 Postdoctoral fellowships, and organizes conferences, workshops, seminars on topics associated with research groups working at the Institute in order to implement their research projects as well as attract new students to do research.

Our institute is also responsible for the implementation of the National Program for the Development of Mathematics in Vietnam, now in the second phase from 2021 to 2030. Under this program, we help organize many teacher training seminars, and outreach activities to encourage young students to learn mathematics, improve the quality of teaching and learning mathematics, as well as disseminate scientific knowledge to the public.

Forum "Math-for-Industry" 2021
-Mathematics for Digital Economy-

Date: December 13-16, 2021.
Venue: Vietnam Institute for Advanced Study in Mathematics
Start 08:30, finish 15:30 each day (Hanoi time)

12/12 Sunday morning from 8am: **IMI-IAB, APCMfI (Council and AGM), Journal Board meetings**
14/12 Tuesday afternoon: **Poster Session and Short Communication**
14/12 Tuesday evening: **Banquet** (depending on the covid-19 situation in Hanoi, Vietnam)
15/12 Wednesday morning: **Special Session: Mathematics of Covid-19**

Organising Committee

Le Minh Ha (Chair), Vietnam Institute for Advanced Study in Mathematics
Trinh Thi Thuy Giang, Vietnam Institute for Advanced Study in Mathematics
Shizuo Kaji, Kyushu University, Japan
Nguyen Ha Nam, Vietnam Institute for Advanced Study in Mathematics
Ta Hai Tung, Hanoi University of Science and Technology, Vietnam
Melanie Roberts, Griffith University in Brisbane, Australia
Osamu Saeki, Kyushu University, Japan
Masato Wakayama, Tokyo University of Science, Japan

Invited Speakers Committee

Ho Tu Bao (Chair), Vietnam Institute for Advanced Study in Mathematics
Alona Ben-Tal, Massey University, New Zealand
Philip Broadbridge, La Trobe University, Australia
Jin Cheng, Fudan University, China
Yasuhide Fukumoto, Kyushu University, Japan
Nguyen Xuan Hung, Ho Chi Minh City University of Technology, Vietnam
Kenji Kajiwara, Kyushu University, Japan
Vu Hoang Linh, Vietnam National University, Hanoi
Vu Ha Van, Yale University, USA and Vingroup Big Data Institute, Vietnam

Theme may include:

Digital economy can be understood as an economy in the digital environment where much more data than ever and connection of everything. It consists of three groups:
- ICT sector
- Industries in which business models are closely related to digital technology (e.g. Finance)
- Traditional industries trying to supplement their practices with digital technology

Math for digital economy may include or be related to:
- Machine Learning/Data Science
- Optimization in Industry
- Information Security
- Blockchain
- Math Modelling
- Big Data
- Business Analytics
- and others

FMfI2021 will include:

* Invited talks
* Emerging Researcher talks
* Student posters
* Special Session: Mathematics of Covid-19
* Short Communication
* Meetings of APCMfI + IMI-IAB + Journal Editorial Boards

VIASM
VIETNAM INSTITUTE FOR ADVANCED STUDY IN MATHEMATICS

Institute of Mathematics for Industry
Kyushu University

APCMfI
Asia Pacific Consortium of Mathematics for Industry

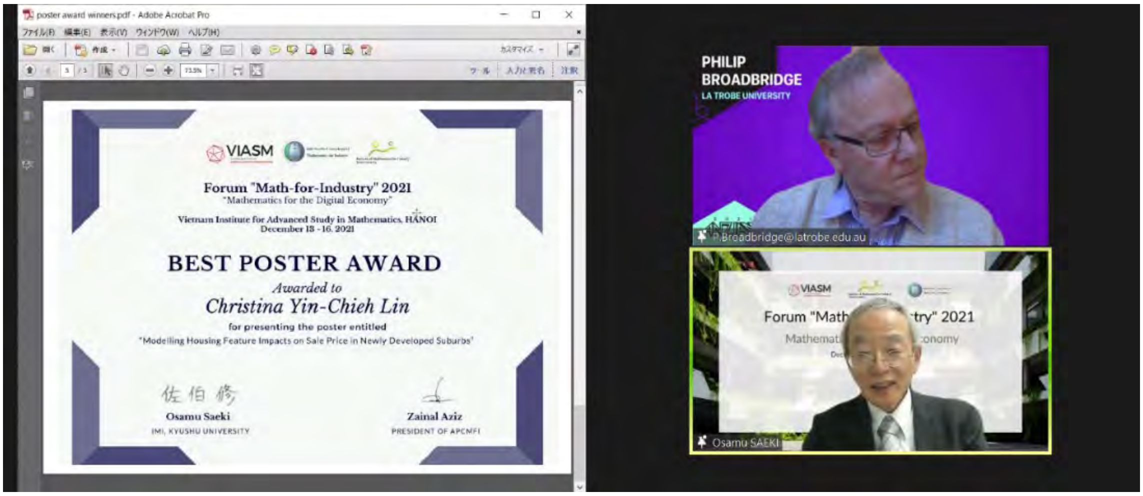

Forum "Math-for-Industry" 2021
"Mathematics for the Digital Economy"

Vietnam Institute for Advanced Study in Mathematics, HANOI
December 13 - 16, 2021

BEST POSTER AWARD

Awarded to
Christina Yin-Chieh Lin

for presenting the poster entitled
"Modelling Housing Feature Impacts on Sale Price in Newly Developed Suburbs"

佐伯修
Osamu Saeki
IMI, KYUSHU UNIVERSITY

Zainal Aziz
PRESIDENT OF APCMFI

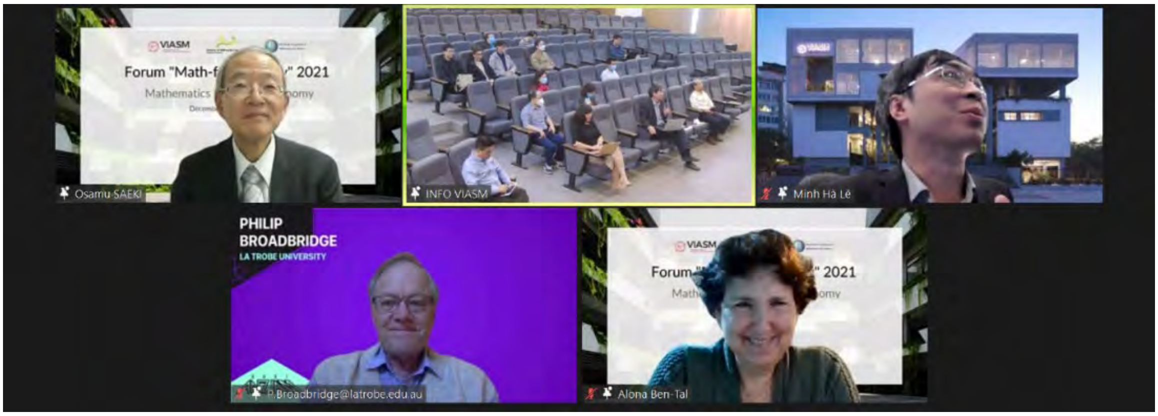

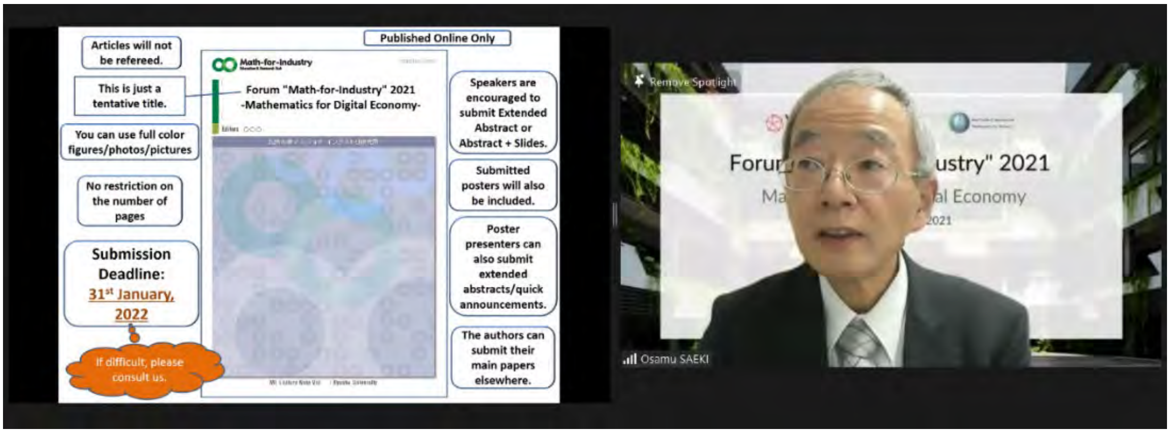

Published Online Only

Articles will not be refereed.

This is just a tentative title.

Forum "Math-for-Industry" 2021
-Mathematics for Digital Economy-

You can use full color figures/photos/pictures

No restriction on the number of pages

Submission Deadline:
31st January, 2022

If difficult, please consult us.

Speakers are encouraged to submit Extended Abstract or Abstract + Slides.

Submitted posters will also be included.

Poster presenters can also submit extended abstracts/quick announcements.

The authors can submit their main papers elsewhere.


Forum "Math-For-Industry" 2021
Mathematics for Digital Economy
Special Session: Mathematics of Covid-19
December 11 - 16, 2021


VIASM

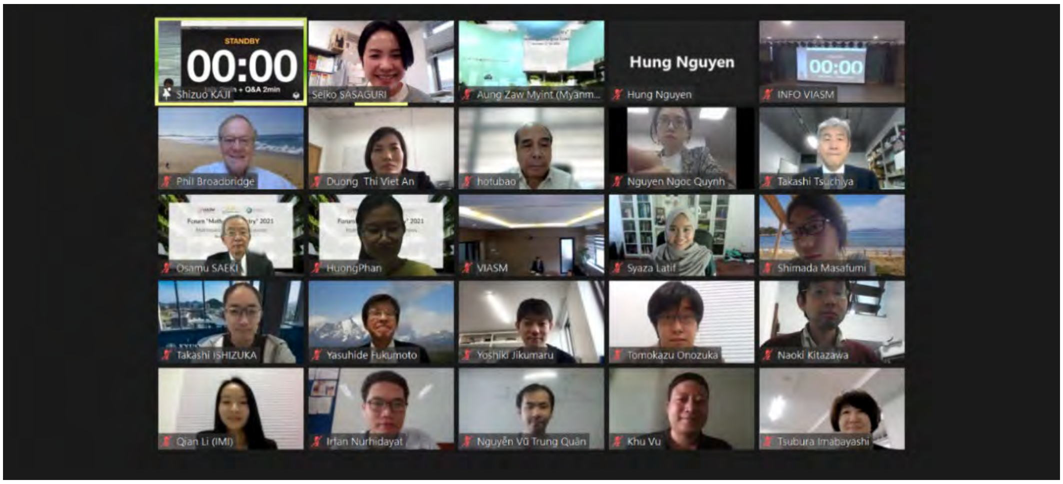
STANDBY
00:00
+ Q&A 2min
Shizuo KAJI
Seiko SASAGURI
Aung Zaw Myint (Myanm...
Hung Nguyen
Hung Nguyen
00:00
INFO VIASM
Phil Broadbridge
Duong Thi Viet An
hotubao
Nguyen Ngoc Quynh
Takashi Tsuchiya
Osamu SAEKI
HuongPhan
VIASM
Syaza Latif
Shimada Masafumi
Takashi ISHIZUKA
Yasuhide Fukumoto
Yoshiki Jikumaru
Tomokazu Onozuka
Naoki Kitazawa
Qian Li (IMI)
Irfan Nurhidayat
Nguyễn Vũ Trung Quân
Khu Vu
Tsubura Imabayashi

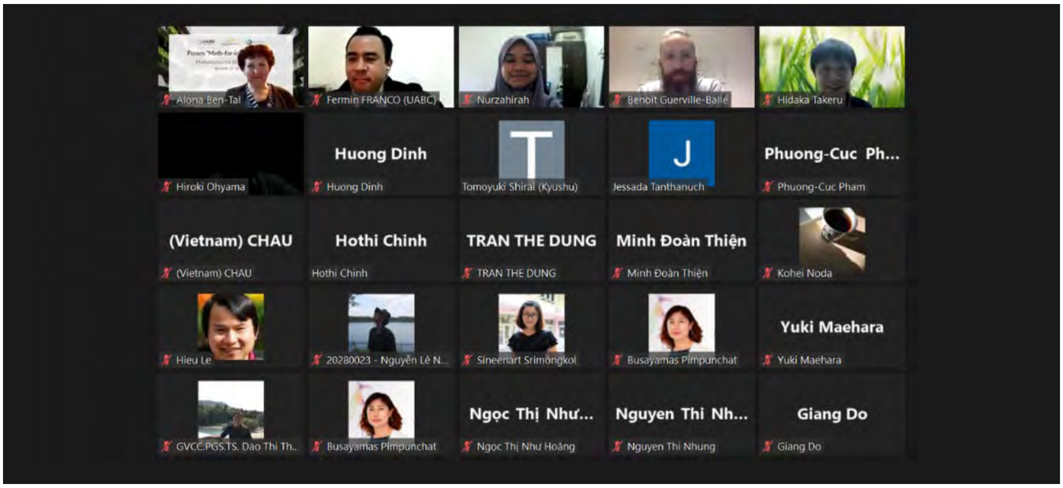
Alona Ben-Tal
Fermin FRANCO (UABC)
Nurzahirah
Benoit Guerville-Ballé
Hidaka Takeru
Hiroki Ohyama
Huong Dinh
Huong Dinh
T
Tomoyuki Shirai (Kyushu)
J
Jessada Tanthanuch
Phuong-Cuc Ph...
Phuong-Cuc Pham
(Vietnam) CHAU
(Vietnam) CHAU
Hothi Chinh
Hothi Chinh
TRAN THE DUNG
TRAN THE DUNG
Minh Đoàn Thiện
Minh Đoàn Thiện
Kohei Noda
Hieu Le
20280023 - Nguyễn Lê N...
Sineenart Srimongkol
Busayamas Pimpunchat
Yuki Maehara
Yuki Maehara
GVCC.PGS.TS. Dao Thi Th...
Busayamas Pimpunchat
Ngọc Thị Như...
Ngọc Thị Như Hoàng
Nguyen Thi Nh...
Nguyen Thi Nhung
Giang Do
Giang Do

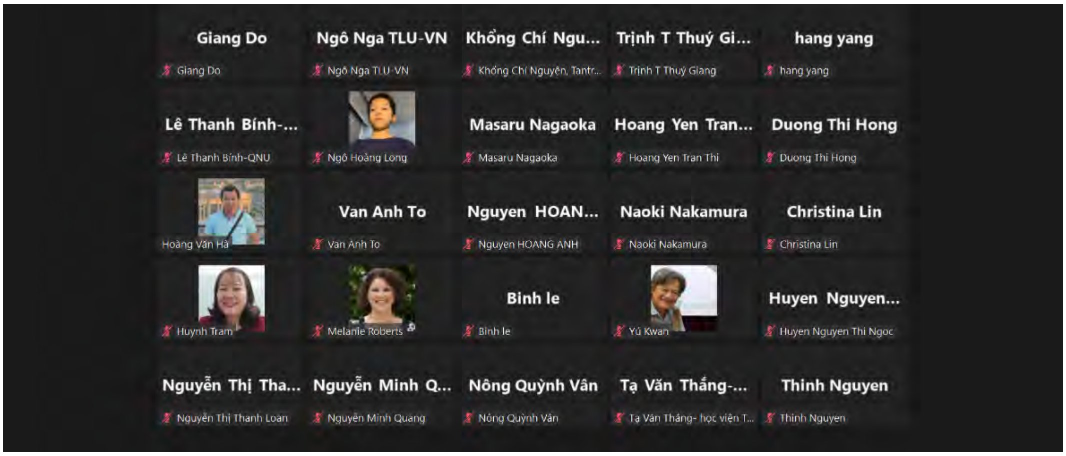
Giang Do
Giang Do
Ngô Nga TLU-VN
Ngô Nga TLU-VN
Khổng Chí Ngu...
Khổng Chí Nguyên, Tantr...
Trịnh T Thuý Gi...
Trịnh T Thuý Giang
hang yang
hang yang
Lê Thanh Bình-...
Lê Thanh Bình-QNU
Ngô Hoàng Long
Masaru Nagaoka
Masaru Nagaoka
Hoang Yen Tran...
Hoang Yen Tran Thi
Duong Thi Hong
Duong Thi Hong
Hoàng Văn Hà
Van Anh To
Van Anh To
Nguyen HOAN...
Nguyen HOANG ANH
Naoki Nakamura
Naoki Nakamura
Christina Lin
Christina Lin
Huynh Tram
Melanie Roberts
Binh le
Binh le
Yú Kwan
Huyen Nguyen...
Huyen Nguyen Thi Ngoc
Nguyễn Thị Tha...
Nguyễn Thị Thanh Loan
Nguyễn Minh Q...
Nguyễn Minh Quang
Nông Quỳnh Vân
Nông Quỳnh Vân
Tạ Văn Thắng-...
Tạ Văn Thắng- học viên T...
Thinh Nguyen
Thinh Nguyen

Local news about FMfI2021

I am very pleased to share that the FMfI2021 has been covered in leading Vietnamese magazines and newspapers. This shows the Forum as well as Math for Industry have gained positive local recognition, and the collective effort of the FMfI2021 team did not go unnoticed.

1. *Local News about FMfI2021(from Vietnam)*
   https://apcmfi.org/event/view/179
2. *Các nhà khoa học Việt ứng dụng Toán học trong ứng phó với Covid-19*
   https://dantri.com.vn/giao-duc-huong-nghiep/cac-nha-khoa-hoc-viet-ung-dung-toan-hoc-trong-ung-pho-voi-covid19-20211213172455652.htm?zarsrc=31&utm_source=zalo&utm_medium=zalo&utm_campaign=zalo
3. *Ứng dụng Toán học trong các hoạt động phòng chống Covid-19*
   https://vov2.vov.vn/giao-duc-dao-tao/ung-dung-toan-hoc-trong-cac-hoat-dong-phong-chong-covid-19-31383.vov2
4. *Ứng dụng Toán học trong các hoạt động phòng chống Covid-19*
   https://vietnamnet.vn/vn/giao-duc/toan-hoc-co-nhieu-ung-dung-trong-viec-chong-lai-covid-19-800897.html?fbclid=IwAR0O4EiHbcPL39-XxO4wNDXgWkM6MxUc3uVtp76HVpLVo5P-5Dg6j1gldJE
5. *VIASM chủ trì hội nghị quốc tế về ứng dụng toán học cho nền kinh tế số*
   https://khoahocphattrien.vn/thoi-su-trong-nuoc/viasm-chu-tri-hoi-nghi-quoc-te-ve-ung-dung-toan-hoc-cho-nen-kinh-te-so/20211213105218775p882c918.htm
6. *Ứng dụng toán học cho nền kinh tế số như thế nào?*
   https://dantri.com.vn/giao-duc-huong-nghiep/ung-dung-toan-hoc-cho-nen-kinh-te-so-nhu-the-nao-20211212113916798.htm
7. *Giáo sư Katsuki Fujisawa: "Không thể tạo ra tiến bộ nếu không có Toán học"*
   https://dantri.com.vn/giao-duc-huong-nghiep/giao-su-katsuki-fujisawa-khong-the-tao-ra-tien-bo-neu-khong-co-toan-hoc-20211225093121436.htm

Program FMfI2021 Vietnam
December 12-16

THEME: Mathematics for Digital Economy

Join the FMfI2021:

https://zoom.us/j/93911359124?pwd=R0lmZmYycEpJT1BVbGRPZnRLM2tpUT09

- Meeting ID: 939 1135 9124
- Passcode: 107102

Sunday 12 Dec
8.00. **IMI IAB**
9.00. **APCMfI Board**
10.00. **APCMfI AGM**
11.00. **Journal Boards**

Monday 13 Dec	
08.30–09.00	Registration
09.00-09.30	**Welcome and Opening**
09.30-10.10	**Nathan Kutz** USA
10.10-10.30	Refreshment break
10.30-11.10	**Washio Takashi** Japan
11.10-11.50	**Ngo Duc Thanh** Vietnam
11.50-12.30	**Graham Williams** Australia
12.30-13.30	Lunch
13.30-14.10	**Alexander Lipton** Israel
14.10-14.20	Break
14.20-15.00	**Julian Jang-Jaccard** New Zealand
15.00-15.40	**Volkan Cevher** Switzerland

Tuesday 14 Dec	
08.30-09.10	**Kazue Sako** Japan
09.10-09.50	**Lim Ee-Peng** Singapore
09.50-10.00	Break
10.00-10.40	**Hien Nguyen** Australia
10.40-11.20	**Yu Jiang** China
11.20-12.00	**Takashi Tsuchiya** Japan
12.00-13.30	Lunch
13.30-14.00	**Short communications** Aung Zaw Myint Myanmar Jessada Tanthanuch Thailand
14.00-16.00	**Poster Session**

Wednesday 15 Dec	
Mathematics of Covid-19	
08.30-09.10	**Stefan Canzar** Chile
09.10-09.50	**Michael Lydeamore** Australia
09.50-10.00	Break
10.00-10.40	**Emily Harvey** New Zealand
10.40-11.20	**Nguyen Ngoc Doanh** Vietnam
11.20-12.00	**Shingo Iwami** Japan
12.00-13.30	Lunch
13.30–14.10	**Mai Anh Tien** Singapore
14.10–14.20	Break
14.20-15.00	**Vincent Y. F. Tan** Singapore
15.00-15.40	**Amir Mosavic** Hungary

Thursday 16 Dec	
08.30-09.10	**Yaniv Gal** New Zealand
09.10-09.50	**Caleb Moses** New Zealand
09.50-10.00	Break
10.00-10.40	**Xiaoping Lu** Australia
10.40-11.20	**Kohei Hatano** Japan
11.20-12.00	**Nguyen Dinh Hoa** Japan
12.00-13.30	Lunch
13.30–14.10	**Jin Cheng** China
14.10–14.20	Break
15.00-15.20	**Closing** **Osamu Saeki**
17.00-20.00	**Banquet**

Session Chairs	
Mon 9.30-10.10	Osamu Saeki
10.30-12.30	Yasuhide Fukumoto
13.30-15.40	Ho Tu Bao
Tue 8.30-9.50	Zainal Aziz
10.00-12.00	Hoang Linh Vu
13.30-14.00	Hung Nguyen Xuan
14.00-16.00	Shizuo Kaji
Wed 8.30-9.50	Philip Broadbridge
10.00-12.00	Alona Ben-tal
13.30-15.40	Jin Cheng
Thu 8.30-9.50	Melanie Roberts
10.00-12.00	Kenji Kajiwara
13.30-14.10	Le Minh Ha

World Time (December 2021)

USA (EST)	Chile	Europe	Myanmar	Vietnam	Singapore/China	Japan	Australia (AEDT)	New Zealand
18.00	22.00	2.00	7.30	8.00	9.00	10.00	12.00	14.00
19.00	23.00	3.00	8.30	9.00	10.00	11.00	13.00	15.00
20.00	0.00	4.00	9.30	10.00	11.00	12.00	14.00	16.00
21.00	1.00	5.00	10.30	11.00	12.00	13.00	15.00	17.00
22.00	2.00	6.00	11.30	12.00	13.00	14.00	16.00	18.00
23.00	3.00	7.00	12.30	13.00	14.00	15.00	17.00	19.00
0.00	4.00	8.00	13.30	14.00	15.00	16.00	18.00	20.00
1.00	5.00	9.00	14.30	15.00	16.00	17.00	19.00	21.00

Contents

Learning Dynamical Systems Models from Data

J. Nathan Kutz

Applied Mathematics, University of Washington, USA

A major challenge in the study of dynamical systems is that of model discovery: turning data into reduced order models that are not just predictive, but provide insight into the nature of the underlying dynamical system that generated the data. We introduce a number of data-driven strategies for discovering nonlinear multiscale dynamical systems and their embeddings from data. We consider two canonical cases: (i) systems for which we have full measurements of the governing variables, and (ii) systems for which we have incomplete measurements. For systems with full state measurements, we show that the recent sparse identification of nonlinear dynamical systems (SINDy) method can discover governing equations with relatively little data and introduce a sampling method that allows SINDy to scale efficiently to problems with multiple time scales, noise and parametric dependencies. For systems with incomplete observations, we show that the Hankel alternative view of Koopman (HAVOK) method, based on time-delay embedding coordinates and the dynamic mode decomposition, can be used to obtain a linear model and Koopman invariant measurement systems that nearly perfectly captures the dynamics of nonlinear quasiperiodic systems. Neural networks are used in targeted ways to aid in the model reduction process. Together, these approaches provide a suite of mathematical strategies for reducing the data required to discover and model nonlinear multiscale systems.

Rare Event Search and Fast Data Assimilation for Industry in the Digital Twin Era

Takashi WASHIO

ISIR, Osaka University, and

AIRC, The National Institute of Advanced Industrial Science and Technology, Japan

Modern society has now entered the digital twin era, where simulation models of many systems are constructed, and highly reliable and efficient designs and operations of the systems are expected to be carried out using simulations. Under this movement, enormous research activities on developing simulation techniques and models are currently underway in various fields. However, generic techniques to efficiently construct high quality designs and operation plans of the systems using the simulations have not been sufficiently studied. Such techniques must be developed by fusing mathematical optimization and simulation approaches in elaborating manners.

In this talk, first, we show techniques to efficiently discover rare events, which occur under very special conditions with extremely low probabilities, using simulations guided by mathematical search principles [1]. We demonstrate an efficient scheme to design highly reliable products in industry using the techniques. Second, we show techniques for data assimilation which automatically and efficiently tune the simulation model parameters to reflect real system dynamics [2]. Particularly, our techniques enable to find the accurate parameter values using only a few observations of the real system. We demonstrate quick monitoring of dynamics changes of an industrial factory and its prompt operation alteration to maintain the productivity.

This talk suggests an important R&D direction of applied mathematics for future industry.

REFERENCES

[1] Keiichi Kisamori, Takashi Washio, Yoshio Kameda and Ryohei Fujimaki, A Rare and Critical Condition Search Technique and its Application to Telescope Stray Light Analysis, Proc. the 2018 SIAM International Conference on Data Mining (SDM2018), 2018. Read More: https://epubs.siam.org/doi/pdf/10.1137/1.9781611975321.64
`https://archive.siam.org/meetings/sdm18/`

[2] Keiichi Kisamori, Motonobu Kanagawa and Keisuke Yamazaki, Simulator Calibration under Covariate Shift with Kernels, Proc. the 23rdInternational Conference on Artificial Intelligence and Statistics (AISTATS2020), PMLR: Vol.108, 2020. Read More: http://proceedings.mlr.press/v108/kisamori20a/kisamori20a.pdf
`https://aistats.org/aistats2020/`

OSAKA UNIVERSITY

NEC-AIST
AI Cooperative
Research Laboratory

Rare Event Search and Fast Data Assimilation for Industry in the Digital Twin Era

FMfI 2021
December, 13th, 2021

Takashi Washio

Professor: The Institute of Scientific and Industrial Research,
Osaka University
Director: NEC-AIST AI CRL, Artificial Intelligence Research Center,
National Institute of Advanced Industrial Science and Technology

This presentation includes research work with Keiichi Kisamori, Keisuke Yamazaki, Yoshio Kameda and Ryohei Fujimaki in NEC-AIST AI CRL.

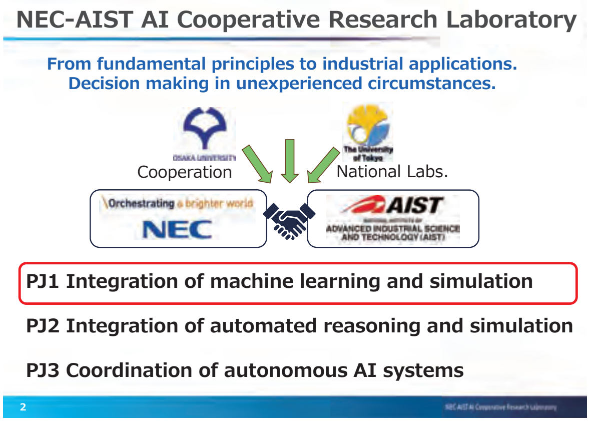

NEC-AIST AI Cooperative Research Laboratory

From fundamental principles to industrial applications.
Decision making in unexperienced circumstances.

PJ1 Integration of machine learning and simulation

PJ2 Integration of automated reasoning and simulation

PJ3 Coordination of autonomous AI systems

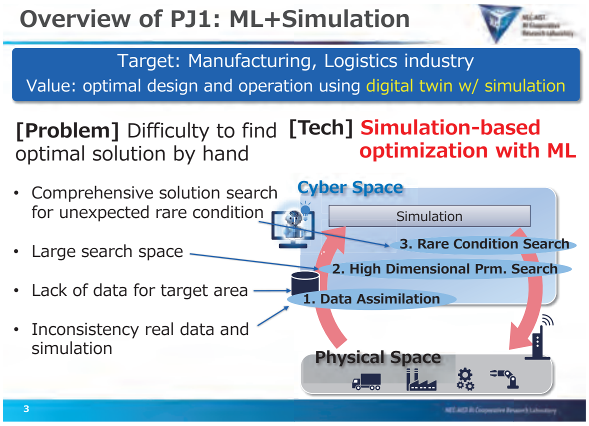

Overview of PJ1: ML+Simulation

Target: Manufacturing, Logistics industry
Value: optimal design and operation using digital twin w/ simulation

[Problem] Difficulty to find optimal solution by hand

- Comprehensive solution search for unexpected rare condition
- Large search space
- Lack of data for target area
- Inconsistency real data and simulation

[Tech] **Simulation-based optimization with ML**

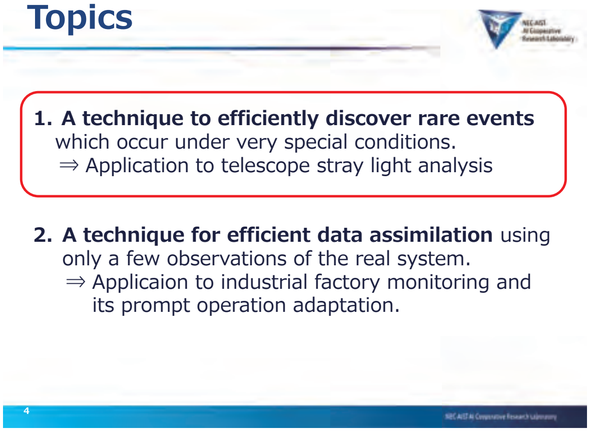

Topics

1. **A technique to efficiently discover rare events** which occur under very special conditions.
   ⇒ Application to telescope stray light analysis

2. **A technique for efficient data assimilation** using only a few observations of the real system.
   ⇒ Applicaion to industrial factory monitoring and its prompt operation adaptation.

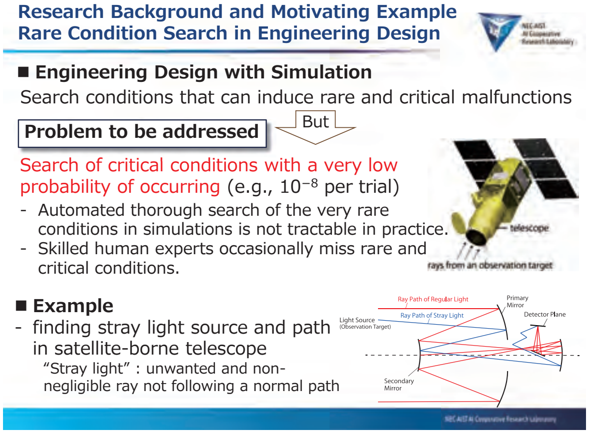

Research Background and Motivating Example
Rare Condition Search in Engineering Design

■ **Engineering Design with Simulation**

Search conditions that can induce rare and critical malfunctions

Problem to be addressed

But

Search of critical conditions with a very low probability of occurring (e.g., 10^{-8} per trial)

- Automated thorough search of the very rare conditions in simulations is not tractable in practice.
- Skilled human experts occasionally miss rare and critical conditions.

■ **Example**

- finding stray light source and path in satellite-borne telescope
  "Stray light" : unwanted and non-negligible ray not following a normal path

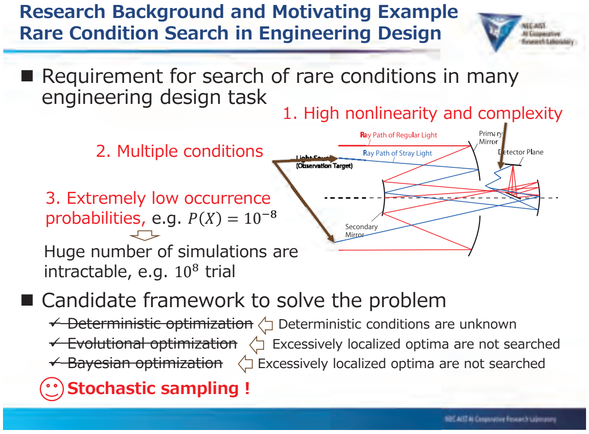

Research Background and Motivating Example
Rare Condition Search in Engineering Design

■ Requirement for search of rare conditions in many engineering design task

1. High nonlinearity and complexity

2. Multiple conditions

3. Extremely low occurrence probabilities, e.g. $P(X) = 10^{-8}$

Huge number of simulations are intractable, e.g. 10^8 trial

■ Candidate framework to solve the problem

✓ ~~Deterministic optimization~~ ⇦ Deterministic conditions are unknown
✓ ~~Evolutional optimization~~ ⇦ Excessively localized optima are not searched
✓ ~~Bayesian optimization~~ ⇦ Excessively localized optima are not searched

☺ **Stochastic sampling !**

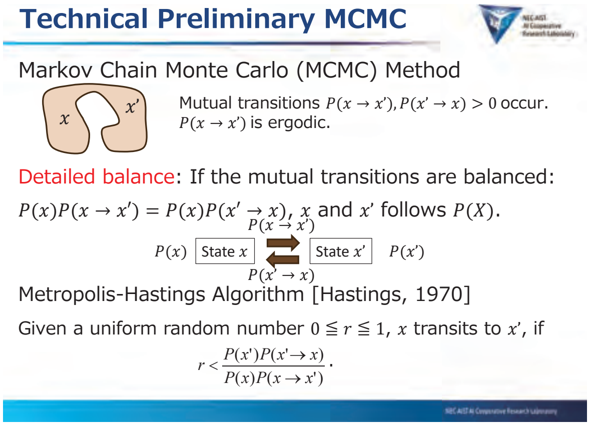

Technical Preliminary MCMC

Markov Chain Monte Carlo (MCMC) Method

Mutual transitions $P(x \to x'), P(x' \to x) > 0$ occur.
$P(x \to x')$ is ergodic.

Detailed balance: If the mutual transitions are balanced:

$P(x)P(x \to x') = P(x)P(x' \to x)$, x and x' follows $P(X)$.

Metropolis-Hastings Algorithm [Hastings, 1970]

Given a uniform random number $0 \leqq r \leqq 1$, x transits to x', if

$$r < \frac{P(x')P(x' \to x)}{P(x)P(x \to x')}.$$

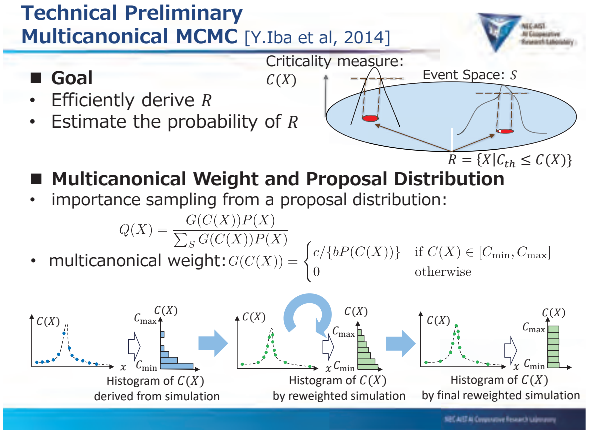

Technical Preliminary Multicanonical MCMC [Y.Iba et al, 2014]

- **Goal**
  - Efficiently derive R
  - Estimate the probability of R

- **Multicanonical Weight and Proposal Distribution**
  - importance sampling from a proposal distribution:

$$Q(X) = \frac{G(C(X))P(X)}{\sum_S G(C(X))P(X)}$$

  - multicanonical weight: $G(C(X)) = \begin{cases} c/\{bP(C(X))\} & \text{if } C(X) \in [C_{\min}, C_{\max}] \\ 0 & \text{otherwise} \end{cases}$

Histogram of $C(X)$ derived from simulation

Histogram of $C(X)$ by reweighted simulation

Histogram of $C(X)$ by final reweighted simulation

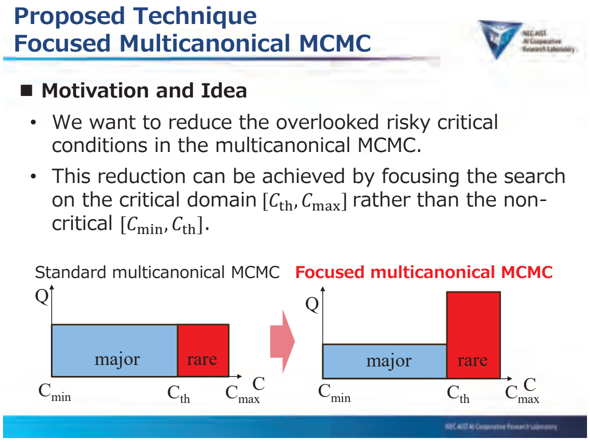

Proposed Technique Focused Multicanonical MCMC

- **Motivation and Idea**
  - We want to reduce the overlooked risky critical conditions in the multicanonical MCMC.
  - This reduction can be achieved by focusing the search on the critical domain $[C_{\text{th}}, C_{\max}]$ rather than the non-critical $[C_{\min}, C_{\text{th}}]$.

Standard multicanonical MCMC

Focused multicanonical MCMC

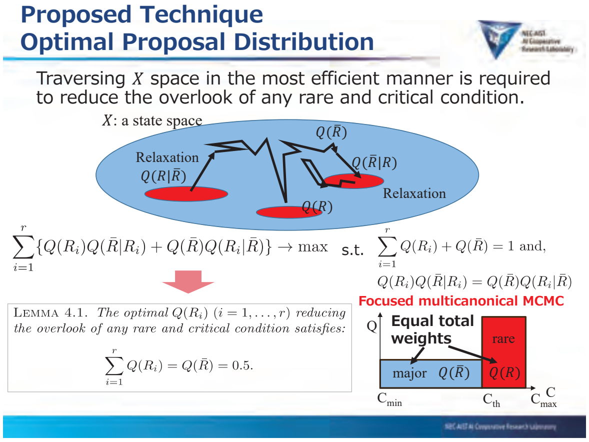

Proposed Technique Optimal Proposal Distribution

Traversing X space in the most efficient manner is required to reduce the overlook of any rare and critical condition.

$$\sum_{i=1}^{r}\{Q(R_i)Q(\bar{R}|R_i) + Q(\bar{R})Q(R_i|\bar{R})\} \to \max \quad \text{s.t.} \quad \sum_{i=1}^{r} Q(R_i) + Q(\bar{R}) = 1 \text{ and,}$$

$$Q(R_i)Q(\bar{R}|R_i) = Q(\bar{R})Q(R_i|\bar{R})$$

LEMMA 4.1. *The optimal* $Q(R_i)$ $(i = 1, \ldots, r)$ *reducing the overlook of any rare and critical condition satisfies:*

$$\sum_{i=1}^{r} Q(R_i) = Q(\bar{R}) = 0.5.$$

Focused multicanonical MCMC

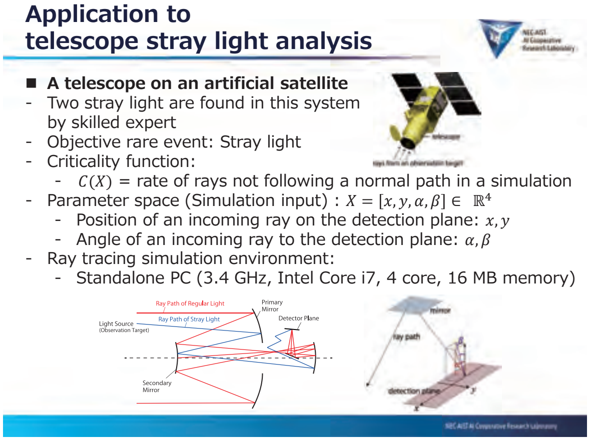

Application to telescope stray light analysis

- **A telescope on an artificial satellite**
- Two stray light are found in this system by skilled expert
- Objective rare event: Stray light
- Criticality function:
  - $C(X)$ = rate of rays not following a normal path in a simulation
- Parameter space (Simulation input) : $X = [x, y, \alpha, \beta] \in \mathbb{R}^4$
  - Position of an incoming ray on the detection plane: x, y
  - Angle of an incoming ray to the detection plane: α, β
- Ray tracing simulation environment:
  - Standalone PC (3.4 GHz, Intel Core i7, 4 core, 16 MB memory)

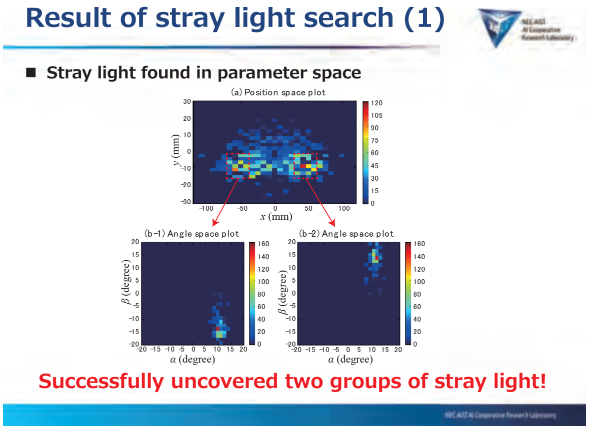

Result of stray light search (1)

- **Stray light found in parameter space**

Successfully uncovered two groups of stray light!

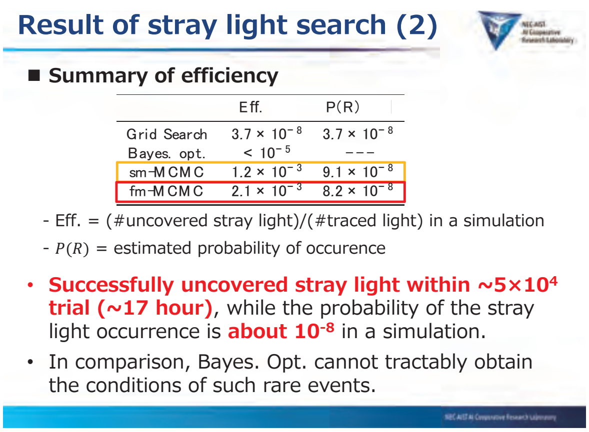

Result of stray light search (2)

■ **Summary of efficiency**

	Eff.	P(R)
Grid Search	3.7×10^{-8}	3.7×10^{-8}
Bayes. opt.	$< 10^{-5}$	---
sm-MCMC	1.2×10^{-3}	9.1×10^{-8}
fm-MCMC	2.1×10^{-3}	8.2×10^{-8}

- Eff. = (#uncovered stray light)/(#traced light) in a simulation

- $P(R)$ = estimated probability of occurence

- **Successfully uncovered stray light within ~5×10^4 trial (~17 hour)**, while the probability of the stray light occurrence is **about 10^{-8}** in a simulation.
- In comparison, Bayes. Opt. cannot tractably obtain the conditions of such rare events.

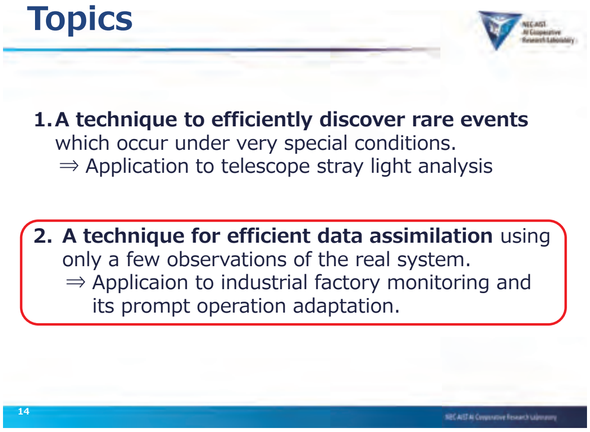

Topics

1. **A technique to efficiently discover rare events** which occur under very special conditions.
   ⇒ Application to telescope stray light analysis

2. **A technique for efficient data assimilation** using only a few observations of the real system.
   ⇒ Applicaion to industrial factory monitoring and its prompt operation adaptation.

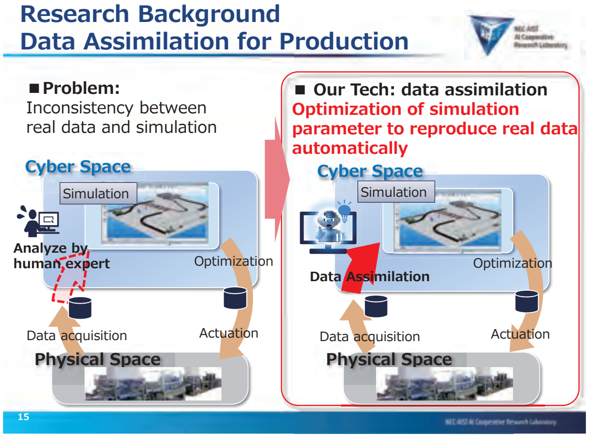

Research Background
Data Assimilation for Production

■ **Problem:**
Inconsistency between real data and simulation

■ **Our Tech: data assimilation**
Optimization of simulation parameter to reproduce real data automatically

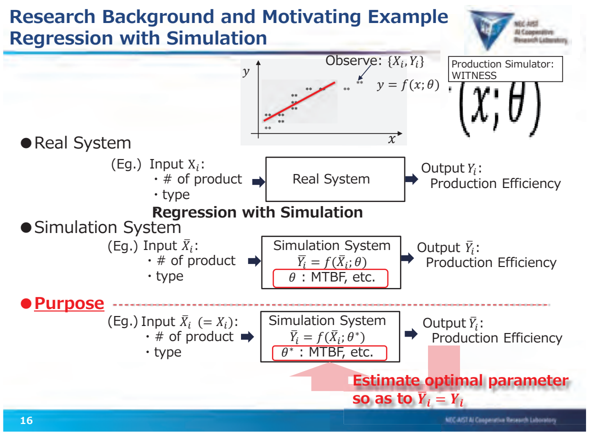

Research Background and Motivating Example
Regression with Simulation

- Real System
  (Eg.) Input X_i:
  ・# of product
  ・type
  → Real System → Output Y_i: Production Efficiency

Regression with Simulation

- Simulation System
  (Eg.) Input $\bar{X}_i$:
  ・# of product
  ・type
  → Simulation System $\bar{Y}_i = f(\bar{X}_i;\theta)$ θ : MTBF, etc. → Output $\bar{Y}_i$: Production Efficiency

- **Purpose**
  (Eg.) Input $\bar{X}_i$ $(= X_i)$:
  ・# of product
  ・type
  → Simulation System $\bar{Y}_i = f(\bar{X}_i;\theta^*)$ θ^* : MTBF, etc. → Output $\bar{Y}_i$: Production Efficiency

Estimate optimal parameter so as to $\bar{Y}_i = Y_i$

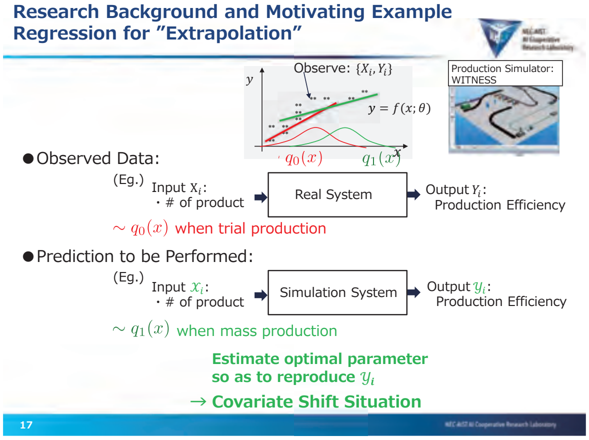

Research Background and Motivating Example
Regression for ”Extrapolation”

- Observed Data:
  (Eg.) Input X_i:
  ・# of product
  → Real System → Output Y_i: Production Efficiency
  $\sim q_0(x)$ when trial production

- Prediction to be Performed:
  (Eg.) Input x_i:
  ・# of product
  → Simulation System → Output y_i: Production Efficiency
  $\sim q_1(x)$ when mass production

Estimate optimal parameter so as to reproduce y_i

→ Covariate Shift Situation

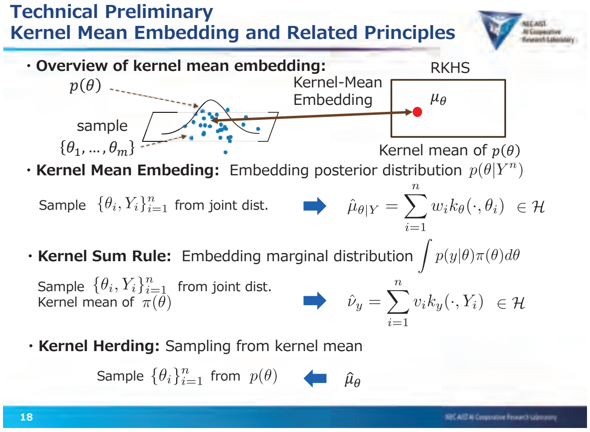

Technical Preliminary
Kernel Mean Embedding and Related Principles

- **Overview of kernel mean embedding:**

- **Kernel Mean Embeding:** Embedding posterior distribution $p(\theta|Y^n)$

  Sample $\{\theta_i, Y_i\}_{i=1}^n$ from joint dist. ➡ $\hat{\mu}_{\theta|Y} = \sum_{i=1}^n w_i k_\theta(\cdot, \theta_i) \in \mathcal{H}$

- **Kernel Sum Rule:** Embedding marginal distribution $\int p(y|\theta)\pi(\theta)d\theta$

  Sample $\{\theta_i, Y_i\}_{i=1}^n$ from joint dist.
  Kernel mean of $\pi(\theta)$ ➡ $\hat{\nu}_y = \sum_{i=1}^n v_i k_y(\cdot, Y_i) \in \mathcal{H}$

- **Kernel Herding:** Sampling from kernel mean

  Sample $\{\theta_i\}_{i=1}^n$ from $p(\theta)$ ⬅ $\hat{\mu}_\theta$

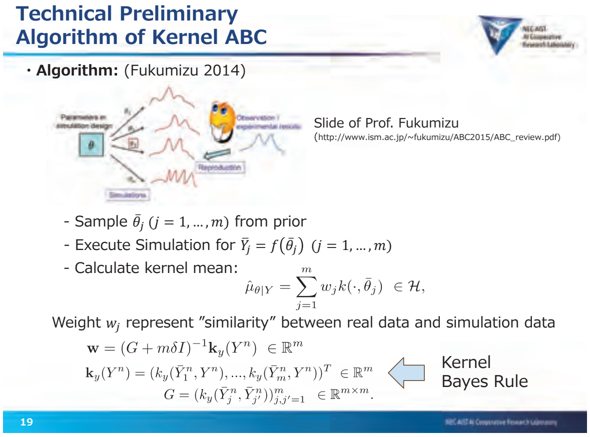

Technical Preliminary
Algorithm of Kernel ABC

- **Algorithm:** (Fukumizu 2014)

Slide of Prof. Fukumizu
(http://www.ism.ac.jp/~fukumizu/ABC2015/ABC_review.pdf)

- Sample $\bar{\theta}_j$ $(j = 1, \dots, m)$ from prior
- Execute Simulation for $\bar{Y}_j = f(\bar{\theta}_j)$ $(j = 1, \dots, m)$
- Calculate kernel mean:

$$\hat{\mu}_{\theta|Y} = \sum_{j=1}^{m} w_j k(\cdot, \bar{\theta}_j) \ \in \mathcal{H},$$

Weight w_j represent ”similarity” between real data and simulation data

$$\mathbf{w} = (G + m\delta I)^{-1}\mathbf{k}_y(Y^n) \ \in \mathbb{R}^m$$
$$\mathbf{k}_y(Y^n) = (k_y(\bar{Y}_1^n, Y^n), \dots, k_y(\bar{Y}_m^n, Y^n))^T \ \in \mathbb{R}^m$$
$$G = (k_y(\bar{Y}_j^n, \bar{Y}_{j'}^n))_{j,j'=1}^m \ \in \mathbb{R}^{m \times m}.$$

Kernel
Bayes Rule

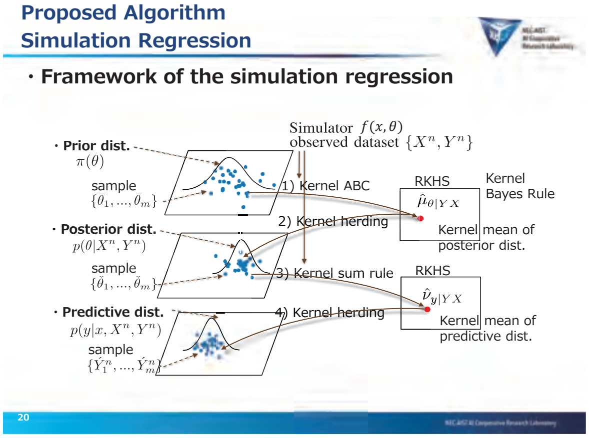

Proposed Algorithm
Simulation Regression

- **Framework of the simulation regression**

Simulator $f(x, \theta)$
observed dataset $\{X^n, Y^n\}$

- **Prior dist.**
  $\pi(\theta)$
  sample
  $\{\bar{\theta}_1, \dots, \bar{\theta}_m\}$
- **Posterior dist.**
  $p(\theta|X^n, Y^n)$
  sample
  $\{\check{\theta}_1, \dots, \check{\theta}_m\}$
- **Predictive dist.**
  $p(y|x, X^n, Y^n)$
  sample
  $\{\acute{Y}_1^n, \dots, \acute{Y}_m^n\}$

1) Kernel ABC
2) Kernel herding
3) Kernel sum rule
4) Kernel herding

RKHS
$\hat{\mu}_{\theta|YX}$
Kernel mean of posterior dist.

Kernel
Bayes Rule

RKHS
$\hat{\nu}_{y|YX}$
Kernel mean of predictive dist.

Proposed Algorithm
Simulation Regression (Cont’d)

- **Kernel ABC for regression**
  - Generate sample $\bar{\theta}_j \ \in \mathbb{R}^{d_\theta} \ \sim \pi(\theta)$ for $j = 1, \dots, m$
  - Generate pseudo-data $\bar{Y}_j^n \ \in \mathbb{R}^n \ \sim p(y|X^n, \bar{\theta}_j)$ by simulator$f(\bar{X}; \bar{\theta}_j)$ for $j = 1, \dots, m$.
  - Calculate kernel mean $\hat{\mu}_{\theta|YX}$

Key point of our extension

$$\hat{\mu}_{\theta|YX} = \sum_{j=1}^{m} w_j k(\cdot, \bar{\theta}_j)$$

$$\mathbf{w} = (G + m\delta I)^{-1}\mathbf{k}_y(Y^n) \ \in \mathbb{R}^m$$
$$\mathbf{k}_y(Y^n) = (k_y(\bar{Y}_1^n, Y^n), \dots, k_y(\bar{Y}_m^n, Y^n))^T \ \in \mathbb{R}^m$$
$$G = (k_y(\bar{Y}_j^n, \bar{Y}_{j'}^n))_{j,j'=1}^m \ \in \mathbb{R}^{m \times m}.$$

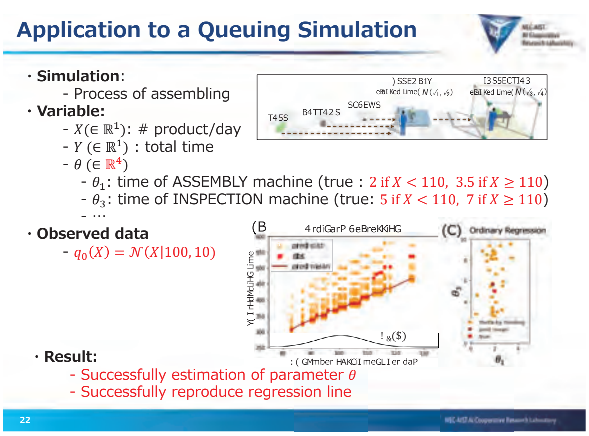

Application to a Queuing Simulation

- **Simulation**:
  - Process of assembling
- **Variable:**
  - $X (\in \mathbb{R}^1)$: # product/day
  - $Y \ (\in \mathbb{R}^1)$: total time
  - $\theta \ (\in \mathbb{R}^4)$
    - θ_1: time of ASSEMBLY machine (true : $2 \text{ if } X < 110, \ 3.5 \text{ if } X \geq 110$)
    - θ_3: time of INSPECTION machine (true: $5 \text{ if } X < 110, \ 7 \text{ if } X \geq 110$)
    - …
- **Observed data**
  - $q_0(X) = \mathcal{N}(X|100, 10)$

- **Result:**
  - Successfully estimation of parameter θ
  - Successfully reproduce regression line

Proposed Algorithm
Covariate Shift Situation

- **Kernel ABC for covariate shift**

$$\ln \tilde{p}(Y^n|X^n, \theta) = \sum_{i=1}^{n} \beta(X_i) \ln p(Y_i|X_i, \theta) \qquad \text{where} \qquad \beta_i = \beta(X_i) = \frac{q_1(X_i)}{q_0(X_i)}$$

- **How to express β_i in RKHS ??**
  - β_i weighted kernel :

$$\tilde{k}_y(Y^n, Y^{n\prime}) = \exp\left\{-\frac{1}{2\sigma^2}\sum_{i=1}^{n} \underline{\beta_i} (Y_i - Y_i')^2\right\}$$

Key point of our extension

  - β_i weighted kernel mean:

$$\hat{\mu}_{\vartheta|YX} = \sum_{j=1}^{m} \tilde{w}_j k(\cdot, \bar{\theta}_j),$$
$$\tilde{\mathbf{w}} = (\tilde{w}_1, \dots, \tilde{w}_m)^T \ \in \mathbb{R}^m$$
$$= (\tilde{G} + m\delta I)^{-1}\tilde{\mathbf{k}}_y(Y^n).$$
$$\tilde{\mathbf{k}}_y(Y^n) = (\tilde{k}_y(\bar{Y}_1^n, Y^n), \dots, \tilde{k}_y(\bar{Y}_m^n, Y^n))^T$$
$$\tilde{G} = (\tilde{k}_y(\bar{Y}_j^n, \bar{Y}_{j'}^n))_{j,j'=1}^m \ \in \mathbb{R}^{m \times m}$$

Kernel representation of importance weight β_i

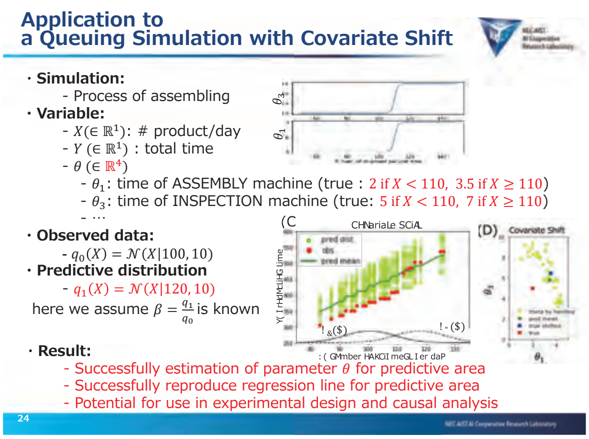

Application to
a Queuing Simulation with Covariate Shift

- **Simulation:**
  - Process of assembling
- **Variable:**
  - $X (\in \mathbb{R}^1)$: # product/day
  - $Y \ (\in \mathbb{R}^1)$: total time
  - $\theta \ (\in \mathbb{R}^4)$
    - θ_1: time of ASSEMBLY machine (true : $2 \text{ if } X < 110, \ 3.5 \text{ if } X \geq 110$)
    - θ_3: time of INSPECTION machine (true: $5 \text{ if } X < 110, \ 7 \text{ if } X \geq 110$)
    - …
- **Observed data:**
  - $q_0(X) = \mathcal{N}(X|100, 10)$
- **Predictive distribution**
  - $q_1(X) = \mathcal{N}(X|120, 10)$

here we assume $\beta = \frac{q_1}{q_0}$ is known

- **Result:**
  - Successfully estimation of parameter θ for predictive area
  - Successfully reproduce regression line for predictive area
  - Potential for use in experimental design and causal analysis

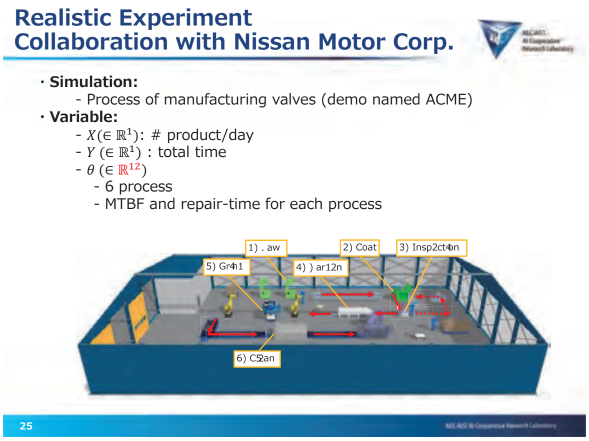

Realistic Experiment
Collaboration with Nissan Motor Corp.

- **Simulation:**
  - Process of manufacturing valves (demo named ACME)
- **Variable:**
  - $X (\in \mathbb{R}^1)$: # product/day
  - Y $(\in \mathbb{R}^1)$: total time
  - θ $(\in \mathbb{R}^{12})$
    - 6 process
    - MTBF and repair-time for each process

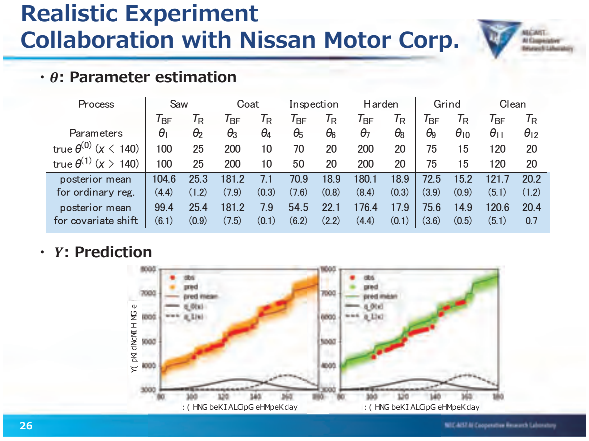

Realistic Experiment
Collaboration with Nissan Motor Corp.

- **θ: Parameter estimation**

Process	Saw		Coat		Inspection		Harden		Grind		Clean	
Parameters	T_{BF} θ_1	T_{R} θ_2	T_{BF} θ_3	T_{R} θ_4	T_{BF} θ_5	T_{R} θ_6	T_{BF} θ_7	T_{R} θ_8	T_{BF} θ_9	T_{R} θ_{10}	T_{BF} θ_{11}	T_{R} θ_{12}
true $\theta^{(0)}$ $(x < 140)$	100	25	200	10	70	20	200	20	75	15	120	20
true $\theta^{(1)}$ $(x > 140)$	100	25	200	10	50	20	200	20	75	15	120	20
posterior mean for ordinary reg.	104.6 (4.4)	25.3 (1.2)	181.2 (7.9)	7.1 (0.3)	70.9 (7.6)	18.9 (0.8)	180.1 (8.4)	18.9 (0.3)	72.5 (3.9)	15.2 (0.9)	121.7 (5.1)	20.2 (1.2)
posterior mean for covariate shift	99.4 (6.1)	25.4 (0.9)	181.2 (7.5)	7.9 (0.1)	54.5 (6.2)	22.1 (2.2)	176.4 (4.4)	17.9 (0.1)	75.6 (3.6)	14.9 (0.5)	120.6 (5.1)	20.4 0.7

- **Y: Prediction**

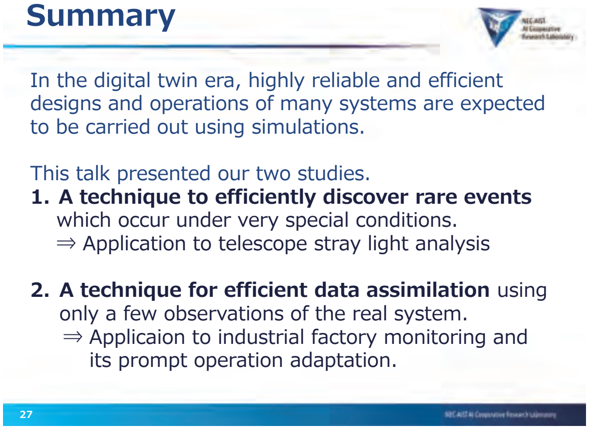

Summary

In the digital twin era, highly reliable and efficient designs and operations of many systems are expected to be carried out using simulations.

This talk presented our two studies.

1. **A technique to efficiently discover rare events** which occur under very special conditions.
   ⇒ Application to telescope stray light analysis

2. **A technique for efficient data assimilation** using only a few observations of the real system.
   ⇒ Applicaion to industrial factory monitoring and its prompt operation adaptation.

Climate change modelling in Southeast Asia and future climate information for the society

Thanh NGO-DUC

Department of Space and Applications, University of Science and Technology of Hanoi, Vietnam
(joint work with CORDEX-SEA's team & Quentin DESMET, LEGOS, France)

Today, 8.6% of the world population is living in Southeast Asia (SEA). Any change in the climate system can have unequivocal impacts on the region's socio-economic structures and living conditions. Given the high exposure and vulnerability of the region to extreme events, countries in SEA need to implement adaptation measures to lower their risk. Detailed information on future climate scenarios is thus needed. However, such information is still lacking in the region or generally based on global climate models (GCMs) that may have large uncertainties in a complex region such as SEA. In order to fill the gap, the Coordinated Regional Climate Downscaling EXperiment - Southeast Asia (CORDEX-SEA) project was established and had successfully gathered members from several countries to carry out a high resolution multi-model regional climate downscaling experiment.

In this presentation, an overview of climate change modeling activities in Southeast Asia and the recent findings of the CORDEX-SEA downscaling activities with the Coupled Model Intercomparison Project Phase 5 (CMIP5) are first introduced. We address how simulation of present-day extremes is influenced by the choices of various physical parameterizations to determine which schemes are well suited to simulate the climate extremes over the region. Future projected rainfall, extremes, and surface wind in association with tropical cyclone activities in SEA are subsequently analyzed. Lastly, we focus on a regional evaluation of 26 CMIP6 GCMs over SEA by introducing a novel ranking method based on temperature, rainfall, and wind distributions. The evaluation provides the CORDEX-SEA community with a reduced number of CMIP6 models with better performance over the region, which can be used in a further downscaling experiment.

Simply Deploying AI and ML

Graham Williams

Software Innovation Institute, Australian National University, Australia

With the extraordinary growth in research outputs in artificial intelligence, machine learning, and data science, industry struggles to keep pace. Developers in industry generally have limited time to explore and experiment with new algorithms coming out of our research labs at their current pace. Trialling a new technique can take considerable effort, even when the developers in industry have solid experience and data at the ready. The MLHub.ai initiative is a fully open source framework that aims to facilitate the exploration of new algorithms with minimal initial overhead. This presentation will set the scene and introduce a framework for easing our access to the latest research, illustrating its utility with industry collaborators.

Forex Trading Utilizing Consensus as a Service on Blockchains

Alexander Lipton

Jerusalem Business School, Hebrew University of Jerusalem, Israel

(joint work with Artur Sepp, Sygnum Bank, Zurich, Switzerland)

We present an automated market-making (AMM) cross-settlement mechanism for digital assets on interoperable blockchains, focusing on central bank digital currencies (CBDCs) and stable coins. We develop an innovative approach for generating fair exchange rates for on-chain assets consistent with traditional off-chain markets. We illustrate the efficacy of our approach on realized FX rates for G-10 currencies.

Artificial Intelligence (AI) for Intrusion Detection and Math

Julian Jang-Jaccard

Massey University, New Zealand

Cybersecurity Lab at Massey University, founded in 2016, has been one of the fastest-growing research labs in NZ dedicated to providing cutting-edge research theory, tools, and methodologies to improve the cybersecurity posture. With generous funds awarded from the NZ government, the lab has been dedicated to developing a set of novel cyber-resilient systems using the advancement of the latest AI techniques, both including machine and deep learnings, that can rapidly detect and classify various intrusions including malware. In this presentation, I will present a set of AI-based techniques (e.g., Autoencoder, Multi-Layer Perceptron, Deep Q-learning based Reinforcement Learning, Generative Adversarial Network) we have developed in the last few years and discuss the type of math skills demanded in these areas.

Optimization challenges in adversarial machine learning

Volkan Cevher

EPFL - Swiss Federal Institute of Technology Lausanne, Switzerland

(joint work with Panayotis Mertikopoulos, Thomas Pethick, Ya-Ping Hsieh, Nadav Hallak, Ali Kavis)

Thanks to neural networks (NNs), faster computation, and massive datasets, machine learning (ML) is under increasing pressure to provide automated solutions to even harder real-world tasks beyond human performance with ever faster response times due to potentially huge technological and societal benefits. Unsurprisingly, the NN learning formulations present a fundamental challenge to the back-end learning algorithms despite their scalability, in particular due to the existence of traps in the non-convex optimization landscape, such as saddle points, that can prevent algorithms from obtaining "good" solutions.

In this talk, we describe our recent research that has demonstrated that the non-convex optimization dogma is false by showing that scalable stochastic optimization algorithms can avoid traps and rapidly obtain locally optimal solutions. Coupled with the progress in representation learning, such as over-parameterized neural networks, such local solutions can be globally optimal.

Unfortunately, this talk will also demonstrate that the central min-max optimization problems in ML, such as generative adversarial networks (GANs), robust reinforcement learning (RL), and distributionally robust ML, contain spurious attractors that do not include any stationary points of the original learning formulation. Indeed, we will describe how algorithms are subject to a grander challenge, including unavoidable convergence failures, which could explain the stagnation in their progress despite the impressive earlier demonstrations. We will conclude with promising new preliminary results from our recent progress on some of these difficult challenges.

Cryptography and Transparency

Kazue Sako

Waseda University, Japan

In a digitalized society, we everyday use computers to receive messages from our friends, buy tickets online, and receive personal ads for attractive products on sale. However, as these are represented as digital data, it is difficult to verify whether these data sent from other computers are trustworthy. In this talk, we will discuss some tools using cryptography that makes the procedures occurring on the other computer transparent, thus increasing trustworthiness.

Keywords: verifiability, digital signature, zero-knowledge proofs, blockchain.

Forum:
Maths for Industry
2021.12.14

Cryptography and Transparency

Kazue Sako
Dept. Computer Science and Engineering
Waseda University

We will be using Green and Red Buttons

Providing nonverbal feedback and reactions during meetings (participants)

To provide nonverbal feedback or reactions to the host of the meeting:

1. Join a Zoom meeting as a participant.
2. Click the **Reactions** button.
3. Choose from the following icons or click ••• to choose from a full set of emojis. Click the icon again to remove it.
   - Clapping Hands 👏
   - Thumbs Up 👍
   - Heart ❤
   - Tears of Joy 😂
   - Open Mouth 😮
   - Party Popper (Tada, Celebration) 🎉
   - Yes ✅
   - No ❎
   - Slow Down ⏪
   - Speed Up ⏩
   - Raise Hand / Lower Hand ✋

The icon will appear in your video panel and next to your name in the participants list.

Zoom Poll 1

Do you know there are public-key encryptions and secret-key encryptions

- ✅ Yes
- ⏪ I have heard of it, but not sure how they're different
- ❎ No
- ⏩ Don't want to answer

Cryptographic Foundations I

Secret-key Encryption
a.k.a Symmetric key encryption

Public-key Encryption
a.k.a Asymmetric key encryption

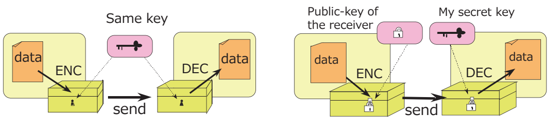

Self Introduction

Prof. Kazue Sako

- Majored mathematics in Kyoto University
- Soon after joining NEC, my boss gave me an article on RSA cryptosystem

RSA Cryptosystem(Rivest-Shamir-Adleman)1978

Key Setup
Find e,d and N s.t. for all M
$M^{ed} = M \pmod N$
Make e,N public
Secret key: d

Encryption
$C = M^e \pmod N$
Anyone can encrypt

Decryption
$M = C^d \pmod N$
Secret key is needed

RSA Cryptosystem(Rivest-Shamir-Adleman)197

N is a product of 2 primes p,q

Key Setup
Find e,d and N s.t. for all M
$M^{ed} = M \pmod N$
Make e,N public
Secret key: d

ed=1 mod Φ(N)
Φ：Euler Function
Fermat's little theorem

Factorization of N(2048bits) being difficult, **d** is kept secure!

Encryption
$C = M^e \pmod N$

Anyone can encrypt

Decryption
$M = C^d \pmod N$

Secret key is needed

Self Introduction

Prof. Kazue Sako

- Majored mathematics in Kyoto University
- Soon after joining NEC, my boss gave me an article on RSA cryptosystem
- I fell in love with cryptography. They are the tools to make our society more secure, more privacy–friendly and more fair.
- I joined Waseda University from 2020, determined that it's young students who will use these tools to make our society better.

Self Introduction

Prof. Kazue Sako

- Majored mathematics in Kyoto University
- Soon after joining NEC, my boss gave me an article on RSA cryptosystem
- I fell in love with cryptography. They are the tools to make our society more secure, more privacy–friendly and more fair.
- I joined Waseda University from 2020, determined that it's young students who will use these tools to make our society better.
- Former President of Japan Society of Industrial and Applied Mathematics (JSIAM)
- Member of Science Council of Japan
- Vice Chair of MyDataJapan

Today's talk

Cryptography and Transparency

In a digitalized society, we everyday use computers to receive messages from our friends, buy tickets online, and receive personal ads for attractive products on sale. However, as these are represented as digital data, it is difficult to verify whether these data sent from other computers are trustworthy. In this talk, we will discuss some tools using cryptography that makes the procedures occurring on the other computer transparent, thus increasing trustworthiness.

Today's title

Cryptography and Transparency

If you used encryption, wouldn't everything is obscured and not transparent?

Zoom Poll 2

Do you know digital signature schemes?

- ✓ Yes
- I have heard of it, but not sure what they are
- ✕ No
- Don't want to answer

Cryptographic Foundations II

Public-key encryption **Digital Signature scheme**

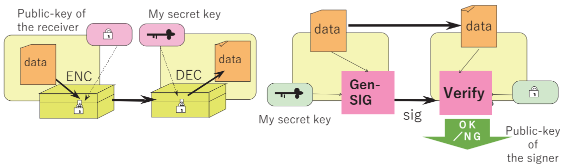

Zoom Poll 3

Did you know that in cryptocurrency Bitcoin, encryption function is not used?

- Yes
- No
- Not true. Encryption is indeed used in Bitcoin
- Don't want to answer

Bitcoin and Digital Signature schemes

Public key is the account number(address) !

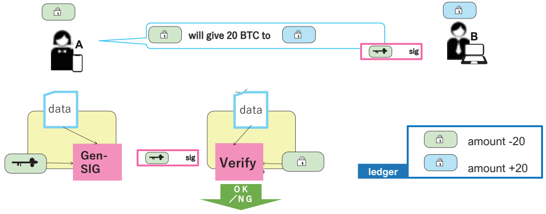

Today's title

Cryptography and Transparency

Cryptography/ Digital signatures clarifies who said what.

Cryptography ensures that one can not cheat in the system.

Cryptography ensures that if anyone cheated, it can be detected.

Cryptography provides transparency to operations in IT systems, even the software running on the other computer is not visible.

Today's title

Cryptography and Transparency

Cryptography provides transparency to operations in IT systems, even the software running on the other computer is not visible.

Ex: voting

Example: secret e-voting

How can we design a system to avoid cheating?

What kind of cheating do we want to prevent in e-voting?

What kind of cheating do we want to prevent in e-voting?

Only legitimate voters vote, but once

Tally must be correct

But vote secrecy must be maintained!

How do we do in paper-based voting?

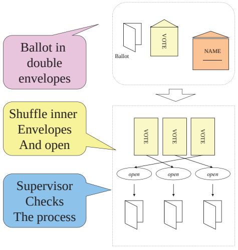

Ballot in double envelopes

Shuffle inner Envelopes And open

Supervisor Checks The process

Mixnet based voting protocol

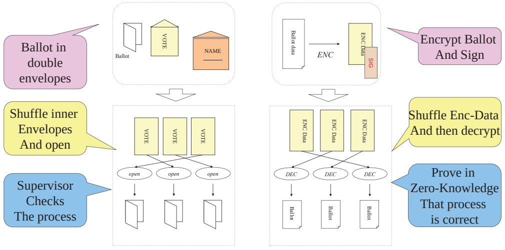

Ballot in double envelopes

Shuffle inner Envelopes And open

Supervisor Checks The process

Encrypt Ballot And Sign

Shuffle Enc-Data And then decrypt

Prove in Zero-Knowledge That process is correct

How to shuffle digital data?

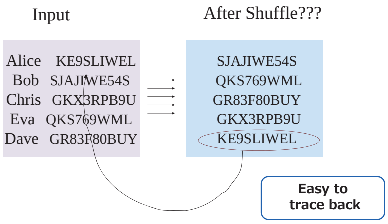

Input

Alice KE9SLIWEL
Bob SJAJIWE54S
Chris GKX3RPB9U
Eva QKS769WML
Dave GR83F80BUY

After Shuffle???

SJAJIWE54S
QKS769WML
GR83F80BUY
GKX3RPB9U
KE9SLIWEL

Easy to trace back

Probabilistic Encryption

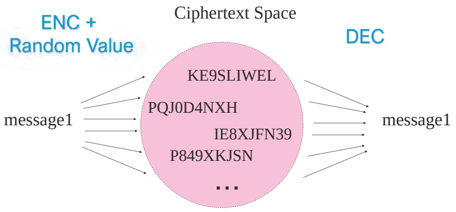

ENC + Random Value

Ciphertext Space

DEC

message1

KE9SLIWEL
PQJ0D4NXH
IE8XJFN39
P849XKJSN
…

message1

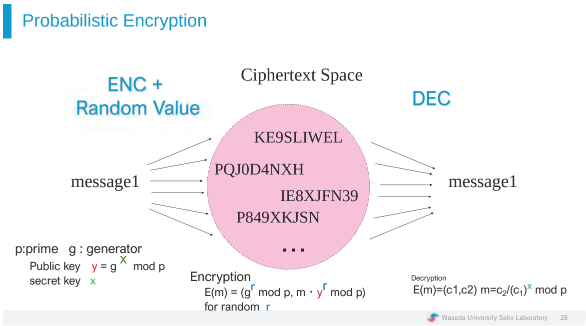

Probabilistic Encryption

p:prime g : generator

Public key $y = g^{x} \bmod p$

secret key x

Encryption

$E(m) = (g^{r} \bmod p, m \cdot y^{r} \bmod p)$

for random r

Decryption

$E(m)=(c1,c2)$ $m=c_2/(c_1)^{x} \bmod p$

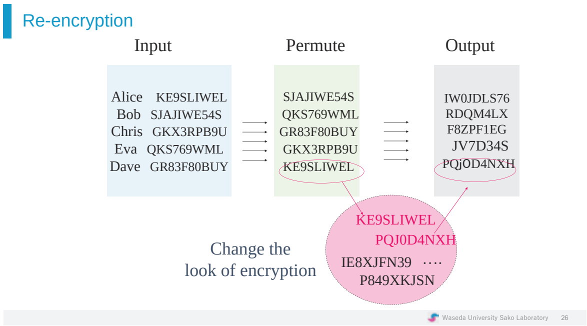

Re-encryption

Input		Permute	Output
Alice	KE9SLIWEL	SJAJIWE54S	IW0JDLS76
Bob	SJAJIWE54S	QKS769WML	RDQM4LX
Chris	GKX3RPB9U	GR83F80BUY	F8ZPF1EG
Eva	QKS769WML	GKX3RPB9U	JV7D34S
Dave	GR83F80BUY	KE9SLIWEL	PQjOD4NXH

Change the
look of encryption

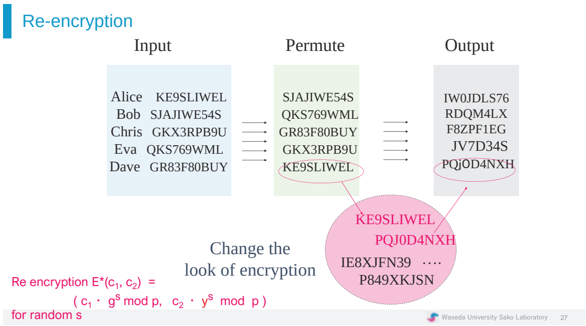

Re-encryption

Input		Permute	Output
Alice	KE9SLIWEL	SJAJIWE54S	IW0JDLS76
Bob	SJAJIWE54S	QKS769WML	RDQM4LX
Chris	GKX3RPB9U	GR83F80BUY	F8ZPF1EG
Eva	QKS769WML	GKX3RPB9U	JV7D34S
Dave	GR83F80BUY	KE9SLIWEL	PQjOD4NXH

Change the
look of encryption

Re encryption $E^*(c_1, c_2) =$

$(c_1 \cdot g^{s} \bmod p, \ c_2 \cdot y^{s} \bmod p)$

for random s

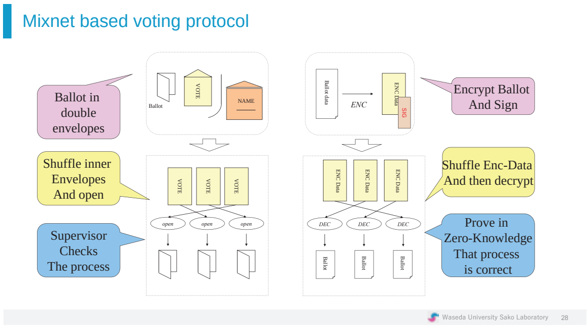

Mixnet based voting protocol

Ballot in
double
envelopes

Shuffle inner
Envelopes
And open

Supervisor
Checks
The process

Encrypt Ballot
And Sign

Shuffle Enc-Data
And then decrypt

Prove in
Zero-Knowledge
That process
is correct

Zero-knowledge Proofs

A powerful tool to ensure correctness without
revealing the witness

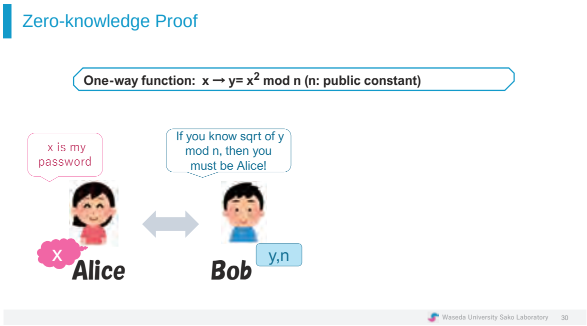

Zero-knowledge Proof

One-way function: $x \rightarrow y= x^2 \bmod n$ (n: public constant)

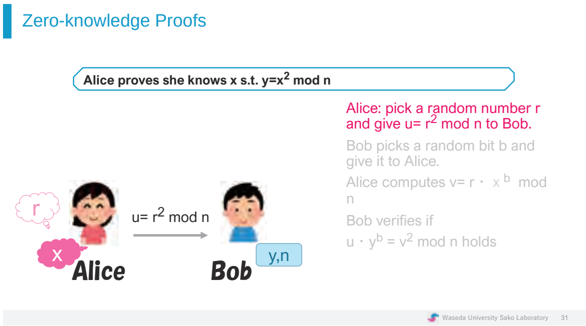

Zero-knowledge Proofs

Alice proves she knows x s.t. $y=x^2$ mod n

Alice: pick a random number r and give u= r^2 mod n to Bob.

Bob picks a random bit b and give it to Alice.

Alice computes v= r・ x^b mod n

Bob verifies if

u・y^b = v^2 mod n holds

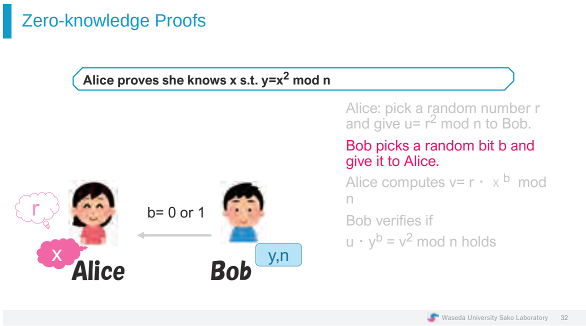

Zero-knowledge Proofs

Alice proves she knows x s.t. $y=x^2$ mod n

Alice: pick a random number r and give u= r^2 mod n to Bob.

Bob picks a random bit b and give it to Alice.

Alice computes v= r・ x^b mod n

Bob verifies if

u・y^b = v^2 mod n holds

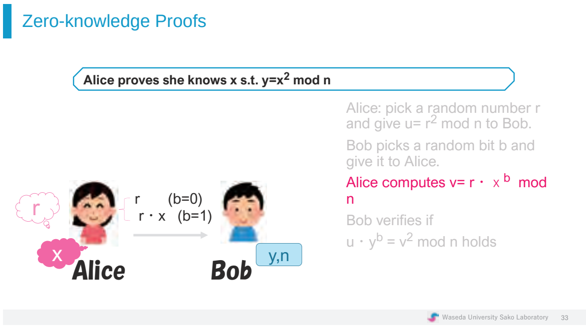

Zero-knowledge Proofs

Alice proves she knows x s.t. $y=x^2$ mod n

Alice: pick a random number r and give u= r^2 mod n to Bob.

Bob picks a random bit b and give it to Alice.

Alice computes v= r・ x^b mod n

Bob verifies if

u・y^b = v^2 mod n holds

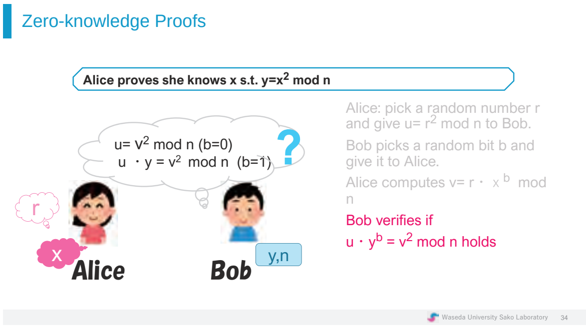

Zero-knowledge Proofs

Alice proves she knows x s.t. $y=x^2$ mod n

Alice: pick a random number r and give u= r^2 mod n to Bob.

Bob picks a random bit b and give it to Alice.

Alice computes v= r・ x^b mod n

Bob verifies if

u・y^b = v^2 mod n holds

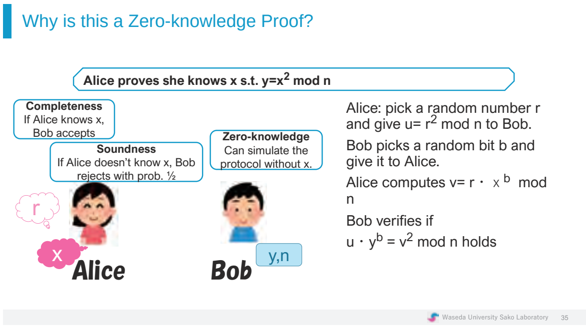

Why is this a Zero-knowledge Proof?

Alice proves she knows x s.t. $y=x^2$ mod n

Completeness
If Alice knows x, Bob accepts

Soundness
If Alice doesn't know x, Bob rejects with prob. ½

Zero-knowledge
Can simulate the protocol without x.

Alice: pick a random number r and give u= r^2 mod n to Bob.

Bob picks a random bit b and give it to Alice.

Alice computes v= r・ x^b mod n

Bob verifies if

u・y^b = v^2 mod n holds

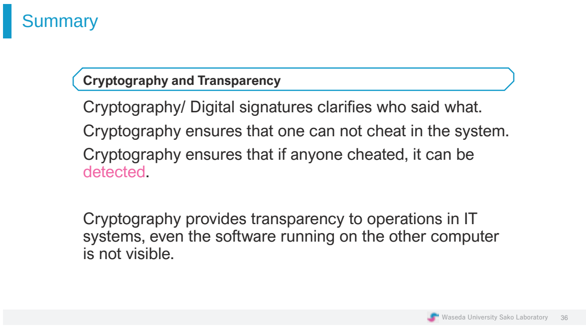

Summary

Cryptography and Transparency

Cryptography/ Digital signatures clarifies who said what.

Cryptography ensures that one can not cheat in the system.

Cryptography ensures that if anyone cheated, it can be detected.

Cryptography provides transparency to operations in IT systems, even the software running on the other computer is not visible.

ICIAM: International Congress on Industrial and Applied Mathematics

Data Mining for Labor Market Intelligence

Ee-Peng Lim

School of Computing and Information Systems, Singapore Management University, Singapore

Global economy and technology disruptions have created major impacts to labor markets in recent years. To fully understand these impacts to companies and rank-and-file people, we need to introduce new labor market intelligence capabilities using data mining. In this talk, we will review labor market intelligence and the underlying data mining problems. We will also illustrate how data mining can be used to analyse trends in job supply as well as patterns in job seeking behavior from big data. Finally, we will cover the challenges in labor market intelligence research and how one may overcome these challenges.

FMfI2021, Hanoi, December 2021

Data Mining for Labor Market Intelligence

LIM Ee Peng
Lee Kong Chian Professor of Computer Science
Director, Living Analytics Research Centre
Singapore Management University

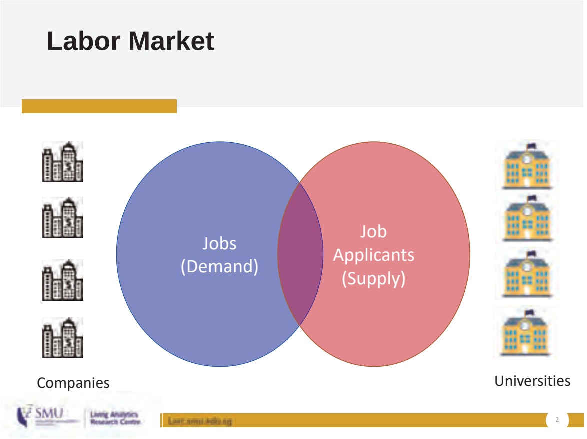

Labor Market

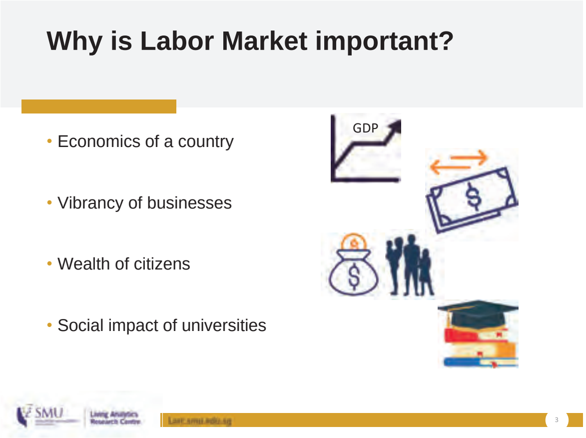

Why is Labor Market important?

- Economics of a country
- Vibrancy of businesses
- Wealth of citizens
- Social impact of universities

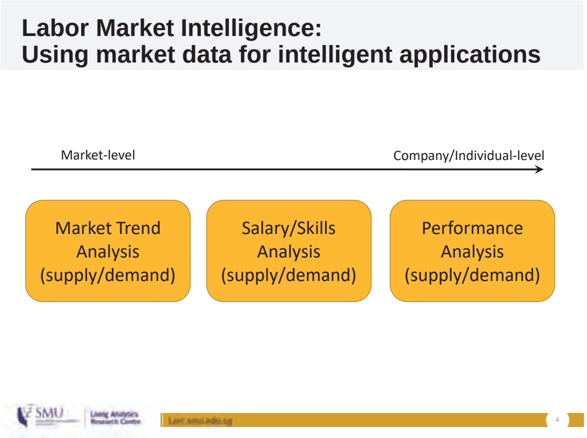

Labor Market Intelligence: Using market data for intelligent applications

Market Trend Analysis (supply/demand)

Salary/Skills Analysis (supply/demand)

Performance Analysis (supply/demand)

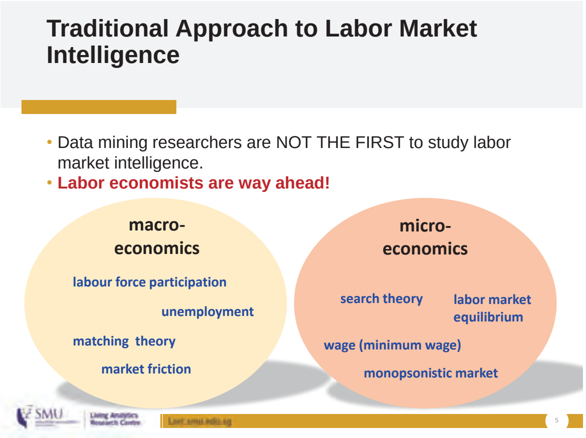

Traditional Approach to Labor Market Intelligence

- Data mining researchers are NOT THE FIRST to study labor market intelligence.
- **Labor economists are way ahead!**

macro-economics

labour force participation
unemployment
matching theory
market friction

micro-economics

search theory
labor market equilibrium
wage (minimum wage)
monopsonistic market

Limitations of Existing Approaches

- Simplified model assumptions:
  E.g., every worker/firm behaves the same way.
  E.g., worker decides jobs based on salary only.
- Focus on modeling variables derived from aggregated data or survey data, not actual micro-data.
  E.g., number of workers, average wage, etc.
- Models for explanation but not models for applications
  E.g., Economic models are good for explaining the trends and outcomes, but insufficient for developing IT solutions.

Advantages of Data Mining Approach: Accuracy, Timeliness and Usability

- Accuracy
  Economic models are good for descriptive analytics but not predictive analytics.
- Timeliness
  As new market data are collected, data mining models can be updated immediately, especially when there are major disruptions
- Usability:
  Personalized solutions to job applicants and companies

Warning! But Opportunity ☺

- Data mining research for labor market intelligence is still at very nascent stage.
- Labor market related datasets for data mining are not standardized nor publicly available.
- Many new data mining techniques have not been applied yet.

Market Trend Analysis

Market Trend Analysis (supply/demand)

Past Research
- Labor Force Survey
- Employer Skills Survey
- Census of Population
- Time series modelling (e.g, autoregressive model)

Modeling & Forecasting Research
- Job datasets and websites
- Univariate time series to multivariate/multimodal time series
- Time series model using deep learning

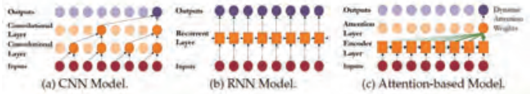

(a) CNN Model. (b) RNN Model. (c) Attention-based Model.

Lim, Bryan, and Stefan Zohren. "Time-series forecasting with deep learning: a survey." *Philosophical Transactions of the Royal Society A* 379.2194 (2021): 20200209.

Salary and Skills Analysis

Salary/Skills Analysis (supply/demand)

Past Research
- Labor Force Survey
- Employer Skills Survey
- Census of Population
- Knowledge Bases (e.g., O*Net)

Prediction & NLP Research
- Job website data
- Salary Prediction for Jobs
- Skill Modeling from Job Postings
- Skill Extraction from Job Descriptions

Measuring the Popularity of Job Skills

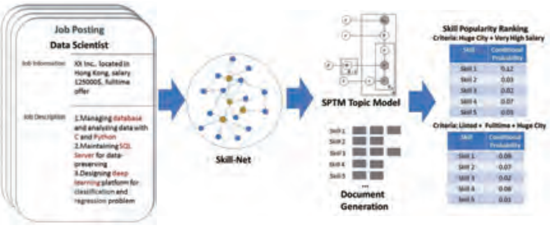

Xu, T., Zhu, H., Zhu, C., Li, P., & Xiong, H. (2018, April). Measuring the popularity of job skills in recruitment market: A multi-criteria approach. In *Proceedings of the AAAI Conference on Artificial Intelligence* (Vol. 32, No. 1).

Skill Entity Recognition (SER): A Deep Learning Approach

- To detect skill mentions in job description.
- Related Work: dictionary-based
  - limited dictionary size and heterogeneity
- NLP-Based Approach
  - Annotate skill data for 1800 job posts.
  - Augment FLAIR, contextual string embedding, with dimension removal and sectional labels
    Stack a CRF-based SER on FLAIR.
  - Our SER approach outperforms state-of-the-art models such as BERT.
  - Further link skill mentions to known skill entities in knowledge graph (Wikipedia).

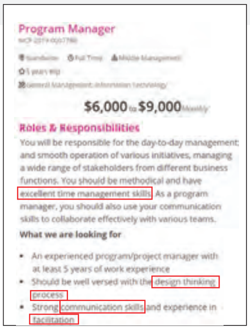

Program Manager

$6,000 to $9,000 Monthly

Roles & Responsibilities

You will be responsible for the day-to-day management and smooth operation of various initiatives, managing a wide range of stakeholders from different business functions. You should be methodical and have excellent time management skills. As a program manager, you should also use your communication skills to collaborate effectively with various teams.

What we are looking for

- An experienced program/project manager with at least 5 years of work experience
- Should be well versed with the design thinking process
- Strong communication skills and experience in facilitation

Skill Wikifier
https://research.larc.smu.edu.sg/skill-wikifier/demo

Skill Wikifier extracts skill mentions from a job posting and links them to Wikipedia entries. Copy and paste your job posting below to try out the software

Your Job Posting

Requirements
- 5+ years of working experience in a data science position
- Solid understanding of machine learning, statistical analysis and predictive techniques
- Knowledge of data management and visualization techniques
- Deep understanding of business modelling and how data science informs business decisions
- Highly skilled in statistical and modelling packages, visualization and familiar with time-series analyses
- Highly proficient and experienced in Python and its data manipulation and machine learning libraries
- Experience with SQL and NoSQL databases
- Experience with data processing using Spark is a plus

Performance Analysis

Performance Analysis (supply/demand)

Past Research
- Employee Engagement Survey
- Productivity Survey
- Employee Turnover Analysis
- Wage and Employee Performance

Company/User Profiling and Recommendation Research
- Datasets: Recruitment site data
- Employee Turnover Prediction
- Applicant User Profiling
- Jobs/Skills Recommendation

Contagious Effect for Employee Turnover Prediction

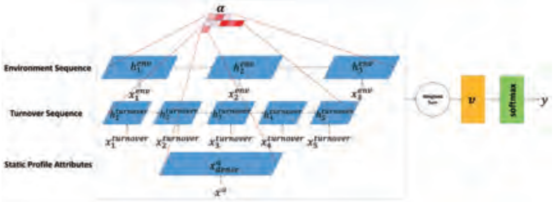

Teng, M., Zhu, H., Liu, C., Zhu, C., & Xiong, H. (2019). Exploiting the Contagious Effect for Employee Turnover Prediction. *Proceedings of the AAAI Conference on Artificial Intelligence*, *33*(01), 1166-1173.

What other research gaps?

Market Trend Analysis (supply/demand)

Salary/Skills Analysis (supply/demand)

Performance Analysis (supply/demand)

Modeling & Forecasting Research

Prediction & NLP Research

Company/User Profiling & Recommendation Research

Data Mining Models for Multiple Types of Analysis

On Learning User/Job Latent Attributes from Job Application Data

- **Our Proposed Approach**: Probabilistic Labor Market Model that captures behavior of people and jobs in the market by learning their attributes, and how they may interact.
- Users $U = \{u_1, u_2, \dots u_M\}$ with attributes gender, education level, age
- Jobs $P = \{p_1, p_2, \dots p_N\}$ each job $p_j \in P$ has an offer salary interval $[w_j^{min}, w_j^{max}]$
- Applications A – an $M \times N$ matrix

$$A_{ij} = \begin{cases} 1 & \text{if user } u_i \text{ is observed to apply job } p_j \\ 0 & \text{otherwise} \end{cases}$$

Probabilistic Labor Model

- Probability of user u_i applying job p_j

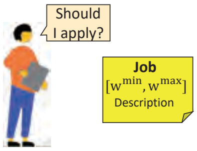

$$\hat{a}_{ij} = a_{ij}^{salary} \cdot a_{ij}^{topic} \cdot a_{ij}^{access}$$

Salary-based probability

Topic-based probability

Accessibility-based probability

Hendrik Santoso Sugiarto and Ee Peng Lim. On Modeling Labor Markets for Fine-grained Insights. Best Paper. The 5th Workshop on Data Science for Social Good, 2020.

Salary Criteria

- User u_i is interested in job p_j if
  job's offers salary ≥ her reserved salary v_i
  (this is a range!) (cannot be observed)

Salary Criteria

- User u_i is interested in job p_j if
  job's offers salary ≥ her reserved salary v_i
- But each user has different **optimisms m_i** $\in [0,1]$.
  If u_i is extreme-optimistic ($m_i = 1$) and u_i will focus on $w_j^{max} - v_i$
  If u_i is extreme-optimistic ($m_i = 0$) and u_i will focus on $w_j^{min} - v_i$
- Probability of u_i interested in p_j based on salary:

$$a_{ij}^{salary} = \sigma\left(m_i\left(w_j^{max} - v_i\right) + (1 - m_i)\left(w_j^{min} - v_i\right)\right)$$

$$\sigma(x) = 1/(1 - e^{-x})$$

Topic and Accessibility Criteria

- Probability of u_i interested in p_j based on topic:

$$a_{ij}^{topic} = cosine(\boldsymbol{y}_i, \boldsymbol{z}_j)$$

User topics Job topics

$\boldsymbol{y}_i$ and $\boldsymbol{z}_j$ are K-dimensional vectors.

- Probability of u_i noticing p_j:

$$a_{ij}^{access} = q_i \cdot r_j$$

User effort Job visibility

Learning the PLM Model

- Likelihood of application

$$\hat{a}_{ij} = a_{ij}^{salary} \cdot a_{ij}^{topic} \cdot a_{ij}^{access}$$

- Objective Function:

$$F(U, P, A) = \sum_{(u_i,p_j)\in D+} (A_{i,j} - \hat{a}_{i,j})^2 + \sum_{(u_i,p_j)\in D-} (A_{i,j} - \hat{a}_{i,j})^2$$

Probabilistic Labor Market (PLM) Model

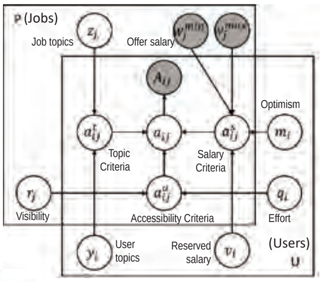

Experiments

- Evaluate PLM model against other models.
- Examine the user variables learned from data.
  - Reserved salary
  - Optimism
  - Effort
- Singapore Jobs Dataset (SJD):
  - # user: 33,866
  - # jobs: 68,091
  - # applications: 827,380

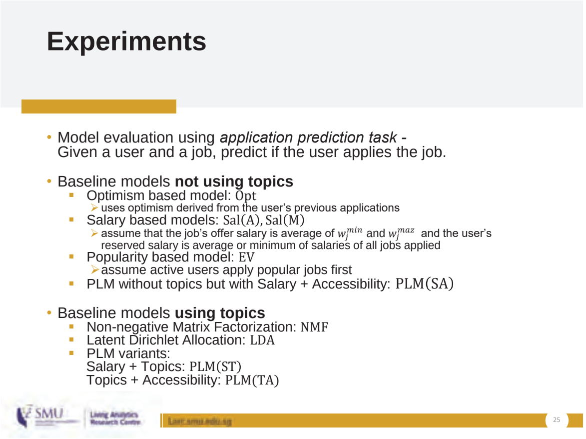

Experiments

- Model evaluation using *application prediction task* -
  Given a user and a job, predict if the user applies the job.

- Baseline models **not using topics**
  - Optimism based model: Opt
    - uses optimism derived from the user's previous applications
  - Salary based models: Sal(A), Sal(M)
    - assume that the job's offer salary is average of w_j^{min} and w_j^{max} and the user's reserved salary is average or minimum of salaries of all jobs applied
  - Popularity based model: EV
    - assume active users apply popular jobs first
  - PLM without topics but with Salary + Accessibility: PLM(SA)

- Baseline models **using topics**
  - Non-negative Matrix Factorization: NMF
  - Latent Dirichlet Allocation: LDA
  - PLM variants:
    Salary + Topics: PLM(ST)
    Topics + Accessibility: PLM(TA)

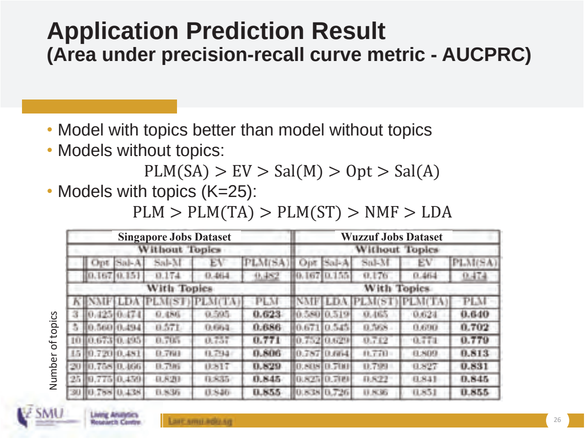

Application Prediction Result
(Area under precision-recall curve metric - AUCPRC)

- Model with topics better than model without topics
- Models without topics:
  $$\mathrm{PLM(SA)} > \mathrm{EV} > \mathrm{Sal(M)} > \mathrm{Opt} > \mathrm{Sal(A)}$$
- Models with topics (K=25):
  $$\mathrm{PLM} > \mathrm{PLM(TA)} > \mathrm{PLM(ST)} > \mathrm{NMF} > \mathrm{LDA}$$

	Singapore Jobs Dataset					Wuzzuf Jobs Dataset				
	Without Topics					Without Topics				
	Opt	Sal-A	Sal-M	EV	PLM(SA)	Opt	Sal-A	Sal-M	EV	PLM(SA)
	0.167	0.151	0.174	0.464	0.482	0.167	0.155	0.176	0.464	0.474
	With Topics					With Topics				
K	NMF	LDA	PLM(ST)	PLM(TA)	PLM	NMF	LDA	PLM(ST)	PLM(TA)	PLM
3	0.425	0.474	0.486	0.595	**0.623**	0.580	0.519	0.465	0.624	**0.640**
5	0.560	0.494	0.571	0.664	**0.686**	0.671	0.545	0.568	0.690	**0.702**
10	0.673	0.495	0.705	0.757	**0.771**	0.752	0.629	0.712	0.774	**0.779**
15	0.720	0.481	0.760	0.794	**0.806**	0.787	0.664	0.770	0.809	**0.813**
20	0.758	0.466	0.796	0.817	**0.829**	0.808	0.700	0.799	0.827	**0.831**
25	0.775	0.459	0.820	0.835	**0.845**	0.825	0.709	0.822	0.841	**0.845**
30	0.788	0.438	0.836	0.846	**0.855**	0.838	0.726	0.836	0.851	**0.855**

Number of topics

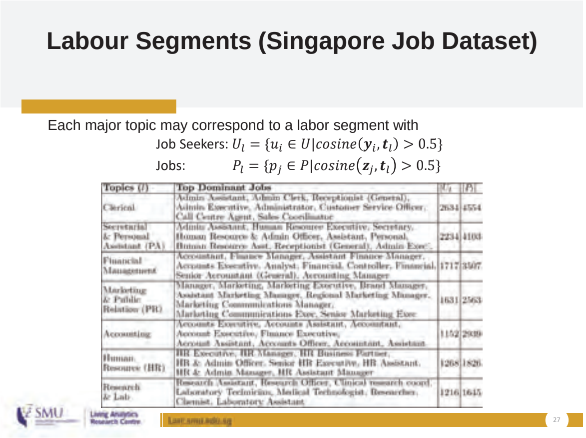

Labour Segments (Singapore Job Dataset)

Each major topic may correspond to a labor segment with

Job Seekers: $U_l = \{u_i \in U | cosine(\boldsymbol{y}_i, \boldsymbol{t}_l) > 0.5\}$

Jobs: $P_l = \{p_j \in P | cosine(\boldsymbol{z}_j, \boldsymbol{t}_l) > 0.5\}$

Topics (l)	Top Dominant Jobs	$\|U_l\|$	$\|P_l\|$
Clerical	Admin Assistant, Admin Clerk, Receptionist (General), Admin Executive, Administrator, Customer Service Officer, Call Centre Agent, Sales Coordinator	2634	4554
Secretarial & Personal Assistant (PA)	Admin Assistant, Human Resource Executive, Secretary, Human Resource & Admin Officer, Assistant, Personal, Human Resource Asst, Receptionist (General), Admin Exec.	2234	4103
Financial Management	Accountant, Finance Manager, Assistant Finance Manager, Accounts Executive, Analyst, Financial, Controller, Financial, Senior Accountant (General), Accounting Manager	1717	3507
Marketing & Public Relation (PR)	Manager, Marketing, Marketing Executive, Brand Manager, Assistant Marketing Manager, Regional Marketing Manager, Marketing Communications Manager, Marketing Communications Exec, Senior Marketing Exec	1631	2563
Accounting	Accounts Executive, Accounts Assistant, Accountant, Account Executive, Finance Executive, Account Assistant, Accounts Officer, Accountant, Assistant	1152	2939
Human Resource (HR)	HR Executive, HR Manager, HR Business Partner, HR & Admin Officer, Senior HR Executive, HR Assistant, HR & Admin Manager, HR Assistant Manager	1268	1826
Research & Lab	Research Assistant, Research Officer, Clinical research coord, Laboratory Technician, Medical Technologist, Researcher, Chemist, Laboratory Assistant	1216	1645

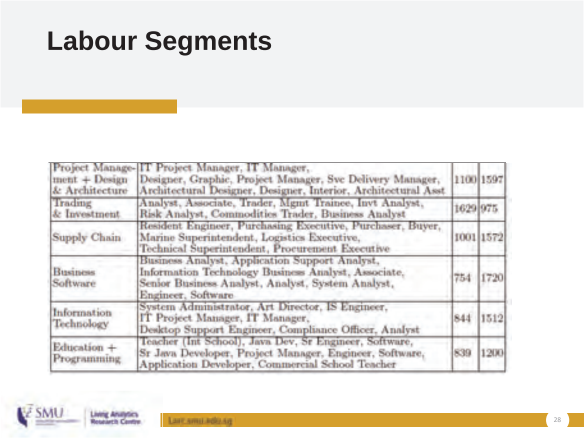

Labour Segments

Project Management + Design & Architecture	IT Project Manager, IT Manager, Designer, Graphic, Project Manager, Svc Delivery Manager, Architectural Designer, Designer, Interior, Architectural Asst	1100	1597
Trading & Investment	Analyst, Associate, Trader, Mgmt Trainee, Invt Analyst, Risk Analyst, Commodities Trader, Business Analyst	1629	975
Supply Chain	Resident Engineer, Purchasing Executive, Purchaser, Buyer, Marine Superintendent, Logistics Executive, Technical Superintendent, Procurement Executive	1001	1572
Business Software	Business Analyst, Application Support Analyst, Information Technology Business Analyst, Associate, Senior Business Analyst, Analyst, System Analyst, Engineer, Software	754	1720
Information Technology	System Administrator, Art Director, IS Engineer, IT Project Manager, IT Manager, Desktop Support Engineer, Compliance Officer, Analyst	844	1512
Education + Programming	Teacher (Int School), Java Dev, Sr Engineer, Software, Sr Java Developer, Project Manager, Engineer, Software, Application Developer, Commercial School Teacher	839	1200

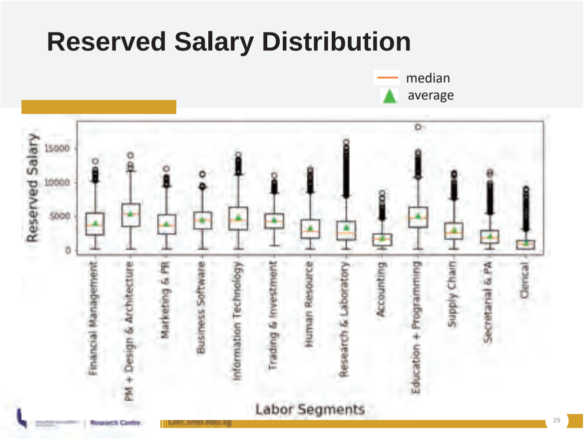

Reserved Salary Distribution

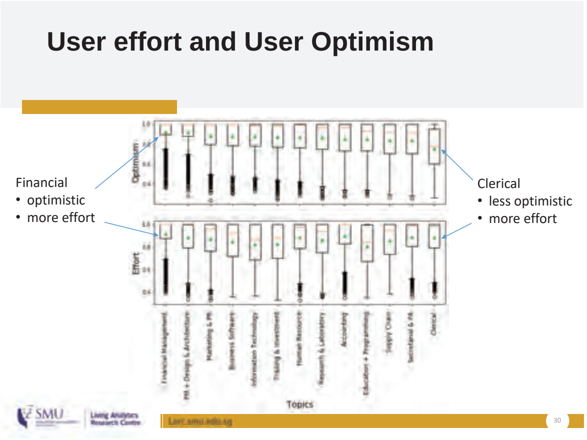

User effort and User Optimism

Financial
- optimistic
- more effort

Clerical
- less optimistic
- more effort

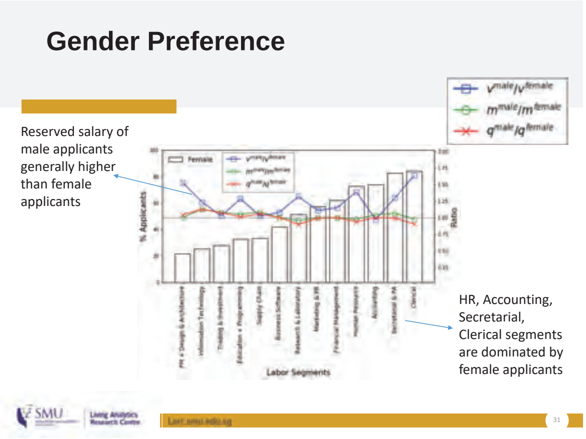

Gender Preference

Reserved salary of male applicants generally higher than female applicants

HR, Accounting, Secretarial, Clerical segments are dominated by female applicants

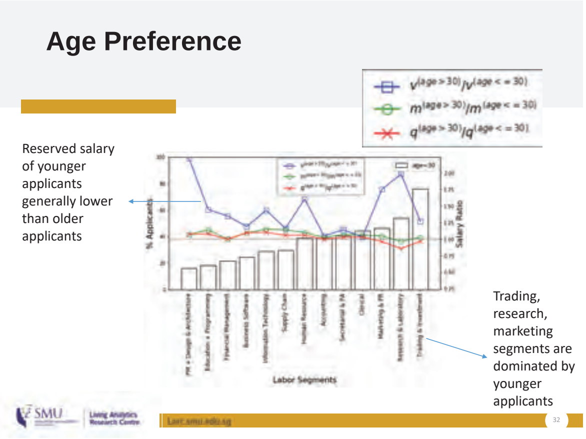

Age Preference

Reserved salary of younger applicants generally lower than older applicants

Trading, research, marketing segments are dominated by younger applicants

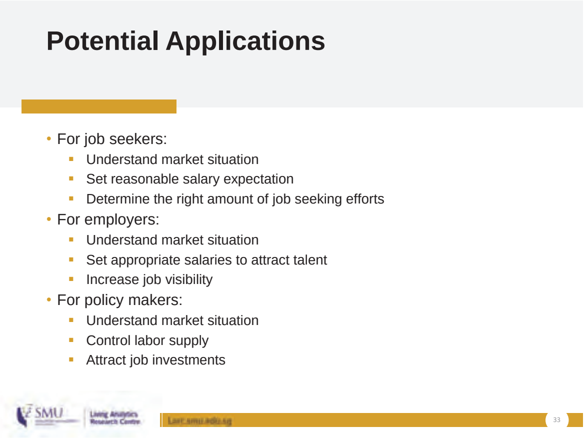

Potential Applications

- For job seekers:
  - Understand market situation
  - Set reasonable salary expectation
  - Determine the right amount of job seeking efforts
- For employers:
  - Understand market situation
  - Set appropriate salaries to attract talent
  - Increase job visibility
- For policy makers:
  - Understand market situation
  - Control labor supply
  - Attract job investments

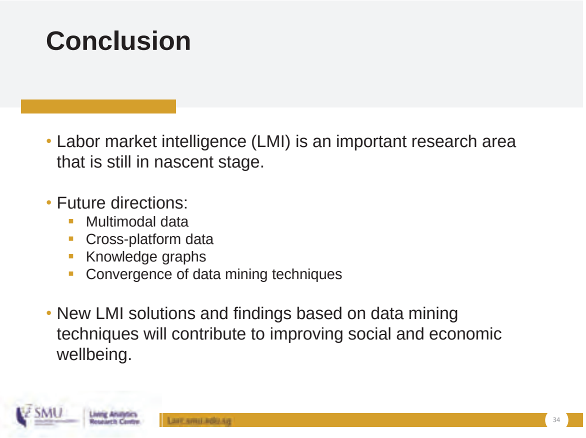

Conclusion

- Labor market intelligence (LMI) is an important research area that is still in nascent stage.
- Future directions:
  - Multimodal data
  - Cross-platform data
  - Knowledge graphs
  - Convergence of data mining techniques
- New LMI solutions and findings based on data mining techniques will contribute to improving social and economic wellbeing.

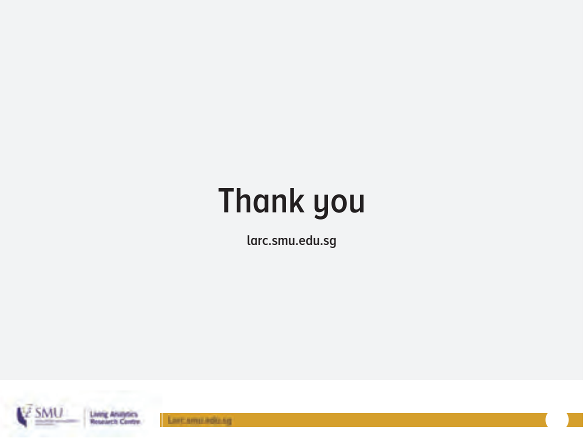

Thank you

larc.smu.edu.sg

Finite sample inference for generic autoregressive models

Hien Duy NGUYEN

School of Mathematics and Physics, University of Queensland, St. Lucia, Australia
Department of Mathematical and Physical Sciences, La Trobe University, Bundoora, Australia

Autoregressive models are a class of time series models that are important in both applied and theoretical statistics. Typically, inferential devices such as confidence sets and hypothesis tests for time series models require nuanced asymptotic arguments and constructions. We present a simple alternative to such arguments that allow for the construction of finite sample valid inferential devices, using a data splitting approach. We prove the validity of our constructions, as well as the validity of related sequential inference tools. A set of simulation studies are presented to demonstrate the applicability of our methodology.

1. INTRODUCTION

Let $(\Omega, \mathcal{F}, \Pr)$ be a probability space, and define a sequence of random variables $(X_t(\omega))_{t\in[T]}$ to be a time series, indexed by $t \in [T] = \{1, \dots, T\}$, where $X_t = X_t(\omega) \in \mathbb{X}$ for some space $\mathbb{X}$. We suppose that the time series $(X_t)_{t\in[T]}$ is order $p \in \mathbb{N}$ autoregressive and parametric, in the sense that for every $\mathbb{A} \subseteq \mathbb{X}^p$,

$$\Pr\Big(\omega : (X_t(\omega))_{t\in[p]} \in \mathbb{A}\Big) = \int_{\mathbb{A}} f(x_1, \dots, x_p; \theta_0)\, \mathrm{d}\boldsymbol{x}_{1\dots p},$$

and for each $\mathbb{B} \subseteq \mathbb{X}$ and $t > p$,

$$\Pr(\omega : X_t(\omega) \in \mathbb{B} | \mathcal{F}_{t-1}) = \int_{\mathbb{B}} f(x_t | \boldsymbol{x}_{t-p\dots t-1}; \theta_0)\, \mathrm{d}x_t.$$

Here, $\theta_0 \in \mathbb{T}$ is a parameter that characterizes the marginal and conditional probability density functions (PDFs)

$$f(x_1, \dots, x_p; \theta_0) \text{ and } f(x_t | \boldsymbol{x}_{t-p\dots t-1}; \theta_0), \text{ for each } t > p,$$

where $\boldsymbol{x}_{a\dots b} = (x_a, x_{a+1}, \dots, x_{b-1}, x_b)$, for $a, b \in \mathbb{N}$ such that $a < b$. The symbol $\mathcal{F}_t = \sigma(X_1, \dots, X_t)$ indicates the sigma algebra generated by the random variables $(X_i(\omega))_{i\in[t]}$. The characterization thus allows us to write the PDF of the time series $\boldsymbol{X}_T = (X_t)_{t\in[T]}$ as

$$f(\boldsymbol{x}_T; \theta_0) = f(x_1, \dots, x_p; \theta_0) \prod_{t=p+1}^{T} f(x_t | \boldsymbol{x}_{t-p\dots t-1}; \theta_0).$$

In this work, we concern ourselves with the problem of drawing inference about θ_0, given that we do not know its value. Specifically, we are concerned with the construction of $100\left(1-\alpha\right)\%$ confidence sets of the form $\mathscr{C}^{\alpha}\left(\boldsymbol{X}_T\right) \subseteq \mathbb{T}$, where

$$\Pr_{\theta_0}\left(\theta_0 \in \mathscr{C}^{\alpha}\left(\boldsymbol{X}_T\right)\right) \geq 1-\alpha,$$

for any $\alpha \in (0,1)$. Here, $\Pr_\theta$ indicates the probability measure under the assumption that the PDF of $\boldsymbol{X}_T$ has form $f\left(\boldsymbol{x}_T;\theta\right)$. We shall also denote the associated expectation operator by E_θ.

Furthermore, we are interested in testing hypotheses of the form

$$\mathrm{H}_0 : \theta_0 \in \mathbb{T}_0 \text{ versus } \mathrm{H}_1 : \theta_0 \in \mathbb{T}_1, \tag{1}$$

where $\mathbb{T}_0, \mathbb{T}_1 \subseteq \mathbb{T}$ and $\mathbb{T}_0 \cap \mathbb{T}_1 = \varnothing$. Here, we wish to construct valid P-values P_T, where

$$\sup_{\theta\in\mathbb{T}_0} \Pr_\theta\left(P_T \leq \alpha\right) \leq \alpha.$$

In order to construct our inference devices, we follow the work of [15], who considered the construction of finite sample valid confidence sets and hypotheses for independent and identically distributed data (IID), using a data splitting construction with generic estimators. Due to the lack of reliance on any estimator specific properties, the authors of [15] refer to their inference procedures as universal inference (UI).

The UI construction consists of demonstrating that a split data likelihood ratio construction is an E-value, in the sense of [14], and [8]; i.e., a positive random variable with expectation less than or equal to 1. The UI construction is extremely flexible and has been adapted for construction of inferential devices using composite likelihood ratios [11] and empirical Bayesian likelihoods [10]. We note that in the simple case of confidence sets for linear first order autoregressive models, our constructions can be compared to the finite sample results of [13] and [3, Sec. 4.1].

Besides our constructions of conventional confidence sets and P-values, using the same construction as that of [15], we also provide anytime valid confidence set and P-value sequences for sequential estimation from online data, in the spirit of [7]. We demonstrate the applicability of some of our constructions via numerical examples.

The paper proceeds as follows. In Section 2, we present our finite sample confidence set and P-value constructions, as well as their anytime valid counterparts. In Section 3, applications of some of our constructions are provided via numerical examples. Final remarks are then provided in Section 4.

2. Finite sample inference devices

Let us split $\boldsymbol{X}_T$ into two contiguous subsequences $\boldsymbol{X}_T^1 = \left(X_1,\dots,X_{T_1}\right)$ and $\boldsymbol{X}_T^2 = \left(X_{T_1+1},\dots,X_T\right)$, where $T_1 \geq p$. We shall also write $T_2 = T - T_1$. Further, let $\hat{\Theta}_T$ be a generic random estimator, such that

$$\hat{\Theta}_T = \hat{\theta}\left(\boldsymbol{X}_T^1\right),$$

for some function $\hat{\theta} : \mathbb{X}^{T_1} \to \mathbb{T}$, and define the likelihood ratio statistic

$$R_T(\theta) = \frac{L\left(\hat{\Theta}_T; \boldsymbol{X}_T\right)}{L(\theta; \boldsymbol{X}_T)},$$

where

$$L(\theta; \boldsymbol{X}_T) = \prod_{t=T_1+1}^{T} f(X_t | \boldsymbol{X}_{t-p\ldots t-1}; \theta)$$

is the conditional likelihood of $[\boldsymbol{X}_T^2 | \boldsymbol{X}_T^1]$.

Lemma 1. *For any* $\theta \in \mathbb{T}$, $\mathrm{E}_\theta [R_T(\theta)] \leq 1$.

Proof. Write $\tilde{\boldsymbol{X}}_{t-p\ldots t-1} = \left(\tilde{X}_{t-p}, \ldots, \tilde{X}_{t-1}\right)$, where $\tilde{X}_t = X_t$, if $t \leq T_1$, and $\tilde{X}_t = x_t$, otherwise. Then

$$\begin{aligned}
&\mathrm{E}_\theta [R_T(\theta)] \\
=&\mathrm{E}_\theta \mathrm{E}_\theta \left[R_T(\theta) | \boldsymbol{X}_T^1\right] \\
=&\mathrm{E}_\theta \int_{\mathbb{X}^{T_2}} \frac{\prod_{t=T_1+1}^{T} f\left(x_t | \tilde{\boldsymbol{X}}_{t-p\ldots t-1}; \hat{\Theta}_T\right)}{\prod_{t=T_1+1}^{T} f\left(x_t | \tilde{\boldsymbol{X}}_{t-p\ldots t-1}; \theta\right)} \prod_{t=T_1+1}^{T} f\left(x_t | \tilde{\boldsymbol{X}}_{t-p\ldots t-1}; \theta\right) \mathrm{d}\boldsymbol{x}_T^2 \\
=&\mathrm{E}_\theta \int_{\mathbb{X}^{T_2}} \prod_{t=T_1+1}^{T} f\left(x_t | \tilde{\boldsymbol{X}}_{t-p\ldots t-1}; \hat{\Theta}_T\right) \mathrm{d}\boldsymbol{x}_T^2 \\
\underset{\text{(i)}}{=}&\mathrm{E}_\theta \int_{\mathbb{X}} \cdots \int_{\mathbb{X}} f\left(x_T | \tilde{\boldsymbol{X}}_{T-p\ldots T-1}; \hat{\Theta}_T\right) \mathrm{d}x_T \cdots f\left(x_{T_1+1} | \tilde{\boldsymbol{X}}_{T_1-p+1\ldots T_1}; \hat{\Theta}_T\right) \mathrm{d}x_{T_1+1} \\
\underset{\text{(ii)}}{=}&\mathrm{E}_\theta 1 = 1,
\end{aligned}$$

where (i) is due to Tonelli's Theorem and (ii) is by definition of conditional PDFs. □

With Lemma 1 in hand, we can now construct $100(1-\alpha)\%$ confidence sets of the form

$$\mathscr{C}^\alpha(\boldsymbol{X}_T) = \{\theta : R_n(\theta) \leq 1/\alpha\}. \tag{2}$$

Proposition 1. *For any* $\alpha \in (0,1)$ *and* $\theta_0 \in \mathbb{T}$,

$$\mathrm{Pr}_{\theta_0}(\theta_0 \in \mathscr{C}^\alpha(\boldsymbol{X}_T)) \geq 1 - \alpha.$$

Proof. By Markov's inequality

$$\mathrm{Pr}_{\theta_0}(R_n(\theta_0) \geq 1/\alpha) \leq \alpha \mathrm{E}_{\theta_0}[R_n(\theta_0)] \underset{\text{(i)}}{=} \alpha,$$

where (i) is by Lemma 1. Then, we complete the proof by noting that

$$\begin{aligned}
\mathrm{Pr}_{\theta_0}(\theta_0 \in \mathscr{C}^\alpha(\boldsymbol{X}_T)) &= 1 - \mathrm{Pr}_{\theta_0}(R_n(\theta_0) \geq 1/\alpha) \\
&\geq 1 - \alpha.
\end{aligned}$$

□

To test hypotheses of form (1), we require an additional estimator

$$\tilde{\Theta}_T \in \left\{ \tilde{\theta} \in \mathbb{T} : L\left(\tilde{\theta}; \boldsymbol{X}_T\right) \geq L\left(\theta; \boldsymbol{X}_T\right), \text{ for all } \theta \in \mathbb{T} \right\}. \tag{3}$$

Then, we may construct the test statistic

$$S_T = R_T\left(\tilde{\Theta}_T\right)$$

and its P-value $P_T = 1/S_T$.

Proposition 2. *For any* $\alpha \in (0,1)$ *and* $\mathbb{T}_0 \subset \mathbb{T}$*,*

$$\sup_{\theta \in \mathbb{T}_0} \Pr_\theta\left(P_T \leq \alpha\right) \leq \alpha.$$

Proof. For each $\theta \in \mathbb{T}_0$, we have

$$\begin{aligned} \mathrm{E}_\theta\left[S_T\right] &= \mathrm{E}_\theta\left[\frac{L\left(\hat{\Theta}_T; \boldsymbol{X}_T\right)}{L\left(\tilde{\Theta}_T; \boldsymbol{X}_T\right)}\right] \\ &\underset{\text{(i)}}{\leq} \mathrm{E}_\theta\left[\frac{L\left(\hat{\Theta}_T; \boldsymbol{X}_T\right)}{L\left(\theta; \boldsymbol{X}_T\right)}\right] \\ &= \mathrm{E}_\theta\left[R_T\left(\theta\right)\right] \underset{\text{(ii)}}{=} 1, \end{aligned}$$

where (i) is by definition (3) and (ii) is due to Lemma 1. Finally, by Markov's inequality, we have

$$\Pr_\theta\left(S_T \geq 1/\alpha\right) \leq \alpha \implies \Pr_\theta\left(P_T \leq \alpha\right) \leq \alpha,$$

as required. ☐

2.1. **Anytime valid inference.**

Let

$$M_T\left(\theta\right) = \frac{\prod_{t=p+1}^{T} f\left(X_t | \boldsymbol{X}_{t-p \dots t-1}; \hat{\Theta}_{t-1}\right)}{\prod_{t=p+1}^{T} f\left(X_t | \boldsymbol{X}_{t-p \dots t-1}; \theta\right)},$$

for each $T \geq p+1$, and $M_T\left(\theta\right) = 1$, for each $T \leq p$. We firstly show that $\left(M_T\left(\theta\right)\right)_{T \in \mathbb{N} \cup \{0\}}$ is a martingale adapted to the natural filtration $\mathcal{F}_T = \sigma\left(X_1, \dots, X_T\right)$. Here, $\left(\hat{\Theta}_T\right)_{T \geq p+1}$ is a non-anticipatory sequence of estimators of θ_0, such that $\hat{\Theta}_T$ is dependent only on $\boldsymbol{X}_T$.

Lemma 2. *For each* $T \in \mathbb{N}$ *and* $\theta \in \mathbb{T}$*,* $E_\theta\left[M_T\left(\theta\right) | \mathcal{F}_{T-1}\right] = M_{T-1}\left(\theta\right)$*.*

Proof. For $T > p+1$,

$$\begin{aligned}
&\mathrm{E}_{\theta}\left[M_T\left(\theta\right)|\mathcal{F}_{T-1}\right] \\
=&\int_{\mathbb{X}} \frac{\prod_{t=p+1}^{T} f\left(\tilde{X}_t|\boldsymbol{X}_{t-p\ldots t-1};\hat{\Theta}_{t-1}\right)}{\prod_{t=p+1}^{T} f\left(\tilde{X}_t|\boldsymbol{X}_{t-p\ldots t-1};\theta\right)} f\left(x_T|\boldsymbol{X}_{T-p\ldots T-1}\right)\mathrm{d}x_T \\
=&\frac{\prod_{t=p+1}^{T-1} f\left(X_t|\boldsymbol{X}_{t-p\ldots t-1};\hat{\Theta}_{t-1}\right)}{\prod_{t=p+1}^{T-1} f\left(X_t|\boldsymbol{X}_{t-p\ldots t-1};\theta\right)} \int_{\mathbb{X}} f\left(x_T|\boldsymbol{X}_{T-p\ldots T-1};\hat{\Theta}_{T-1}\right)\mathrm{d}x_T \\
\underset{\text{(i)}}{=}&M_{T-1}\left(\theta\right).
\end{aligned}$$

where $\tilde{X}_T = x_T$ and $\tilde{X}_t = X_t$, for $t < T$. Here, (i) is due to the properties of conditional density functions. For $T \le p+1$, the result holds by definition. □

We now wish to test the hypotheses (1) in a sequential manner. To do so, we first require an additional sequence of parameter estimates $\left(\tilde{\Theta}_T\right)_{T\ge p+1}$, where

(4)
$$\tilde{\Theta}_T \in \left\{\tilde{\theta} \in \mathbb{T} : \prod_{t=p+1}^{T} f\left(X_t|\boldsymbol{X}_{t-p\ldots t-1};\tilde{\theta}\right) \ge \prod_{t=p+1}^{T} f\left(X_t|\boldsymbol{X}_{t-p\ldots t-1};\theta\right), \text{ for all } \theta \in \mathbb{T}\right\}.$$

Define

$$N_T = M_T\left(\tilde{\Theta}_T\right)$$

for $T \ge p+1$ and $N_T = 1$ for $T \le p$.

Proposition 3. *For each* $\alpha \in (0,1)$ *and* $\mathbb{T}_0 \subset \mathbb{T}$*,*

$$\sup_{\theta\in\mathbb{T}_0} \Pr_{\theta}\left(\sup_{T\ge 0} N_T \ge 1/\alpha\right) \le \alpha.$$

Proof. By Lemma 2, $\left(M_T\left(\theta\right)\right)_{T\in\mathbb{N}}$ is a Martingale, and hence by Lemma 3, we have

$$\Pr_{\theta}\left(\sup_{T\ge 0} M_T\left(\theta\right) \ge 1/\alpha\right) \le \alpha M_0\left(\theta\right) \le \alpha.$$

Note that for each T and $\theta \in \mathbb{T}_0$,

$$\begin{aligned}
N_T &= \frac{\prod_{t=p+1}^{T} f\left(X_t|\boldsymbol{X}_{t-p\ldots t-1};\hat{\Theta}_{t-1}\right)}{\prod_{t=p+1}^{T} f\left(X_t|\boldsymbol{X}_{t-p\ldots t-1};\tilde{\Theta}_T\right)} \\
&\underset{\text{(i)}}{\le} \frac{\prod_{t=p+1}^{T} f\left(X_t|\boldsymbol{X}_{t-p\ldots t-1};\hat{\Theta}_{t-1}\right)}{\prod_{t=p+1}^{T} f\left(X_t|\boldsymbol{X}_{t-p\ldots t-1};\theta\right)} \\
&= M_T\left(\theta\right),
\end{aligned}$$

where (i) is due to definition (4). Thus, for each $\theta \in \mathbb{T}_0$, we have

$$\Pr_\theta \left(\sup_{T \geq 0} N_T \geq 1/\alpha \right) \leq \Pr_\theta \left(\sup_{T \geq 0} M_T \left(\theta\right) \geq 1/\alpha \right) \leq \alpha.$$

□

We observe that if we define $\bar{P}_T = 1/N_T$, then the sequence $\left(\bar{P}_T\right)_{T \in \mathbb{N}}$ is also valid, in the sense that

$$\sup_{\theta \in \mathbb{T}_0} \Pr_\theta \left(\inf_{T \geq 0} \bar{P}_T \leq \alpha \right) \leq \alpha.$$

Now, we shall construct sequential confidence sets of the forms

$$\mathscr{D}_T^\alpha = \left\{ \theta \in \mathbb{T} : M_T \left(\theta\right) \leq 1/\alpha \right\}.$$

Proposition 4. *For any* $\alpha \in (0,1)$ *and* $\theta_0 \in \mathbb{T}$,

$$\Pr_{\theta_0} \left(\theta_0 \in \mathscr{D}_T^\alpha, \textit{ for all } T \in \mathbb{N} \right) \geq 1 - \alpha.$$

Proof. Note that $\left\{\theta_0 \in \mathscr{D}_T^\alpha\right\} = \left\{M_T\left(\theta_0\right) \leq 1/\alpha\right\}$ and so

$$\Pr_{\theta_0} \left(\theta_0 \in \mathscr{D}_T^\alpha, \text{ for all } T \in \mathbb{N} \right) = \Pr_{\theta_0} \left(\sup_{T \geq 0} M_T \left(\theta_0\right) \leq 1/\alpha \right) \underset{\text{(i)}}{\geq} 1 - \alpha,$$

where (i) is due to Lemmas 2 and 3. □

Observe that by definition we also have

$$\Pr_{\theta_0} \left(\theta_0 \in \bar{\mathscr{D}}_T^\alpha \right) \geq 1 - \alpha,$$

where $\bar{\mathscr{D}}_T^\alpha = \bigcap_{t=1}^T \mathscr{D}_T^\alpha$, for each $\alpha \in (0,1)$ and $T \in \mathbb{N}$.

3. NUMERICAL EXAMPLES

3.1. **Normal autoregressive model.** Let $\left(X_t\right)_{t \in \mathbb{Z}}$ be a random sequence defined as

$$X_t = \theta_0 X_{t-1} + E_t, \tag{5}$$

where $\left(E_t\right)_{t \in \mathbb{Z}}$ is an IID sequence, with $E_t \sim \mathrm{N}\left(0,1\right)$, for each $t \in \mathbb{Z}$. We shall construct a confidence interval for θ_0 using the finite sample (FS) procedure.

We take as data $\boldsymbol{X}_T$, and split the data into two halves $\boldsymbol{X}_T^1 = \left(X_1, \dots, X_{T_1}\right)$ and $\boldsymbol{X}_T^2 = \left(X_{T_1+1}, \dots, X_T\right)$, where $T_1 = T/2$ (assuming that T is even, for convenience). Let $\hat{\Theta}_T$ be an estimator of θ_0 depending only on $\boldsymbol{X}_T^1$. We use $\hat{\Theta}_T$ to construct the ratio

$$\begin{aligned} R_T\left(\theta\right) &= \frac{\prod_{t=T_1+1}^T f\left(X_t | \boldsymbol{X}_{t-p \dots t-1}; \hat{\Theta}_T\right)}{\prod_{t=T_1+1}^T f\left(X_t | \boldsymbol{X}_{t-p \dots t-1}; \theta\right)} \\ &= \frac{\prod_{t=T_1+1}^T \phi\left(X_t; \hat{\Theta}_T X_{t-1}, 1\right)}{\prod_{t=T_1+1}^T \phi\left(X_t; \theta X_{t-1}, 1\right)} \\ &= \exp\left\{ \frac{1}{2} \sum_{t=T_1+1}^T \left[\left(X_t - \hat{\Theta}_T X_{t-1}\right)^2 - \left(X_t - \theta X_{t-1}\right)^2 \right] \right\}, \end{aligned}$$

where

$$\phi\left(y;\mu,\sigma^2\right)=\left(2\pi\sigma^2\right)^{-1/2}\exp\left\{-\frac{1}{2}\frac{\left(y-\mu\right)^2}{\sigma^2}\right\},$$

is the normal density function with mean $\mu\in\mathbb{R}$ and variance $\sigma^2>0$.

Thus, by Proposition 1, we obtain $100\left(1-\alpha\right)\%$ confidence intervals (CIs) of form (2):

(6)

$$\mathscr{C}^{\alpha}\left(\boldsymbol{X}_T\right)=\left\{\theta\in\mathbb{R}:\frac{1}{2}\sum_{t=T_1+1}^{T}\left[\left(X_t-\hat{\Theta}_T X_{t-1}\right)^2-\left(X_t-\theta X_{t-1}\right)^2\right]\le\log\left(1/\alpha\right)\right\}.$$

Here, we can use the typical least squares (LS) estimator

$$\hat{\Theta}_T=\arg\min_{\theta\in\mathbb{R}}\sum_{t=2}^{T_1}\left(X_t-\theta X_{t-1}\right)^2=\frac{\sum_{t=2}^{T_1}X_{t-1}X_t}{\sum_{t=2}^{T_1}X_{t-1}^2}. \tag{7}$$

We can compare the performance of CIs of form (6) to the typical asymptotic normal CIs (cf. [2, Sec. 5.2]) for the LS estimator

$$\Theta_T^{\mathrm{LS}}=\frac{\sum_{t=2}^{T}X_{t-1}X_t}{\sum_{t=2}^{T}X_{t-1}^2}, \tag{8}$$

using the distributional limit

$$T^{1/2}\left(\Theta_T^{\mathrm{LS}}-\theta_0\right)\xrightarrow{\mathrm{d}}\mathrm{N}\left(0,1-\theta_0^2\right). \tag{9}$$

To assess the relative performance of the FS and LS CIs, we perform a small simulation study. We simulate $r=1000$ samples of size $T=100$ from model (5) with $\theta_0=0.5$ and construct 90% CIs. To compare the performances of the CIs, we compute coverage proportion (CP) (proportion of the r CIs of each type that contain θ_0) and the average length (AL) of the CIs.

We obtain the results $\mathrm{CP}_{\mathrm{FS}}=0.998$ and $\mathrm{CP}_{\mathrm{LS}}=0.895$, and $\mathrm{AL}_{\mathrm{FS}}=0.643$ and $\mathrm{AL}_{\mathrm{LS}}=0.286$. We thus observe that both the LS and FS CIs obtain the correct nominal level of confidence, although the FS CIs are conservative with respect to coverage. This conservativeness is also reflected in the lengths of the intervals, where the FS CIs over twice as long as the LS CIs. However, this is expected given that the FS CIs are constructed only by Markov's inequality application, whereas the LS CIs makes use of the information geometry of the normal distribution. Figure 1 provides a visualization of 20 pairs of FS and LS CIs from the simulation study. We observe that in many cases, the FS CIs provide useful inference regarding the presence of non-zero autocorrelation θ_0, even if the intervals can be larger than necessary.

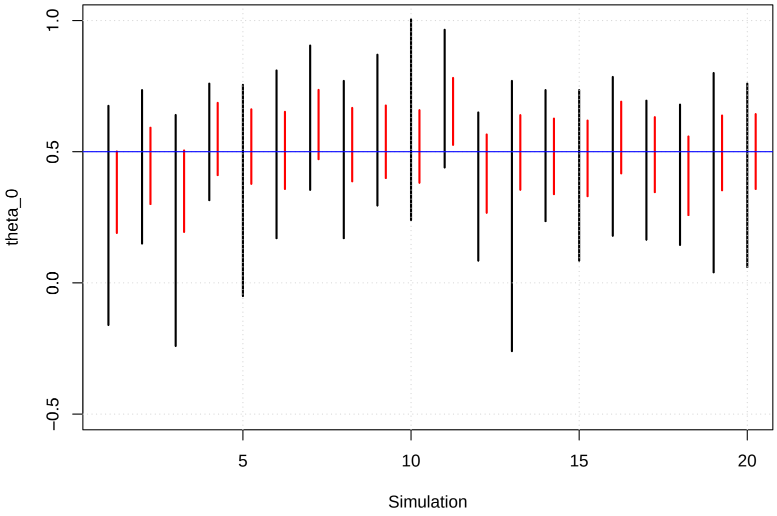

FIGURE 1. A visualization of 20 pairs of 90% CIs for $\theta_0 = 0.5$ in the normal autoregressive model. The FS CIs are colored black and LS CIs are colored red.

3.2. **Cauchy autoregressive model.** We now consider model (5) with $E_t \sim \text{Cauchy}\,(0,1)$, which implies that the ratio statistic has form

$$\begin{aligned} R_T(\theta) &= \frac{\prod_{t=T_1+1}^{T} f\left(X_t | \boldsymbol{X}_{t-p\ldots t-1}; \hat{\Theta}_T\right)}{\prod_{t=T_1+1}^{T} f\left(X_t | \boldsymbol{X}_{t-p\ldots t-1}; \theta\right)} \\ &= \frac{\prod_{t=T_1+1}^{T} \kappa\left(X_t - \hat{\Theta}_T X_{t-1}\right)}{\prod_{t=T_1+1}^{T} \kappa\left(X_t - \theta X_{t-1}\right)} \\ &= \prod_{T=T_1+1}^{T} \frac{1 + \left(X_t - \theta X_{t-1}\right)^2}{1 + \left(X_t - \hat{\Theta}_T X_{t-1}\right)^2}, \end{aligned}$$

where $\kappa(y) = \pi^{-1}\left\{1/\left(1+y^2\right)\right\}$ is the PDF of a the law $\text{Cauchy}\,(0,1)$. This implies a $100\,(1-\alpha)\,\%$ FS CI for θ_0 of the form

$$\mathscr{C}^{\alpha}\left(\boldsymbol{X}_T\right) = \left\{ \prod_{T=T_1+1}^{T} \frac{1 + \left(X_t - \theta X_{t-1}\right)^2}{1 + \left(X_t - \hat{\Theta}_T X_{t-1}\right)^2} \le \frac{1}{\alpha} \right\}.$$

We again use the LS estimator $\hat{\Theta}_T$ to construct the FS CI and compare our construction to the LS CI using the distributional limit (9) as an approximation, since

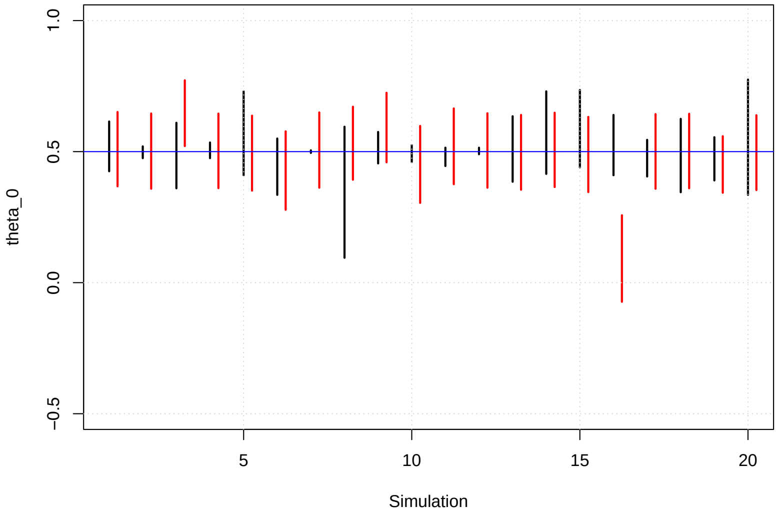

FIGURE 2. A visualization of 20 pairs of 90% CIs for $\theta_0 = 0.5$ in the Cauchy autoregressive model. The FS CIs are colored black and LS CIs are colored red.

the Cauchy model does not satisfy the required regularity conditions of [2, Sec. 5.2]. The comparison is made via the same simulation study as described in Section 3.1.

We obtain the results $\mathrm{CP}_{\mathrm{FS}} = 0.995$ and $\mathrm{CP}_{\mathrm{LS}} = 0.944$, and $\mathrm{AL}_{\mathrm{FS}} = 0.236$ and $\mathrm{AL}_{\mathrm{LS}} = 0.285$. We notice now that the LS CIs no longer achieve the nominal 90% confidence level, and are now also conservative, although not as conservative as the FS CIs. Interestingly, even though the FS CIs are more conservative, they are on average shorter than the LS CIs. We observe this via Figure 2, which visualizes 20 pairs of FS and LS CIs from the simulation study.

4. UNIT ROOT TEST

We assume again Model (5), with $E_t \sim \mathrm{N}(0,1)$. However, we now wish to test the hypotheses

$$\mathrm{H}_0 : \theta_0 = 1 \text{ versus } \mathrm{H}_1 : \theta_0 \in (-1,1)\,. \tag{10}$$

This is the classical normal unit root test setting of [4], which is usually tested using the LS estimator (8) as the test statistic.

Under the null hypothesis, it is known that the LS estimator has a non-normal asymptotic distribution that is highly irregular and requires numerical integration or simulation in order to approximate its quantiles and density (see, e.g., [1, 5, 12]).

TABLE 1. Unit root test results at the $\alpha = 0.1$ level of significance.

θ_0	FS	Asymptotic
0.00	1.000	1.000
0.50	1.000	1.000
0.90	0.990	1.000
0.95	0.904	1.000
1.00	0.005	0.106

However, to perform our FS test, we can simply construct the test statistic

$$S_T = R_T(1) = \exp\left\{\frac{1}{2}\sum_{t=T_1+1}^{T}\left[\left(X_t - \hat{\Theta}_T X_{t-1}\right)^2 - \left(X_t - X_{t-1}\right)^2\right]\right\}, \tag{11}$$

where we use (7) for $\hat{\Theta}_T$. By Proposition 2, $P_T = 1/S_T$ is a P-value, satisfying $\Pr_{\theta_0=1}(P_T \le \alpha) \le \alpha$.

We can assess the performance of the FS test based on statistic (11) versus the usual test, based on (8), using the quantiles provided in [1, Tab. 1]. We simulate $r = 1000$ samples of size $T = 1000$ and test (10) with $\theta_0 \in \{0, 0.5, 0.9, 0.09, 1\}$. We then compare the asymptotic test to the FS test on the basis of proportion of rejection (PR) out of the r samples at the $\alpha = 0.1$ level of significance. Our results are presented in Table 1.

From Table 1, we observe that the FS test is more conservative than the asymptotic test, as to be expected from the previous results, along with the Markov's inequality construction. However, the test does not require knowledge of any special distribution, and can more easily implemented, as a tradeoff.

5. FINAL REMARKS

Remark 1. The anytime valid inference results of Propositions 3 and 4 can be stated in terms of stopping times of the test and confidence event sequences. This can be achieved via [6, Lem. 3].

Remark 2. It is noteworthy that the process of splitting the data may be somewhat arbitrary. However, one alleviate the need of making a choice by averaging over the results of choices of splits. That is, let $(T_{1,i})_{i\in[n]}$ be a sequence of n values $T_{1,i} \in \{p+1, \dots, T-1\}$, for each $i \in [n]$, and let $\left(\hat{\Theta}_{T,i}\right)_{i\in[n]}$ be a sequence of estimators, where $\hat{\Theta}_{T,i}$ depends only on the data $(X_t)_{t\in[T_{1,i}]}$. Then, the averaged ratio statistic

$$\bar{R}_T(\theta) = \frac{1}{n}\sum_{i=1}^{n}\frac{\prod_{t=T_{1,i}}^{T} f\left(X_t|\boldsymbol{X}_{t-p\dots t-1}; \hat{\Theta}_{T,i}\right)}{\prod_{t=T_{1,i}}^{T} f\left(X_t|\boldsymbol{X}_{t-p\dots t-1}; \theta\right)}$$

is an E-value, in the sense that $\mathrm{E}_\theta\left[\bar{R}_T(\theta)\right] \le 1$. Corresponding versions of Propositions 1 and 2 then follow.

Here, a choice must still be made regarding the n valued sequence $(T_{1,i})_{i\in[n]}$. However, one can make all possible choices, in the sense of taking $(T_{1,i})_{i\in[n]} = (p+1, \dots, T-1)$.

Then, we would have a ratio statistic in the form

$$\bar{R}_T(\theta) = \frac{1}{T-p-1} \sum_{i=p+1}^{T-1} \frac{\prod_{t=i}^{T} f\left(X_t | \boldsymbol{X}_{t-p\ldots t-1}; \hat{\Theta}_{T,i}\right)}{\prod_{t=i}^{T} f\left(X_t | \boldsymbol{X}_{t-p\ldots t-1}; \theta\right)},$$

where $\left(\hat{\Theta}_{T,i}\right)_{i\in\{p+1,\ldots,T-1\}}$ is a sequence of estimators with $\hat{\Theta}_i$ depending only on $(X_t)_{t\in[i]}$, for each $i \in \{p+1,\ldots,T-1\}$. This statistic is also an E-value and requires no user input regarding the choice of split. However, it is a much more expensive statistic than $R_T(\theta)$, since it requires $T-p-1$ estimators to be computed, whereas $R_T(\theta)$ requires only one. The user must thus make a tradeoff between computation and user input.

Since the average of E-values is an E-value, the same discussion can be made regarding the choice of estimator $\hat{\Theta}_T$. One can choose different estimators $\hat{\Theta}_T$ and average over the $R_T(\theta)$ statistics corresponding to each estimator in order to produce a new statistic that remains an E-value.

Remark 3. Our text focuses on ratio statistics $R_T(\theta)$ that are constructed using conditional likelihood objects $L(\theta; \boldsymbol{X}_T)$. However, we may replace the conditional likelihoods with conditional composite likelihoods or conditional integrated likelihoods, in the manner of [11] and [10], respectively. This can be useful in situations where the likelihoods $L(\theta; \boldsymbol{X}_T)$ are intractable or difficult to compute.

Appendix

The following result is often called Ville's Lemma and a proof can be found in [9, Thm. 3.9].

Lemma 3. *Let* $(Y_T)_{T\in\mathbb{N}\cup\{0\}}$ *be a non-negative supermartingale, then, for each* $\alpha > 0$,

$$\Pr\left(\sup_{T\geq 0} Y_T \geq 1/\alpha\right) \leq \alpha \mathrm{E}[Y_0].$$

References

[1] K M Abadir. The limiting distribution of the autocorrelation coefficient under a unit root. *Annals of Statistics*, 21:1058–1070, 1993.

[2] T Amemiya. *Advanced Econometrics.* Harvard University Press, Cambridge, 1985.

[3] B Bercu, B Delyon, and E Rio. *Concentration Inequalities for Sums and Martingales.* Springer, Cham, 2015.

[4] D A Dickey and W A Fuller. Distribution of the estimator for autoregressive time series with a unit root. *Journal of the American Statistical Association*, 74:427–431, 1979.

[5] G B A Evans and N E Savin. Testing for unit roots: 1. *Econometrica*, 49:753–779, 1981.

[6] S R Howard, A Ramdas, J McAuliffe, and J Sekhon. Time-uniform, nonparametric, nonasymptotic confidence sequences. *Annals of Statistics*, 49:1055–1080, 2021.

[7] R Johari, P Koomen, L Pekelis, and D Walsh. Peeking at A/B tests. In *Proceedings of KDD*, pages 1517–1525, 2017.

[8] W M Koolen and P Grunwald. Log-optimal anytime-valid E-values. *International Journal of Approximate Reasoning*, to appear, 2021.

[9] T Lattimore and C Szepesvari. *Bandit Algorithms.* Cambridge University Press, Cambridge, 2020.

[10] H Nguyen and M Gupta. Finite sample inference for empirical Bayesian methods. Technical Report hal-03363121, HAL, 2021.

[11] H D Nguyen, J Bagnall-Guerreiro, and A T Jones. Universal inference with composite likelihoods. In *Proceedings of the 63rd ISI World Statistics Congress*. International Statistical Institute, 2021.

[12] M M Rao. Asymptotic distribution of an estimator of the boundary parameter of an unstable process. *Annals of Statistics*, 6:185–190, 1978.

[13] V Vovk. Strong confidence intervals for autoregression. *ArXiv*, (arXiv:0707.0660v1), 2007.

[14] V Vovk and R Wang. E-values: calibration, combination, and application. *Annals of Statistics*, 49:1736–1754, 2021.

[15] L Wasserman, A Ramdas, and S Balakrishnan. Universal inference. *Proceedings of the National Academy of Sciences*, 117:16880–16890, 2020.

Inversion Analysis for Medical Imaging

Yu Jiang

School of Mathematics, Shanghai University of Finance and Economics, China

Inversion analysis for medical imaging is one of the important fields in the field of inverse problem research. The main purpose of solving this kind of inverse problem is to reconstruct the information that can be used for disease diagnosis from the information obtained from medical images. This talk will mainly cover the latest progress of some medical imaging technologies, such as magnetic resonance elastography, optical tomography related inversion analysis technologies.

Inversion Analysis for Medical Imaging

Yu Jiang
Shanghai University of Finance and Economics
FMfI 2021

Joint work with Gen Nakamura (Hokkaido University)
& Kenji Shirota (Aichi Prefectural University)

Magnetic Resonance Elastography, MRE

- MRI + elastography
- measure the **viscoelasticity** of human tissue
  (Muthupillai et al., *Science*, 269, 1854-1857, 1995.)

⇒ enable us to virtually realize a doctor's palpation

- Diagnosis:
  - the stage of liver fibrosis
  - early stage cancer: breast cancer, pancreatic cancer, prostate cancer, etc.
  - neurological diseases: Alzheimer's disease, hydrocephalus, multiple sclerosis, etc.
- Aid of surgery, postoperative observation, evaluation of treatment
- Nondestructive testing: biological material, polymer material

---

MRE measurements: phase image

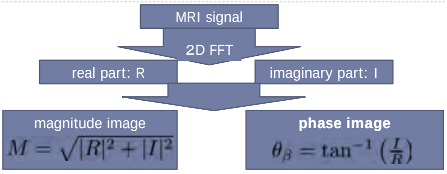

MRI signal

2D FFT

real part: R

imaginary part: I

magnitude image

$M = \sqrt{|R|^2 + |I|^2}$

phase image

$\theta_\beta = \tan^{-1}\left(\frac{I}{R}\right)$

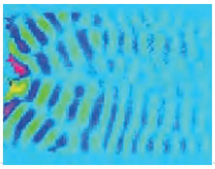

Two types of data analysis (inversion)

- Model independent data analysis

  i.e. Don't need to model tissues, but just assume that the waves are superposition of sinusoidal waves with attenuation
  - Local frequency estimate (LFE, Mayo Clinic)
  - LWV/LAV method (Nakamura-Yoshikawa)
    - Computational and Mathematical Methods in Medicine, 2013, 912920
- Model dependent data analysis

  i.e. Need to model tissues (Jiang – Nakamura, SIAM J. APPL. MATH. 71(6), 2011, 1965–1989)
  - Modified Integral Method (Jiang - Nakamura)
    - Journal of Physics: Conference Series 290, 2011, 012006
  - Least square method (regularization scheme)
  - **Newton type regularization scheme** (Jiang – Nakamura-Shirota)
    - J. Inverse Ill-Posed Probl. 2019; Inverse Problems 2021

Scalar model

- Isotropic incompressible stationary scalar model:

$$\begin{cases} \nabla \cdot [2(\mu + i(2\pi f)\eta)\nabla u] + \rho(2\pi f)^2 u = 0. \\ + \text{boundary conditions} \end{cases}$$

- μ: storage modulus (elastic); η: loss modulus (viscosity)
  ρ: density, f: frequency of external vibration;
- Here, we assumed:

$$\begin{cases} \nabla \cdot \mathbf{u} = 0, \\ \mu(x), \eta(x) \in C^1(\overline{\Omega}); \quad \nabla\mu \cdot \frac{\partial \mathbf{u}}{\partial x_i} = 0, \\ \nabla\eta \cdot \frac{\partial \mathbf{u}}{\partial x_i} = 0 \quad (1 \le i \le 3) \end{cases}$$

Modified Stokes model

- Isotropic+ nearly incompressible

$$\nu = 0.49999..., \ \lambda \ (\text{GPa}) \gg \mu \ (\text{kPa})$$

- Modified Stokes model:

$$\begin{cases} \nabla \cdot [2(\mu + i(2\pi f)\eta)\varepsilon(\mathbf{u})] - \nabla p + \rho(2\pi f)^2 \mathbf{u} = 0, \\ \nabla \cdot \mathbf{u} = 0, \\ + \text{boundary conditions} \end{cases}$$

  - For $\mu, \eta \in L^\infty$ ➔ $(\mathbf{u}, p) \in H^1 \times L^2$
  - Jiang, et. Al., SIAM J. Appl. Math. 71, pp. 1965-1989
  - H. Ammari, Quar. Appl. Math., 2008: isotopic constant elasticity

Modified Stokes model

- 2D numerical simulation (Freefem++)
  - Plane strain assumption

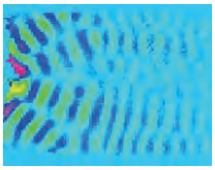

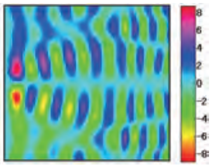

Ux_real

Inverse Problem of MRE

$$\begin{cases} \nabla\cdot[2(\mu+i(2\pi f)\eta)\varepsilon(\mathbf{u})]-\nabla p+\rho(2\pi f)^2\mathbf{u}=0, \\ \nabla\cdot\mathbf{u}=0, \\ +\text{ boundary conditions} \end{cases}$$

- By knowing $\mathbf{u}\in\Omega$
  ➔μ: storage modulus (elastic); η: loss modulus (viscosity)?

Curl operator

- Modified Stokes model (soft tissues: nearly incompressible, isotropic media):

$$\begin{cases} \nabla\cdot[2(\mu+i(2\pi f)\eta)\varepsilon(\mathbf{u})]-\nabla p+\rho(2\pi f)^2\mathbf{u}=0, \\ \nabla\cdot\mathbf{u}=0, \\ +\text{ boundary conditions} \end{cases}$$

- Locally homogeneous (constants):

Curl operator: filter of the pressure term (longitudinal wave)

$$\mathbf{w}=\nabla\times\mathbf{u}$$

$$(\mu+i(2\pi f)\eta)\Delta\mathbf{w}+\rho(2\pi f)^2\mathbf{w}=0$$

Numerical differentiation

- $(\mu+i(2\pi f)\eta)\Delta\mathbf{w}+\rho(2\pi f)^2\mathbf{w}=0$
- $\mu+i(2\pi f)\eta=\dfrac{\rho(2\pi f)^2\mathbf{w}}{\Delta\mathbf{w}}$ (point wisely)
- $\Delta\mathbf{w}=0$ at some point $x\in\Omega$
- Numerical differentiation is ill-posed or unstable!!!
- MRE data: high noise level, ~10%

Lest square problem

- Lest square problem:

$$\min(\|\mathbf{u}(A)-\mathbf{u}^{obs}\|_2+\alpha G(A))$$

$$A=\mu+i(2\pi f)\eta$$

- Iterative method:
- Landweber iteration scheme (Ammari et al.)
- Newton type regularization scheme: Levenberg–Marquardt method (Jiang-Nakamura-Shirota, Inverse Problems (2021))

$$\begin{cases} \nabla\cdot[2(\mu+i(2\pi f)\eta)\varepsilon(\mathbf{u})]-\nabla p+\rho(2\pi f)^2\mathbf{u}=0, \\ \nabla\cdot\mathbf{u}=0, \\ +\text{ boundary conditions} \end{cases}$$

Levenberg-Marquardt method

- Iterative scheme: $u=F(A)$

$$A_{k+1}^\delta=A_k^\delta+\left(F'(A_k^\delta)^*F'(A_k^\delta)+\alpha_k I\right)^{-1}F'(A_k^\delta)^*\left(u^\delta-F(A_k^\delta)\right),\quad k\in\mathbb{Z}_+:=\{0\}\cup\mathbb{N}.$$

- $u^\delta=u^{obs}\in H^1(\Omega;\mathbb{C}^d),\ X:=H^2(\Omega;\mathbb{C}),\ Y:=H^1(\Omega;\mathbb{C}^d)$ For $\mu,\eta\in L^\infty$➔ $(\mathbf{u},p)\in H^1\times L^2$
- $D(F):=\{A=\mu+i\eta : A\in H^2(\Omega;\mathbb{C}), 0<\check{\mu}<\mu<\hat{\mu}, 0<\check{\eta}<\eta<\hat{\eta}\}$
- $F'(A_k^\delta)$: Fréchet derivative

- Satisfies the **tangential cone condition**

$$\|F(\tilde{A})-F(A)-F'(A)(\tilde{A}-A)\|_{H^1(\Omega;\mathbb{C}^d)}\leqslant c\|\tilde{A}-A\|_{H^2(\Omega;\mathbb{C})}\|F(\tilde{A})-F(A)\|_{H^1(\Omega;\mathbb{C}^d)}$$

- Converge to a solution if have a “good” initial guess close to the true value

Implement LM-method numerically

- FreeFEM++ (version 4.9)
- $P := D(F) \subset H^2(\Omega;\mathbb{C}), Y = H^1(\Omega;\mathbb{C}^d)$ and $Q := L^2(\Omega;\mathbb{C})/\mathbb{C}$,
- (u,p) : Hood-Taylor element P2-P1/P3-P2
- $A \in H^2(\Omega;\mathbb{C})$: Hsieh-Clough-Tocher (HCT) element, C1-class
- in FEM space

$$(\alpha I + F'(A_k)^* F'(A_k))\delta A_{k,\alpha} = F'(A_k)^*(u^\delta - F(A_k))$$

$$((\alpha I + F'(A_k)^* F'(A_k))\delta A^h_{k,\alpha}, \phi_h)_{H^2(\Omega;\mathbb{C})} = (F'(A_k)^*(u^\delta - F(A_k)), \phi_h)_{H^2(\Omega;\mathbb{C})}$$

$$\alpha(\delta A^h_{k,\alpha}, \phi_h)_{H^2(\Omega;\mathbb{C})} + (F'(A_k)\delta A^h_{k,\alpha}, F'(A_k)\phi_h)_{H^1(\Omega;\mathbb{C}^d)} = (u^\delta - F(A_k), F'(A_k)\phi_h)_{H^1(\Omega;\mathbb{C}^d)}$$

- linear system

$$(\alpha \boldsymbol{M} + \boldsymbol{F}'_k)\delta \boldsymbol{A}_\alpha = \boldsymbol{b}_k .$$

$$\begin{aligned} \boldsymbol{M} &= \left((\phi_i, \phi_j)_{H^2(\Omega;\mathbb{C})}\right)_{i,j=1,\dots,N} \in \mathbb{R}^{N\times N}, \\ \boldsymbol{F}'_k &= \left((F'(A_k)\phi_i, F'(A_k)\phi_j)_{H^1(\Omega;\mathbb{C}^d)}\right)_{i,j=1,\dots,N} \in \mathbb{C}^{N\times N} \\ \boldsymbol{b}_k &= \left((u^\delta - F(A_k), F'(A_k)\phi_i)_{H^1(\Omega;\mathbb{C}^d)}\right)_{i=1,\dots,N} \in \mathbb{C}^N . \end{aligned}$$

Numerical test (smooth function)

Need to assume $\mu, \eta \in H^2$

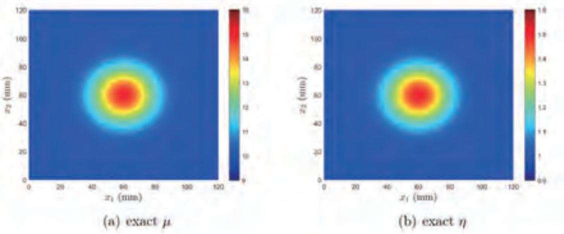

(a) exact μ (b) exact η

$\mu = 10 + 5e^{-\frac{(x-x_0)^2}{2\sigma^2}}$ (kPa), $\eta = 1 + 0.5e^{-\frac{(x-x_0)^2}{2\sigma^2}}$ (kPa),

Numerical test (smooth function, 62.5 **Hz**)

- 6% relative noise (H1 sense)

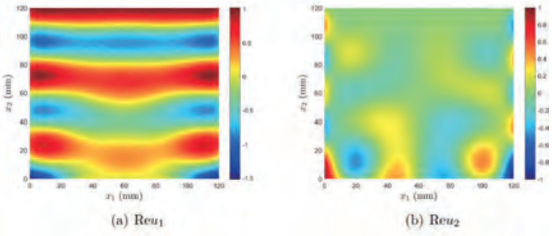

(a) Reu_1 (b) Reu_2

Numerical test (smooth function, 62.5 **Hz**)

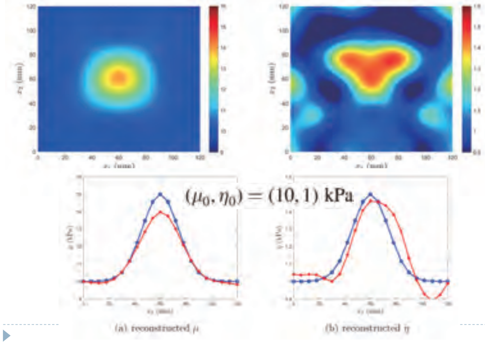

(a) reconstructed μ (b) reconstructed η

Numerical test (smooth function, 125 **Hz**)

- 6% relative noise (H1 sense)

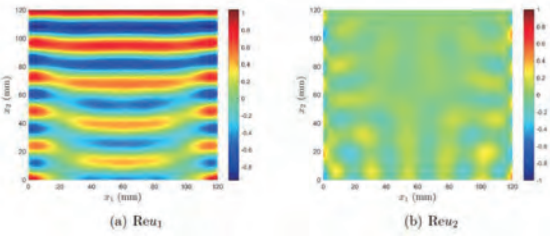

(a) Reu_1 (b) Reu_2

Numerical test (smooth function, 125**Hz**)

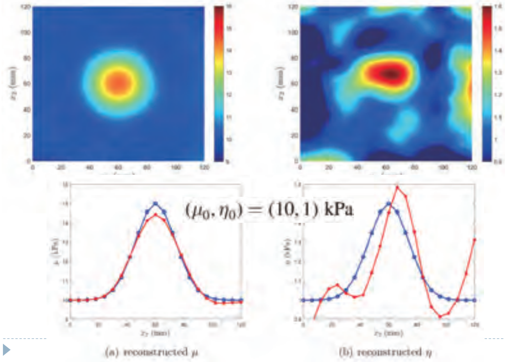

(a) reconstructed μ (b) reconstructed η

Conclusion and future works

- A Newton type regularization scheme to reconstruct $\mu, \eta \in H^2$;

- Need to reconstruct $\mu, \eta \in L^\infty$;
- How to have a good reconstruction of η;
- Real data test.

Thank you for your attention.

A simple mathematical model on spread of Covid-19 with the effect of vaccination and its application to Japan

Takashi Tsuchiya

National Graduate Institute for Policy Studies, Tokyo, Japan

The spread of Covid-19 causes serious damages to Japanese society since 2020. However, the number of new cases is decreasing drastically with the progress of vaccination reaching 70% to 80% in ratio as of November 2021. In this talk, a simple mathematical model is presented to describe the spread of Covid-19 used to predict the number of day-by-day new cases in Tokyo taking the effect of vaccination into account. The dynamics of infection are described with a simplified version of SIR model, where the period of infection of a patient is assumed to be a constant instead of obeying to an exponential distribution in SIR model. Another feature is it takes account of potential spreaders without symptom. The model works fairly well in spite of its simplicity.

In Japan, the timing of the next (sixth) wave of Covid-19 is of great public interest. We discuss the possibility of herd immunity relying on vaccination, and predict the future based on the model and data.

A mathematical model for COVID-19 transmission dynamics with a case study of Myanmar

Aung Zaw Myint

Department of Mathematics, University of Mandalay, Myanmar

We propose a compartmental mathematical model to predict and control the transmission dynamic of COVID-19 disease in Myanmar. We compute the basic reproduction number threshold. We perform local and global stability analysis for infection equilibrium in terms of basic reproduction number, and we conduct a sensitivity analysis in our corona-virus model to determine the relative importance of model parameters to epidemic transmission. Moreover, numerical simulation demonstrates that the disease transmission rate more than effective to mitigate the basic reproduction number.

Some Applications of Mathematics in Medical Works

Jessada TANTHANUCH

School of Mathematics, Institute of Science, Suranaree University of Technology, Thailand

Mathematics, often called the "Queen of the Sciences", is one of the basic sciences. However, this major role of the basic science is able to apply to many medical works. This presentation shows the applications of mathematics research to biomedical engineering applications. The overall concepts of some research by School of Mathematics and School of Biomedical Innovation Engineering, Suranaree University of Technology, Nakhon Ratchasima, Thailand, are given. The research works are the modelling of knee shape, the modelling of the blood flow to heart, the modelling to predict the patients' postoperative WOMAC score after total knee replacement, the applications of support vector machine, twin parametric support vector machine for the medical image classification problems, the development of image processing technique to enhance quality of ultrasound and x-ray images and teeth classification, and the case study of using 3D printing in the preoperative planning for the surgery.

REFERENCES

[1] Thongking, W., Mitsomwang, P., Sindhupakorn, B., Tanthanuch, J. (2022) Analysis and Classification of Abnormal Vertebral Column by Convolutional Neural Network Algorithm., **Suranaree Journal of Social Science.**, Vol 16., No. 1., (January-June 2022)., in press.

[2] Nerysungnoen, B., Chatwongwan, W., Nuengkota, P., Puntanakun, S. and Tanthanuch, J. (2020), The Application of Using 3D Printing for Operation Planning in Maharat Nakhon Ratchasima Hospital: Case report of Changing Mandibular Bone, **Journal of Medicine and Health Science**, Vol 27 No. 3: December 2020., pp 166-178. (in Thai)
https://he01.tci-thaijo.org/index.php/jmhs/article/download/246846/167503/

[3] Tanthanuch, J., Kaptsov, E.I., Meleshko, S.V. (2021) Equation of Rayleigh Noise Reduction Model for Medical Ultrasound Imaging: Symmetry Classification, Conservation Laws and Invariant Solutions., **Journal of Vibration Testing and System Dynamics,** Vol 5 Issue 3, September 2021, pp. 237-247.

[4] Tanthanuch, J., Kaptsov, E.I. and Meleshko, S.V. (2019) Equation of Rayleigh Noise Reduction Model for Medical Ultrasound Imaging: Symmetry Classification and Conservation Laws in Cylindrical Coordinates, **AIP Conference Proceedings**. Vol. 2153, Issue 1, 020022 (2019):
https://doi.org/10.1063/1.5125087

Engineered algorithms for large-scale single-cell RNA sequencing and multimodal data analysis

Stefan Canzar

Gene Center, Ludwig Maximilian University of Munich, Germany

Experimental methods for sequencing DNA or RNA of single cells have transformed biological and medical research. The throughput of this technology has dramatically increased over the last few years, such that today the expression of genes in millions of cells can be measured in a single experiment. The computational interpretation of the produced data, however, often exceeds the capacity of existing algorithms. We have therefore developed method Sphetcher, an efficient algorithm that computes a much smaller set of cells that represent the transcriptional space of the original data as accurately as possible. Sphetcher can compute such a so-called sketch of millions of cells in minutes and facilitates the identification of rare cell types.

Single-cell sequencing in addition allows to reconstruct trajectories that describe dynamic changes in gene expression that occur during the differentiation of cells. We have developed method Trajan that allows to compare such trajectories of, e.g., differentiating immune cells that are involved in the response to an infection.

In algorithm Specter we combine measurements of multiple types of molecules to refine cell types. We showed that Specter is able to resolve subtle transcriptomic differences between subpopulations of memory T cells based on their combined expression of mRNAs and surface proteins. For the joint visualization of such modalities, we extended t-SNE and UMAP, the most popular methods for the visualization of biomedical data.

Mathematical modelling for COVID-19 in the Victorian Public Service

Michael Lydeamore

Department of Econometrics and Business Statistics, Monash University, Australia

(joint work with COVID-19 Modelling and Analytics team, Government of Victoria)

The COVID-19 pandemic has put infectious diseases modelling in the spotlight. Many institutes and governments globally have very suddenly had a desire and need for accurate modelling and analytics on a rapidly evolving situation. During 2020, I was seconded to the Victorian Department of Health, and formed a modelling and analytics team that regularly provided situational reporting, analysis and policy relevant advice to high level decision makers and ministers.

I will discuss three pieces of work that were influential at very different stages of the Victorian COVID-19 experience. The first was a model that was created in a time of little knowledge, but was inclusive of many operational details that normally would not be considered in model construction. This model was used in numerous decisions, including Victoria's PPE planning and hospital equipment procurement.

The second model contains much more detail, including age and complex contact patterns, and was used to inform the gradual easing of restrictions before Victoria's second wave including school and workplace re-opening.

The final piece of work is a data visualisation dashboard known as the "Mystery Case Tracker". This tool brings together infection timelines, contact patterns and geographical coding into a dashboard utilised by the outbreak team to rapidly understand and classify places of risk.

As well as the pieces of work, I'll discuss how analytics and modelling are broadly thought of in these settings, and how approaching issues with an analytics mindset can be helpful in solving problems rapidly.

Modelling COVID-19 on a bipartite contact network of 5 million individuals for the Elimination Strategy in Aotearoa New Zealand

Emily Harvey

M.E. Research & Te Pūnaha Matatini, New Zealand

(joint work with James Gilmour - Department of Physics, University of Auckland,

Oliver MacLaren - Department of Engineering Science, University of Auckland, Dion O ' Neale - Department of Physics, University of Auckland & Te Pūnaha Matatini, Frankie Patten-Elliott - Department of Physics, University of Auckland & Te Pūnaha Matatini, Steven Turnbull - Department of Physics, University of Auckland & Te Pūnaha Matatini, David Wu - Department of Engineering Science, University of Auckland)

Many of the models used for rapid policy advice during the COVID-19 pandemic rely on simplifying assumptions about the homogeneity of populations and the impact of non-pharmaceutical interventions on transmission. In the context of an elimination strategy, with small case numbers, such approximations become increasingly poor representations of reality. We have built a stochastic model of infection dynamics that runs on an empirically-derived, bipartite contact network that explicitly represents each of the 5 million people in Aotearoa NZ. This model includes mechanistic representation of testing, contact tracing, and isolation processes, as well as targeted 'Alert Level' changes. The model has been used to inform government responses to SARS-CoV-2 outbreaks in Aotearoa NZ during 2020 and 2021. We find that the heterogeneity and network structure in our model leads to qualitatively different behaviour, compared with a "well-mixed" model, in a number of scenarios. We highlight some key differences between this model and such well-mixed ODE and branching process models.

Modelling COVID-19 on a bipartite contact network of 5 million individuals

for the *Elimination Strategy* in Aotearoa NZ

Presenter: ***Emily Harvey*** emily@me.co.nz

Team: ***Dion O'Neale***, Oliver Maclaren, James Gilmour, Joshua Looker, Frankie Patten-Elliott, Joel Trent, Steven Turnbull, David Wu & others

Te Pūnaha Matatini
Data • Knowledge • Insight

m.e research

Questions

- *How many* people will get infected, and *when*?
- *Who* will get infected?
- What will happen to the people who get infected?
- *Where*/*how* will people get infected? (What factors drive infection risk?)
- What capacity levels will be needed in test-trace-isolate and in the health system to meet assumed levels of performance?

Te Pūnaha Matatini
Data • Knowledge • Insight

Traditional Epidemic Models

Susceptible → Exposed → Infectious → Recovered

- **Assumes a well-mixed, homogeneous, population**

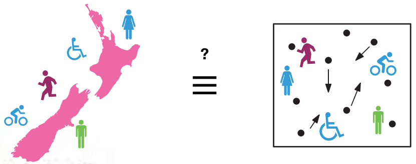

Te Pūnaha Matatini
Data • Knowledge • Insight

Building an Interaction Network

- Explicitly represent each individual along with individual level attributes
- Heterogeneous interaction structure → **contagion spreads on an explicit contact network for the whole of Aotearoa NZ**

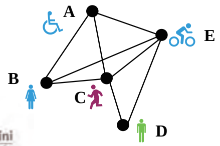

Susceptible
↓
Infectious
↓
Recovered

Te Pūnaha Matatini
Data • Knowledge • Insight

Bipartite Network Model

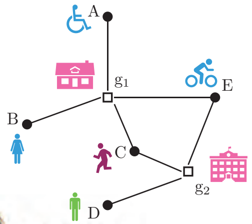

Explicitly represents:

● individuals

☐ groups (interactions)

- Network interactions are through *groups* or *contexts* - the places interaction occurs
- We build the network in *layers* for each type of 'group' from empirical data sources

Te Pūnaha Matatini
Data • Knowledge • Insight

Why bipartite networks ?

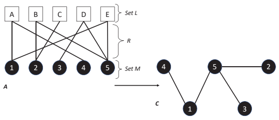

To represent a school with 1000 students we need:

- 1000 + 1 nodes & 1000 links for a bipartite representation

or

- 1000 nodes & 1000 x 999 links for a one-mode representation

Te Pūnaha Matatini
Data • Knowledge • Insight

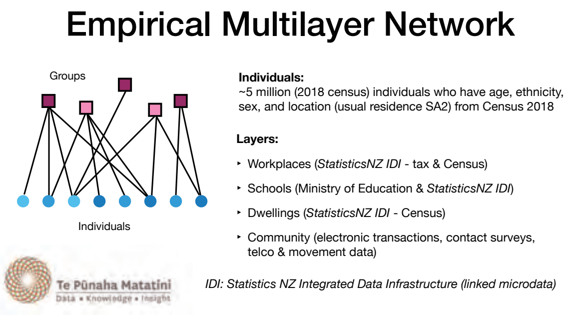

Empirical Multilayer Network

Individuals:
~5 million (2018 census) individuals who have age, ethnicity, sex, and location (usual residence SA2) from Census 2018

Layers:

- Workplaces (*StatisticsNZ IDI* - tax & Census)
- Schools (Ministry of Education & *StatisticsNZ IDI*)
- Dwellings (*StatisticsNZ IDI* - Census)
- Community (electronic transactions, contact surveys, telco & movement data)

IDI: Statistics NZ Integrated Data Infrastructure (linked microdata)

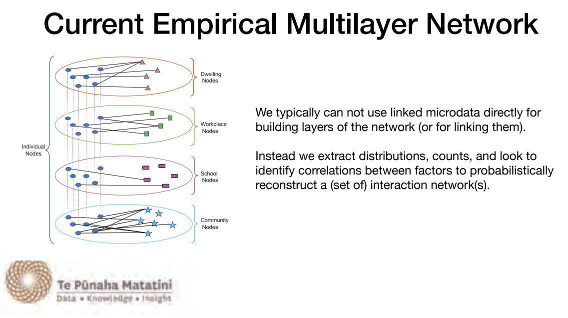

Current Empirical Multilayer Network

We typically can not use linked microdata directly for building layers of the network (or for linking them).

Instead we extract distributions, counts, and look to identify correlations between factors to probabilistically reconstruct a (set of) interaction network(s).

Adding a contagion process

- We use a modified Gillespie algorithm (hence Markovian) with extensions to allow for non-Markovian dynamics including scheduled (delayed) processes, and algorithmic speed ups.
- Contagion spread is stochastic with explicit representations of contact tracing, testing and quarantine/isolation processes (which is where we use the delayed processes).
- For more info contact Oliver Maclaren oliver.maclaren@auckland.ac.nz

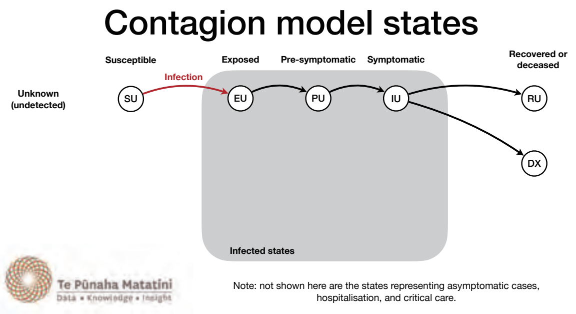

Contagion model states

Note: not shown here are the states representing asymptomatic cases, hospitalisation, and critical care.

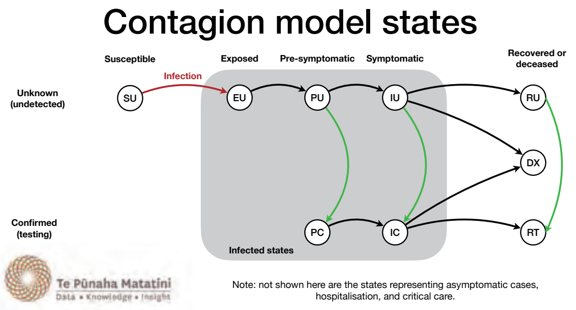

Contagion model states

Note: not shown here are the states representing asymptomatic cases, hospitalisation, and critical care.

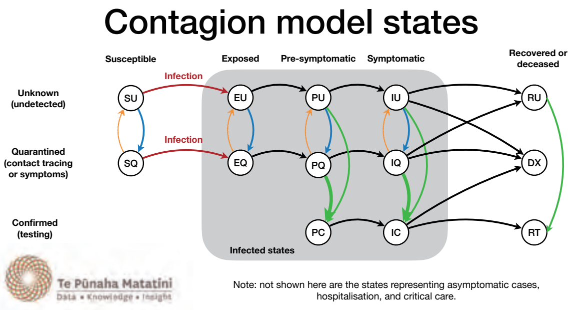

Contagion model states

Note: not shown here are the states representing asymptomatic cases, hospitalisation, and critical care.

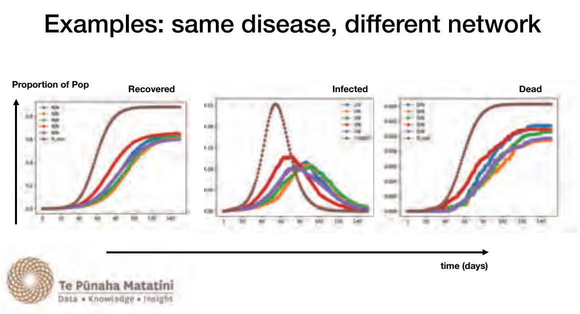

Examples: same disease, different network

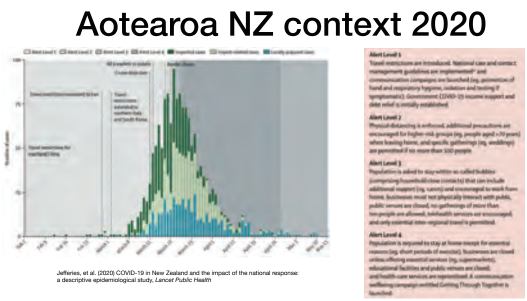

Aotearoa NZ context 2020

Jefferies, et al. (2020) COVID-19 in New Zealand and the impact of the national response: a descriptive epidemiological study, *Lancet Public Health*

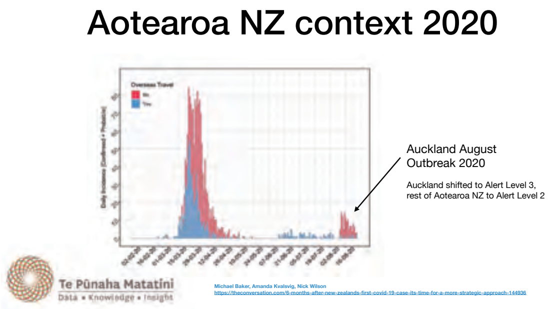

Aotearoa NZ context 2020

Auckland August Outbreak 2020

Auckland shifted to Alert Level 3, rest of Aotearoa NZ to Alert Level 2

Michael Baker, Amanda Kvalsvig, Nick Wilson
https://theconversation.com/6-months-after-new-zealands-first-covid-19-case-its-time-for-a-more-strategic-approach-144936

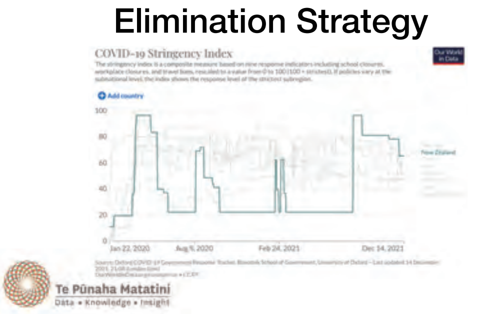

Elimination Strategy

COVID-19 Stringency Index

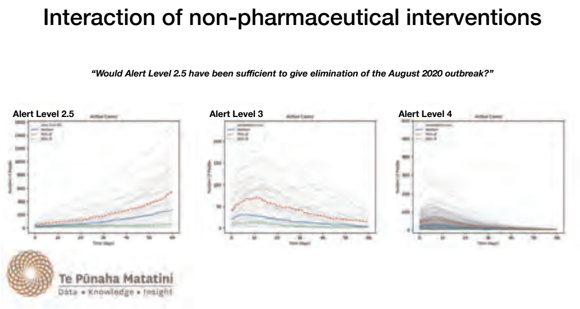

Interaction of non-pharmaceutical interventions

"Would Alert Level 2.5 have been sufficient to give elimination of the August 2020 outbreak?"

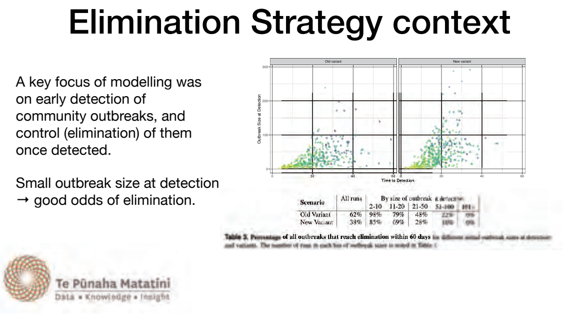

Elimination Strategy context

A key focus of modelling was on early detection of community outbreaks, and control (elimination) of them once detected.

Small outbreak size at detection → good odds of elimination.

Scenario	All runs	By size of outbreak at detection				
		2-10	11-20	21-50	51-100	101+
Old Variant	62%	98%	79%	48%	22%	0%
New Variant	38%	85%	69%	28%	10%	0%

Table 3. Percentage of all outbreaks that reach elimination within 60 days for different initial outbreak sizes at detection and variants. The number of runs in each bin of outbreak sizes is noted in Table 1.

Impact of delays (applying AL3)

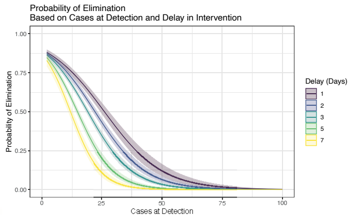

Interaction of increased transmissibility variants: Alpha

Alert Level 3
baseline transmissibility

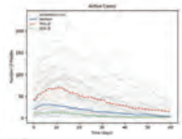

Alert Level 3
50% increased transmissibility

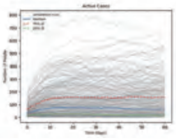

Alert Level 4
50% increased transmission

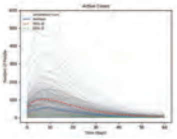

Interaction of increased transmissibility variants: Alpha

- The observed growth rate (R_{eff}) at different Alert Levels does not scale linearly with transmissibility of different variants

Alert Level 3
baseline transmissibility

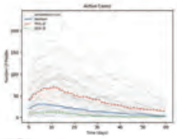

Alert Level 3
50% increased transmission

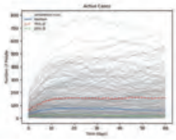

Alert Level 4
50% increased transmission

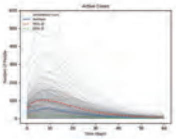

August 2021 (Delta outbreak)

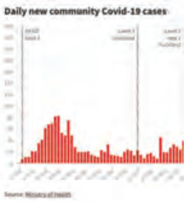

Farah Hancock, Data journalist, RadioNZ

August 2021 (Delta outbreak)

Farah Hancock, Data journalist, RadioNZ

August 2021 (Delta outbreak)

Branching process model

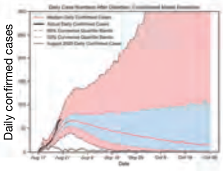

Network model

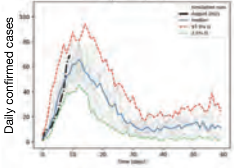

August 2021 (Delta outbreak)

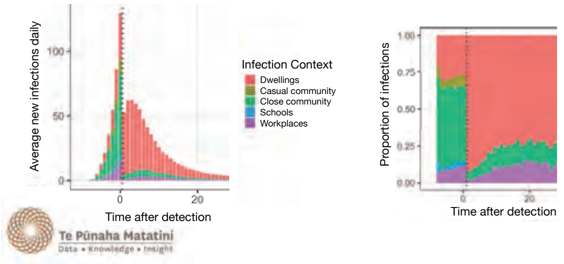

August 2021 (Delta outbreak)

Adjusting ‘control’ level *C(t)* in Branching process model

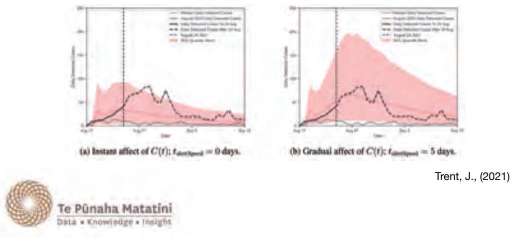

Trent, J., (2021)

Effect of relaxing Alert Levels: Delta, September 2021

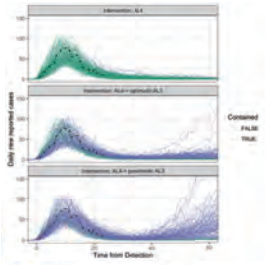

Effect of relaxing Alert Levels: Delta, September 2021

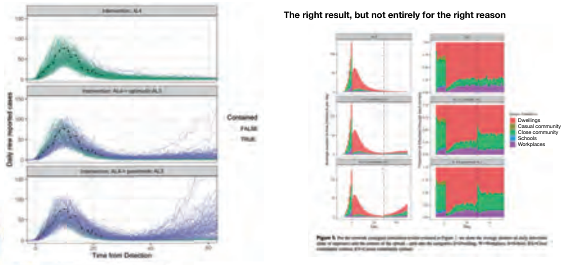

The right result, but not entirely for the right reason

Effect of opening schools: Delta, November 2021

Interactions matter most when they make the contact network more connected

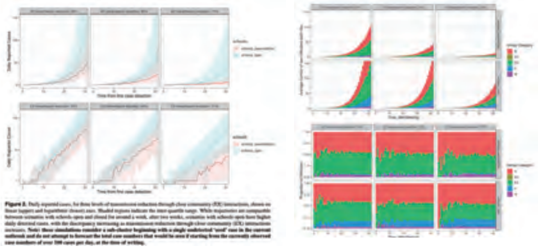

Workplace heterogeneity (Alert Level intervention)

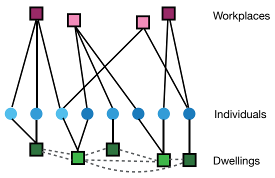

Workplace heterogeneity (Alert Level intervention)

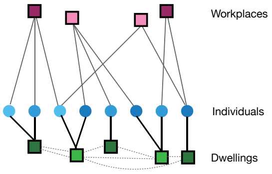

50% reduction in transmission within workplaces

Workplace heterogeneity (Alert Level intervention)

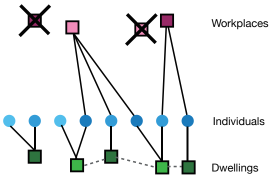

50% of workplaces are closed (not working on site)

Workplace heterogeneity (Alert Level intervention)

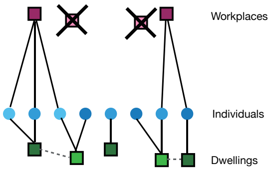

50% of workplaces are closed (not working on site)

Workplace heterogeneity (Alert Level intervention)

All workplaces open, but have transmission reduction measures that lead to an 85% reduction in transmission (equivalent in the average sense)

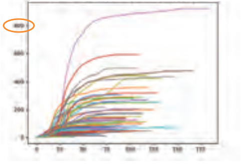

Elimination

76% of workplaces are closed (Alert Level 4), remaining ones have transmission reduction measures that lead to a 37.5% reduction in transmission

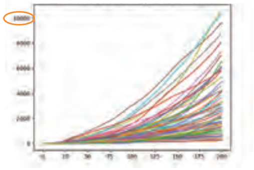

No Elimination

Workplace heterogeneity (Alert Level intervention)

Heterogeneous workplace closure conceptual diagram

Original contact network

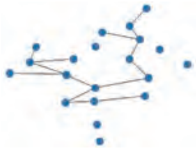

50% edge removal

Where else might this have an effect

- Vaccination clustering *Age (eligibility) and/or Attitudes*
- Ability to stay home from work if symptomatic

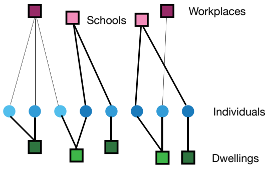

Effect of interventions and heterogeneity

The effect (and effectiveness) of interventions depends on what other interventions are applied and on the specifics of the infection tree:

- The effect of contact tracing (e.g. on reduction in R_{eff}) depends on the Alert Level status, the level of testing, the *time to detection* and other features of the infection tree
- The effect of an increase in transmissibility of the virus on R_{eff} depends on the network structure and number and 'riskiness' of contacts
- Effectiveness of Alert Level changes and other interventions depend on *who* is infected in the initial outbreak

Heterogeneity plays a large role.

Te Pūnaha Matatini
Data • Knowledge • Insight

Thank you for listening

And thanks to TPM, MBIE, DPMC, & HRC for funding.

Te Pūnaha Matatini
Data • Knowledge • Insight

m.e research

SEIR network models for Coronavirus disease (COVID-19) in Vietnam

Doanh Nguyen-Ngoc

UMMISCO & ACROSS, IRD/France and Thuyloi University, Vietnam

(joint work with Alexis Drogoul, UMMISCO, IRD/France and in collaboration with other colleagues)

In this talk, we will introduce some SEIR network models incorporating different spatial scales from province, district and ward levels to cell level to explore the spread of different waves of Coronavirus disease (COVID-19) in Vietnam and to support the Rapid Response Team, Vietnam National Committee Against Covid-19.

Mathematical model based prediction and application to COVID-19

Shingo Iwami

Division of Biological Science, Graduate School of Science, Nagoya University, Japan

If it becomes possible to capture the nonlinear dynamics behind phenomena with a mathematical model and its numerical analysis, it will be possible to predict the future which might be limited. For example, when applied to medical data, it can be expected to evaluate and predict treatment effects and prognosis with high accuracy. In this talk, I will present an example of how the development of a mathematical model that explains clinical data of COVID-19 patients has essentially made it possible to propose treatments and design clinical trials based on predictions.

Securing Vaccine Delivery Against Physical Threats

Mai Anh Tien

School of Computing and Information Systems, Singapore Management University, Singapore
(joint work with Arunesh Sinha, School of Computing and Information Systems, Singapore Management University)

Vaccine delivery in under-resourced locations with security risks is not just logistically challenging but also life threatening. The current COVID pandemic spread and the need to vaccinate has added even more urgency to this issue. In this paper, we propose a framework to plan vaccination drives that balance physical security and desired vaccination coverage with limited resources. We set up the problem as a Stackelberg game between a defender and adversary, where the set of vaccine centers is not fixed a priori. This results in a mixed combinatorial and continuous optimization problem. As part of solving this problem, we provide a novel contribution by identifying general duality conditions of switching max and min when discrete variables are involved. We perform experiments to show effects of various parameters on the problem and show that the solution proposed is scalable in practice.

Towards Minimax Optimal Best Arm Identification In Linear Bandits

Vincent Y. F. Tan

National University of Singapore, Singapore
(joint work with Junwen Yang, National University of Singapore)

We study the problem of best arm identification in linear bandits in the fixed-budget setting. By leveraging properties of the G-optimal design and incorporating it into the arm allocation rule, we design a parameter-free algorithm, Optimal Design-based Linear Best Arm Identification (OD-LinBAI). We provide a theoretical analysis of the failure probability of OD-LinBAI. While the performances of existing methods (e.g., BayesGap) depend on all the optimality gaps, OD-LinBAI depends on the gaps of the top d arms, where d is the effective dimension of the linear bandit instance. Furthermore, we present a minimax lower bound for this problem. The upper and lower bounds show that OD-LinBAI is minimax optimal up to multiplicative factors in the exponent. Finally, numerical experiments corroborate our theoretical findings.

Towards Minimax Optimal Best Arm Identification in Linear Bandits

Junwen Yang, **Vincent Tan**

National University of Singapore

December 10, 2021

Outline

1. Problem setup and preliminaries
2. Algorithm
3. Main results
4. Numerical experiments

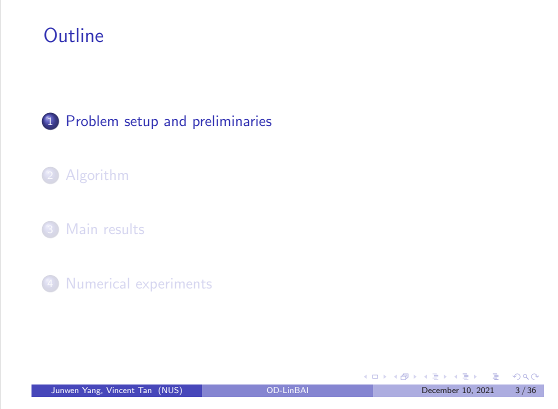

Outline

1. Problem setup and preliminaries
2. Algorithm
3. Main results
4. Numerical experiments

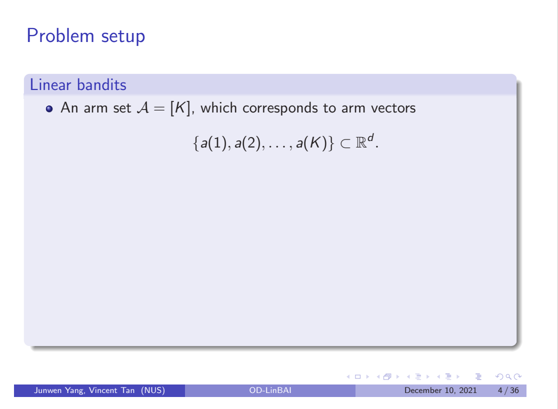

Problem setup

Linear bandits

- An arm set $\mathcal{A} = [K]$, which corresponds to arm vectors

$$\{a(1), a(2), \dots, a(K)\} \subset \mathbb{R}^d.$$

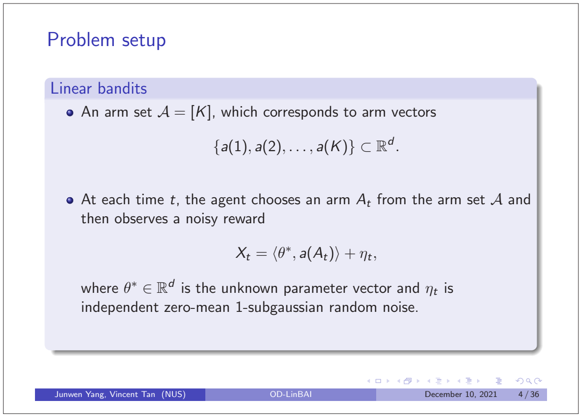

Problem setup

Linear bandits

- An arm set $\mathcal{A} = [K]$, which corresponds to arm vectors

$$\{a(1), a(2), \dots, a(K)\} \subset \mathbb{R}^d.$$

- At each time t, the agent chooses an arm A_t from the arm set $\mathcal{A}$ and then observes a noisy reward

$$X_t = \langle \theta^*, a(A_t) \rangle + \eta_t,$$

where $\theta^* \in \mathbb{R}^d$ is the unknown parameter vector and η_t is independent zero-mean 1-subgaussian random noise.

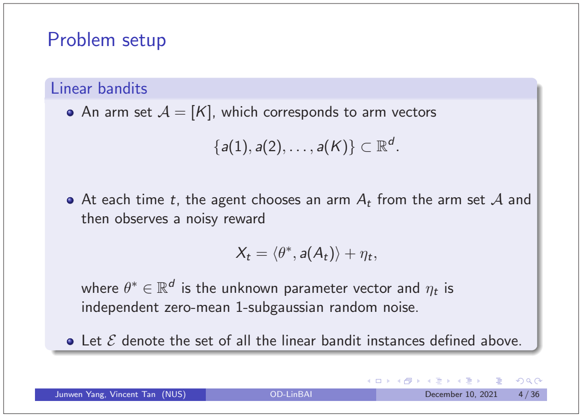

Problem setup

Linear bandits

- An arm set $\mathcal{A} = [K]$, which corresponds to arm vectors

$$\{a(1), a(2), \dots, a(K)\} \subset \mathbb{R}^d.$$

- At each time t, the agent chooses an arm A_t from the arm set $\mathcal{A}$ and then observes a noisy reward

$$X_t = \langle \theta^*, a(A_t) \rangle + \eta_t,$$

where $\theta^* \in \mathbb{R}^d$ is the unknown parameter vector and η_t is independent zero-mean 1-subgaussian random noise.

- Let $\mathcal{E}$ denote the set of all the linear bandit instances defined above.

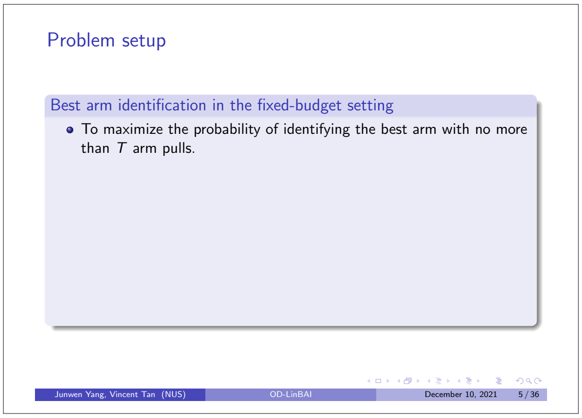

Problem setup

Best arm identification in the fixed-budget setting

- To maximize the probability of identifying the best arm with no more than T arm pulls.

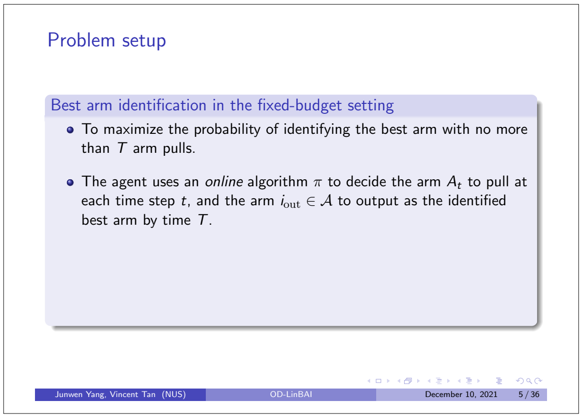

Problem setup

Best arm identification in the fixed-budget setting

- To maximize the probability of identifying the best arm with no more than T arm pulls.
- The agent uses an *online* algorithm π to decide the arm A_t to pull at each time step t, and the arm $i_{\text{out}} \in \mathcal{A}$ to output as the identified best arm by time T.

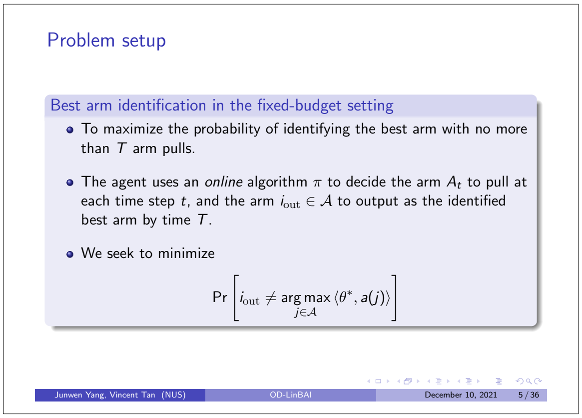

Problem setup

Best arm identification in the fixed-budget setting

- To maximize the probability of identifying the best arm with no more than T arm pulls.
- The agent uses an *online* algorithm π to decide the arm A_t to pull at each time step t, and the arm $i_{\text{out}} \in \mathcal{A}$ to output as the identified best arm by time T.
- We seek to minimize

$$\Pr\left[i_{\text{out}} \neq \arg\max_{j \in \mathcal{A}} \langle \theta^*, a(j) \rangle \right]$$

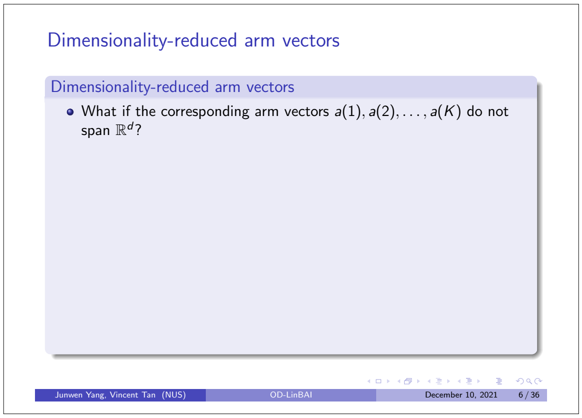

Dimensionality-reduced arm vectors

Dimensionality-reduced arm vectors

- What if the corresponding arm vectors $a(1), a(2), \ldots, a(K)$ do not span $\mathbb{R}^d$?

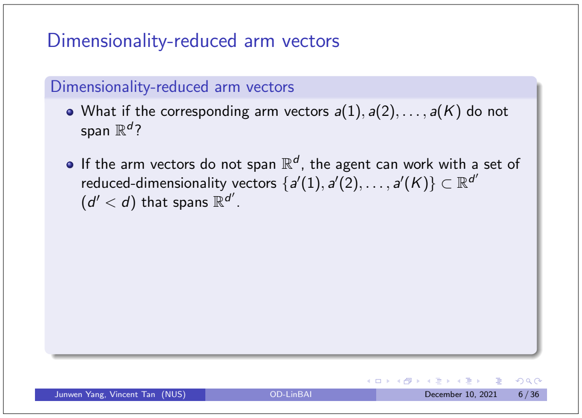

Dimensionality-reduced arm vectors

Dimensionality-reduced arm vectors

- What if the corresponding arm vectors $a(1), a(2), \ldots, a(K)$ do not span $\mathbb{R}^d$?
- If the arm vectors do not span $\mathbb{R}^d$, the agent can work with a set of reduced-dimensionality vectors $\{a'(1), a'(2), \ldots, a'(K)\} \subset \mathbb{R}^{d'}$ $(d' < d)$ that spans $\mathbb{R}^{d'}$.

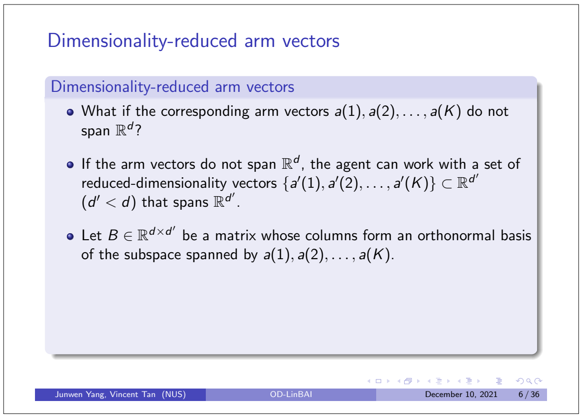

Dimensionality-reduced arm vectors

Dimensionality-reduced arm vectors

- What if the corresponding arm vectors $a(1), a(2), \ldots, a(K)$ do not span $\mathbb{R}^d$?
- If the arm vectors do not span $\mathbb{R}^d$, the agent can work with a set of reduced-dimensionality vectors $\{a'(1), a'(2), \ldots, a'(K)\} \subset \mathbb{R}^{d'}$ $(d' < d)$ that spans $\mathbb{R}^{d'}$.
- Let $B \in \mathbb{R}^{d \times d'}$ be a matrix whose columns form an orthonormal basis of the subspace spanned by $a(1), a(2), \ldots, a(K)$.

Dimensionality-reduced arm vectors

Dimensionality-reduced arm vectors

- What if the corresponding arm vectors $a(1), a(2), \ldots, a(K)$ do not span $\mathbb{R}^d$?
- If the arm vectors do not span $\mathbb{R}^d$, the agent can work with a set of reduced-dimensionality vectors $\{a'(1), a'(2), \ldots, a'(K)\} \subset \mathbb{R}^{d'}$ $(d' < d)$ that spans $\mathbb{R}^{d'}$.
- Let $B \in \mathbb{R}^{d \times d'}$ be a matrix whose columns form an orthonormal basis of the subspace spanned by $a(1), a(2), \ldots, a(K)$.
- Such an orthonormal basis can be calculated efficiently with the reduced singular value decomposition, Gram–Schmidt process, etc.

Dimensionality-reduced arm vectors

Dimensionality-reduced arm vectors

- What if the corresponding arm vectors $a(1), a(2), \ldots, a(K)$ do not span $\mathbb{R}^d$?
- If the arm vectors do not span $\mathbb{R}^d$, the agent can work with a set of reduced-dimensionality vectors $\{a'(1), a'(2), \ldots, a'(K)\} \subset \mathbb{R}^{d'}$ $(d' < d)$ that spans $\mathbb{R}^{d'}$.
- Let $B \in \mathbb{R}^{d \times d'}$ be a matrix whose columns form an orthonormal basis of the subspace spanned by $a(1), a(2), \ldots, a(K)$.
- Such an orthonormal basis can be calculated efficiently with the reduced singular value decomposition, Gram–Schmidt process, etc.
- Set $a'(i) = B^\top a(i)$ for each arm $i \in \mathcal{A}$.

Least Squares Estimator

Ordinary Least Squares (OLS) Estimator

- Let $A_1, A_2, \ldots, A_n \in \mathcal{A} = [K]$ be the arms pulled by the agent and $X_1, X_2, \ldots, X_n \in \mathbb{R}$ be the corresponding noisy rewards.

Least Squares Estimator

Ordinary Least Squares (OLS) Estimator

- Let $A_1, A_2, \ldots, A_n \in \mathcal{A} = [K]$ be the arms pulled by the agent and $X_1, X_2, \ldots, X_n \in \mathbb{R}$ be the corresponding noisy rewards.
- Suppose that the corresponding arm vectors $\{a(A_1), a(A_2), \ldots, a(A_n)\}$ span $\mathbb{R}^d$.
(This is not always true in linear bandits.)

Least Squares Estimator

Ordinary Least Squares (OLS) Estimator

- Let $A_1, A_2, \ldots, A_n \in \mathcal{A} = [K]$ be the arms pulled by the agent and $X_1, X_2, \ldots, X_n \in \mathbb{R}$ be the corresponding noisy rewards.
- Suppose that the corresponding arm vectors $\{a(A_1), a(A_2), \ldots, a(A_n)\}$ span $\mathbb{R}^d$.
(This is not always true in linear bandits.)
- The ordinary least squares (OLS) estimator of θ^* is given by

$$\hat{\theta} = V^{-1} \sum_{t=1}^{n} a(A_t) X_t$$

where $V = \sum_{t=1}^{n} a(A_t) a(A_t)^\top \in \mathbb{R}^{d \times d}$ is invertible.

Least squares estimators

Statistical Property of the Least Squares Estimator

By applying properties of subgaussian random variables, the confidence bounds for the ordinary least squares estimator can be derived as follows.

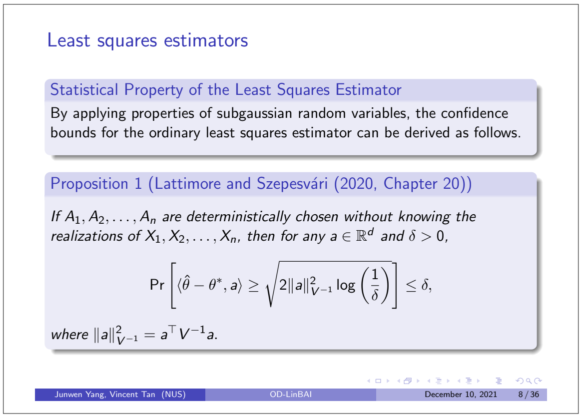

Least squares estimators

Statistical Property of the Least Squares Estimator

By applying properties of subgaussian random variables, the confidence bounds for the ordinary least squares estimator can be derived as follows.

Proposition 1 (Lattimore and Szepesvári (2020, Chapter 20))

If $A_1, A_2, \ldots, A_n$ are deterministically chosen without knowing the realizations of $X_1, X_2, \ldots, X_n$, then for any $a \in \mathbb{R}^d$ and $\delta > 0$,

$$\Pr\left[\langle \hat{\theta} - \theta^*, a \rangle \geq \sqrt{2\|a\|_{V^{-1}}^2 \log\left(\frac{1}{\delta}\right)}\right] \leq \delta,$$

where $\|a\|_{V^{-1}}^2 = a^\top V^{-1} a$.

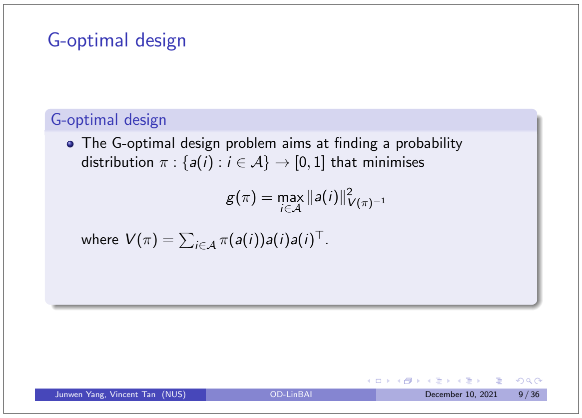

G-optimal design

G-optimal design

- The G-optimal design problem aims at finding a probability distribution $\pi : \{a(i) : i \in \mathcal{A}\} \to [0, 1]$ that minimises

$$g(\pi) = \max_{i \in \mathcal{A}} \|a(i)\|_{V(\pi)^{-1}}^2$$

where $V(\pi) = \sum_{i \in \mathcal{A}} \pi(a(i)) a(i) a(i)^\top$.

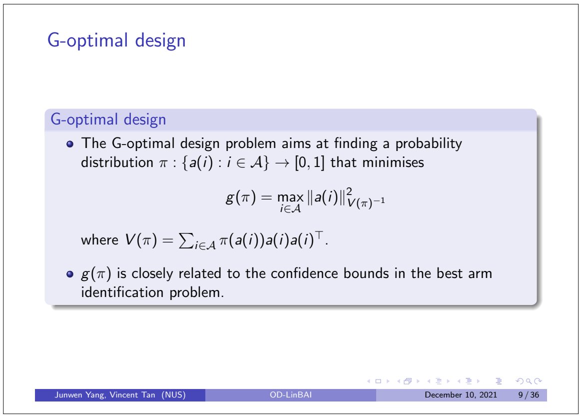

G-optimal design

G-optimal design

- The G-optimal design problem aims at finding a probability distribution $\pi : \{a(i) : i \in \mathcal{A}\} \to [0, 1]$ that minimises

$$g(\pi) = \max_{i \in \mathcal{A}} \|a(i)\|_{V(\pi)^{-1}}^2$$

where $V(\pi) = \sum_{i \in \mathcal{A}} \pi(a(i)) a(i) a(i)^\top$.
- $g(\pi)$ is closely related to the confidence bounds in the best arm identification problem.

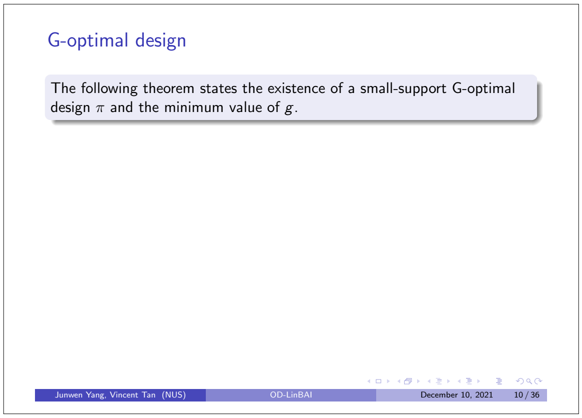

G-optimal design

The following theorem states the existence of a small-support G-optimal design π and the minimum value of g.

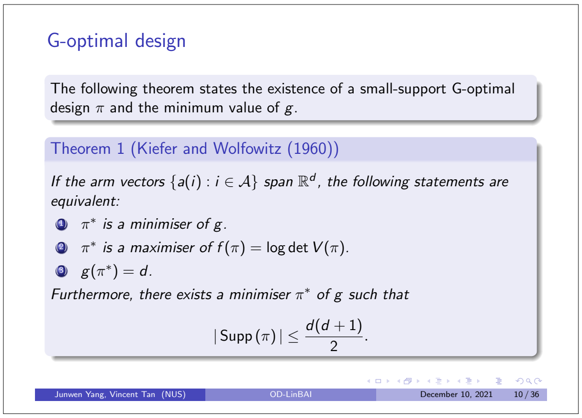

G-optimal design

The following theorem states the existence of a small-support G-optimal design π and the minimum value of g.

Theorem 1 (Kiefer and Wolfowitz (1960))

If the arm vectors $\{a(i) : i \in \mathcal{A}\}$ span $\mathbb{R}^d$, the following statements are equivalent:

1. *π^* is a minimiser of g.*
2. *π^* is a maximiser of $f(\pi) = \log\det V(\pi)$.*
3. *$g(\pi^*) = d$.*

Furthermore, there exists a minimiser π^* of g such that

$$|\operatorname{Supp}(\pi)| \leq \frac{d(d+1)}{2}.$$

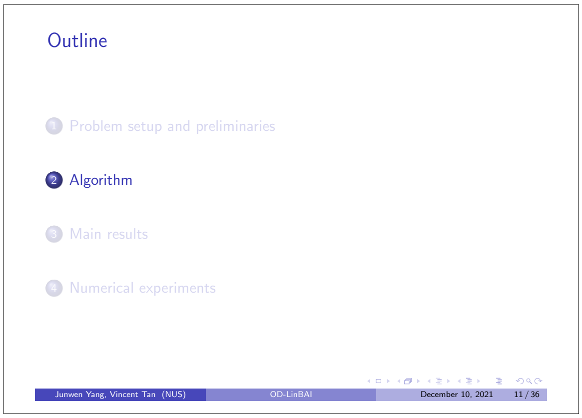

Outline

1. Problem setup and preliminaries
2. Algorithm
3. Main results
4. Numerical experiments

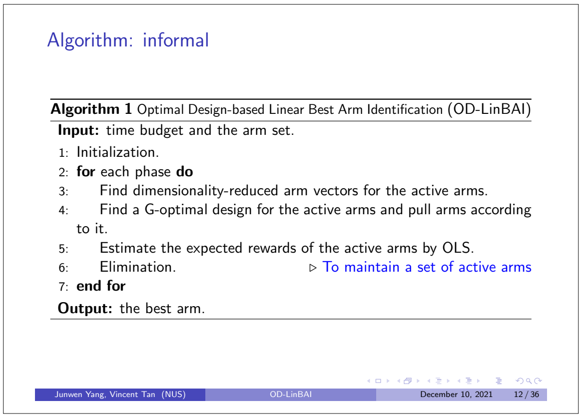

Algorithm: informal

```
Algorithm 1 Optimal Design-based Linear Best Arm Identification (OD-LinBAI)
Input: time budget and the arm set.
1: Initialization.
2: for each phase do
3:     Find dimensionality-reduced arm vectors for the active arms.
4:     Find a G-optimal design for the active arms and pull arms according to it.
5:     Estimate the expected rewards of the active arms by OLS.
6:     Elimination.                         ▷ To maintain a set of active arms
7: end for
Output: the best arm.
```

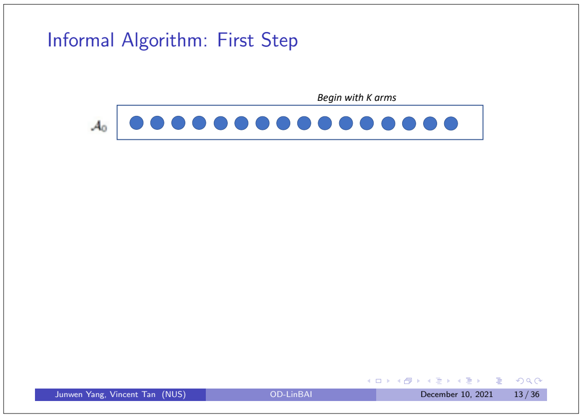

Informal Algorithm: First Step

Begin with K arms

$\mathcal{A}_0$

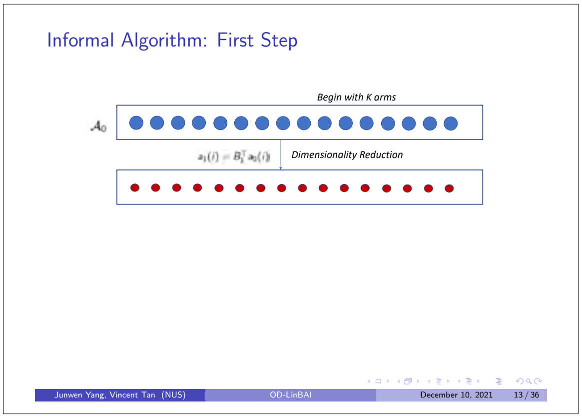

Informal Algorithm: First Step

Begin with K arms

$\mathcal{A}_0$

$a_1(i) = B_1^\top a_0(i)$ *Dimensionality Reduction*

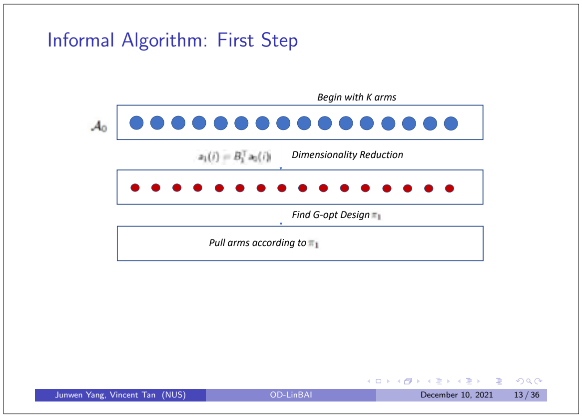

Informal Algorithm: First Step

Begin with K arms

$\mathcal{A}_0$

$a_1(i) = B_1^\top a_0(i)$ *Dimensionality Reduction*

Find G-opt Design π_1

Pull arms according to π_1

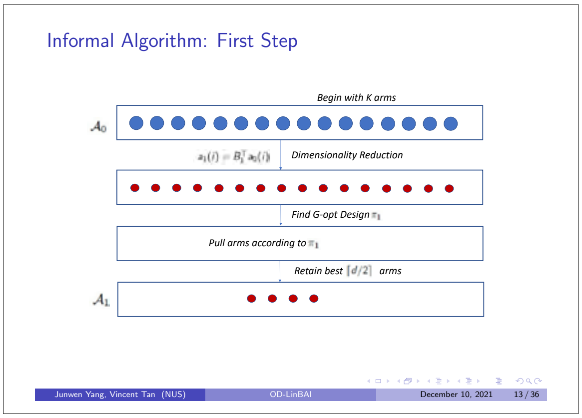

Informal Algorithm: First Step

Begin with K arms

$\mathcal{A}_0$

$a_1(i) = B_1^\top a_0(i)$ *Dimensionality Reduction*

Find G-opt Design π_1

Pull arms according to π_1

Retain best $\lceil d/2 \rceil$ *arms*

$\mathcal{A}_1$

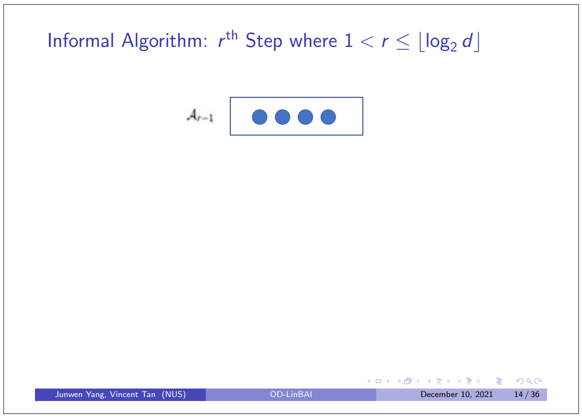

Informal Algorithm: r^{th} Step where $1 < r \leq \lfloor \log_2 d \rfloor$

$\mathcal{A}_{r-1}$

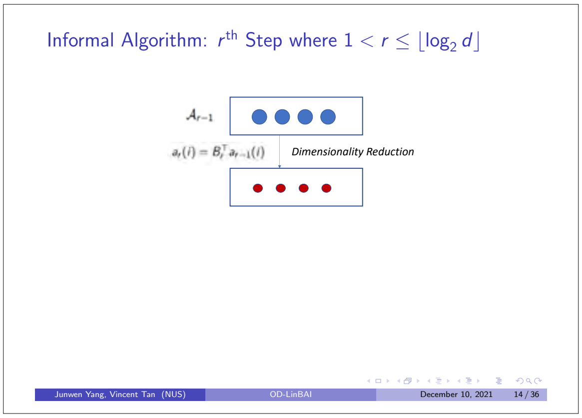

Informal Algorithm: r^{th} Step where $1 < r \leq \lfloor \log_2 d \rfloor$

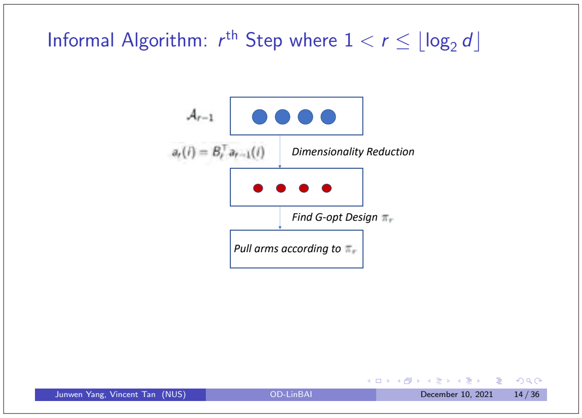

Informal Algorithm: r^{th} Step where $1 < r \leq \lfloor \log_2 d \rfloor$

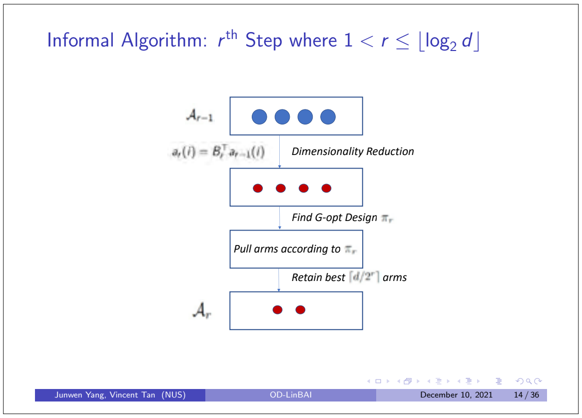

Informal Algorithm: r^{th} Step where $1 < r \leq \lfloor \log_2 d \rfloor$

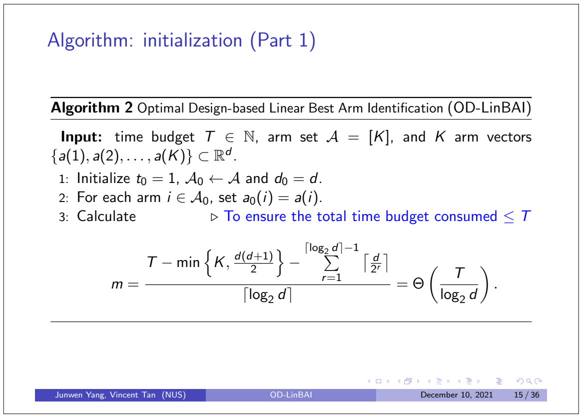

Algorithm: initialization (Part 1)

Algorithm 2 Optimal Design-based Linear Best Arm Identification (OD-LinBAI)

```
Input: time budget $T \in \mathbb{N}$, arm set $\mathcal{A} = [K]$, and $K$ arm vectors $\{a(1), a(2), \dots, a(K)\} \subset \mathbb{R}^d$.
Initialize $t_0 = 1$, $\mathcal{A}_0 \leftarrow \mathcal{A}$ and $d_0 = d$.
For each arm $i \in \mathcal{A}_0$, set $a_0(i) = a(i)$.
Calculate                    ▷ To ensure the total time budget consumed $\leq T$
    $$m = \frac{T - \min\left\{K, \frac{d(d+1)}{2}\right\} - \sum_{r=1}^{\lceil \log_2 d \rceil - 1} \left\lceil \frac{d}{2^r} \right\rceil}{\lceil \log_2 d \rceil} = \Theta\left(\frac{T}{\log_2 d}\right).$$
```

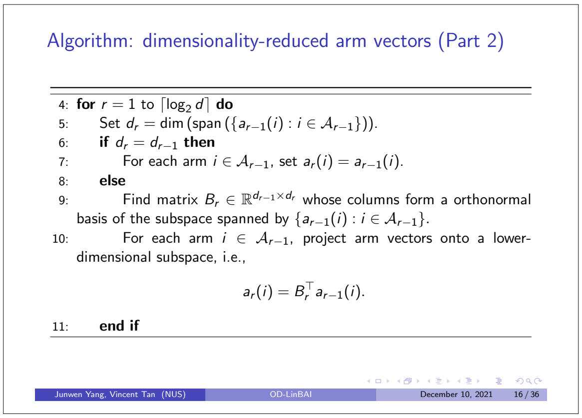

Algorithm: dimensionality-reduced arm vectors (Part 2)

```
for $r = 1$ to $\lceil \log_2 d \rceil$ do
    Set $d_r = \dim(\mathrm{span}(\{a_{r-1}(i) : i \in \mathcal{A}_{r-1}\}))$.
    if $d_r = d_{r-1}$ then
        For each arm $i \in \mathcal{A}_{r-1}$, set $a_r(i) = a_{r-1}(i)$.
    else
        Find matrix $B_r \in \mathbb{R}^{d_{r-1} \times d_r}$ whose columns form a orthonormal basis of the subspace spanned by $\{a_{r-1}(i) : i \in \mathcal{A}_{r-1}\}$.
        For each arm $i \in \mathcal{A}_{r-1}$, project arm vectors onto a lower-dimensional subspace, i.e.,
            $$a_r(i) = B_r^\top a_{r-1}(i).$$
    end if
```

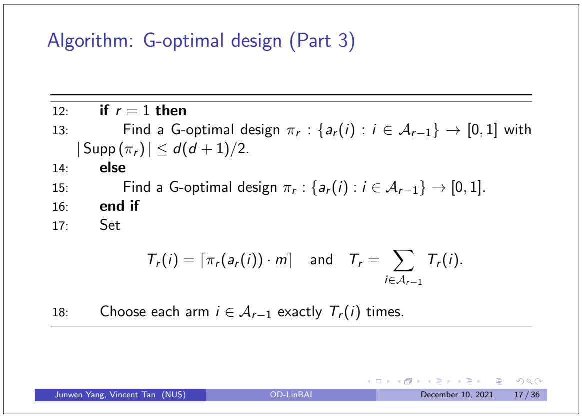

Algorithm: G-optimal design (Part 3)

```
    if $r = 1$ then
        Find a G-optimal design $\pi_r : \{a_r(i) : i \in \mathcal{A}_{r-1}\} \to [0,1]$ with $|\mathrm{Supp}(\pi_r)| \leq d(d+1)/2$.
    else
        Find a G-optimal design $\pi_r : \{a_r(i) : i \in \mathcal{A}_{r-1}\} \to [0,1]$.
    end if
    Set
        $$T_r(i) = \lceil \pi_r(a_r(i)) \cdot m \rceil \quad \text{and} \quad T_r = \sum_{i \in \mathcal{A}_{r-1}} T_r(i).$$
    Choose each arm $i \in \mathcal{A}_{r-1}$ exactly $T_r(i)$ times.
```

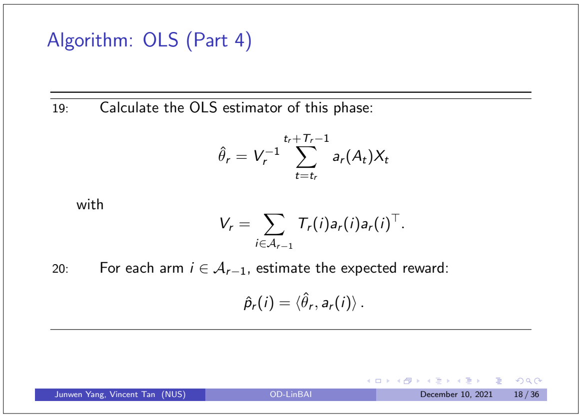

Algorithm: OLS (Part 4)

```
Calculate the OLS estimator of this phase:
    $$\hat{\theta}_r = V_r^{-1} \sum_{t=t_r}^{t_r+T_r-1} a_r(A_t) X_t$$
  with
    $$V_r = \sum_{i \in \mathcal{A}_{r-1}} T_r(i) a_r(i) a_r(i)^\top .$$
For each arm $i \in \mathcal{A}_{r-1}$, estimate the expected reward:
    $$\hat{p}_r(i) = \langle \hat{\theta}_r, a_r(i) \rangle .$$
```

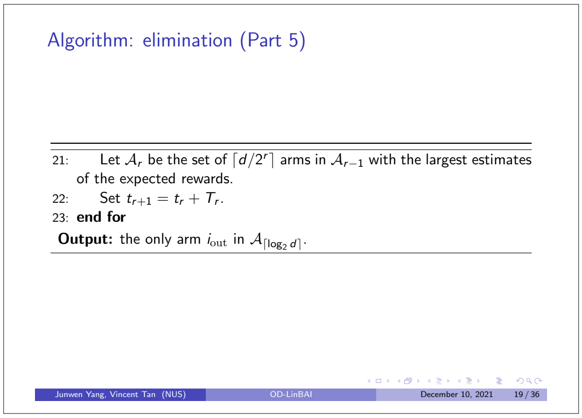

Algorithm: elimination (Part 5)

```
    Let $\mathcal{A}_r$ be the set of $\lceil d/2^r \rceil$ arms in $\mathcal{A}_{r-1}$ with the largest estimates of the expected rewards.
    Set $t_{r+1} = t_r + T_r$.
end for
Output: the only arm $i_{\text{out}}$ in $\mathcal{A}_{\lceil \log_2 d \rceil}$.
```

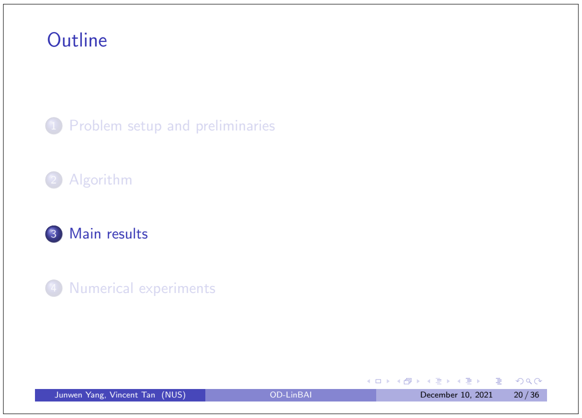

Outline

1. Problem setup and preliminaries
2. Algorithm
3. Main results
4. Numerical experiments

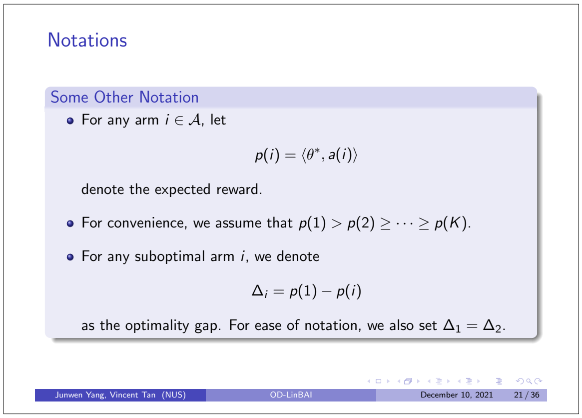

Notations

Some Other Notation

- For any arm $i \in \mathcal{A}$, let

$$p(i) = \langle \theta^*, a(i) \rangle$$

denote the expected reward.

- For convenience, we assume that $p(1) > p(2) \geq \cdots \geq p(K)$.
- For any suboptimal arm i, we denote

$$\Delta_i = p(1) - p(i)$$

as the optimality gap. For ease of notation, we also set $\Delta_1 = \Delta_2$.

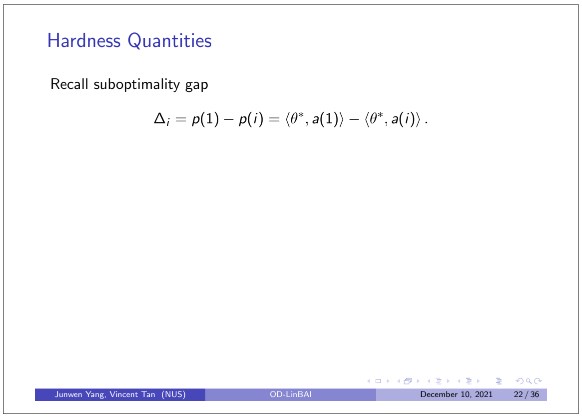

Hardness Quantities

Recall suboptimality gap

$$\Delta_i = p(1) - p(i) = \langle \theta^*, a(1) \rangle - \langle \theta^*, a(i) \rangle .$$

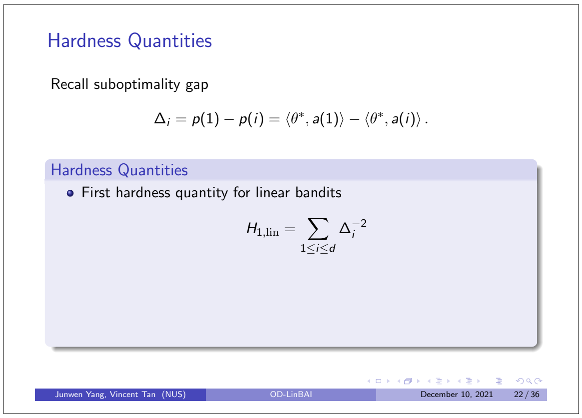

Hardness Quantities

Recall suboptimality gap

$$\Delta_i = p(1) - p(i) = \langle \theta^*, a(1) \rangle - \langle \theta^*, a(i) \rangle .$$

Hardness Quantities

- First hardness quantity for linear bandits

$$H_{1,\text{lin}} = \sum_{1 \leq i \leq d} \Delta_i^{-2}$$

Hardness Quantities

Recall suboptimality gap

$$\Delta_i = p(1) - p(i) = \langle \theta^*, a(1) \rangle - \langle \theta^*, a(i) \rangle .$$

Hardness Quantities

- First hardness quantity for linear bandits

$$H_{1,\mathrm{lin}} = \sum_{1 \le i \le d} \Delta_i^{-2}$$

- Second hardness quantity for linear bandits

$$H_{2,\mathrm{lin}} = \max_{2 \le i \le d} \frac{i}{\Delta_i^2}$$

Hardness quantities

Table: Comparisons of different hardness quantities: H_1, H_2, $H_{1,\mathrm{lin}}$ and $H_{2,\mathrm{lin}}$

$H_1 = \sum_{1 \le i \le K} \Delta_i^{-2}$	$H_2 = \max_{2 \le i \le K} \frac{i}{\Delta_i^2}$	$1 \le \frac{H_1}{H_2} \le \log(2K)$
$H_{1,\mathrm{lin}} = \sum_{1 \le i \le d} \Delta_i^{-2}$	$H_{2,\mathrm{lin}} = \max_{2 \le i \le d} \frac{i}{\Delta_i^2}$	$1 \le \frac{H_{1,\mathrm{lin}}}{H_{2,\mathrm{lin}}} \le \log(2d)$
$1 \le \frac{H_1}{H_{1,\mathrm{lin}}} \le \frac{K}{d}$	$1 \le \frac{H_2}{H_{2,\mathrm{lin}}} \le \frac{K}{d}$	

Upper bound

Theorem 2 (Error Probability of OD-LinBAI)

For any linear bandit instance $\nu \in \mathcal{E}$, OD-LinBAI outputs an arm i_{out} satisfying

$$\Pr\left[i_{\mathrm{out}} \ne 1\right] \le \left(\frac{4K}{d} + 3\log_2 d\right) \exp\left(-\frac{m}{32 H_{2,\mathrm{lin}}}\right)$$

where m was defined in the algorithm and scales as

$$m = \Theta\left(\frac{T}{\log_2 d}\right) \qquad \text{and} \qquad H_{2,\mathrm{lin}} = \max_{2 \le i \le d} \frac{i}{\Delta_i^2}.$$

Existing Works

Comparison to Existing Art

- BayesGap (Hoffman et al., 2014):
  - Not parameter-free (require the knowledge of the problem instance)
  - Error probability: $\exp\left(-\Omega\left(\frac{T}{H_1}\right)\right)$

Existing Works

Comparison to Existing Art

- BayesGap (Hoffman et al., 2014):
  - Not parameter-free (require the knowledge of the problem instance)
  - Error probability: $\exp\left(-\Omega\left(\frac{T}{H_1}\right)\right)$
- Peace (Katz-Samuels et al., 2020):
  - Not parameter-free (require the knowledge of the problem instance)
  - Not minimax optimal

Existing Works

Comparison to Existing Art

- BayesGap (Hoffman et al., 2014):
  - Not parameter-free (require the knowledge of the problem instance)
  - Error probability: $\exp\left(-\Omega\left(\frac{T}{H_1}\right)\right)$
- Peace (Katz-Samuels et al., 2020):
  - Not parameter-free (require the knowledge of the problem instance)
  - Not minimax optimal
- LinearExploration (Alieva et al., 2021):
  - Error probability: $\exp\big(-\Omega(\frac{T}{H_2 \log_2 K})\big)$

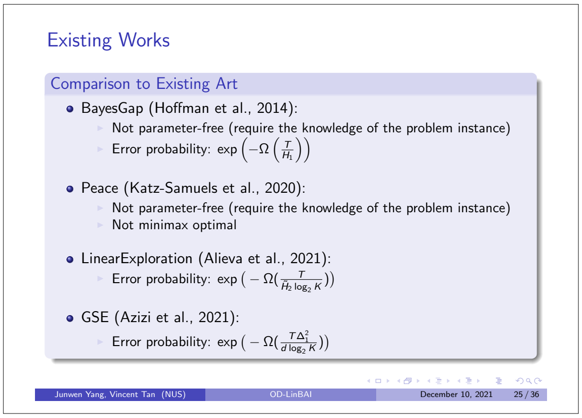

Existing Works

Comparison to Existing Art

- BayesGap (Hoffman et al., 2014):
  - Not parameter-free (require the knowledge of the problem instance)
  - Error probability: $\exp\left(-\Omega\left(\frac{T}{H_1}\right)\right)$
- Peace (Katz-Samuels et al., 2020):
  - Not parameter-free (require the knowledge of the problem instance)
  - Not minimax optimal
- LinearExploration (Alieva et al., 2021):
  - Error probability: $\exp\big(-\Omega(\frac{T}{H_2 \log_2 K})\big)$
- GSE (Azizi et al., 2021):
  - Error probability: $\exp\big(-\Omega(\frac{T\Delta_1^2}{d \log_2 K})\big)$

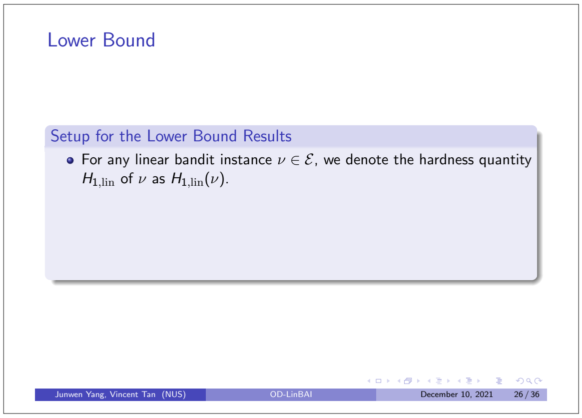

Lower Bound

Setup for the Lower Bound Results

- For any linear bandit instance $\nu \in \mathcal{E}$, we denote the hardness quantity $H_{1,\mathrm{lin}}$ of ν as $H_{1,\mathrm{lin}}(\nu)$.

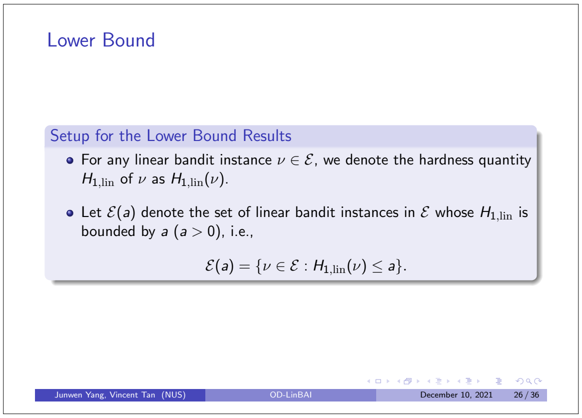

Lower Bound

Setup for the Lower Bound Results

- For any linear bandit instance $\nu \in \mathcal{E}$, we denote the hardness quantity $H_{1,\mathrm{lin}}$ of ν as $H_{1,\mathrm{lin}}(\nu)$.
- Let $\mathcal{E}(a)$ denote the set of linear bandit instances in $\mathcal{E}$ whose $H_{1,\mathrm{lin}}$ is bounded by a ($a > 0$), i.e.,

$$\mathcal{E}(a) = \{\nu \in \mathcal{E} : H_{1,\mathrm{lin}}(\nu) \leq a\}.$$

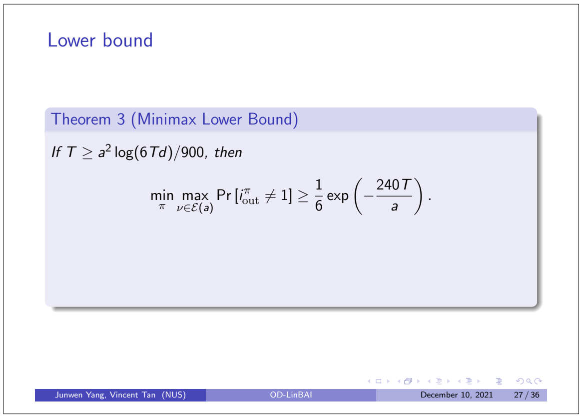

Lower bound

Theorem 3 (Minimax Lower Bound)

If $T \geq a^2 \log(6Td)/900$, then

$$\min_{\pi} \max_{\nu \in \mathcal{E}(a)} \Pr\left[i_{\mathrm{out}}^{\pi} \neq 1\right] \geq \frac{1}{6} \exp\left(-\frac{240T}{a}\right).$$

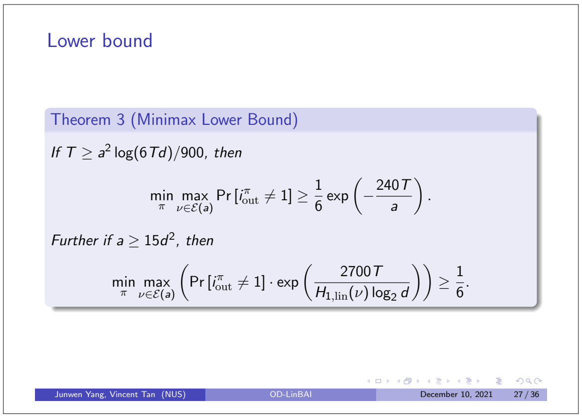

Lower bound

Theorem 3 (Minimax Lower Bound)

If $T \geq a^2 \log(6Td)/900$, then

$$\min_{\pi} \max_{\nu \in \mathcal{E}(a)} \Pr\left[i_{\mathrm{out}}^{\pi} \neq 1\right] \geq \frac{1}{6} \exp\left(-\frac{240T}{a}\right).$$

Further if $a \geq 15d^2$, then

$$\min_{\pi} \max_{\nu \in \mathcal{E}(a)} \left(\Pr\left[i_{\mathrm{out}}^{\pi} \neq 1\right] \cdot \exp\left(\frac{2700T}{H_{1,\mathrm{lin}}(\nu) \log_2 d}\right)\right) \geq \frac{1}{6}.$$

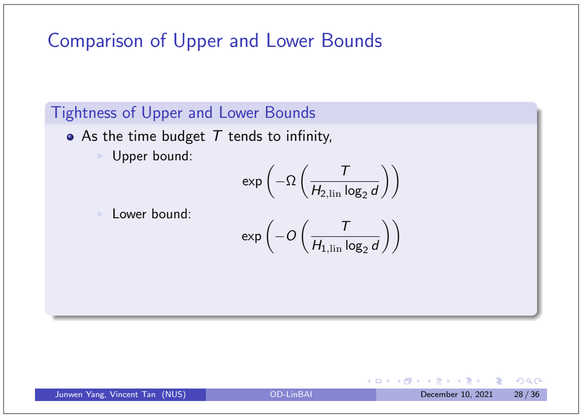

Comparison of Upper and Lower Bounds

Tightness of Upper and Lower Bounds

- As the time budget T tends to infinity,
  - Upper bound:

$$\exp\left(-\Omega\left(\frac{T}{H_{2,\mathrm{lin}} \log_2 d}\right)\right)$$

  - Lower bound:

$$\exp\left(-O\left(\frac{T}{H_{1,\mathrm{lin}} \log_2 d}\right)\right)$$

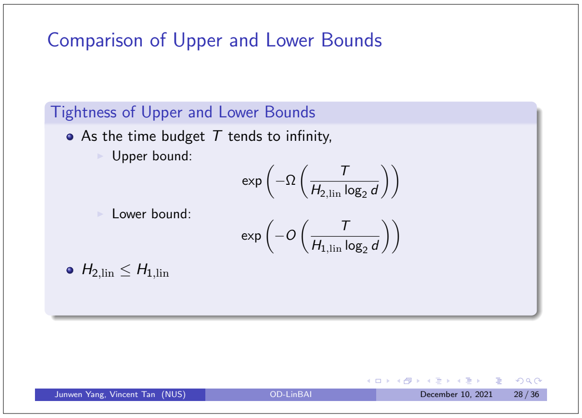

Comparison of Upper and Lower Bounds

Tightness of Upper and Lower Bounds

- As the time budget T tends to infinity,
  - Upper bound:
$$\exp\left(-\Omega\left(\frac{T}{H_{2,\mathrm{lin}}\log_2 d}\right)\right)$$
  - Lower bound:
$$\exp\left(-O\left(\frac{T}{H_{1,\mathrm{lin}}\log_2 d}\right)\right)$$
- $H_{2,\mathrm{lin}} \leq H_{1,\mathrm{lin}}$

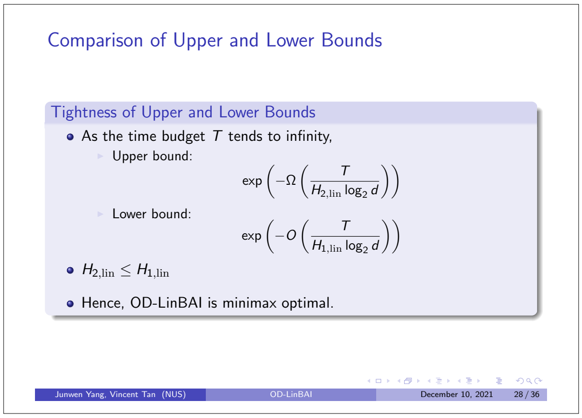

Comparison of Upper and Lower Bounds

Tightness of Upper and Lower Bounds

- As the time budget T tends to infinity,
  - Upper bound:
$$\exp\left(-\Omega\left(\frac{T}{H_{2,\mathrm{lin}}\log_2 d}\right)\right)$$
  - Lower bound:
$$\exp\left(-O\left(\frac{T}{H_{1,\mathrm{lin}}\log_2 d}\right)\right)$$
- $H_{2,\mathrm{lin}} \leq H_{1,\mathrm{lin}}$
- Hence, OD-LinBAI is minimax optimal.

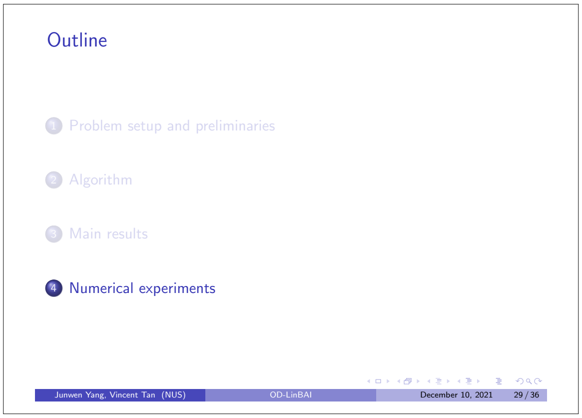

Outline

1. Problem setup and preliminaries
2. Algorithm
3. Main results
4. Numerical experiments

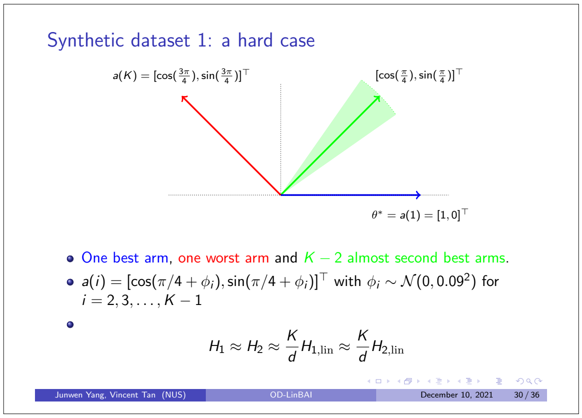

Synthetic dataset 1: a hard case

- One best arm, one worst arm and $K-2$ almost second best arms.
- $a(i) = [\cos(\pi/4 + \phi_i), \sin(\pi/4 + \phi_i)]^\top$ with $\phi_i \sim \mathcal{N}(0, 0.09^2)$ for $i = 2, 3, \ldots, K-1$
-
$$H_1 \approx H_2 \approx \frac{K}{d} H_{1,\mathrm{lin}} \approx \frac{K}{d} H_{2,\mathrm{lin}}$$

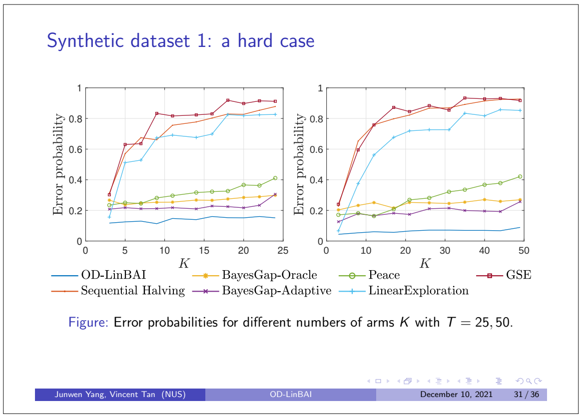

Synthetic dataset 1: a hard case

Figure: Error probabilities for different numbers of arms K with $T = 25, 50$.

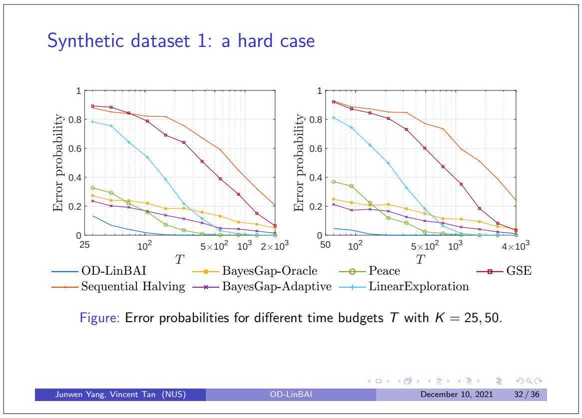

Synthetic dataset 1: a hard case

Figure: Error probabilities for different time budgets T with $K = 25, 50$.

Real-world dataset: Abalone Dataset (Dua and Graff, 2017)

Description the Abalone Dataset

- The age of each abalone is usually hard to determine from physical measurements.
- $K = 400$: 400 groups of 8 attributes (such as sex, length, diameter, etc.) of the abalone
- $d = 9$: $\theta^* \in \mathbb{R}^9$ comes from the linear regression
- To identify the abalone with the largest age with using the 8 attributes from physical measurements

Real-world dataset: Abalone Dataset

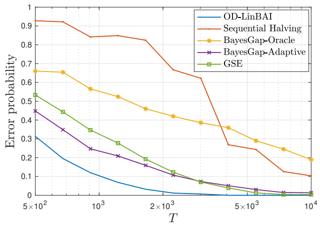

Figure: Error probabilities for different budgets T.

Thanks for listening!

References

Tor Lattimore and Csaba Szepesvári. *Bandit algorithms*. Cambridge University Press, 2020.

Jack Kiefer and Jacob Wolfowitz. The equivalence of two extremum problems. *Canadian Journal of Mathematics*, 12:363–366, 1960.

Matthew Hoffman, Bobak Shahriari, and Nando Freitas. On correlation and budget constraints in model-based bandit optimization with application to automatic machine learning. In *Artificial Intelligence and Statistics*, pages 365–374. PMLR, 2014.

Julian Katz-Samuels, Lalit Jain, Kevin G Jamieson, et al. An empirical process approach to the union bound: Practical algorithms for combinatorial and linear bandits. *Advances in Neural Information Processing Systems*, 33, 2020.

Ayya Alieva, Ashok Cutkosky, and Abhimanyu Das. Robust pure exploration in linear bandits with limited budget. In *International Conference on Machine Learning*, pages 187–195. PMLR, 2021.

MohammadJavad Azizi, Branislav Kveton, and Mohammad Ghavamzadeh. Fixed-budget best-arm identification in contextual bandits: A static-adaptive algorithm. *arXiv preprint arXiv:2106.04763*, 2021.

Dheeru Dua and Casey Graff. UCI machine learning repository, 2017. URL `http://archive.ics.uci.edu/ml`.

Global and Local Prediction Methods of COVID-19 Time Series with Machine Learning

Amir Mosavi

Obuda University, Hungary

(joint work with Sina Ardebili, Annamaria R. Varkonyi-Koczy)

This presentation is devoted to the advancement of the machine learning-based methods for accurate prediction of the Covid-19 outbreak prediction. Advancement of the novel models for time-series prediction of COVID-19 is of utmost importance. Machine learning (ML) methods have recently shown promising results. The present study aims to engage an artificial neural network-integrated by grey wolf optimizer for COVID-19 outbreak predictions by employing the global and local dataset. For the case study, the training and testing processes have been performed by time-series data related to January 22 to September 15, 2020 and validation has been performed by time-series data related to September 16 to October 15, 2020. Results have been evaluated by employing mean absolute percentage error (MAPE) and correlation coefficient (r) values. ANN-GWO provided a MAPE of 6.23, 13.15 and 11.4% for training, testing and validating phases, respectively. According to the results, the developed model could successfully cope with the prediction task.

Deep learning in diagnostic applications: the good, the bad, and the ugly.

Yaniv Gal

MoleMap Ltd, New Zealand

Artificial Intelligence (AI) in general, and deep learning (DL) in particular, have recently gained popularity in both academic and commercial applications due to its ability to automatically identify meaningful features in the data and calculate a complex decision boundary between in the constructed feature space.

The medical device industry has recognised the potential of deep learning to support clinicians' diagnosis and gradually integrate deep learning into the clinical workflow to enforce diagnostic decisions and significantly reduce the likelihood of human error. Skin cancer diagnosis is an example for such application, where dermatologist rely mainly (or solely) on visual inspection in order to diagnose suspicious skin lesions. Deep learning, which can extract subtle features from dermoscopic images provides accurate diagnosis to support the clinicians in their decision and reduce error rates.

While the question of whether AI will ever replace the clinician's decision making is still in debate, it is undeniable that the diagnostic performance of these algorithms is continuously improving and in some case is comparable or even surpasses human specialists. Moreover, advances in deep-learning training techniques and improved network architectures now allow training these models with less data and yet, lower the risk of overfitting, which makes these algorithms even more accessible and increases their attractiveness. However, once a model is trained on labelled data, it is impossible to explain its decisions on new data, in a way that will be meaningful for the user (i.e. clinician). This lack of "explainability" in deep learning creates a landscape where clinical decisions that are supported by AI require the clinician to either blindly trust the trained model or monitor the automated decision to a level that diminishes the utility that it brings, until enough trust is gained.

Furthermore, when a trained AI model is given a sample that it was not trained on (i.e. unknown class), it is impossible to predict the output of the system and such cases often lead to a wrong diagnostic result that is presented by the AI model with high score, implicitly suggesting that the result should be trusted.

This talk reviews some of the benefits, pitfalls, and challenges of using modern AI models in real-world diagnostic applications. We use the AI technology that is currently developed by Kāhu, New Zealand, for skin cancer detection as a case study, and describe what is a desirable solution to the above challenges may be.

Language models in industry and around the world

Caleb Moses

Dragonfly Data Science, Wellington, New Zealand

Language Models have been a strong focus for research in the AI industry following the publication of the Bidirectional Encoder Representations from Transformers (BERT) neural network architecture published by Google in 2018. More recently, major tech companies have been engaged in an arms race to build ever more complex language models trained on increasingly massive text datasets, also aimed at as many languages as possible.

I will discuss the latest language model trends and their implications for the digital economy, as well as their ethical implications. In addition, I will discuss non-English language models and their differences as well as the current situation for under-resourced minority languages around the world.

Option pricing with transaction costs – mathematical modelling in new digital economy

Xiaoping Lu

School of Mathematics and Applied Statistics, University of Wollongong, Australia

Mathematics plays an important role in modern finance, particularly in pricing options, which are financial derivatives with complicated structures. When transaction costs are considered, there is no longer a unique fair price between the buyer and the writer of an option, as both parties wish to recover the costs incurred in trading the underlying stocks from the prices that they are willing to pay or receive for the option. Mathematically, transaction costs make option pricing problems much more complicated, especially for American options and options under stochastic volatility. In this talk, we shall discuss the valuation problems for options with transaction costs, and examine how transaction costs affect option prices and the optimal exercise policy for American options.

U O W

Option pricing with transaction costs

–mathematical modeling in new digital economy

Xiaoping Lu

School of Mathematics and Applied Statistics
University of Wollongong

Acknowledgement

Most of the work reported here are carried out with Dr D. Yan and Prof. S.-P. Zhu

---

What is an option?

An option is a contract between two parties, a buyer (holder) and a seller (writer), that gives the buyer right but not obligation with the following conditions:

- at a prescribed time in the future, the expiry date, the holder of the option *may*
- buy (sell) a prescribed asset, known as the underlying, for
- a prescribed price, known as the exercise price or strike price.

An option giving the right to *buy* is called a *call* option, and the right to *sell* is a *put* option.

European or American?

There are two main styles of options:

- European Option:

  The holder can only exercise their right at the expiration date. This type of options are characterized by their time to expiry and exercise price.

- American Option:

  It allows the holder to exercise before the expiry when the underlying asset price is deemed profitable (optimal).

  Because of this flexibility, the price of an American option is dictated by the concept of *optimal exercise price*.

Value of an option

- In an option contract, the holder has right, but not obligation to buy or sell. Therefore, the option has value for the holder, which must be paid for.
- The writer does have a potential obligation, as he/she has to sell or buy if the holer decides to buy or sell the asset. The writer needs to be compensated for this obligation.
- However, how much would one pay for this right? that is, what is the value of an option?
- Accurate evaluation of an option would give answer to the above question, and more.
- The Black–Scholes model is the foundation of modern financial theory.

The Black–Scholes model

Under the Black–Scholes (B–S) framework, the value of an option, denoted by $V(S, t)$, is governed by the following partial differential equation (PDE)

$$\frac{\partial V}{\partial t} + \frac{1}{2}\sigma^2 S^2 \frac{\partial^2 V}{\partial S^2} + rS\frac{\partial V}{\partial S} - rV = 0,$$

where S is the current price of the underlying stock;
t, the current time;
σ, the volatility of the underlying;
r, the risk-free interest rate.

This equation is referred to as the **B–S PDE**. The solution of the PDE subject to appropriate conditions gives rise to the **fair price** of the corresponding option.

Boundary and final Conditions

The B–S PDE can be solved analytically for the value of European options, subject to conditions on S and t. For a European put:

- at the time of expiry, i.e. at $t = T$, the payoff of the option is the value of
$$V(S,T) = \max(K - S, 0).$$
where K is the pre-determined exercise price or the strike.
- If $S = 0$, at any time the option will take the present value of K received at expiry T,
$$V(0,t) = Ke^{-r(T-t)}.$$
- As $S \to \infty$ the option is unlikely to be exercised, so
$$V(S,t) \to 0,\ S \to \infty.$$

Optimal boundary for American option

For an American option, there exists an optimal exercise price, $S_f(t)$, which divides the domain of S into a continuation/holding region and an exercise region. For an American put

- $$V(S_f(t),t) = K - S_f(t),\ S = S_f(t),$$
which is derived from the option value being simply the intrinsic value when the optimal exercise price is reached. While in the exercise region
$$V(S,t) = K - S,\ 0 \leq S < S_f(t).$$
- Another condition, $\dfrac{\partial V}{\partial S}(S_f(t),t) = -1$, is needed to ensure smoothness between the option value and the payoff function at $S = S_f(t)$.

A complete B–S PDE system for American put

$$\begin{cases} \dfrac{\partial V}{\partial t} + \dfrac{1}{2}\sigma^2 S^2 \dfrac{\partial^2 V}{\partial S^2} + rS\dfrac{\partial V}{\partial S} - rV = 0, \\ V(S,T) = \max(K - S, 0), \\ V(S_f(t),t) = K - S_f(t), \\ \dfrac{\partial V}{\partial S}(S_f(t),t) = -1, \\ V(S,t) = 0,\ S \to \infty. \end{cases} \tag{1}$$

In theory, the solution of PDE system (1) gives the value of the American put V and the optimal exercise price S_f at any time t ($0 < t < T$) and at stock price $S \geq S_f$.

However, the problem is highly nonlinear due to the fact that S_f is unknown, constituting a **moving boundary problem**, for which an analytic solution is not attainable except in special cases.

B–S model assumptions

- The asset price S follows the lognormal walk
$$dS = \mu S dt + \sigma S dW_t,$$
where μ is the drift rate, dW_t is normally distributed with a mean 0 and standard deviation $\sqrt{dt}$.
- The risk-free interest rate r and the asset volatility σ are known.
- There are **no transaction costs** associated with hedging a portfolio.
- The underlying pays no dividends (can be dropped).
- There is no arbitrage possibilities.
- Trading of the underlying can be done **continuously**.
- Short selling is permitted.

Limitations of B–S model

Under the assumptions, the B–S PDE or a variant incorporating dividends or time-dependent r or σ is satisfied by any derivative security whose price depends only on current S and t.

The B–S model set up the foundation for modern derivative pricing. However, there are some limitations:

- The value of an option is independent of μ.
$\Longrightarrow$ Two investors with different views on μ agree on the value of the option.
- Transaction costs are not taken into consideration. In practice, trading of underlying assets attracts fees.
- The model is based on a continuous hedging strategy.
$\Longrightarrow$ The strategy could lead to an unrealistic high option selling price, when transaction costs are considered.

Option pricing with transaction costs

- In the presence of transaction costs, both the holder/buyer and the writer/seller of an option would want to recover their costs from the price they are willing to pay or receive.
- The market is incomplete due to the market friction — there is no longer a unique price for the buyer and the writer of an option.
- Instead, the holder price p_h and the writer price p_w form a bid-ask spread,
$$p_h < p_{BS} < p_w,$$
where p_{BS} is the B–S price.
- Continuous hedging is impossible, as it could lead to unreal high writer price and possible negative buyer price.
- The standard B–S model is no longer suitable.

The Leland Model

The assumptions are those for the B–S model, except

- it is a discrete hedging strategy.

  the portfolio is re-balanced every δt, where δt is a non-infinitesimal constant interval.
- The costs associated with the trading of the underlying are proportional to the value of the transaction.

  the costs for a transaction of ν shares valued at S are $\kappa|\nu|S$, where κ is a constant rate and ν is the number of shares traded: bought $\nu > 0$ and sold $\nu < 0$.

Leland, Option pricing and replication with transaction costs, *J. Finance*, **40(5)** (1985).

Wilmott et al., Hedging option portfolios in the presence of transaction costs, *Adv. Futures Opt Res.*, **7** (1994).

The discrete hedging strategy

Consider a financial market, where investors have access to both stocks and options.

A hedged portfolio of a writer of an option, who is shorting one unit of option and long holding Δ unit of the stock, can be expressed as

$$\Pi = -V + \Delta S$$

The change in the value of the hedged portfolio in a time-step δt is

$$\delta\Pi = -\delta V + \Delta\delta S - \kappa S|\nu|. \qquad (2)$$

On the other hand, the portfolio of a holder is $\Pi = V - \Delta S$, and the change in the value of the portfolio in a time-step is

$$\delta\Pi = \delta V - \Delta\delta S - \kappa S|\nu|. \qquad (3)$$

The discrete hedging strategy

The random walk in discrete time is given by

$$\delta S = \mu S\delta t + \sigma S\phi\sqrt{\delta t},$$

where ϕ is drawn from a standard normal distribution.

Applying Itô's lemma to V, we obtain for the writer

$$\begin{aligned}\delta\Pi &= \sigma S\left(\Delta - \frac{\partial V}{\partial S}\right)\phi\sqrt{\delta t} \\ &\quad - \left(\frac{1}{2}\sigma^2 S^2\frac{\partial^2 V}{\partial S^2}\phi^2 + \mu S\frac{\partial V}{\partial S} + \frac{\partial V}{\partial t} - \mu\Delta S\right)\delta t - \kappa S|\nu|\end{aligned}$$

Following the hedging strategy, we choose $\Delta = \frac{\partial V}{\partial S}$, which is the number of the stock held at time t.

The discrete hedging strategy

The number of stocks held at time $t + \delta t$ due to hedging is $\Delta_{t+\delta t} = \frac{\partial V}{\partial S}(S + \delta S, t + \delta t)$.

So the number of traded stocks is

$$\nu = \frac{\partial V}{\partial S}(S + \delta S, t + \delta t) - \frac{\partial V}{\partial S}(S, t)$$

Applying Taylor's expansion of $\Delta_{t+\delta t}$, we obtain

$$\nu \approx \sigma S\frac{\partial^2 V}{\partial S^2}\phi\sqrt{\delta t}.$$

Thus, the expected transaction costs during one time step δt is

$$\mathbb{E}\left[\kappa S|\nu|\right] = \sqrt{\frac{2}{\pi}}\kappa\sigma S^2\left|\frac{\partial^2 V}{\partial S^2}\right|\sqrt{\delta t}$$

The discrete hedging strategy

Under the hedging strategy, the writer of the option is expected to make as much from his/her portfolio as if he/she puts the money in the bank, then

$$\mathbb{E}\left[\delta\Pi\right] = r\Pi\delta t.$$

This leads to

$$\frac{\partial V}{\partial t} + \frac{1}{2}\sigma^2 S^2\frac{\partial^2 V}{\partial S^2} + \sqrt{\frac{2}{\pi\delta t}}\kappa\sigma S^2\left|\frac{\partial^2 V}{\partial S^2}\right| + rS\frac{\partial V}{\partial S} - rV = 0$$

Following similar argument, the governing equation for the holder of the option can be derived as

$$\frac{\partial V}{\partial t} + \frac{1}{2}\sigma^2 S^2\frac{\partial^2 V}{\partial S^2} - \sqrt{\frac{2}{\pi\delta t}}\kappa\sigma S^2\left|\frac{\partial^2 V}{\partial S^2}\right| + rS\frac{\partial V}{\partial S} - rV = 0$$

The modified B–S PDE

Thus, the following PDE (Wilmott et al. 1994) is derived

$$\frac{\partial V}{\partial t} + \frac{1}{2}\sigma^2 S^2\frac{\partial^2 V}{\partial S^2} \pm \sqrt{\frac{2}{\pi\delta t}}\kappa\sigma S^2\left|\frac{\partial^2 V}{\partial S^2}\right| + rS\frac{\partial V}{\partial S} - rV = 0, \quad (4)$$

where the '+' sign is for the writer of the option, and the '$-$' for the buyer.

This equation is a modified B–S PDE with an extra term due to the transaction costs, which can be used to price a portfolio of options.

The pricing equation is nonlinear because of the transaction costs term so analytical solution is not available.

However, it is not difficult to solve (4) with simple finite difference methods.

The Laland Equation

For a single option, (4) reduces to the Leland equation

$$\frac{\partial V}{\partial t} + \frac{1}{2}\tilde{\sigma}^2 S^2 \frac{\partial^2 V}{\partial S^2} + rS\frac{\partial V}{\partial S} - rV = 0, \qquad (5)$$

where $\tilde{\sigma}^2 = \sigma^2\left(1 \pm \sqrt{\frac{8}{\pi\delta t}}\frac{\kappa}{\sigma}\right)$.

The Leland equation (5) only differs from the standard B–S PDE in the adjusted volatility term, $\tilde{\sigma}$, which is referred to as the **Leland number**.

As a result, for a European option, the B–S formula could be used to determine the option prices for the writer and the buyer, respectively.

Complications of American options

The Leland model can be used to price American options with appropriate boundary conditions.

However, the optimal exercise boundary associated with an American option again makes the problem more complicated.

Unlike in the case of European options, the price for the writer of an American option cannot be determined independently.

- The holder of an American option has the right to decide if and when to exercise their right.
  — Mathematically, a holder's problem is a moving boundary problem.
- Once the holder makes the decision, the writer has obligation to fulfill the holder's right.
  —The writer's problem is one with known time-dependent boundary (the holder's optimal exercise price).

Pros and cons of discrete hedging strategy

This strategy is basically a modified B–S model, which is easy to implement, especially for a single option case.

However, there are some inherent problems:

- Perfect hedging is not possible, which leads unavoidable hedging errors.

  —More frequent re-balancing would reduce the hedging error, but increase transaction costs.
- Investors' risk preferences are not incorporated in the model, which could lead to the mispricing of an option.

  —The only choice an investor could make is the re-balancing interval.

Utility indifference pricing

Utility indifference price — the price at which the investor is indifferent, in the sense that his or her expected utility under optimal trading maintains the same, whether he or she trades stocks in the market with or without an option in the portfolio.

Utility indifference pricing is pioneered by Davis et al. for the pricing of European options with proportional transaction costs.

Davis et al., European option pricing with transaction costs, *SIAM J. Control and Optim.*, **31(2)** (1993).

The method by Davis et al. was later extended for pricing American options by others, however, only Zakamouline provided analysis on the early exercise boundary as well as prices for the holder and writer.

Zakamouline, American option pricing and exercising with transaction costs, *J. Comput. Finance*, **8(3)** (2005).

Pros and cons of utility indifference method

Utility indifference formulation takes into consideration of the investors' risk preferences in terms of their utility functions.

The core idea of utility indifference method is utility maximization.

Mathematically, one needs to solve three-dimensional Hamilton-Jacobi-Bellman (HJB) equations corresponding to the investor's portfolios with or without an option.

Since an analytical solution is not attainable, the HJB equations have to be solved numerically.

The analysis in Zakamouline (2005) is insightful, but it is also very sophisticated and computationally expensive. As a result, a key aspect of the utility indifference pricing is to find an efficient numerical technique or approximate approach.

Our new utility indifference method

For a pricing method to work well in practice, it should not be too complicated.

To achieve a balance, we propose a new method based on utility maximization, following the discrete hedging idea to re-balance one's portfolio at regular interval only.

Yan and Lu (2021), Utility-indifference pricing of European options with proportional transaction costs, *Journal of Computational and Applied Mathematics*.

The key point in our approach is that we deduce the expected number of stocks traded in one time-step, instead of treating it as a process. This reduces the HJB equation to two dimensional for the portfolio without an option, thus, provides considerable time-savings.

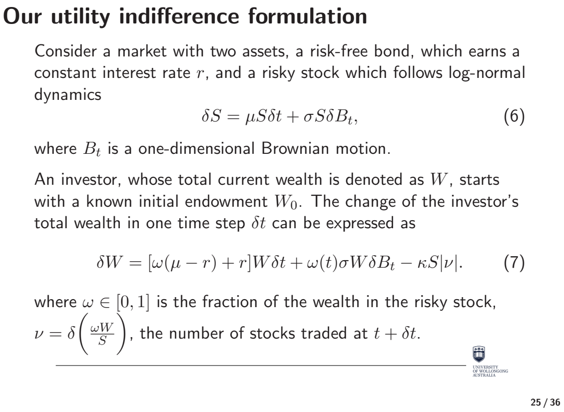

Our utility indifference formulation

Consider a market with two assets, a risk-free bond, which earns a constant interest rate r, and a risky stock which follows log-normal dynamics

$$\delta S = \mu S \delta t + \sigma S \delta B_t, \tag{6}$$

where B_t is a one-dimensional Brownian motion.

An investor, whose total current wealth is denoted as W, starts with a known initial endowment W_0. The change of the investor's total wealth in one time step δt can be expressed as

$$\delta W = [\omega(\mu - r) + r]W\delta t + \omega(t)\sigma W \delta B_t - \kappa S|\nu|. \tag{7}$$

where $\omega \in [0,1]$ is the fraction of the wealth in the risky stock, $\nu = \delta\left(\frac{\omega W}{S}\right)$, the number of stocks traded at $t + \delta t$.

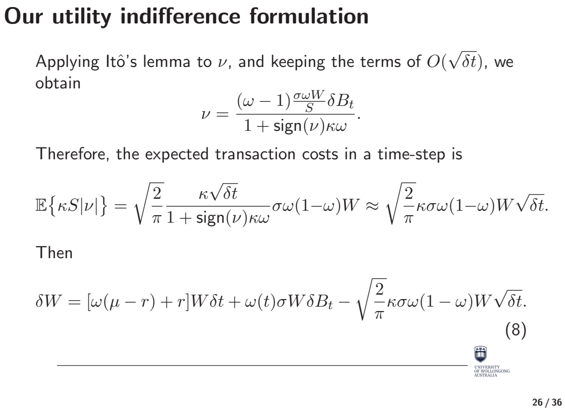

Our utility indifference formulation

Applying Itô's lemma to ν, and keeping the terms of $O(\sqrt{\delta t})$, we obtain

$$\nu = \frac{(\omega - 1)\frac{\sigma\omega W}{S}\delta B_t}{1 + \mathsf{sign}(\nu)\kappa\omega}.$$

Therefore, the expected transaction costs in a time-step is

$$\mathbb{E}\{\kappa S|\nu|\} = \sqrt{\frac{2}{\pi}}\frac{\kappa\sqrt{\delta t}}{1 + \mathsf{sign}(\nu)\kappa\omega}\sigma\omega(1-\omega)W \approx \sqrt{\frac{2}{\pi}}\kappa\sigma\omega(1-\omega)W\sqrt{\delta t}.$$

Then

$$\delta W = [\omega(\mu - r) + r]W\delta t + \omega(t)\sigma W \delta B_t - \sqrt{\frac{2}{\pi}}\kappa\sigma\omega(1-\omega)W\sqrt{\delta t}. \tag{8}$$

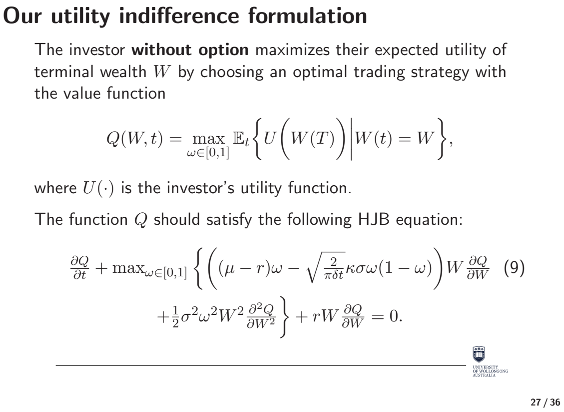

Our utility indifference formulation

The investor **without option** maximizes their expected utility of terminal wealth W by choosing an optimal trading strategy with the value function

$$Q(W,t) = \max_{\omega\in[0,1]} \mathbb{E}_t\left\{U\Big(W(T)\Big)\Big| W(t) = W\right\},$$

where $U(\cdot)$ is the investor's utility function.

The function Q should satisfy the following HJB equation:

$$\frac{\partial Q}{\partial t} + \max\nolimits_{\omega\in[0,1]}\left\{\left((\mu - r)\omega - \sqrt{\tfrac{2}{\pi\delta t}}\kappa\sigma\omega(1-\omega)\right)W\frac{\partial Q}{\partial W} \right. \tag{9}$$
$$\left. + \tfrac{1}{2}\sigma^2\omega^2W^2\frac{\partial^2 Q}{\partial W^2}\right\} + rW\frac{\partial Q}{\partial W} = 0.$$

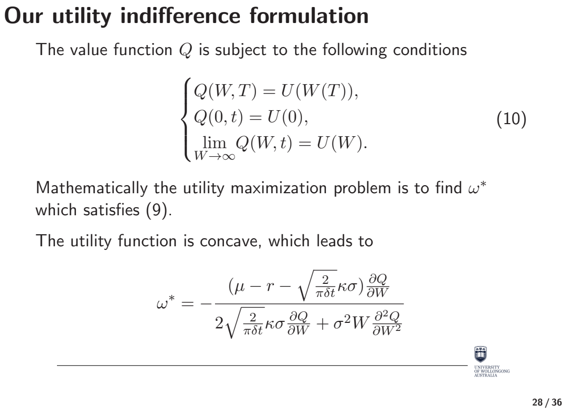

Our utility indifference formulation

The value function Q is subject to the following conditions

$$\begin{cases} Q(W,T) = U(W(T)), \\ Q(0,t) = U(0), \\ \lim\limits_{W\to\infty} Q(W,t) = U(W). \end{cases} \tag{10}$$

Mathematically the utility maximization problem is to find ω^* which satisfies (9).

The utility function is concave, which leads to

$$\omega^* = -\frac{(\mu - r - \sqrt{\frac{2}{\pi\delta t}}\kappa\sigma)\frac{\partial Q}{\partial W}}{2\sqrt{\frac{2}{\pi\delta t}}\kappa\sigma\frac{\partial Q}{\partial W} + \sigma^2 W\frac{\partial^2 Q}{\partial W^2}}$$

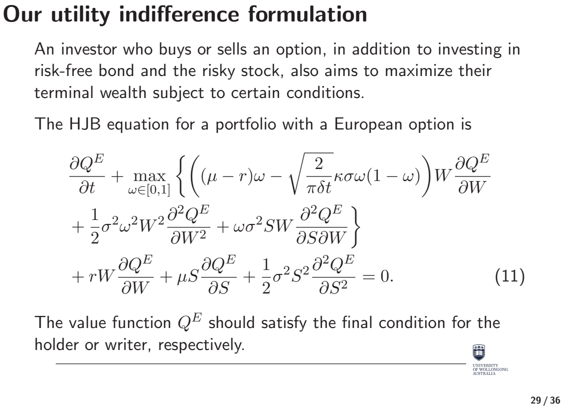

Our utility indifference formulation

An investor who buys or sells an option, in addition to investing in risk-free bond and the risky stock, also aims to maximize their terminal wealth subject to certain conditions.

The HJB equation for a portfolio with a European option is

$$\frac{\partial Q^E}{\partial t} + \max_{\omega\in[0,1]}\left\{\left((\mu - r)\omega - \sqrt{\frac{2}{\pi\delta t}}\kappa\sigma\omega(1-\omega)\right)W\frac{\partial Q^E}{\partial W}\right.$$
$$\left. + \frac{1}{2}\sigma^2\omega^2W^2\frac{\partial^2 Q^E}{\partial W^2} + \omega\sigma^2 SW\frac{\partial^2 Q^E}{\partial S\partial W}\right\}$$
$$+ rW\frac{\partial Q^E}{\partial W} + \mu S\frac{\partial Q^E}{\partial S} + \frac{1}{2}\sigma^2S^2\frac{\partial^2 Q^E}{\partial S^2} = 0. \tag{11}$$

The value function Q^E should satisfy the final condition for the holder or writer, respectively.

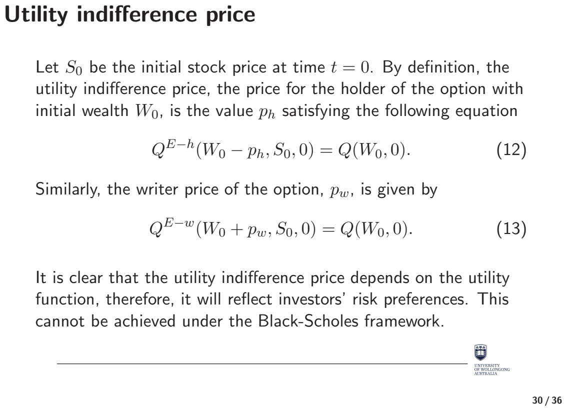

Utility indifference price

Let S_0 be the initial stock price at time $t = 0$. By definition, the utility indifference price, the price for the holder of the option with initial wealth W_0, is the value p_h satisfying the following equation

$$Q^{E-h}(W_0 - p_h, S_0, 0) = Q(W_0, 0). \tag{12}$$

Similarly, the writer price of the option, p_w, is given by

$$Q^{E-w}(W_0 + p_w, S_0, 0) = Q(W_0, 0). \tag{13}$$

It is clear that the utility indifference price depends on the utility function, therefore, it will reflect investors' risk preferences. This cannot be achieved under the Black-Scholes framework.

Utility indifference price for American options

The same principle applies for American options. However, due to the embedded optimality problem, not only we have to consider the portfolio for the holder and that for the writer separately, but also take into consideration if the holder would excise their right.

In utility indifference pricing, the holder takes the pay-off and continues to optimize the portfolio, whereas the writer pays the pay-off, also continues to optimize the portfolio until expiry.

As a result, the HJB system is more complicated, and much more calculations need to be done. Here we omit the lengthy equations, only present the results. More details can be found in

Lu, Yan, and Zhu (2022), Optimal exercise of American puts with transaction costs under utility maximization, *Applied Mathematics and Computation*.

Numerical examples

For our utility indifference approach, the following exponential utility is applied

$$U(y) = 1 - e^{-\lambda y},$$

where λ is a constant that represents the degree of risk preference, with $\lambda > 0$ being risk averse, $\lambda = 0$ risk-neutral, and $\lambda < 0$ risk seeking.

Unless otherwise mentioned, all of the calculations are carried out for the following parameters: the risk-less interest rate $r = 0.06$, volatility $\sigma = 0.45$, strike price $K = 10$, expiry $T = 0.5$ (years), hedging frequency $\delta t = \frac{1}{10}$(year) with various values of other parameters and initial values.

The HJB equations are solved by a policy iteration scheme.

Comparison of European put prices

Table 1: European put price for $\lambda = 0.05$, $\mu = 0.1$ and $\kappa = 0.08\%$.

S_0	B-S price	Holder price		Writer price	
		Hedging	Indifference	Hedging	Indifference
8	2.16882	2.16469	2.16864	2.17294	2.18112
9	1.56714	1.56202	1.56685	1.57224	1.57697
10	1.10312	1.09760	1.10278	1.10863	1.11031
11	0.76002	0.75464	0.75969	0.76539	0.76508
12	0.51476	0.50990	0.51447	0.51961	0.51819

It can be observed that the writer price and holder price deviate similar amount from the B–S price for hedging strategy, but the writer price in utility indifference pricing deviates more than the holder price from the B–S price.

Comparison of American put prices

Table 2: American put price for $\lambda = 0.05$, $\mu = 0.1$ and $\kappa = 0.08\%$.

S_0	B-S	Holder price		Writer price	
		Hedging	Indifference	Hedging	Indifference
8	2.24869	2.24495	2.24835	2.25234	2.25576
9	1.61421	1.60921	1.61380	1.61913	1.62054
10	1.13088	1.12535	1.13043	1.13634	1.13568
11	0.77643	0.77100	0.77599	0.78181	0.77985
12	0.52451	0.51959	0.52411	0.52939	0.52682

Similar trend for the writer and holder prices is observed for American options. This is because when the investor's risk preference is considered (utility indifference approach) the asymmetry between the writer and holder of an option contract is reflected in their prices.

Comparison of optimal exercise prices

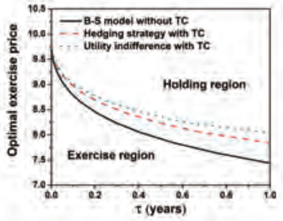

Figure 1: $\mu = 0.1$, $r = 0.02$, $\sigma = 0.2$, $\lambda = 0.1$, $T = 1$ and $\kappa = 1\%$.

The holder would exercise earlier with transaction costs.

Conclusion

- Pricing options with transaction costs (market incomplete) is more difficult than pricing without transaction costs (market complete), which is especially true for American options due to the holder's early exercise right.
- Utility indifference pricing is better in terms of optimization, taking into consideration of investors' risk preferences. But it involves lengthy computation, suitable for simple vanilla options whose prices depend only on stock price and time.
- Hedging strategy is easy to implement, suitable for options whose interest rate or stock volatility is also a random variable, for example, as in our paper
  Lu, Zhu & Yan (2021). Nonlinear PDE model for European options with transaction costs under Heston stochastic volatility. *Communications in Nonlinear Science and Numerical Simulation*.

Blackwell game and its applications in online prediction tasks

Kohei Hatano

Kyushu University / RIKEN AIP

We review the Blackwell game, which is a classical game and a multi-objective extension of the Von Neumann's min-max game, online convex optimization(OCO), the standard framework of online prediction in the machine learning literature, and discuss their relationship. Then we will show some examples of online prediction tasks such as online load balancing, which seemingly do not fit to OCO, can be reduced to Blackwell games and resulting algorithms.

Mutuality between AI and Optimization

Nguyen Dinh Hoa

International Institute for Carbon-Neutral Energy Research & Institute of
Mathematics for Industry Kyushu University, Japan

AI and optimization are often considered from different perspectives by different research communities. However, it is undeniable that they are closely related to each other, where optimization is a core part of many machine learning algorithms, while AI can be employed to support optimization schemes. This talk presents examples of such mutuality with illustrations in energy systems. Moreover, directions for future research are also introduced.

Mutuality between AI and Optimization

Nguyen Dinh Hoa

International Institute for Carbon-Neutral Energy Research
Institute of Mathematics for Industry
Kyushu University
Emails: hoa.nd@i2cner.kyushu-u.ac.jp, hoa@imi.kyushu-u.ac.jp

FMfI 2021
Hanoi, December 13–16, 2021

Outline

❑ **Introduction**
❑ **Optimization for AI**
❑ **AI for Optimization**
❑ **Conclusions**

Self Introduction

- **Education:**
  - 2010–2013: PhD, The University of Tokyo, Tokyo, Japan.
  - 2007–2009: MEng, Chulalongkorn University, Bangkok, Thailand.
  - 2002–2007: BSc (Talented Program), Hanoi University of Technology, Hanoi, Vietnam.
- **Career:**
  - 12/2021–now: Associate Professor, I^{2}CNER and IMI, Kyushu University, Fukuoka, Japan.
  - 11/2017–3/2018: Visiting Scholar, University of Illinois at Urbana-Champaign, USA.
  - 12/2016–12/2021: Assistant Professor, I^{2}CNER and IMI, Kyushu University, Fukuoka, Japan.
  - 1/2015–12/2016: Postdoctoral Researcher, Toyota Technological Institute, Nagoya, Japan.
  - 10/2013–1/2015, 10/2009–9/2010: Lecturer, Hanoi University of Technology, Hanoi, Vietnam.

My Research

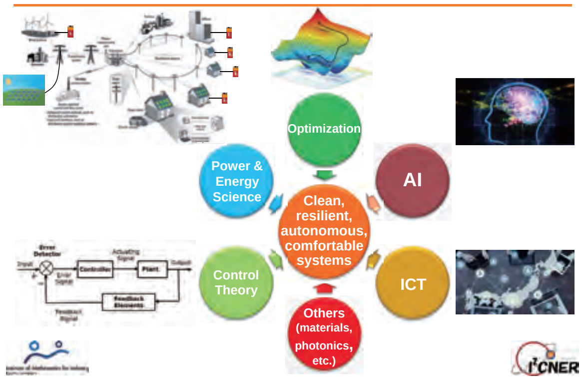

Outline

❑ Introduction
❑ **Optimization for AI**
❑ AI for Optimization
❑ Conclusions

Optimization for AI

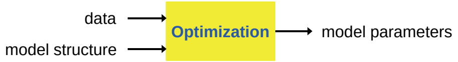

- Many AI algorithms aim to learn models or ‘relations’ (dynamics, behaviors, etc.), given a finite set of data $\{(x_i, y_i)\}_{i=1,\ldots,n}$.
- Central to those algorithms is to find optimal model parameters via solving

$$\min_{\theta} \frac{1}{n} \sum_{i=1}^{n} l(y_i, f_\theta(x_i))$$

$f_\theta(\cdot)$: model or relation to be found
θ: vector of parameters
$l(\cdot)$: loss function

Optimization for AI

$$\{(x_i, y_i)\}_{i=1,\dots,n} \longrightarrow \boxed{\min_{\theta} \frac{1}{n}\sum_{i=1}^{n} l(y_i, f_\theta(x_i))} \longrightarrow \theta$$

$$f_\theta(\cdot) \longrightarrow$$

- How to solve this programming and problem nature lead to different types of AI algorithms: centralized, decentralized, or fully decentralized (distributed).

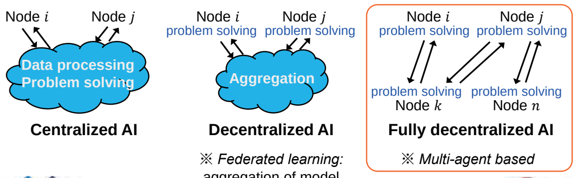

Centralized AI

Decentralized AI

※ *Federated learning:* aggregation of model parameters instead of data

Fully decentralized AI

※ *Multi-agent based*

Example 1: Electric Demand Prediction

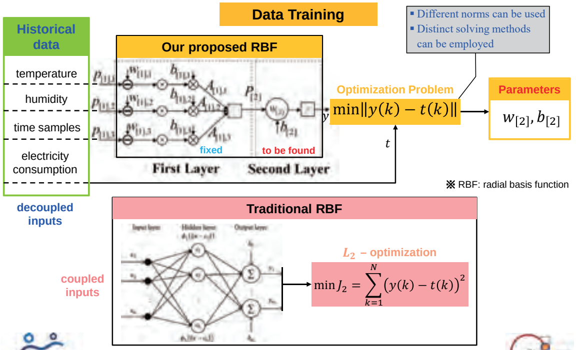

- Different norms can be used
- Distinct solving methods can be employed

※ RBF: radial basis function

A. T. Nguyen, D. H. Nguyen, "A Machine Learning-based Approach for The Prediction of Electricity Consumption", 2019 Asian Control Conference (ASCC 2019), Fukuoka, Japan.

Example 1: Electric Demand Prediction

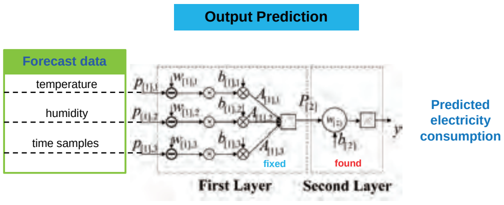

A. T. Nguyen, D. H. Nguyen, "A Machine Learning-based Approach for The Prediction of Electricity Consumption", 2019 Asian Control Conference (ASCC 2019), Fukuoka, Japan.

Example 1: Electric Demand Prediction

Model is trained using electric demand in Tokyo during 25/9 – 25/10/2018

$$\min|y(k) - t(k)|$$

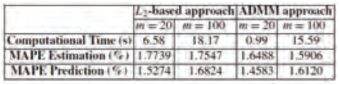

	L_2-based approach		ADMM approach	
	$m = 20$	$m = 100$	$m = 20$	$m = 100$
Computational Time (s)	6.58	18.17	0.99	15.59
MAPE Estimation (%)	1.7739	1.7547	1.6488	1.5906
MAPE Prediction (%)	1.5274	1.6824	1.4583	1.6120

※ ADMM: alternating direction method of multipliers

D. H. Nguyen, "L_1 Optimization for Sparse Structure Machine Learning Based Electricity Demand Prediction", in "Optimization in Large Scale Problems: Industry 4.0 and Society 5.0 Applications", Springer Optimization and Its Applications, Springer Nature Switzerland AG, 2019.

Example 1: Electric Demand Prediction

Electricity demand prediction for Tokyo on October 26, 2018

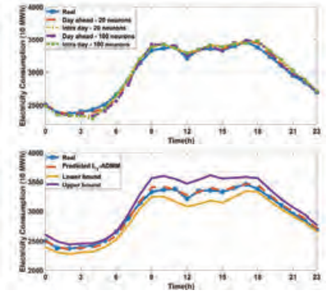

Prediction at different times and using different numbers of neurons

Prediction interval using standard deviation method

D. H. Nguyen, "L_1 Optimization for Sparse Structure Machine Learning Based Electricity Demand Prediction", in "Optimization in Large Scale Problems: Industry 4.0 and Society 5.0 Applications", Springer Optimization and Its Applications, Springer Nature Switzerland AG, 2019.

Example 2: Occupancy Analysis

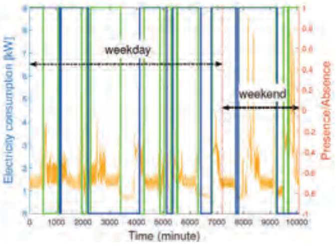

A dataset of electricity consumption and consumer occupancy

Feature vectors construction

SVM model training

Occupancy prediction

Useful for demand response and energy management strategies

D. H. Nguyen, "Residential Energy Consumer Occupancy Prediction based on Support Vector Machine", Sustainability, vol. 13(15), 8321, 2021.

Example 2: Occupancy Analysis

Essence of SVM

$$\max \sum_{i=1}^{m} \alpha_i - \frac{1}{2}\sum_{i,j=1}^{m} \alpha_i\alpha_j y_i y_j \underline{K(x_i, x_j)}$$

$\triangleq \phi(x_i)^T\phi(x_j)$: kernel

feature map

$$\text{s.t.} \sum_{i=1}^{m} \alpha_i y_i = 0$$

$$0 \le \alpha_i \le C, i = 1, \dots, m$$

New data are labeled by

$y = \mathrm{sgn}(\sum_{i=1}^{m} \alpha_i y_i K(x_i, x) + b)$

D. H. Nguyen, "Residential Energy Consumer Occupancy Prediction based on Support Vector Machine", Sustainability, vol. 13(15), 8321, 2021.

Example 2: Occupancy Analysis

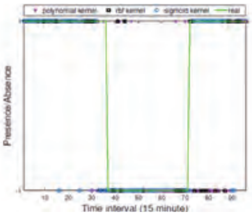

Kernel \ Index	Confusion matrix		Accuracy	Precision	TPR TNR	F₁-score	MCC	Balanced accuracy
polynomial	45	16	77.08%	88.24%	73.77%	80.36%	54.02%	78.72%
	6	29			82.86%			
sigmoid	51	10	89.58%	100%	83.61%	91.07%	80.64%	91.81%
	0	35			100%			
rbf	47	14	83.33%	95.92%	77.05%	85.46%	68.68%	85.67%
	2	33			94.29%			

D. H. Nguyen, "Residential Energy Consumer Occupancy Prediction based on Support Vector Machine", Sustainability, vol. 13(15), 8321, 2021.

Outline

- ❑ Introduction
- ❑ Optimization for AI
- ❑ **AI for Optimization**
- ❑ Conclusions

AI for Optimization

- A lot of optimization problems whose optimal spaces cannot be found analytically or in polynomial time (NP-hard), e.g., non-convex or combinatorial programming.
- **AI can be a useful aid to solution finding:**
  - Simulated annealing (SA)
  - Gaussian processes (GP)
  - Nature and bio-inspired algorithms (GA, PSO, ACO, etc.)
  - …

Example 3: Objective Function Parameter Learning

Energy trading between prosumers (<u>pro</u>ducer + con<u>sumer</u>)

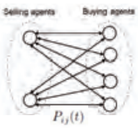

Time-varying, bipartite graph

$$\min \sum_{t=1}^{T}\sum_{i=1}^{n} C_i(P_i(t))$$ Objective function for a trading period

$$\text{s.t.} \quad P_{ij}(t) + P_{ji}(t) = 0 \; \forall \, j \in \mathcal{N}_i(t)$$ Bilateral trading constraint

$$P_{i,tr}^{\min} \le P_{i,tr}(t) = \sum_{j \in \mathcal{N}_i(t)} P_{ij}(t) \le P_{i,tr}^{\max}$$ Trading capacity constraint

$$P_{ij}(t) \le (\ge)\, 0 \text{ if peer } i \text{ is a seller (buyer) } \forall \, j \in \mathcal{N}_i(t)$$

$$C_i(P_i(t)) = a_i(t)P_{i,tr}^2(t) + b_i(t)P_{i,tr}(t) + \sum_{j \in \mathcal{N}_i} d_{ij}P_{ij}(t)$$

<u>Question:</u> How to ensure successful trading of all prosumers with preferred energy prices and amounts?

※ ***Answers are based on optimal solutions derived from KKT conditions***

D. H. Nguyen, "Optimal Solution Analysis and Decentralized Mechanisms for Peer-to-Peer Energy Markets", IEEE Transactions on Power Systems, vol. 36(2), pp. 1470-1481, 2021.

Answer 1: Heuristic Variation of Parameters

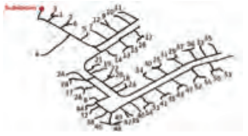

Diagram of the IEEE European Low Voltage Test Feeder

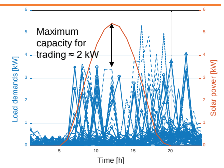

Maximum capacity for trading ≈ 2 kW

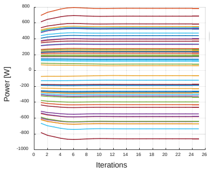

<u>Before learning</u>
Maximum traded power is << 2 kW available

<u>After learning</u>
Maximum traded power ≈ maximum capacity

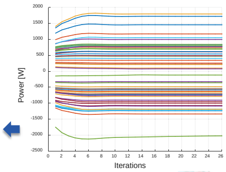

D. H. Nguyen, "Optimal Solution Analysis and Decentralized Mechanisms for Peer-to-Peer Energy Markets", IEEE Transactions on Power Systems, vol. 36(2), pp. 1470-1481, 2021.

Answer 2: Analytical Cooperative Learning

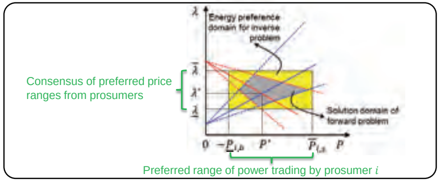

Consensus of preferred price ranges from prosumers

Preferred range of power trading by prosumer i

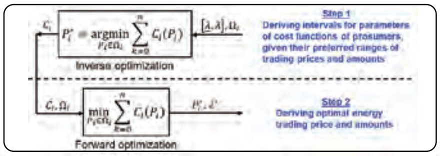

D. H. Nguyen, "A Cooperative Learning Approach for Decentralized Peer-to-Peer Energy Trading Markets And Its Structural Robustness Against Cyberattacks", IEEE Access, vol. 9, pp. 148862-148872, 2021.

Outline

- ❑ Introduction
- ❑ Optimization for AI
- ❑ AI for Optimization
- ❑ **Conclusions**

Conclusions

- ❑ Optimization is a core of many AI algorithms → finding better solving schemes for optimization problems will advance AI algorithms
- ❑ AI can be leveraged to help solve difficult optimization problems
- ❑ AI and optimization, together with data science, are essential parts in a lot of current and future systems and applications (energy, materials, biology, medicine, etc.) → blend to make the best use of them

Thank you for listening!

Q & A

Contact: hoa.nd@i2cner.kyushu-u.ac.jp

What can we find from Big Data with random Noise?

Jin Cheng

School of Mathematical Sciences, Fudan University & Shanghai Key Laboratory of Contemporary Applied Mathematics, China

The rapid development of science and technology has produced a large amount of data with random noise. How to extract useful information from big data effectively is one of the fundamental problems in artificial intelligence, machine learning and other fields. From the perspective view of mathematics, there are some essential difficulties to be overcome. We consider the following two kinds of problems, Problem 1: How to use a large number of data with "large" random errors to construct more accuracy functions; Problems 2: How to obtain useful information in some areas that cannot be observed or difficult to observe data.

To solve these two difficult problems, we obtain that: 1. Tikhonov regularization based theory and algorithms for big data with random noise. The "more" data can be used to reduce the noise level of the data; 2. Theory and algorithms of how to use the physical mechanism "differential equation"; to reconstruct the unknown function in the place where the data may not be observed or is difficult to observe. We can also construct the indicator functions which can be used to describe the accuracy between the approximate solution and the true solution.

Poster Session

Following the tradition of FMfI, we held a poster session this year as well. The poster session at FMfI has served as an ideal venue, especially for early-career researchers and students to get their work and themselves known by and receive comments from various people in academia and industry. However, it was challenging for both the organisers and the presenters to have a poster session online this year. Instead of placing posters on the wall, the presenters submitted PDF files describing their work, which were made downloadable online during the forum. Additionally, the presenters gave two-minute flash talks on the second day of the forum. The audience asked questions live to compensate for the lack of interaction over a cup of coffee. Most of the contribution was from postdocs and students, and it was an excellent opportunity for them to give a presentation for an international audience with various backgrounds. The topics ranged from purely-mathematical ones such as algebraic geometry to detailed statistical analysis of real data.

Out of 28 presentations, one best and four excellent posters were chosen by the votes of the jury. The following presenters were awarded the Best Poster Award and Excellent Poster Awards respectively at the closing ceremony.

・Best Poster Award
Modelling Housing Feature Impacts on Sale Price in Newly Developed Suburbs
Christina Yin-Chieh LIN, Department of Engineering Science, University of Auckland

・Excellent Poster Awards
Augmented Lagrangian Method for Convex Piecewise Linear-Quadratic Optimization Problems
NGUYEN Thi Van Hang, Department of Optimization and Control, Institute of Mathematics, Vietnam Academy of Science and Technology

Optimal control problem in linear elasticity
NGUYEN Quang Huy, School of Applied Mathematics and Informatics, Hanoi University of Science and Technology

The impact of extreme weather events on calorie intake – income relationship: semiparametric estimates for Vietnam
TRINH Huong Thi, Department of Mathematics and Statistics, Thuongmai University, Hanoi

Differential Geometry Formulation of Hanging Membranes
Yoshiki JIKUMARU, Institute of Mathematics for Industry, Kyushu University, Japan

Poster Session Committee Members
Shizuo Kaji and Nguyen Ha Nam

VIASM

Forum "Math-for-Industry" 2021
"Mathematics for the Digital Economy"

Vietnam Institute for Advanced Study in Mathematics, HANOI
December 13 - 16, 2021

BEST POSTER AWARD

Awarded to

Christina Yin-Chieh Lin

for presenting the poster entitled
"Modelling Housing Feature Impacts on Sale Price in Newly Developed Suburbs"

佐伯修
Osamu Saeki
IMI, KYUSHU UNIVERSITY

Zainal Aziz
PRESIDENT OF APCMFI

VIASM

Forum "Math-for-Industry" 2021
"Mathematics for the Digital Economy"

Vietnam Institute for Advanced Study in Mathematics, HANOI
December 13 - 16, 2021

EXCELLENT POSTER AWARD

Awarded to

Nguyen Thi Van Hang

for presenting the poster entitled
"Augmented Lagrangian Method for Convex Piecewise Linear-Quadratic Optimization Problems"

佐伯修
Osamu Saeki
IMI, KYUSHU UNIVERSITY

Zainal Aziz
PRESIDENT OF APCMFI

VIASM

Forum "Math-for-Industry" 2021
"Mathematics for the Digital Economy"

Vietnam Institute for Advanced Study in Mathematics, HANOI
December 13 - 16, 2021

EXCELLENT POSTER AWARD

Awarded to

Trinh Thi Huong

for presenting the poster entitled
"The impact of extreme weather events on calorie intake – income relationship: semiparametric estimates for Vietnam "

佐伯修
Osamu Saeki
IMI, KYUSHU UNIVERSITY

Zainal Aziz
PRESIDENT OF APCMFI

VIASM

Forum "Math-for-Industry" 2021
"Mathematics for the Digital Economy"

Vietnam Institute for Advanced Study in Mathematics, HANOI
December 13 - 16, 2021

EXCELLENT POSTER AWARD

Awarded to

Nguyen Quang Huy

for presenting the poster entitled
"Optimal control problem in linear elasticity"

佐伯修
Osamu Saeki
IMI, KYUSHU UNIVERSITY

Zainal Aziz
PRESIDENT OF APCMFI

VIASM

Forum "Math-for-Industry" 2021
"Mathematics for the Digital Economy"

Vietnam Institute for Advanced Study in Mathematics, HANOI
December 13 - 16, 2021

EXCELLENT POSTER AWARD

Awarded to

Yoshiki Jikumaru

for presenting the poster entitled
"Differential Geometry Formulation of Hanging Membranes"

佐伯修
Osamu Saeki
IMI, KYUSHU UNIVERSITY

Zainal Aziz
PRESIDENT OF APCMFI

Poster Session Contents

Density estimates for jump diffusion processes
Ngoc Khue TRAN

This poster has not been published. All the results of this poster are already published in "Applied Mathematics and Computation", 420 (2022), 126814.

Complex symmetry in Fock space
PHAM Viet Hai

This poster has not been published. All the results of this poster were taken from the paper "Hai, Pham Viet and Khoi, Le Hai, Complex symmetry of weighted composition operators on the Fock space. J. Math. Anal. Appl. 433 (2016), no. 2, 1757–1771 MR3398790".

On the non-connectivity of moduli spaces of line arrangements

Benoît Guerville-Ballé
IMI - Kyushu Univeristy, Japan
FMfI 2021, December 13-16, 2021

Moduli space of complex line arrangements

Definition

A line combinatorics $\mathcal{C} = (\mathcal{L}, \mathcal{P})$ is the data of an ordered finite set $\mathcal{L}$ and a subset $\mathcal{P}$ of the power set of $\mathcal{L}$ which verify:

- for all $P \in \mathcal{P}$, $\#P \geq 2$,
- for all $L_1, L_2 \in \mathcal{L}$, it exists a unique $P \in \mathcal{P}$ such that $L_1 \in P$ and $L_2 \in P$.

Line arrangements in $\mathbb{CP}^2$ are classically studied as **simpler case of singular plane algebraic curves**. They are defined as a finite collection of distinct lines in $\mathbb{CP}^2$. The incidence structure of a line arrangement $\mathcal{A} = \{L_1, \dots, L_n\}$, given by $\mathcal{P} = \{P \subset \mathcal{A} \mid \bigcap_{L \in P} L \neq \emptyset,\ \forall P \subsetneq Q \subset \mathcal{A},\ \bigcap_{L \in Q} L = \emptyset\}$, forms naturally a line combinatorics. This line combinatorics, is named the **combinatorics of** $\mathcal{A}$ and it is denoted by $\mathcal{C}(\mathcal{A})$. It can be described as the incidence graph $\Gamma_{\mathcal{A}}$ of the lines of $\mathcal{A}$, with vertices composed by the lines and singular points, joined by an edge if $P \in L$.

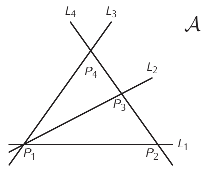

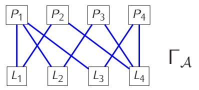

Definition

The *realization space* $R(\mathcal{A})$ of a line arrangement $\mathcal{A}$ (or of its combinatorics $\mathcal{C}(\mathcal{A})$) is the set of all arrangements which have isomorphic combinatorics, or equivalently whose incidence graphs are isomorphic to $\Gamma_{\mathcal{A}}$. The *moduli space* $\mathcal{M}(\mathcal{A})$ of $\mathcal{A}$ is the quotient of $R(\mathcal{A})$ by the action of $\mathrm{PGL}_3(\mathbb{C})$:

$$\mathcal{M}(\mathcal{A}) = \{\, \mathcal{B} \mid \mathcal{C}(\mathcal{B}) \sim \mathcal{C}(\mathcal{A}) \,\} \,/\, \mathrm{PGL}_3(\mathbb{C}).$$

Notation: The connected component of $\mathcal{M}(\mathcal{A})$ which contains the arrangement $\mathcal{A}$ is denoted by $\mathcal{M}(\mathcal{A})^{\mathcal{A}}$.

Main Question: How to construct arrangements or combinatorics which have a non-connected moduli space?

Small examples: Up to 7 lines, the moduli space of a line arrangement is path-connected. The first example of a line arrangement with a non-connected moduli space is the **MacLane arrangement** [1]. It is fomed by 8 lines each contains three triple points. For 9 line arrangements, see [2], there are three types of arrangements with a non-connected moduli space: those which contains a MacLane arrangement, the **Falk-Sturmfels arrangements** and the **Nazir-Yoshinaga arrangements**.

The splitting-polygon structure

Definition

- Let $\mathcal{C} = (\mathcal{L}, \mathcal{P})$ be a line combinatorics and let $3 \leq r \leq \#\mathcal{A}$. A *plinth* Ψ in $\mathcal{C}$ is form by two tuples: the *support* $S = (S_1, \dots, S_r) \subset \mathcal{L}$ and the *pivot-points* $(P_1, \dots, P_r) \subset \mathcal{P}$ such that, for each P_i, we have $S_i \notin P_i$ and $S_{i+1} \notin P_i$.

  A line arrangement $\mathcal{A}$ is said to have a plinth if its combinatorics does.
- A plinth Ψ is said to be projectively rigid in $\mathcal{M}(\mathcal{A})^{\mathcal{A}}$ (resp. in $\mathcal{M}(\mathcal{A})$), if for all arrangement $\mathcal{A}'$ in $\mathcal{M}(\mathcal{A})^{\mathcal{A}}$ (resp. in $\mathcal{M}(\mathcal{A})$), it exists a projective transformation $\tau \in \mathrm{PGL}_3(\mathbb{C})$ such that $\tau(S_i) = S'_i$ and $\tau(P_i) = P'_i$, for all $i \in \{1, \dots, r\}$.

Let $\mathcal{A}$ be a line arrangement such that, for a fixed integer $3 \leq r \leq \#\mathcal{A}$, the lines $(S_1, \dots, S_r) \in \mathcal{A}$ and the singular points $(P_1, \dots, P_r) \in \mathrm{Sing}(\mathcal{A})$ form a plinth Ψ.

- Q_1^λ is a generic point of S_1 which is determined by a parameter $\lambda \in \mathbb{C}$.
- E_1^λ is the line which passes through Q_1^λ and P_1.
- Q_2^λ is the intersection point of S_2 and E_1^λ.
- E_i^λ is the lines which passes through Q_i^λ and P_i.
- Q_{i+1}^λ is the intersection points of E_i^λ and S_{i+1}.
- R_1^λ is the intersection point of E_r^λ and S_1

We denote by A^λ the arrangement $\mathcal{A} \cup \{E_1^\lambda, \dots, E_r^\lambda\}$.

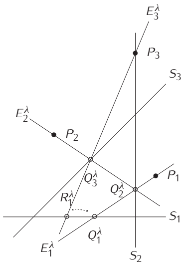

Definition

The tuple $E^\lambda = (E_1^\lambda, \dots, E_r^\lambda)$ forms a *splitting-polygon* on the plinth Ψ if:

1. $Q_1^\lambda = R_1^\lambda$,
2. for all $i, j \in \{1, \dots, n\}$, we have $E_i^\lambda \notin \mathcal{A}$, and $E_i^\lambda \neq E_j^\lambda$,
3. each line E_i^λ contains $\#\mathcal{A} + r - \#P_i - 2$ singular points in $\mathcal{A}^\lambda$.

Notation: The combinatorics of the arrangement $\mathcal{A}^\lambda$ is denoted by $\mathcal{C}(\mathcal{A})_\Psi$ when E^λ form a splitting-polygons on Ψ.

Theorem (____, [3])

Let $(S_1, \dots, S_r)$ and $(P_1, \dots, P_r)$ be a projectively rigid plinth Ψ of an arrangement $\mathcal{A}$ of $\mathcal{M}(\mathcal{A})^{\mathcal{A}}$. If E^{λ_1} and E^{λ_2} are two distinct splitting-polygons on Ψ, then $\mathcal{M}(\mathcal{C}(\mathcal{A})_\Psi)$ splits over $\mathcal{M}(\mathcal{A})^{\mathcal{A}}$.
More precisely, the line arrangements $\mathcal{A}^{\lambda_1}$ and $\mathcal{A}^{\lambda_2}$ are in different connected components of $\mathcal{M}(\mathcal{C}(\mathcal{A})_\Psi)$.

Applications

Let $\mathcal{A} = \{L_1, \dots, L_5\}$ be the arrangement of 5 lines defined by the equations:

$$\begin{array}{lll} L_1 : z = 0 & L_2 : x = 0 & L_3 : x - z = 0 \\ L_4 : y = 0 & L_5 : y - z = 0 & \end{array}$$

The line combinatorics of $\mathcal{A}$ is given by

$$\big\{\{L_1, L_2, L_3\}, \{L_1, L_4, L_5\}, \{L_2, L_4\}, \{L_2, L_5\}, \{L_3, L_4\}, \{L_3, L_5\}\big\}.$$

We consider on $\mathcal{A}$ the projectively rigid plinth Ψ defined by (L_1, L_2, L_4) for the support and $(\{L_3, L_4\}, \{L_3, L_5\}, \{L_2, L_5\})$ for the pivot-points.

Let $Q_1^\lambda = [1 : \lambda : 0]$ be a generic point of L_1. Following the previous construction, we deduce that the equations of E_1^λ, E_2^λ and E_3^λ are:

$$E_1^\lambda :\ \lambda x + y - \lambda z = 0, \quad E_2^\lambda :\ (1 - \lambda)x - y + \lambda z = 0, \quad E_3^\lambda :\ (\lambda - 1)x + \lambda y - \lambda z = 0.$$

The points Q_1^λ and R_1^λ are equal if and only if the lines L_1, E_1^λ and E_3^λ are collinear. Algebraically speaking, we have a splitting-triangle if and only if the following determinant vanishes.

$$\Delta_\Psi(\lambda) = \begin{vmatrix} 0 & \lambda & (\lambda - 1) \\ 0 & 1 & \lambda \\ 1 & -\lambda & -\lambda \end{vmatrix} = \lambda^2 - \lambda + 1.$$

Let $\lambda_1 = \frac{1+i\sqrt{3}}{2}$ and $\lambda_2 = \frac{1-i\sqrt{3}}{2}$ be the two roots of Δ_Ψ. The arrangements $\mathcal{A}^{\lambda_1}$ and $\mathcal{A}^{\lambda_2}$ share the same combinatorics $\mathcal{C}(\mathcal{A})_\Psi$ which is the MacLane combinatorics. By the previous Theorem, they lie in different connected components of the moduli space $\mathcal{M}(\mathcal{C}(\mathcal{A}_\Psi))$.

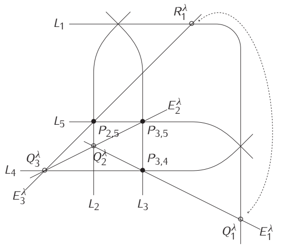

In addition of the MacLane arrangements, the splitting-polygons structure allows to reconstruct the Falk-Sturmfels arrangements and the Nazir-Yoshinaga arrangements.

Theorem (____, [3])

The tuples (L_1, L_2, L_4) and $\{\{L_3, L_4, L_6\}, \{L_1, L_6, L_8\}, \{L_2, L_5, L_8\}\}$ form a projectively rigid plinth Φ of the MacLane combinatorics.
The moduli space of the combinatorics $\mathcal{C}(\mathcal{A})_{\Psi,\Phi}$ is not path-connected and it admits 4 connected components.

References

[1] S. MacLane. *Some interpretations of abstract linear dependence in terms of projective geometry.* Am. J. Math., 58:236-240, 1936.

[2] F. Ye. *Classification of moduli spaces of arrangements of nine projective lines.* Pac. J. Math., 265(1):243-256, 2013.

[3] B. Guerville-Ballé *On the non-connectivity of moduli spaces of arrangements: the splitting-polygons structure.* arXiv:2111.00399.

Contact & Info:
ℹ www.benoit-guervilleballe.com
✉ benoit.guerville-balle@math.cnrs.fr

FLAT FAMILIES OF CYCLIC COVERS (OF CURVES)

Dang Quoc Huy
Vietnam Institute for Advanced Study in Mathematics

Wildly ramified covers of curves

We know from classical topology that the group $\pi_1(\mathbb{A}^1_{\mathbb{C}})$ is trivial. In algebraic geometry, the étale fundamental group π_1^{et} is the direct analog of π_1. For instance, if X is a connected scheme of finite type over $\mathbb{C}$, then $\pi_1^{\mathrm{et}}(X) \cong \widehat{\pi_1(X(\mathbb{C}))}$. Regarding positive characteristic, Grothendieck proved that every curve C over a field k of characteristic $p > 0$ lifts to a curve $\mathscr{C}$ over $W(k)$, hence in characteristic zero. Moreover,

$$(\pi_1^{\mathrm{et}}(C))^{p'} \cong (\pi_1^{\mathrm{et}}(\mathscr{C}_\eta))^{p'}$$

[3, XIII, Corollaire 2.12], where $(G)^{p'}$ denotes the "prime-to-p" part of a group G. However, the p-part of $\pi_1^{\mathrm{et}}(\mathbb{A}^1_k)$ is **no** longer trivial as there always exists an étale $\mathbb{Z}/p$-cover defined by the equation $y^p - y = x$. That cover, also known as an Artin-Schreier cover, is the simplest example of a *wildly ramified* Galois cover, which distinguishes characteristic p from characteristic zero.

Moduli space of Artin-Schreier curves

An Artin-Schreier (AS) curve is a $\mathbb{Z}/p$-Galois cover of the projective line over a field k in characteristic p. Any such cover, say $\phi : Y \to \mathbb{P}^1_k$, is defined by the equation

$$y^p - y = f(x) \in k(x).$$

Moreover, $f(x)$ is unique up to adding an element of the form $b^p - b$, where $b \in k(x)$. Hence, we might assume that $f(x)$ is "reduced". Suppose $\{P_1, \ldots, P_r\}$ is the set of poles of $f(x)$ in $\mathbb{P}^1_k$, and $d_j \not\equiv 0 \pmod p$ is the order of the pole of $f(x)$ at P_j. Then d_j is also the ramification jump at P_j, and

$$g_Y = \Big(\sum_{j=1}^{r}(d_j+1) - 2\Big)(p-1)/2, \tag{1}$$

is the genus of Y. Equation (1) shows that all the Artin-Schreier k-curves with the same genus g_Y have the same $\sum_{j=1}^{r}(d_j+1)$. We denote by $\mathcal{AS}_g$ the moduli space of Artin-Schreier curves of genus g.
The moduli space $\mathcal{AS}_g$ can be partitioned by locally closed strata corresponding to the partitions of $d+2$ [5]. In particular, the partition $\overrightarrow{E} = \{e_1, \ldots, e_r\}$ of $d+2$ is associated with the stratum $\Gamma_{\overrightarrow{E}}$, which is the collection of all the curves in $\mathcal{AS}_g$ which are branched at s number of points $\{P_1, P_2, \ldots, P_s\}$, with ramification jump $e_i - 1$ at P_i. The following well-known fact will relate the geometry of $\mathcal{AS}_g$ with equicharacteristic deformations of Artin-Schreier covers.

Equicharacteristic deformations and the geometry of $\mathcal{AS}_g$

Given two partitions $\overrightarrow{E}_1$ and $\overrightarrow{E}_2$ of $d+2$. The stratum $\Gamma_{\overrightarrow{E}_1}$ is contained in the closure of $\Gamma_{\overrightarrow{E}_2}$ if and only if there exists a deformation over $k[[t]]$ from a point in $\Gamma_{\overrightarrow{E}_1}$ to one in $\Gamma_{\overrightarrow{E}_2}$.

Therefore, equal characteristic deformations between Artin-Schreier curves give full information about the geometry of the moduli space $\mathcal{AS}_g$! For example, suppose $p = 5$ and $g = 14$. One can explicitly construct some deformations between the curves in different stata of $\mathcal{AS}_{14}$ (see [1, Theorem 3.7]) to obtain the following diagram.
There is an edge between two strata if one is contained in the closure of the other. Hence, it follows from the diagram that the moduli space $\mathcal{AS}_{14}$ is connected. Moreover, the irreducible components of $\mathcal{AS}_{14}$ are the closures of the following strata: $\Gamma_{\{5,4\}}$,$\Gamma_{\{3,3,3\}}$, $\Gamma_{\{4,3,2\}}$, $\Gamma_{\{5,2,2\}}$, and $\Gamma_{\{3,2,2,2\}}$. Furthermore, the intersection of $\overline{\Gamma}_{\{3,3,3\}}$ and $\overline{\Gamma}_{\{3,2,2,2\}}$ is $\Gamma_{\{9\}}$, the intersection of $\overline{\Gamma}_{\{4,3,2\}}$ and $\overline{\Gamma}_{\{5,2,2\}}$ is $\Gamma_{\{7,2\}}, \ldots$

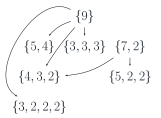

The moduli space of $\mathcal{AS}_{14}$

Differential Hurwitz Tree

Thanks to a local-global principle, it suffices to study the good reduction of the formal disc over $R := k[[t]]$'s covers! Suppose we are given an order-p-cover of the disc. One can derive from that action a minimal semi-stable model for which the specializations of the fixed points are distinct and lie in the smooth locus of the special fiber. Moreover, one can enrich the dual graph of the model with the *depth Swan conductor* and the *differential conductor* (see [4, Definition 3.2.10]) of each component of the special fiber. The description leads to a combinatorial-differential object called a *differential Hurwitz tree*. For instance, suppose χ is a $\mathbb{Z}/5$-action that arises from the Galois group of the extension

$$y^5 - y = \frac{x + 2t^{10}}{x^5(x - t^{10})^2(x - t^5)^5} =: f(x,t).$$

Then the Hurwitz tree associated with χ has the following form.

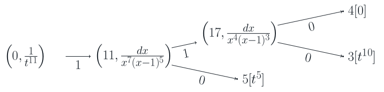

We say the above tree is of *type* $\{12\} \to \{4,3,5\}$. At each vertex v of the tree, the first component of the dual is the depth Swan conductor at the boundary of the disc corresponds to v. If the depth is positive, the second component is the differential conductor at the boundary of the disc. When the depth is 0, the second component is a polynomial in $k[x^{-1}]$, which represents the *degeneration type* of χ. The rational number below each edge e is the "thickness" of the corresponding annulus. The integer at a leaf is the conductor (the ramification-jump-plus-one) of the corresponding branch point.

Exact Hurwitz tree and equicharacteristic deformations

Suppose $\overrightarrow{E}_1 = \{e\} \prec \overrightarrow{E}_2 = \{e_1, \ldots, e_r\}$. Then there is a deformation from each curve of $\Gamma_{\overrightarrow{E}_1}$ to a curve of $\Gamma_{\overrightarrow{E}_2}$ if and only if there exists a differential Hurwitz tree of type $\{e\} \to \{e_1, \ldots, e_r\}$.

The above result implies that the equicharacteristic deformations problem can be translated to the exact Hurwitz tree problem. By studying exact differential forms (in characteristic $p > 0$), we obtain the following result (c.f. [1, Theorem 1.1] [2, Theorem 1.2]).

The connectedness of the moduli space

The moduli space $\mathcal{AS}_g$ is connected when g is sufficiently large. In particular,

1. When $p = 2, 3$, the moduli space $\mathcal{AS}_g$ is connected for any g.
2. When $p = 5$, $\mathcal{AS}_g$ is connected for any $g \geq 14$ and $g = 0, 2$. It is disconnected otherwise.

Toward the moduli space of cyclic covers

Similarly, a $\mathbb{Z}/p^n$-cover $\phi_n : Y_n \to \mathbb{P}^1_k$ can be represented by

$$\wp(y_1, \ldots, y_n) = \big(f_1(x), \ldots, f_n(x)\big) \in W_n(k(x))$$

where $\wp(y) := F(x) - x$ is the Artin-Schreier-Witt isogeny. Suppose $\{P_1, \ldots, P_r\}$ is the set of poles of the f_i's. Then the degree of the different at P_j is

$$\deg(\mathscr{D}_{P_j}) = \sum_{i=1}^{n}(\iota_{j,i}+1)(p^i - p^{i-1}) \tag{2}$$

where $\iota_{j,i}$ is the i-th upper jump at P_j. It follows from (2) that $\mathbb{Z}/p^n$-covers of fixed genus on each sub-cover have the same $d_i := \sum_{j=1}^{r}(\iota_{j,i}+1)$. We hence use an $r \times n$ matrix as below to record the ramification data of the cover.

$$\begin{bmatrix} \iota_{1,1}+1 & \iota_{1,2}+1 & \ldots & \iota_{1,n}+1 \\ \iota_{2,1}+1 & \iota_{2,2}+1 & \ldots & \iota_{n,n}+1 \\ \ldots & \ldots & \ldots & \ldots \\ \iota_{r,1}+1 & \iota_{r,2}+1 & \ldots & \iota_{r,n}+1 \end{bmatrix}$$

Denote by $\mathcal{ASW}_{d_1,\ldots,d_n}$ the moduli space of $\mathbb{Z}/p^n$-covers whose j-th sub-covers have $\sum_{i=1}^{j} d_i(p^i - p^{i-1})$ as the degree of the different. The moduli space can be partitioned into strata which are parameterized by $r \times n$ matrices like the one above! In addition, by generalizing the Hurwitz tree technique, we prove the following.

Cyclic covers deform in towers

Suppose $\phi : Z \to X$ is a cyclic G-Galois cover of curves over k, and $\psi : Y \to X$ is its H-Galois sub-cover (where H is a quotient of G). Suppose, moreover, that $\Psi : \mathcal{Y}_R \to \mathcal{X}_R$ is a deformation of ψ over a complete discrete valuation R of characteristic p. Then there exists a deformation $\Phi : \mathcal{Z}_R \to \mathcal{X}_R$ of ϕ over R that contains Ψ as a sub-cover. That is, one can always fill in the following commutative diagram of cyclic covers,

$$\begin{tikzcd}
\operatorname{Spec} k \arrow[d] & X \arrow[l] \arrow[d] & Y \arrow[l, "\psi"'] \arrow[d] & Z \arrow[l, "\lambda"'] \arrow[d, dotted] \\
\operatorname{Spec} R & \mathcal{X} \arrow[l] & \mathcal{Y} \arrow[l, "\Psi"] & \mathcal{Z} \arrow[l, dotted, "\Lambda"]
\end{tikzcd}.$$

In particular, the canonical morphism $\mathcal{ASW}_{d_1,\ldots,d_m,d_{m+1},\ldots d_n} \to \mathcal{ASW}_{d_1,\ldots,d_m}$ maps closures surjectively to closures.

References

[1] Huy Dang. "Connectedness of the moduli space of Artin-Schreier curves of fixed genus". In: *Journal of Algebra* 547 (2020), pp. 398–429. ISSN: 0021-8693. DOI: `https://doi.org/10.1016/j.jalgebra.2019.11.034`. URL: `http://www.sciencedirect.com/science/article/pii/S0021869319306659`.

[2] Huy Dang. "Hurwitz trees and deformations of Artin-Schreier covers". In: *arXiv e-prints*, arXiv:2002.03719 (Feb. 2020), arXiv:2002.03719. arXiv: `2002.03719 [math.AG]`.

[3] Alexander Grothendieck. *Revêtements étales et groupe fondamental. Fasc. I: Exposés 1 à 5*. Vol. 1960/61. Séminaire de Géométrie Algébrique. Institut des Hautes Études Scientifiques, Paris, 1963, iv+143 pp. (not consecutively paged) (loose errata).

[4] Shigeki Matsuda. "On the Swan conductor in positive characteristic". In: *Amer. J. Math.* 119.4 (1997), pp. 705–739. ISSN: 0002-9327. URL: `http://muse.jhu.edu/journals/american_journal_of_mathematics/v119/119.4matsuda.pdf`.

[5] Rachel Pries and Hui June Zhu. "The *p*-rank stratification of Artin-Schreier curves". In: *Ann. Inst. Fourier (Grenoble)* 62.2 (2012), pp. 707–726. ISSN: 0373-0956. DOI: `10.5802/aif.2692`. URL: `http://dx.doi.org/10.5802/aif.2692`.

The impact of extreme weather events on calorie intake – income relationship Semiparametric estimates for Vietnam

Huong T. TRINH[1,2*], Michel SIMIONI[3], Huyen T. N. NGUYEN [1], Loan T. T. NGUYEN [4], Anh T. V TO[5]

[1]Thuongmai University, Hanoi, [2]Vietnam Institute for Advanced Studies in Mathematics
[3]INRA, UMR 1110 MOISA, Montpellier, France
[4]Hanoi National University of Education [5]Ministry of Education and Training

[*]trinhthihuong@tmu.edu.vn

A. INTRODUCTION

- A huge literature has been devoted to the estimation of the relationship between food con-sumption measured in calories and household income.
- Most of these countries are now affected by climate change and experience more and more frequent extreme weather events.
- This climate dimension has never been taken into account when estimating the calorie-intake and income relationship.

Main contribution

- The semiparametric modeling is a powerful tool in estimating nonlinear relationship such as that linking calorie-intake to income.
- We estimate additive semiparametric specifications of the calorie intake and income relationship: the linking calorie-intake to income and its interacts it with extreme weather events.

B.METHOD

We use two kinds of semiparametric regression models:

$$\mathbb{E}(log(Y)) = \alpha_0 + s(log(HHINC)) + \Sigma_{k=1}^{3} s(Extreme_k) + \Sigma_j \beta_j X_j$$

$$\mathbb{E}(log(Y)) = \alpha_0 + s(log(HHINC)) + \Sigma_{k=1}^{3} s(Extreme_k, log(HHINC)) + \Sigma_j \beta_j X$$

where Y is per capita macronutrients.

C. DATASET

- Six waves of the Vietnam Household Living Standard Survey, or VHLSS: 2010, 2012, 2014, 2016 and 2018.
- Food consumption (kg) ⇒ Kilocalories (household levels) ⇒ transfer to per capita macronutrient.
- Household incomes.
- Extreme weather events (flood, typhoon, drought): as dummy variables and the duration between the occurrence of the extreme event and the time at which the household was surveyed.
- Focus on rural area in Vietnam.

E. DISCUSSION

- The number of households in rural areas effected by disasters have increased from 2010 to 2016, especially drought event in 2016 due to "El Nio" event in 2016.
- The results highlight the non-linear relationship between macronutrients and income: It is strongly increasing for low income levels and that becomes increasing with a much lower slope or even constant from a certain income threshold.
- The effects of flood and typhoon are direct and immediate for households, while households who experienced drought take more time to recovery.
- Households with higher income are more resilient to natural disasters.
- The results raise the importance of the long-run policies on economic growth to strengthen resilience of rural households sustainably, especially under the digital economy, climate change and infectious diseases.

H. REFERENCES

1.Arouri, M., Nguyen, C., & Youssef, A. B. (2015). Natural disasters, household welfare, and resilience: evidence from rural Vietnam. World development, 70, 59-77
2. Trinh, H. T., Simioni, M., & Thomas-Agnan, C. (2018). Assessing the nonlinearity of the calorie-income relationship: An estimation strategy–With new insights on nutritional transition in Vietnam. World Development, 110, 192-204.
3. Wood, S. N. (2017). Generalized additive models: an introduction with R. CRC press.

D. RESULTS

Figure: Percentage of household experienced extreme event and by years

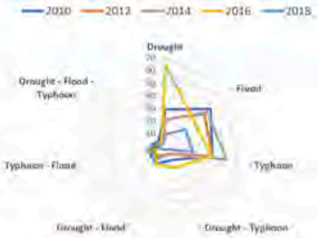

Figure: GAM model of Per capita calorie intake

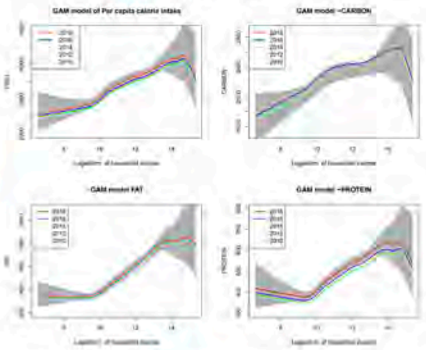

Figure: GAM model 3 D

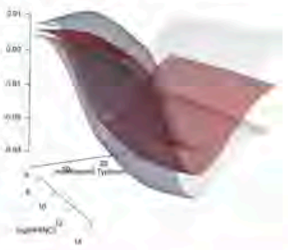

FMfI, VIASM - Hanoi 2021 Forum "Math-for-Industry" 2021 "Mathematics for Digital Economy" December 13-16, 2021

Optimality conditions based on the Fréchet second-order subdifferential

Duong Thi Viet An [1] and Nguyen Dong Yen [2]

[1]Thai Nguyen University of Sciences, Thai Nguyen city, Vietnam
[2]Institute of Mathematics, Vietnam Academy of Science and Technology, Hanoi, Vietnam

Optimization Problem

Let X be a Banach space, $C \subset X$ and $f : X \to \mathbb{R}$ a function. Consider the problem

$$\min\{f(x) \mid x \in C\}. \tag{P}$$

Motivating Results

- **Theorem 1** ([5, Theorem 3.45]) Let $X = \mathbb{R}^n$. Suppose that $\bar{x} \in C$ is a local solution of (P) and f is twice continuously differentiable at $\bar{x}$. Then
$$\langle \nabla f(\bar{x}), v\rangle \geq 0,\ \forall v \in T_C(\bar{x}), \tag{1}$$
and for every $v \in T_C(\bar{x})$ such that $\langle \nabla f(\bar{x}), v\rangle = 0$, we have
$$\langle \nabla f(\bar{x}), w\rangle + \langle \nabla^2 f(\bar{x})v, v\rangle \geq 0 \quad \forall w \in T_C^2(\bar{x}, v), \tag{2}$$
where $T_C(\bar{x})$ is the tangent cone to C at $\bar{x}$ and $T_C^2(\bar{x}, v)$ is the second-order tangent set to C at $\bar{x}$ in direction v (see the definitions in [5, Chapter 3]).
- **Theorem 2** ([3, Theorem 3.3]) Consider the problem (P) with $C = X$. Suppose that $\bar{x}$ is a local solution of (P) and there exists $\ell > 0$ satisfying
$$||\nabla f(x) - \nabla f(\bar{x})|| \leq \ell ||x - \bar{x}||$$
for all x in some neighborhood of $\bar{x}$. Then $\nabla f(\bar{x}) = 0$ and the Fréchet second-order subdifferential $\widehat{\partial}^2 f(\bar{x})$ (see the definition in [4, p. 122]) is positive semi-definite, i.e., $\langle z, u\rangle \geq 0$ for any $u \in X$ and $z \in \widehat{\partial}^2 f(\bar{x})(u)$.

Our Contributions

- For problems in the classical setting, where f is twice continuously differentiable, we show that strengthened second-order necessary optimality conditions are valid if C is generalized polyhedral convex (see the definition in [2, p. 133]).
- For problems in a new setting, where f is just assumed to be differentiable and C is generalized polyhedral convex, we establish sharp second-order necessary optimality conditions based on the Fréchet second-order subdifferential of f and the second-order tangent set to C.

Main Results

Theorem 3 ([1, Theorem 3]) Let C be a generalized polyhedral convex set in a Banach space X. If $\bar{x}$ is a local solution of (P), then (1) holds, and the conditions
(i) $\langle \nabla f(\bar{x}), w\rangle \geq 0$ for all $w \in T_C^2(\bar{x}, v)$, where $v \in T_C(\bar{x})$ is such that $\langle \nabla f(\bar{x}), v\rangle = 0$,
(ii) $\langle \nabla^2 f(\bar{x})v, v\rangle \geq 0$ for every $v \in T_C(\bar{x})$ satisfying $\langle \nabla f(\bar{x}), v\rangle = 0$
are fulfilled.

Theorem 4 ([1, Theorem 5]) Assume that $\bar{x}$ is a local solution of (P), where C is a generalized polyhedral convex set. Suppose that there exists a constant $\ell > 0$ such that
$$||\nabla f(x) - \nabla f(\bar{x})|| \leq \ell ||x - \bar{x}|| \tag{3}$$
for every x in some neighborhood of $\bar{x}$. Then, (1) is valid and, for each $v \in T_C(\bar{x})$ such that $-v \in T_C(\bar{x})$ and $\langle \nabla f(\bar{x}), v\rangle = 0$, one has
$$\langle \nabla f(\bar{x}), w\rangle \geq 0 \tag{4}$$
and
$$\langle z, v\rangle \geq 0 \tag{5}$$
for any $w \in T_C^2(\bar{x}, v)$ and $z \in \widehat{\partial}^2 f(\bar{x})(v)$.

Remarks

1. If C is not a generalized polyhedral convex set, then the assertions (i) and (ii) of Theorem 3 may not hold anymore.
2. Theorem 4 asserts that inequality (5) holds for any $z \in \widehat{\partial}^2 f(\bar{x})(v)$ if the critical direction v satisfies the *additional condition* $-v \in T_C(\bar{x})$.

Open Questions

- **Open Question 1:** When f is just assumed to be differentiable and C is not a generalized polyhedral convex set, how to verify necessary optimality condition for (P) by using Fréchet second-order subdifferential?
- **Open Question 2:** Is it possible to obtain a sufficient optimality condition by using Fréchet second-order subdifferential for (P)?

References

[1] An, D.T.V., Yen, N.D.: Optimality conditions based on the Fréchet second-order subdifferential. *Journal of Global Optimization*, 81, 351–365 (2021)

[2] Bonnans, J.F., Shapiro, A.: Perturbation Analysis of Optimization Problems. Springer, New York (2000)

[3] Chieu, N.H., Lee, G.M., Yen, N.D.: Second-order subdifferentials and optimality conditions for C^1-smooth optimization problems. *Applied Analysis and Optimization*, 1, 461–476 (2017)

[4] Mordukhovich, B.S.: Variational Analysis and Generalized Differentiation, Volume I: Basic Theory. Springer, Berlin (2006)

[5] Ruszczynski, A.: Nonlinear Optimization. Princeton University Press, New Jersey (2006)

About the Presenter

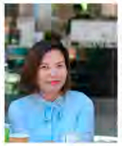

- Since 11/2011: Lecturer, Thai Nguyen University of Sciences, Thai Nguyen, Vietnam
- 01/2021–12/2022: Researcher, Postdoctoral Fellowship at Hangzhou Dianzi University, Hangzhou, China
- 10/2019–10/2020: Researcher, IM-Simons Postdoctoral Fellowship at Institute of Mathematics, VAST, Hanoi, Vietnam
- 07/2014 – 07/2018: Ph.D. student, Institute of Mathematics, VAST, Hanoi, Vietnam.

Supervisor: Prof. Dr.Sc. Nguyen Dong Yen

Dr. Duong Thi Viet An (TNUS)   Optimality conditions based on the Fréchet second-order subdifferential   Email: andtv@tnus.edu.vn

An algorithm for counting the number of solutions for brick Wang tiling

Yang Hang, Graduate School of Mathematics, Kyushu university, yang.hang.685@s.kyushu-u.ac.jp

Abstract

Wang tiling problem is an important problem in Graph Theory and Combinatorics. Brick Wang tiling [3] is a problem in the range of Wang tiling with permissive restrictions, and in many situations there exist multiple solutions. We develop an algorithm to get the specific number of valid solutions of brick Wang tiling. We discuss the validity conditions of the method. We use Mathematica to implement our algorithm and check the data.

1 Wang Tile

correct Wang tiling

incorrect Wang tiling

A Wang tile is a square tile with each edge colored. An edge in a Wang tile is also called a leg. Wang tiles are pasted side by side to form a tile graph. In a tiling problem, adjacent tiles must have the same color on the shared leg.
The tiling problem was first introduced by Hao Wang in 1961 [5]. He discussed the question whether an infinite plane can or cannot be covered by a given set of Wang tiles as described above.
Lately, Wang tiling problem is studied widely and aperiodic Wang tile sets that tile the plane were discovered [4,6]. Some special types of Wang tile, such as brick Wang tile, were illustrated in [3].

2 Application of Wang Tile

Wang tiling has applications in computer graphics [7] . Generating wall patterns is one of its applications [2]. Brick Wang tiles are a special set of Wang tiles introduced by Derouet-Jourdan in 2016 to model wall patterns. In their algorithm, a set of proper fractions is regarded as color set and the border of bricks is determined by proper fractions [2]. In [3] the result is generalized by providing a linear algorithm to decide and solve the tiling problem for arbitrary planar regions with holes.

computer graphics

wall patterns generated by Wang tile

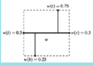

reflection

3 Brick Wang tiling Problem

A Brick Wang tile is a Wang tile with one pair of opposite legs of the same color and the other pair of different colors.

brick Wang tile

non-brick Wang tile

A Brick Wang tiling Problem consists of:
1 a tile graph T_G
2 a color set C
3 valid prototile set $W = \{w, e, s, n | w, e, s, n \in C, (w = e \wedge s \neq n) \vee (w \neq e \wedge s = n)\}$
In tiling problem we assign colors to legs to ensure that prototiles formed by 4 legs of each tile are in the prototile set, that also means to ensure each tile is a brick Wang tile.
Our target is to enumerate the specific number of valid solutions in a certain Brick Wang Tiling problem.
We also have the following problem setting:
1. Color set={ red , blue , green }
2. Boundary legs [1] are colored in advance.
3. Tile graph is connected.

This tile graph has 6 valid tilings

4 Model and tools

The enumeration vector ($N_l = (r_l, b_l, g_l)$) is introduced to describe the possibilities that one leg can be tiled by red, blue or green respectively [1].
We define operations on vectors. A special operation is ¬ ($\neg N_l = (b_l + g_l, r_l + g_l, r_l + b_l)$ when $N_l = (r_l, b_l, g_l)$) is used to describe the situation where one leg must have a different color from its opposite leg.

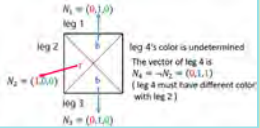

Matrices composed by enumeration vectors are used to denote the paths composed of a series of uncolored legs. Two objects (paths, circles, etc.) are equivalent as long as they have the same matrix. Hence we reduce the number of circles in a tile graph by replacing one circle with its equivalent path.

References

[1] H. Yang, Brick Wang tiling problem and its enumeration (unpublished)
[2] A. Derouet-Jourdan, M. Salvati, T. Jonchier, Generating Stochastic Wall Patterns On-the-fly with Wang Tiles, EUROGRAPHICS 2019 Volume 38(2) 255-265 (2019), DOI: 10.1111/cgf.13635
[3] A. Derouet-Jourdan, S. Kaji, Y. Mizoguchi, A linear algorithm for Brick Wang tiling, Japan Journal of Industrial and Applied Mathematics (2019)36:749C761
[4] E. Jeandel, M. Rao, An aperiodic set of 11 Wang tiles (2015), arXiv:1506.06492
[5] H. Wang, Proving theorems by pattern recognition-II. Bell Syst Tech J 40(1), 1-41 (1961)
[6] K. Culik II, An aperiodic set of 13 Wang tiles. Discrete Math, 160(1C3), 245C251 (1996)
[7] M.F Cohen., J. Shade., S. Hiller, O. Deussen., Wang tiles for image and texture generation. ACM Trans. Graph.22(3), 287C294 (2003)
[8] T. Matsushima, Y. Mizoguchi, A. Derouet-Jourdan, Verification of a brick Wang tiling algorithm, EPiC Series in Computing Volume 39, 107–116 (2016).

5 Our results

Lemma 1 *Assume that 1,2,3,4 are the four legs of one tile. We can get the vector* N_4 *corresponding to the leg 4 by the formula* $N_4 = (N_1 N_3)\ (\neg N_2) + (\neg N_1 N_3)\ N_2$ *if we know the vectors* N_1, N_2, N_3 *corresponding to the legs 1,2,3 respectively. (We assume leg 2 is opposite to leg 4 . In formula* $N_1 N_3$ *is the inner product.)*

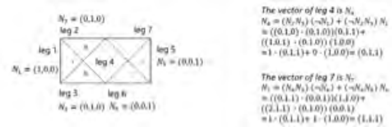

Lemma 2 *A circle is equivalent to a path described by matrix* M_{O1O2}

$$= \begin{bmatrix} tr(M_1F_{r1}M_2F_{r2}) & tr(M_1F_{r1}M_2F_{b2}) & tr(M_1F_{r1}M_2F_{g2}) \\ tr(M_1F_{b1}M_2F_{r2}) & tr(M_1F_{b1}M_2F_{b2}) & tr(M_1F_{b1}M_2F_{g2}) \\ tr(M_1F_{g1}M_2F_{r2}) & tr(M_1F_{g1}M_2F_{b2}) & tr(M_1F_{g1}M_2F_{g2}) \end{bmatrix}$$

where tr *is the trace of matrix.*

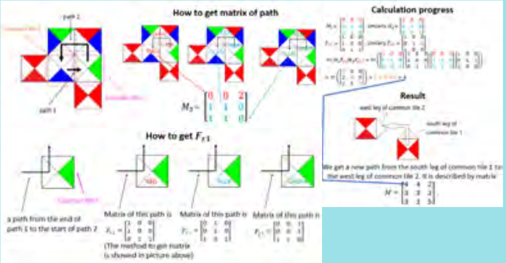

Proposition 3 *The number of valid solutions is* $N_u N_v$ *when* N_u *and* N_v *are different vectors of one certain (shared) leg got from different sides.*
Proposition 4 *The number of valid solutions is* $tr(M)$ *when there is only one circle described by matrix* M.

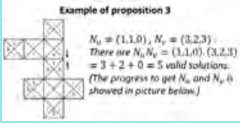

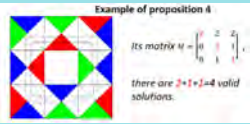

Algorithm 5a *When a tile Graph is a tree, we choose a leg* $u\ v$ *(subjectively) and let this leg divide the tree into two smaller trees. We get their vectors* $N_u\ N_v$ *by Applying Lemma 1 repeatedly. utilize Proposition 3 to get the number of valid solutions.*

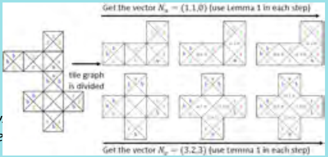

N_u and N_v are get by this progress linearly

Algorithm 5b *If there exist circles, then we apply Lemma 2 repeatedly and reduce the number of circles until there is only one circle. Then by Proposition 4 we get the number of valid solutions.*

6 Conclusion

1. We formalized a brick Wang tiling problem and introduced an algorithm for counting the number of solutions.
2. We introduced an enumeration vector and its operations for counting solutions formally. We showed the correctness of our algorithms using graph theory.
3. We implemented our algorithm using Mathematica.

7 Future works

1. The correctness of our algorithm is showed only for a limited class of graphs. We need to extend the target class of graphs and prove its correctness.
2. We will prepare a formal proof of our algorithm using a formal theorem prover system such as Coq [8] .
3. We are considering an application area for a formal verified class of Wang tile patterns using a brick Wang tiling.

The ground state of the semi-relativistic Pauli-Fierz Hamiltonian

Takeru Hidaka
(Institute of Mathematics for Industry Kyushu University, Japan)
Email: t-hidaka@imi.kyushu-u.ac.jp

Abstract

The existence of the ground state for the massless semi-relativistic Pauli-Fierz model in quantum electrodynamics is considered.

(Joint work with F. Hiroshima and I. Sasaki)

This work was supported by, JSPS KAKENHI Grant Number JP16H03942, JP20H01808, JP16K17612 and JSPS KAKENHI Grant Number JP20K03628.

Background

We are interested in the spectrum of Hamiltonians of quantum field theory. The existence of the ground state implies the stability of quantum systems.

Definition of ground states

A ground state Φ is an eigenvector of the Hamiltonian associated with the minimum of the spectrum E. E is called the ground state energy. By definition,
(ψ,Hψ)≧E(ψ, ψ) (∀ψ), HΦ=EΦ, Φ≠0.
Here (ψ,Φ) stands for the inner product ψ and Φ.

Particle-field interaction models

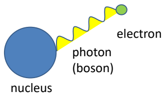

Let H_P and $H_{f,m}$ be a particle Hamiltonian and a free field Hamiltonian respectively, where m is an artificial mass of boson. The decoupled Hamiltonian, $H_{0,m}$, is given by

$$H_{0,m} = H_P \otimes 1 + 1 \otimes H_{f,m}.$$

The spectrum of $H_{0,m}$ is well known.

Spectrum of $H_{0,m}$

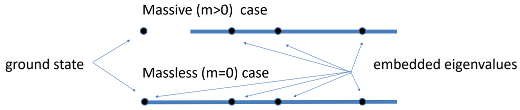

Add interaction

Spectrum of an Hamiltonian for a particle-field interaction model

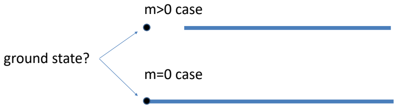

Perturbation for embedded eigenvalues is not trivial.

Strategy

1. Define a Hamiltonian as a self-adjoint operator acting in a given Hilbert space.
2. Prove the existence of ground states when m>0.

   $m\to0^+$
3. Prove the existence of ground states when m=0.

Nonrelativistic Pauli-Fierz model

The Pauli-Fierz Hamiltonian describes low energy electrons minimally coupled to a quantized radiation field A. The Hamiltonian is given by

$$H = \frac{1}{2M}(p \otimes 1 - A)^2 + V \otimes 1 + 1 \otimes H_{f,m}$$

and the existence of the ground state of H for all m≧0 is shown in [GLL 01].

Nelson model

The Nelson model describes a system of quantum mechanical particles linearly coupled to a scalar Bose field. The Hamiltonian of the Nelson model is of the form

$$H = \left(\frac{1}{2M}p^2 + V\right) \otimes 1 + 1 \otimes H_{f,m} + \phi.$$

No ground states exist if an infrared regular condition is failed and m=0 [Hirok 06].

Semi-relativistic Pauli-Fierz model

The semi-relativistic Pauli-Fierz (SRPF) Hamiltonian is defined by

$$H = \sqrt{(p \otimes 1 - A)^2 + M^2} + V \otimes 1 + 1 \otimes H_{f,m}.$$

The existence of the ground state of the SRPF Hamiltonian is initially proven by Könenberg, Matte and Stockmeyer for *M>0* and *m≧0* [KMS 11]. We show that H is the self-adjoint operator for all M≧0 and m≧0 in [HH 15]. When *m>0*, the existence of the ground state Φ_m for some confining potentials is proven in [HH16], and it is also shown that Φ_m decays exponentially [Hir 14]. The SRPF Hamiltonian has two singularities: **m=0** and **M=0.** We consider the massless SRPF Hamiltonian:

$$H = |p \otimes 1 - A| + V \otimes 1 + 1 \otimes H_{f,m=0}.$$

The existence of the ground state for the massless SRPF Hamiltonian is proven in [HH21]. The uniqueness of the ground state is shown by [Hir 14].

References

[GLL 01] M. Griesemer, E. H. Lieb and M. Loss, Ground states in non-relativistic quantum electrodynamics, *Invent. Math.* **145** (2001) 557--595.
[HH 15] T. Hidaka and F. Hiroshima, Self-adjointness of the semi-relativistic Pauli-Fierz Hamiltonian, *Rev. Math. Phys*. **27** (2015) 1550015 18pp.
[HH 16] T. Hidaka and F. Hiroshima, Spectrum of the semi-relativistic Pauli-Fierz model I, *J. Math. Anal. Appl.* **437** (2016) 330--349.
[HHS 21] T. Hidaka, F. Hiroshima and I. Sasaki, Spectrum of the semi-relativistic Pauli-Fierz model II, to appear in *J. Spectr. Theory*.
[Hirok 06] M. Hirokawa, Infrared catastrophe for Nelson's model—non-existence of ground state and soft-boson divergence, *Publ. Res. Inst. Math. Sci.* **42**, (2006) 897–922.
[Hir 14] F. Hiroshima, Functional integral approach to semi-relativistic Pauli-Fierz models, *Adv. Math.* **259** (2014) 784--840.
[KMS 11] M. Könenberg, O. Matte and E. Stockmeyer, Existence of ground states of hydrogen-like atoms in relativistic QED I: The semi-relativistic Pauli-Fierz operator, *Rev. Math. Phys.* **23** (2011) 375--407.

FEM Study on the Elastic Deformation Process of Materials in Industry

Phuong Cuc Hoang[1], Thi Thanh Mai Ta[2]
HANOI UNIVERSITY OF SCIENCE AND TECHNOLOGY
School of Applied Mathematics and Informatics
`cuc.hp185332@sis.hust.edu.vn, mai.tathithanh@hust.edu.vn`

1. Introduction

Elastic deformation is a temporary deformation when a material is subjected to force within its elastic limits. This means that the shape of the material reverses itself after the removal of force or load. The study of elastic deformation is a matter of concern in the industry to make objective assessments of the structure of the material.
Weak Formulation in Hilbert Space: Let V be a Hilbert space, α be a continuous bilinear form on $V \times V$,i.e., $\alpha \in \mathcal{L}(V \times V; \mathbb{R})$ and L be a continuous linear form on V,,i.e. $L \in \mathcal{L}(V; \mathbb{R})$. Find $\mathbf{u} \in V$ such that:

$$\alpha(\mathbf{u}, \mathbf{v}) = L(\mathbf{v}) \qquad \forall \mathbf{v} \in V.$$

Finite Element Method: is a powerful numerical method that uses computational power to calculate approximate solutions of structural mechanics problems. It is widely used in all majors engineering industries.
The FEM approaches this problem by splitting the body into a number of small elements that are connected together at nodes. This process is called *discretization* and the collection of nodes and elements is called *the mesh*. Discretization is useful because the equilibrium requirement now only needs to be satisfied over a finite number of discrete elements, instead of continuously over the entire body.

2. Setting of the problem

We have the domain: $\Omega \subset \mathbb{R}^2$ and $f : \Omega \to \mathbb{R}^2$.
Let $\mathcal{A}(\mathbf{u}) : \Omega \to \mathbb{R}^{2,2}$ be the *stress tensor*.
Let $\varepsilon(\mathbf{u}) : \Omega \to \mathbb{R}^{2,2}$ be the *strain rate tensor* defined as:

$$\varepsilon(\mathbf{u}) = \frac{1}{2}(\nabla \mathbf{u} + \nabla \mathbf{u}^T).$$

According to Hooke's law, the stress tensor is related to the strain rate tensor by the relation:

$$\mathcal{A}(\mathbf{u}) = \lambda tr(\varepsilon(\mathbf{u}))\mathcal{I} + 2\mu\varepsilon(\mathbf{u}),$$

where λ and μ are the so-called *Lamé coefficients*, and $\mathcal{I}$ is the identity matrix.
We have:

- The coefficient $(\lambda + \frac{2}{3}\mu)$ describes the compressibility of the medium; very large values correspond to almost incompressible materials.
- *Young modulus* E and *Poisson coefficient* ν:
  $$E = \mu\frac{3\lambda + 2\mu}{\lambda + \mu} \quad \text{and} \quad \nu = \frac{1}{2}\frac{\lambda}{\lambda + \mu}.$$
  Or:
  $$\mu = \frac{E}{2(1+\nu)} \quad \text{and} \quad \lambda = \frac{E\nu}{(1+\nu)(1-2\nu)}.$$
- The Poisson coefficient is such that $-1 \leq \nu < \frac{1}{2}$, and owing to the assumption $\lambda \geq 0$, we infer $\nu \geq 0$. An almost incompressible material corresponds to a Poisson coefficient very close to $\frac{1}{2}$.

The equilibrium conditions under the external load f can be expressed as:

$$div(\mathcal{A}(\mathbf{u})) + f = 0 \quad in \quad \Omega.$$

Adding boundary conditions, we get a **linear elastic equation system**:

$$\begin{cases} -div(\mathcal{A}(\mathbf{u})) = f & in \quad \Omega, \\ \mathbf{u} = 0 & on \quad \Gamma_D, \\ \mathcal{A}(\mathbf{u})n = g_N & on \quad \Gamma_N. \end{cases}$$

3. Numerical method

Variational formulation
Take the scalar product of the equilibrium equation with a test function $\mathbf{v} : \Omega \to \mathbb{R}^2$:

$$-\int_\Omega div(\mathcal{A}(\mathbf{u})).\mathbf{v}\mathrm{d}x = \int_\Omega f.\mathbf{v}\mathrm{d}x.$$

Apply Green's formula:

$$-\int_\Omega div(\mathcal{A}(\mathbf{u})).\mathbf{v}\mathrm{d}x = \int_\Omega \mathcal{A}(\mathbf{u}).\nabla\mathbf{v}\mathrm{d}x - \int_{\partial\Omega} \mathbf{v}.\mathcal{A}(\mathbf{u})n\mathrm{d}s.$$

We have $\mathbf{u} = 0$ on Γ_D:

$$\int_\Omega \mathcal{A}(\mathbf{u}).\nabla\mathbf{v}\mathrm{d}x = \int_\Omega f.\mathbf{v}\mathrm{d}x + \int_{\Gamma_N} g_N.\mathbf{v}\mathrm{d}s.$$

And:

$$\mathcal{A}(\mathbf{u}) = \lambda tr(\varepsilon(\mathbf{u}))\mathcal{I} + 2\mu\varepsilon(\mathbf{u}) = \lambda div(\mathbf{u})\mathcal{I} + 2\mu\varepsilon(\mathbf{u}).$$

Therefore:

$$\int_\Omega \mathcal{A}(\mathbf{u}).\nabla\mathbf{v}\mathrm{d}x = \int_\Omega 2\mu\varepsilon(\mathbf{u}) : \varepsilon(\mathbf{v})\mathrm{d}x + \lambda div\mathbf{u}div\mathbf{v}\mathrm{d}x.$$

The weak formulation of elastic equation:
Seek $\mathbf{u} \in (H^1_{\Gamma_D}(\Omega))^d$ such that:

$$\alpha(\mathbf{u}, \mathbf{v}) = L(\mathbf{v}) \quad \forall \mathbf{v} \in (H^1_{\Gamma_D}(\Omega))^d,$$

with the continuous bilinear form:

$$\alpha(\mathbf{u}, \mathbf{v}) = \int_\Omega 2\mu\varepsilon(\mathbf{u}) : \varepsilon(\mathbf{v})\mathrm{d}x + \lambda div\mathbf{u}.div\mathbf{v}\mathrm{d}x,$$

and the continuous linear form:

$$L(\mathbf{v}) = \int_\Omega f.\mathbf{v}\mathrm{d}x + \int_{\Gamma_N} g_N.\mathbf{v}\mathrm{d}s.$$

The mesh

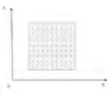

A triangulation is generated on Ω using $buildmesh$ function. This computational domain is regular and its elements have no inner common vertices. The geometric angles of the triangle > 0, and as the edge of the triangle move towards 0, the area of triangles also gradually moves toward 0.

4. Assembling the stiffness matrices

The basic formulation is:

$$\{F\} = [K].\{\mathbf{u}\},$$

where:

- $\{F\}$ is the force vector that also includes moments.
- $[K]$ is the stiffness matrix of the entire structure - global stiffness matrix.
- $\{\mathbf{u}\}$ is the vector of displacements.

The global stiffness matrix is constructed by assembling individual element stiffness matrices.
According to *Maxwell's Reciprocity Theorem*, the stiffness matrix is symmetric.

5. Numerical experiments

The parameters

No.	Materials	E (MPa)	ν
1	Aluminum	0.69 E+5	0.33
2	Steel	0.20 E+6	0.291

Deformation of the bridge under the influence of gravity
Steel Material

Aluminum Material

Deformation of the swing arm machine under the force applied to the rim of the part
Steel Material

Aluminum Material

Deformation of the material composite bar under the influence of gravity

(a) Original (b) Aluminum (c) Steel

(a) (b) (c)

(a) Original.
(b) Circle is steel, outside is aluminum.
(c) Circle is aluminum, outside is steel.

6. Conclusion and perspective

- When the object is acted on by the same force of equal magnitude, it will cause other deformations depending on the Young modulus E of the object.
- Objects with high E have less deformation than objects with low E.
- We can combine multiple materials in one object to improve the performance of the product.

7. Forthcoming Research

We will develop the study of the elastic deformation of objects made from a variety of materials with complex shapes in 2D, 3D and applications in industry.

8. Acknowledgements

The authors wish to express our gratitude to the Vietnam Institute for Advanced Study in Mathematics (VIASM) and University Kyushu, Japan for giving us the precious opportunity to present our research.

References

[1] Alexandre Ern and Jean-Luc Guermond, *Theory and Practice of Finite Elements*, volume 159 of Applied Mathematical Sciences. Springer, New York, 2004.

[2] Roberto Font and Francisco Periago, *The Finite Element Method with FreeFEM++ for beginners*, 2013.

[3] FreeFEM Documentation, *A system of the elasticity*.

The complexity of the parity argument with potential

Takashi Ishizuka
Graduate School of Mathematics, Kyushu University, Japan
ishizuka.takashi.664@s.kyushu-u.ac.jp

Introduction

Computational Complexity for Search Problems :
We are interested in the complexity class $\mathtt{TFNP}$ (Total Functions in $\mathtt{NP}$).

Every search problem in $\mathtt{TFNP}$ satisfies the following

TOTALITY: For every input, a solution always exists.
CHECKABLITY: Checking the correctness of each solution is easy.

The class $\mathtt{PPAD}$ is a subclass of $\mathtt{TFNP}$ and closely related to Game Theory [Das09, Pap94, Yan09]. EndofLine is a $\mathtt{PPAD}$-complete problem.

EndofLine [Pap94]

Input:
- An implicit digraph with potential $G(1, m, S, P, V) = (\Sigma^n, E)$

Task: Find a string $x \in \Sigma^n$ satisfying one of the following:
- $P((S(x)) \neq x$;
- $S(P(x)) \neq x \neq \pi$.

The blue vertex is a known source. The red vertices are solutions.

Overview of Complexity Class $\mathtt{TFNP}$

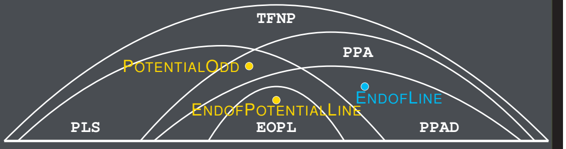

Related Works:
Goldberg and Hollender [GH18] showed that the following variants of EndofLine have the same complexity:
- given k sources and $l \neq k$ sinks, find another sink or source;
- given k sources, k sinks or k other souces.

Our Contribution:
- We show that the following variants of EndofPotentialLine, defined below, have the same complexity:
  - given k sources, find another degree-1 vertex or a non-increasing arc;
  - given k sources, find k distinct vertices that are at least one of a sink, other source, and a non-increasing arc.
- We consider the complexity of weighted variants of Odd, called PotentialOdd.

Basics

Complexity Class TFNP:
We consider a polynomial-time computable and polynomial-balanced relation $R \subseteq \{0,1\}^* \times \{0,1\}^*$:
- We can decide whether $(x, y) \in R$ in $\mathtt{P}$ for all (x, y); and
- For each $(x, y) \in R$, $|y| \leq \mathrm{poly}(|x|)$.

R has totality if for each $x \in \{0,1\}^*$, there is a $y \in \{0,1\}^*$ s.t. $(x, y) \in R$.

Total Search problem R

Input: a string $x \in \{0,1\}^*$
Task: Find a string $y \in \{0,1\}^*$ such that $(x, y) \in R$.

Polynomial-time reduction:
Let R, Q be search problems.
R is reducible to Q, denoted by $R \leq_P Q$, iff there are two polynomial-time computable functions f and g such that
- for every input x of R, $f(x)$ is an input of Q;
- for each solution y to Q w.r.t. $f(x)$, $g(x, y)$ is a solution to R w.r.t. x.

Complete Problem:
Let $\mathcal{C}$ be a complexity class.
A search problem R is $\mathcal{C}$-complete iff $R \in \mathcal{C}$ and $Q \leq_P R \ \forall Q \in \mathcal{C}$.

Complexity Class EOPL:
The class of all problems that are reducible to EndofPotentialLine.

EndofPotentialLine [FGMS20]

Input:
- An implicit digraph with potential $G(1, m, S, P, V) = (\Sigma^n, E)$
- A known source $\pi \in \Sigma^n$ s.t. $S(\pi) \neq \pi = P(\pi)$ and $V(\pi) = 1$

Task: Find a string $x \in \Sigma^n$ satisfying one of the following:
- $P((S(x)) \neq x$;
- $S(P(x)) \neq x \neq \pi$;
- $S(x) \neq x, P((S(x))) = x$, and $V(S(x)) - V(x) \leq 0$.

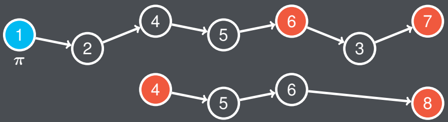

The blue vertex is a known source. The red vertices are solutions.

Main Results [Ish21]

Multiple-Source EndofLine

Input:
- An implicit digraph with potential $G(1, m, S, P, V) = (\Sigma^n, E)$
- A set $\Pi \subseteq \Sigma^n$ s.t. $\forall \pi \in \Pi$, $S(\pi) \neq \pi = P(\pi)$ and $V(\pi) = 1$

Task: Find a string $x \in \Sigma^n$ satisfying one of the following:
- $P((S(x)) \neq x$;
- $S(P(x)) \neq x \neq \pi$;
- $S(x) \neq x, P((S(x))) = x$, and $V(S(x)) - V(x) \leq 0$.

Theorem
- Multiple-Source EndofLine is also $\mathtt{EOPL}$-complete,

i.e., this problem has the same complexity as EndofPotentialLine.

PotentialOdd

Input:
- An implicit graph $G(d, m, N, V) = (\Sigma^n, E)$
- an odd-degree vertex $\pi \in \Sigma^n$

Task: Find a vertex $x \in \Sigma^n$ satisfying one of the following:
- $x \neq \pi$ and x has odd-degree;
- $V(x) \geq V(y)$ for every $y \in N(y)$ with $\{x, y\} \in E$;
- $V(x) \leq V(y)$ for every $y \in N(y)$ with $\{x, y\} \in E$.

Theorem
- If $d \leq 3$, then PotentialOdd is $\mathtt{EOPL}$-complete.
- If $d \geq 4$, then PotentialOdd is $\mathtt{PPA} \cap \mathtt{PLS}$-complete.

References

[Das09] C. Daskalakis. “Nash equilibria: Complexity, symmetries, and approximation,” Comput. Sci. Rev., Vol. 3(2), pp.87-100, 2009.
[FGMS20] J. Fearnley, S. Gordon, R. Mehta, and R. Savani. “Unique end of potential line,” J. Comput. Syst. Sci., Vol. 114, pp.1-35, 2020.
[GH18] P. W. Goldberg and A. Hollender. “The Hairy ball problem is PPAD-complete,” J. Comput. Syst. Sci., Vol. 122, pp.33-62, 2021.
[Ish21] T. Ishizuka. “The complexity of the parity argument with potential,” J. Comput. Syst. Sci., Vol.120, pp.12-41, 2021.
[Pap94] C. Papadimitriou. “On the Complexity of the Parity Argument and Other Inefficient proofs of Existence,” J. Comput. Syst. Sci., Vol. 48(3), pp.498-532, 1994.
[Yan09] M. Yannakakis. “Equilibrium, fixed points, and complexity classes,” Comput. Sci. Rev., Vol. 3(2), pp.71-85, 2009.

The work was partly supported by JSPS KAKENHI Grant Number 21J10845, Japan.

Differential Geometry Formulation of Hanging Membranes

Yoshiki Jikumaru (Institute of Mathematics for Industry, Kyushu University, y-jikumaru@imi.Kyushu-u.ac.jp)
Joint work with Yohei Yokosuka (Kagoshima University)

1. Introduction

Antoni Gaudi, famous for his design of the Sagrada Familia, proposed a mechanically efficient structure obtained by “a reversed hanging chain”.

Previous research of hanging membranes (surfaces):

1. Structures: A. Gaudi (Sagrada Familia, 1880’s [6]), H. Isler (roof design, 1960’s [4])
2. A well-known method: Thrust Network Analysis [3]

In our poster: we consider hanging membranes with “good” mechanical properties, and related numerical analysis


Sagrada Familia (Façana de la Passió) [6]

2. Hanging chains (catenary, classical)

$X:[\alpha,\beta]\to R^2, X(s)=(x(s),z(s))$, s : arclength,
$\boldsymbol{e}=X'$: unit tangent, ν: unit normal
$\boldsymbol{T}=T\boldsymbol{e}$: internal force along tangent direction
$\boldsymbol{q}$: loading per unit length (constant vector)

Equilibrium equation: $-\boldsymbol{T}+(\boldsymbol{T}+d\boldsymbol{T})+\boldsymbol{q}ds=\boldsymbol{0} \Leftrightarrow \frac{d\boldsymbol{T}}{ds}+\boldsymbol{q}=\boldsymbol{0}$

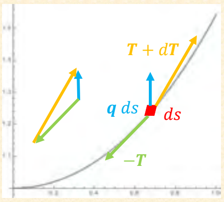

Equilibrium of force (chain)


Gateway arch, St. Louis Missouri, the United States [7]

Equilibrium equation for the hanging chain

Internal stress resultant: $T+\langle\,\boldsymbol{q},X\,\rangle=const.$
Equilibrium equation: $\kappa(\langle\boldsymbol{q},X\rangle+b)\ -\langle\boldsymbol{q},\nu\rangle=0$
(κ: curvature of X)

Variational principle for the hanging chain

Functional: $E(X)=\int_\alpha^\beta(\langle\boldsymbol{q},X\rangle+b)ds$
$X_\varepsilon=X+\varepsilon\cdot\delta X+O(\varepsilon^2)$: variation of X

$$\delta E=-\int_\alpha^\beta(\kappa(\langle\boldsymbol{q},X\rangle+b)-\langle\boldsymbol{q},\nu\rangle)\,\langle\nu,\delta X\rangle ds$$

*Exact solution: $q=(0,\gamma)\Longrightarrow z=\frac{T_0}{\gamma}\cosh\frac{\gamma}{T_0}\,x$

3. Hanging membranes [1]

$X:M\to R^3, X=X(x,y)$: immersion (surface in $\mathbb{R}^3$)
$I=A_1^2dx^2+A_2^2dy^2$: 1st fundamental form
$e_1=X_x/A_1$, $e_2=X_y/A_2$: unit tangent, $\nu=e_1\times e_2$: unit normal
$\boldsymbol{T}^{(1)}=TA_2\boldsymbol{e}_1dy, \boldsymbol{T}^{(2)}=TA_1\boldsymbol{e}_2dx$: in-plane stress resultants
$\boldsymbol{q}$: loading per unit area (constant vector)

Equilibrium equation: $\boldsymbol{T}_x^{(1)}dx+\boldsymbol{T}_y^{(2)}dy+\boldsymbol{q}dA=0$

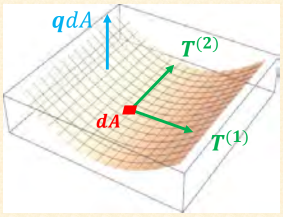

Equilibrium of force (membrane)


Casa Mila [8]

Equilibrium equation for the hanging membrane

In-plane stress resultant: $T+\langle\,\boldsymbol{q},X\,\rangle=const.$
Equilibrium equation: $2H(\langle\boldsymbol{q},X\rangle+b)\ -\langle\boldsymbol{q},\nu\rangle=0$
(H: mean curvature of X)

Variational principle for the hanging membrane

Functional: $E(X)=\int_M(\langle\boldsymbol{q},X\rangle+b)dA$
$X_\varepsilon=X+\varepsilon\cdot\delta X+O(\varepsilon^2)$: variation of X

$$\delta E=-\int_M(2H(\langle\boldsymbol{q},X\rangle+b)-\langle\boldsymbol{q},\nu\rangle)\langle\nu,\delta X\rangle d\mathrm{A}$$

4. Numerical analysis for hanging membranes

Equilibrium equation in conformal coordinates: $(-(\langle\boldsymbol{q},X\rangle+b)X_x)_x+\big(-(\langle\boldsymbol{q},X\rangle+b)X_y\big)_y+\boldsymbol{q}A_1A_2=0$

“discretization”

Our discretized equation [1]:

$$\sum_{j:\,adjacent\ to\ i} w_{ij}(X_j-X_i)+\boldsymbol{q}\ =\boldsymbol{0}$$

$$w_{ij}=-\frac{1}{A_i}\left(\left\langle\boldsymbol{q},\frac{X_i+X_j}{2}\right\rangle+b\right)$$

”Force density” [5]

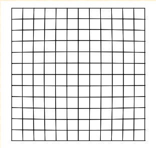
Plane view

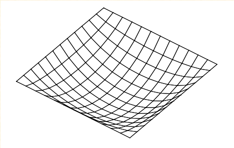
Perspective view

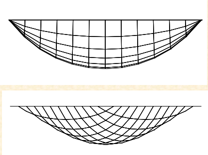
Elevation view

References:
[1] Y. Jikumaru and Y. Yokosuka, in preparation.
[2] V. V. Novozhilov, Thin shell theory, 2nd edn., Groningen, Noordhoff, 1964.
[3] P. Block and J. Oschendorf, Thrust Network Analysis: A New Methodology for Three-dimensional Equilibrium, *J. Int. Assoc. Shell Spat. Struct.* **48**(3) (2007) 167-173.
[4] J. Chilton, The Engineer’s Contribution to Contemporary Architecture: Heinz Isler, Thomas Telford: London (2000) 5–159.
[5] H.-J. Schek, Force density method for form finding and computation of general networks, *Comput. Methods Appl. Mech. Engrg.*, **3** (1974) 115–134.
[6] A. Gaudi, Sagrada Familia: https://en.wikipedia.org/wiki/Sagrada_Fam%C3%ADlia
[7] Gateway arch: https://www.gatewayarch.com/
[8] Casa Mila: https://en.wikipedia.org/wiki/Casa_Mil%C3%A0

Reeb graphs of smooth functions with prescribed preimages

Naoki Kitazawa
Institute of Mathematics for Industry, Kyushu University.
n-kitazawa@imi.kyushu-u.ac.jp

Abstract

This poster is on realization of graphs as Reeb graphs of smooth functions of several good classes with prescribed preimages. The Reeb space of a (smooth) map c is the space of all connected components of preimages of a (smooth) map. For smooth functions of a wide class, the Reeb space is a graph and it is called the Reeb graph. Reeb spaces (graphs) are important in singularity theory of differentiable maps, its applications to geometry of manifolds and some applied mathematics.

1 Preliminaries.

- Manifolds are spaces which are locally regarded as the Euclidean space of a fixed dimension and have local coordinates.
- Differentiable (smooth) manifolds are manifolds for differential calculus.

Smooth maps and singular points.

$f : M \to N$: a smooth map between smooth manifolds.
$p \in M$ is a singular point of f : at p
(the rank of the differential df_p)$< \min\{\dim M, \dim N\}$ and $f(p)$ is a singular value.

Euclidean spaces, unit spheres and unit disks.

$\mathbb{R}^k$: the k-dim. Euclidean space and for $p \in \mathbb{R}^k$ ($\mathbb{R}^1$ is denoted by $\mathbb{R}$).
$||p||$: the distance between $p \in \mathbb{R}^k$ and the origin 0 where the underlying metric is the standard metric.
$S^k := \{p \in \mathbb{R}^{k+1} \mid ||x|| = 1\}$: the k-dim. unit sphere.
$D^k := \{p \in \mathbb{R}^k \mid ||x|| \leq 1\}$: the k-dim. unit disk.

Graph.

$G := (V, E)$: a graph s.t.

- V : the vertex set. $E \neq \emptyset$: the edge set.
- It may be a multigraph. It is with no loops and finite.

→ A 1-dim. compact polyhedron.

2 Morse(-Bott) functions.

Definition 1. $f : M \to \mathbb{R}$ is a Morse function: a smooth function s.t. at each singular point p it is represented by $(x_1, \cdots, x_m) \mapsto \Sigma_{j=1}^{m-i(p)} {x_j}^2 - \Sigma_{j=1}^{i(p)} {x_{m-i(p)+j}}^2) + f(p)$ for some integer $0 \leq i(p) \leq m$ and suitable coordinates.

→ $i(p)$ is chosen uniquely. Singular points appear discretely.

A Morse-Bott function: a smooth function locally represented as the composition of a submersion with a Morse function around each singular point.

3 Reeb spaces, Reeb graphs and realization of graphs.

For a map between spaces $f : M \to N \cdots$
$p_1 {\sim_f} p_2$: $p_1, p_2 \in M$ are in a same connected component of $f^{-1}(p)$ for some $p \in N$.
→ $\sim_f$ is an eq. rel. on M.

Definition 2. $W_f := M/{\sim_f}$ is the Reeb space of f.

$q_f : M \to W_f$: the quotient map. $\exists ! \bar{f}$ s.t. $f = \bar{f} \circ q_f$.

Some important properties.

- Reeb spaces often inherit invariants for the manifolds such as homology groups.
- They are often graphs (a Reeb graph: the graph W_f in Fact 1).
- In applications of mathematics such as visualizations, they are strong tools.

Fact 1 ([4]). *f : a smooth function with finitely many singular values on a closed manifold.*
→ W_f is a graph with the vertex set $V := \{p \in W_f \mid {q_f}^{-1}(p)$ has at least one singular point.$\}$.

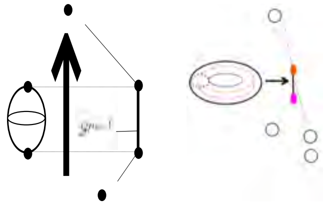

A Morse function on the unit sphere $S^{m-1} \subset \mathbb{R}^m$ and its Reeb graph and preimages for $m \geq 2$: isolated dots and "S^{m-1}" are for preimages (**left**). A Morse-Bott function on a torus and its Reeb graph and preimages (**right**).

Main Problem (**A realization).** For a given graph $G = (V, E)$, can we construct a smooth function f of a certain good class s.t. the Reeb graph W_f is isomorphic to G (with prescribed preimages)?

4 Existing studies on Main Problem and Main Theorem.

- Construction of smooth functions on closed surfaces (see [5] and [2]).

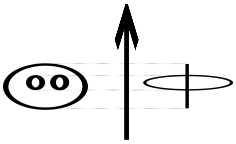

A function on a closed orientable surface of genus 2 and its Reeb graph.

- Construction of Morse functions s.t. connected components of preimages contain no singular points are **copies of a unit sphere** ([3]).

Main Theorem ([1]). *l : a non-negative integer valued function on E of the graph $G := (V, E)$.*
$g : G \to \mathbb{R}$: a continuous function which is injective on each edge.
→ $\exists M$: a 3-dim. closed, connected and orientable manifold.
$\exists f : M \to \mathbb{R}$: a smooth function satisfying the following.

1. *W_f and G are isomorphic as graphs (we identify them suitably).*
2. *${q_f}^{-1}(a)$ is a closed and orientable surface of genus $l(e)$ ($a \in \text{Int } e$).*
3. *$g(a) = \bar{f}(a)$ ($a \in V$: $\bar{f} \circ q_f = f$).*
4. *f is a Morse function, or if not, f is a function which is locally a Morse-Bott function around each singular point except finitely many singular points.*

Some local functions.

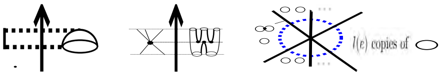

- (**First**) A Morse function around a vertex v of degree 1 adjacent to an edge e satisfying $l(e) = 0$.
- (**Second**) A Morse function around a vertex v where r does not have a local extremum s.t. for any edge $e \ni v$, $l(e) = 0$.
  ⇒ This is due to [3]. Our Main Theorem extends this to the case $l(e) > 0$ may hold.
- (**Third**) A smooth map into the plane (onto the disk surrounded by the dotted blue circle). We need this to obtain a smooth function around a vertex of degree 1 adjacent to an edge e satisfying $l(e) > 0$.
  ⇒ The straight lines show the singular values of the map into the plane. This map is locally regarded as the product map of a Morse function and the identity map on a line.
  ⇒ Circles and "$l(e)$ copies $\cdots$" are for preimages of the corresponding points in the plane.
  ⇒ We compose the map with a function in the first figure to obtain a desired function.

5 Future work.

Problem 1. Can we obtain higher dimensional variants of our Main Theorem?

⇒ [4] has a result where connected components of preimages containing no singular points are compact (closed) manifolds of general dimensions. However, different from our study, explicit types of singular points are not studied.

Problem 2. Find useful applications to visualizations, data analysis etc.

⇒ Our problem may give new methods in function fittings. For example, in suitable situations, datasets may be regarded as the union of (finitely many) prescribed preimages in our problem and our solution to Main Problem may give rise to a suitable fitting function.

6 Acknowledgement.

This work is supported by JSPS KAKENHI Grant Number JP17H06128 (Principal Investigator: Osamu Saeki).

References

[1] N. Kitazawa, *On Reeb graphs induced from smooth functions on 3-dimensional closed orientable manifolds with finitely many singular values*, accepted for publication in Topol. Methods in Nonlinear Anal. after a refereeing process, arxiv:1902.08841.

[2] Y. Masumoto and O. Saeki, *A smooth function on a manifold with given Reeb graph*, Kyushu J. Math. 65 (2011), 75–84.

[3] L. P. Michalak, *Realization of a graph as the Reeb graph of a Morse function on a manifold*. Topol. Methods in Nonlinear Anal. 52 (2) (2018), 749–762, arxiv:1805.06727.

[4] O. Saeki, *Reeb spaces of smooth functions on manifolds*, International Mathematics Research Notices, maa301, https://doi.org/10.1093/imrn/maa301, arxiv:2006.01689.

[5] V. Sharko, *About Kronrod-Reeb grpah of a function on a manifold*, Methods of Functional Analysis and Topology 12 (2006), 389–396.

Strategic Delegation in Bilateral Environmental Agreements under Heterogeneity

Qian Li
Institute of Mathematics for Industry, Kyushu University, Japan
q-li@imi.kyushu-u.ac.jp

1. Introduction

Transboundary pollutant problems can be solved via international cooperation, of which a common way is forming bilateral environmental agreements (BEAs). Former studies modelling the formation of BEAs regard each country as a single player, without considering the domestic politics. In this study, we construct a political-economy model of strategic environmental policymaking with heterogeneous countries. In both the developed and developing countries, domestic households that have heterogeneous environmental preferences vote for the government separately and then these governments negotiate about each country's individual abatement levels and transfers between them.

2. The model setting

There are two countries, of which one is developing country and another is developed country. In each of them, there are households who have different environmental preferences, denoted as θ_i^h. In the former country (denoted as 1), each household's payoff function is

$$\pi_1^h = \theta_1^h(x_1 + x_2) - \gamma c {x_1}^2, \qquad (1)$$

while in the later (denoted as 2), it becomes

$$\pi_2^h = \theta_2^h(x_1 + x_2) - c {x_2}^2. \qquad (2)$$

$0 < \gamma < 1$ suggests that each household in developing country has lower abatement cost than developed one, for the same abatement level. Moreover, $\theta_1^m < \theta_2^m$ means that the median voter in country 1 has a lower monetary valuation over the improvement of environmental quality than that in country 2. The formation of the agreement can be represented using a three-stage game, the framework of which is represented as follows:

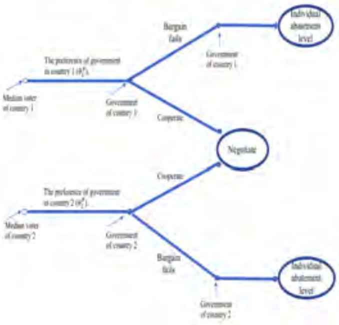

6. References

[1] Buchholz, W., Haupt, A. Peters, W. (2005). International environmental agreements and strategic voting. Scandinavian Journal of Economics. 107, 175–195.

[2] Harstad, B. (2008). Do side payments help? Collective decisions and strategic delegation. Journal of the European Economic Association, 6(2/3), 468–477.

[3] Siqueira, K. (2003). International externalities, strategic interaction, and domestic politics. Journal of Environmental Economics and Management, 45, 674–691.

3. Cooperative environmental policies

Cooperative environmental policies mean that the elected governments decide individual abatement levels and transfers in order to maximize their aggregate payoff.

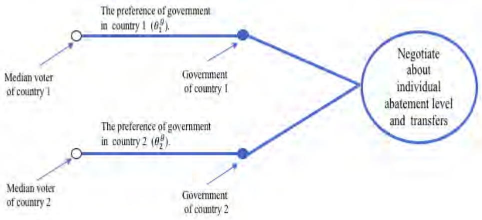

After solving the game via backwards induction, the equilibrial individual abatement levels suggest that $x_{1c}^* = \frac{\theta_1^g+\theta_2^g}{2c\gamma} > x_{2c}^* = \frac{\theta_1^g+\theta_2^g}{2c}$, where subscript c represents the cooperative case. In addition, the elected governments' environmental preferences are that $\theta_1^{g*} < \theta_1^m$ and $\theta_2^{g*} < \theta_2^m$. These confirm the results in [1] and [2] that households have incentives to delegate less green government when cooperate, in the asymmetric case.

4. Non-cooperative environmental policies

Under the non-cooperative environmental policies, each government decides the abatement level individually in order to maximize its own payoff, which can be shown as follows.

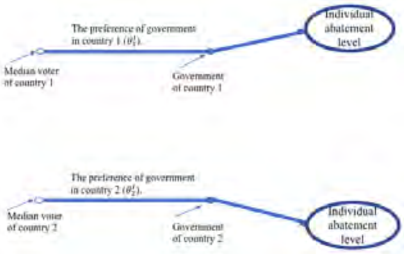

The equilibrial results show that households will delegate sincerely. The abatement level of each country is $x_{1I}^* = \frac{\theta_1^m}{2c\gamma}$ and $x_{2I}^* = \frac{\theta_2^m}{2c}$, where I means the non-cooperative case.

5. Conclusions

We prove that cooperation is effective in improving the abatement levels.

1. Under cooperative environmental policies, the governments being elected in both the developing and the developed country have lower environmental preferences than the median household. The developing country always abate more than the developed one.
2. Under both the cooperative and non-cooperative environmental policies, the government being elected in the developed country has a higher environmental preference than the developing one.
3. Cooperation brings higher total abatement level and is always effective since it brings higher aggregate payoff, which is in contrast with [3].

Modelling Housing Feature Impacts on Sale Price in Newly Developed Suburbs

Christina Yin-Chieh Lin (UOA), Andreas W. Kempa-Liehr (UOA), Andrew Mason (UOA)
Department of Engineering Science
University of Auckland

BACKGROUND

Shortage of affordable housing is a growing crisis all around the world. Surveys conducted by Gallup's World Poll from 2015 to 2017 across 140 different countries indicate that on average 27% of a country's population cannot afford adequate housing. Countries are looking for new housing solutions to create sustainable and affordable housing conditions for middle-class families. One new solution is the mass development of entirely new suburbs that support a local community. Auckland Council has presented a plan to develop outer suburbs such as Fairview Heights and Hobsonville and expand the current city into `Greater Auckland'. These new suburbs have not been adequately studied because this is a relatively new approach to property development. Modelling housing feature impacts in the new suburbs will be increasingly relevant to future developers.

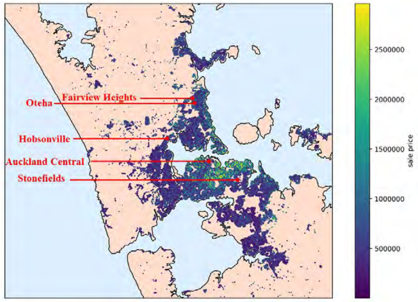

Figure 1 Map of Greater Auckland

OBJECTIVES

This study focuses on analyzing newly developed suburbs in Auckland to understand housing feature impacts on sale price in these new suburbs and provide interpretable. Defining a reliable point of reference for our model is critical for conveying the results to non-experts in machine learning, such as housing developers. Our chosen point of reference is the price of a standard house in the new suburbs over time. Modelling housing feature impacts relative to a standard house will create a unique solution to our regression problem that is easy to interpret. The main objectives of this study are to:

- Understand the impact of individual housing features on sale price in a new suburb.
- Validate the robustness of our proposed model by making predictions for a new suburb.

METHODS

This study proposes separating the effects of price change over time from the effects of individual housing features by decomposing the problem into two components:

- Price of a standard house over time
- Impacts of individual housing features on sale price relative to the standard house

The chosen formula for our model is:

$$
\begin{aligned}
Log(P_i) =& w_0 + w_A(A_i - \bar{A}) + w_L(L_i - \bar{L}) + \sum_{b\in\mathcal{B}\setminus\bar{B}} w_b^{\mathrm{B}} \mathbb{1}_{B_i=b} \\
&+ \sum_{c\in\mathcal{C}\setminus\bar{C}} w_c^{\mathrm{C}} \mathbb{1}_{C_i=c} + \sum_{g\in\mathcal{G}\setminus\bar{G}} w_g^{\mathrm{G}} \mathbb{1}_{G_i=g} \\
&+ \sum_{f\in\{0,1\}\setminus\bar{F}} w^{\mathrm{F}} \mathbb{1}_{F_i} + \sum_{s\in\mathcal{S}} w_s^{\mathrm{S}} \mathbb{1}_{S_i=s} \\
&+ \frac{1}{N(M_i)} \sum_{m\in\mathcal{M}} w_m^{\mathrm{M}} \mathbb{1}_{M_i-5\le m\le M_i+6} + \varepsilon_i
\end{aligned}
$$

RESULTS

We conduct a case study on modelling house sales in three new Auckland suburbs-Fairview Heights, Oteha, and Stonefields. The estimated percentage change in price for individual housing features compared to a standard house are calculated from the fitted coefficients of housing features. A house with only one bedroom is estimated to have a price approximately 37.25% lower than the price of a standard house with three bedrooms. A house with four bedrooms is estimated to be 10.43% higher in price than the standard house, but the increase in price for each added bedroom plateaus above four bedrooms. This indicates that most buyers are not satisfied with single-bedroom houses, but five bedrooms or above can become excessive. Additionally, houses with at least one free-standing garage are estimated to have prices 5.01% higher than those who do not.

Area	Floor Area in excess of 184m^2	Land Area in excess of 256m^2
Price Change	2.43% per 10m^2	0.56% per 100m^2

Bedrooms	1	2	3	4	5	6+
Price Change	-37.25%	-10.53%	0.00%	10.43%	12.82%	10.89%

Bathrooms	1	2	3	4	5+
Price Change	-3.63%	0.00%	0.63%	1.82%	0.37%

Garages	0	1	2	3+
Price Change	-0.73%	0.00%	6.41%	6.22%

Garage Type	No Free-Standng Garage	At Least 1 Free-Standing Garage
Price Change	0.00%	5.01%

Figure 2 Percentage price change from housing features

RESULTS

We use our ridge regression model fitted on Fairview Heights, Oteha, and Stonefields to make house price predictions for sales in the Hobsonville suburb. Root mean square error (RMSE) is $129,779 after back transformation. The box plot of residuals against sale years does not show any clear trend of residual changes across time (see Fig. 3). Residuals are relatively uniform across sale years. This implies that the non-linear house price trend over time is effectively captured by our model. There is one clear outlier with a residual just above one million in magnitude. This outlier property is a townhouse sold in 2018 and with a floor area of 400m^2. This is more than twice the median floor area of other townhouses, but the actual sale price is unexpectedly low for unknown reasons. Overall, approximately 91% of our predictions are within $200,000 of the true sale price.

Figure 3 Scatter plot of predicted price against actual price

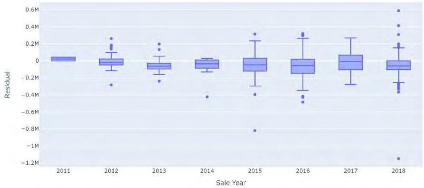

Figure 4 Box plot of prediction residuals against sale year

CONCLUSIONS

- The proposed method of modelling sale prices relative to a 'standard' house effectively captures the non-linear effects of individual housing features and price change over time.
- Our model is able to predict house prices in the new suburb of Hobsonville with reasonable accuracy.
- The insights from our model has the potential to be applied to other new suburbs to assist with the planning phase of suburb development.

Homotopifying abstraction of abstraction of algebra

Yuki Maehara

Institute of Mathematics for Industry, Kyushu University

Starting problem

One often wants to mix algebra and geometry:

- algebraic topology studies topological spaces using algebraic invariants, and
- algebraic geometry studies geometric structures arising from algebra.

But "natural" algebraic structures in geometric (or at least homotopical) situations tend to be too complicated to deal with by hand.

Approach: category theory

We will squint just enough so that homotopical and usual algebra look the same. More precisely, we adopt an abstract approach to algebra provided by category theory.

My contribution

The Gray tensor product is a crucial tool for the category theoretic treatment of algebra. I constructed a homotopical version of this tensor product, and showed that it satisfies a suitable analogue of

- unit law: $1X = X = X1$,
- associative law: $(XY)Z = X(YZ)$,
- distributive law: $\begin{cases} X(Y+Z) = XY + XZ, \\ (X+Y)Z = XZ + YZ. \end{cases}$

More precisely:

Main theorem of [1]

The 2-quasi-categorical Gray tensor product forms part of a homotopical biclosed monoidal structure.

The proof of this theorem required a good understanding of 2-quasi-categories, which was provided by the following.

Main theorem of [2]

The model structure for 2-quasi-categories can be characterised using the inner horn inclusions and the equivalence extensions.

"Natural" algebraic structures

"Natural" algebraic structures in geometry (homotopy theory) usually only satisfy weak versions of familiar algebraic equations.

Example: $\pi_1(X, x)$ v.s. $\Omega(X, x)$

Given a topological space X with a basepoint x, its fundamental group is

$$\pi_1(X, x) = \{\text{loops in } X \text{ based at } x\}.$$

More precisely, its elements are continuous maps

$$\alpha : [0, 1] \to X$$

with $\alpha(0) = \alpha(1) = x$.

Multiplication is given by concatenation of loops; $\alpha * \beta$ first traces α and then β at double speed.

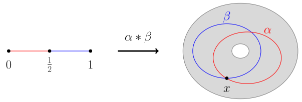

This is, however, not quite a group yet. For example, it's associative only up to reparametrisation:

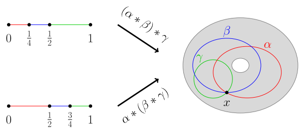

So actually,

$$\pi_1(X, x) = \left\{ \begin{matrix} \text{loops in } X \text{ based at } x \text{ modulo} \\ \text{continuous deformation (homotopy)} \end{matrix} \right\}.$$

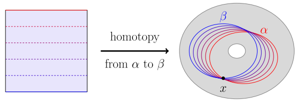

But the "natural" object here is really the space of all loops before quotienting by homotopy. In this space, denoted $\Omega(X, x)$, the associativity (and the other group axioms) hold only up to homotopy/path.

When we need the Gray tensor product

Each notion of algebraic structure gives rise to a monad. The Gray tensor product plays an important role when we are characterising the corresponding category of algebras, or when combining monads using distributive laws.

Example: (monad for) groups

Recall that the free group TX on a set X consists of strings like

$$x \cdot y, \quad z^{-1}, \quad \Big(x \cdot \big(y \cdot (y^{-1} \cdot x^{-1})\big)\Big) \cdot z$$

subject to the "obvious" relations identifying, for instance, $x \cdot (x^{-1} \cdot y)$ with y.

If X was a group, then we can evaluate these strings into actual elements in X. *e.g.*

$$T\mathbb{R}_{>0} \to \mathbb{R}_{>0}$$
$$2 \cdot \pi \mapsto 2\pi$$
$$(6 \cdot 0.5) \cdot 3^{-1} \mapsto 1$$

In fact, we have a bijection:

$$\begin{matrix} \text{group structures on } X \\ \wr\wr \\ TX \to X \text{ satisfying certain conditions} \\ (T\text{-algebra structures on } X) \end{matrix}$$

Example: monad for rings

A ring R consists of a compatible pair of an abelian group structure $(R, +, 0)$ and a monoid structure $(R, *, 1)$. On the level of monads, this is witnessed by an (abstract) distributive law between the monads for monoids and for abelian groups.

Monads

A monad (T, η, μ) on a category $\mathcal{C}$ looks like

$$\begin{tikzcd} \mathcal{C} \arrow[rr, bend left=50, "\mathrm{id}"] \arrow[rr, "T" description] \arrow[rr, bend right=50, "TT"'] & {} \arrow[d, phantom, "\Uparrow\mu"] \arrow[u, phantom, "\Downarrow\eta"] & \mathcal{C} \end{tikzcd}$$

where

- TX is the free T-algebra on X,
- $\eta_X : X \to TX$ witnesses that TX contains X,
- $\mu_X : TTX \to TX$ witnesses that TX is canonically a T-algebra.

The category $\mathcal{C}^T$ of T-algebras is the universal ("largest") one equipped with:

$$\begin{tikzcd} \mathcal{C}^T \arrow[r, "U"] \arrow[dr, "U"'] & \mathcal{C} \arrow[d, "T"] \arrow[dl, phantom, "\swarrow"] \\ & \mathcal{C} \end{tikzcd}$$

(More precisely, $\mathcal{C}^T$ is the lax limit of the monad regarded as a 2-functor.)

References

[1] Yuki Maehara.
The Gray tensor product for 2-quasi-categories.
Adv. Math., 377:107461, 78, 2021.

[2] Yuki Maehara.
Inner horns for 2-quasi-categories.
Adv. Math., 363:107003, 56, 2020.

Acknowledgements

This poster is based on my PhD project, which was supported by an International Macquarie University Research Training Program Scholarship (Allocation Number: 2017127).

Contact Information

- Web: https://yukimaehara.github.io
- Email: y-maehara@imi.kyushu-u.ac.jp

Non-log liftable log del Pezzo surfaces of rank one in characteristic five

Masaru Nagaoka, Institute of Mathematics for Industry, Kyushu University, m-nagaoka@imi.kyushu-u.ac.jp

Background

- A(n algebraic) variety ≒ a topological space that locally resembles the set of solutions of polynomial equations over an algebraically closed field (e.g., $\{x^2+y^2=1\} \subset \mathbb{C}^2_{[x,y]}$, $\mathbb{P}^1_{\mathbb{C}}$: the projective line over $\mathbb{C}$)
- Each variety V is endowed with the canonical divisor K_V intrinsically (≒ certain linear sum of subvarieties of codimension one).
- **M**inimal **M**odel **P**rogram ≒ a procedure to classify varieties with mild singularities up to weak equivalence (= birational equivalence)
- According to MMP, there are three building blocks of varieties: General type ("$K_V > 0$"), Calabi-Yau ("$K_V = 0$"), Fano ("$-K_V > 0$").
- **A log del Pezzo surface (LDP)**
  := a 2-dimensional Fano variety (with mild singularities)
- An LDP V has several invariants: rank (we assume rank $=1$ here), $\mathrm{Dyn}(V)$ **(invariants of singularities on** V**),** $K_V^2 \in \mathbb{Q}_{>0}$ **(volume).**
- When the defining polynomials are defined over a field F of characteristic $p>0$, some LDPs have quite different (=**pathological**) properties from varieties over $p=0$ (or over $\mathbb{C}$).

Similarities between $p = 0$ and $p > 0$

$$\begin{tikzcd} U \\ W \arrow[u] \arrow[d] \\ V \end{tikzcd}$$

- Each LDP is obtained from the projective plane $\mathbb{P}^2$ or $\mathbb{P}^1$-fibrations / $\mathbb{P}^1$ by finite steps of **Sarkisov links** of the following type:

  ①: Choose another LDP (e.g., $\mathbb{P}^2$).

  ②: Extract a K-negative divisor (e.g., blow up at smooth pt).

  ③: Contract a K_W-non-negative divisor.

  or ①+②: Choose a $\mathbb{P}^1$-fibration over $\mathbb{P}^1$ (+ extra conditions).
  ③: Contract a K_W-non-negative divisor.

Differences between $p = 0$ and $p > 0$

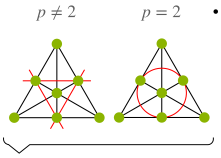

- E.g. (Sarkisov-like construction)

  ①: Choose the projective plane $\mathbb{P}^2_{[x_0:x_1:x_2]}$.

  ②: Blow up at seven points $[x_0 : x_1 : x_2] = [a_0 : a_1 : a_2]$ with $a_i \in \{0,1\}$ and $(a_0, a_1, a_2) \neq (0^3)$.

  ③: Contract lines passing through 3 pts.

$$\begin{tikzcd} \mathbb{P}^2 \\ W \arrow[u] \arrow[d] \\ V_0 \end{tikzcd}$$

$\cap$

- The following holds only in $p = 2$:
  - Three lines $\{x_0 = x_1 + x_2\}, \{x_1 = x_2 + x_0\}, \{x_2 = x_0 + x_1\}$ are the same as $L = \{x_0 + x_1 + x_2 = 0\}$.
  - L is contracted in ③ to the 7-th singularity of the output V_0.
  - V_0 is an LDP satisfying pathological properties such as **(ND): No LDPs in $p = 0$ have the same invariants** $(\mathrm{Dyn}(V_0), K^2_{V_0})$ and **(NK): The Kawamata-Viehweg vanishing (of cohomologies) fails for** V_0. It also satisfies (NL) to be described below.

Methods to connect $p > 0$ to $p = 0$

- LDPs have log resolutions: birational morphisms from smooth surfaces such that the preimages of the singularities are "good"
- In $p > 0$, there is the ring of Witt vectors $W(F)$ with the residue field $= F$ and the fractional field G of characteristic 0. In particular, each variety "over $W(F)$" has fibers over F ($p > 0$) and over G ($p = 0$).
- The notion of **non-log liftability (NL): No log resolutions of the given LDP are "defined over** $W(F)$**"** was introduced in [1] to be compared with pathological properties such as (ND) and (NK).

Main Questions

- What kind of LDPs (of rank one) do satisfy (NL)?
- Are there any implication between (ND), (NK), and (NL)?

Previous works

- [2] (ND)⇒(NL) and (NK)⇒(NL) in general.
- [2] Du Val del Pezzo surfaces (= LDPs with milder singularities) satisfying (NK) (resp.(ND), (NL)) are classified. As a consequence, (NK)⇒(ND)⇒(NL) in this case.
- [3] In $p > 5$, ∄LDPs satisfying (NK), (ND), or (NL).

Main results ($p = 5$) [4]

- (1) An LDP V satisfies (NL) $\Longleftrightarrow$ V is constructed as follows:

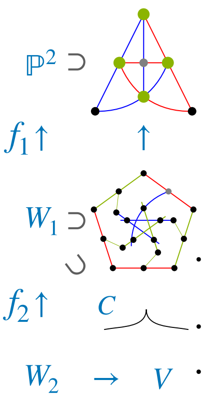

①: Choose the projective plane $\mathbb{P}^2_{[x_0:x_1:x_2]}$.

②-1: Blow up at four points $[x_0 : x_1 : x_2] = [a_0 : a_1 : 1]$ with $a_i \in \{\pm 1\}$along certain lines with multiplicity two.

(A reduced irreducible singular member $C \in |-K_{W_1}|$ has a cusp only in $p = 5$.)

②-2: Blow up at the cusp of C with multiplicity $n \in \mathbb{Z}_{>0}$.

③: Contract K_{W_2}-non-negative divisors.

- (2) The isomorphism classes of LDPs with fixed $\mathrm{Dyn}(-)$ correspond to either the singleton or $F \backslash \{0,1\}$.
- (3) An LDP V satisfies (ND)
  $\Longleftrightarrow$ V is constructed as above with $n > 2$.
- (4) An LDP V satisfies (NK)
  ⇒ V is constructed as above with $n > 2$.
- In particular, (NK)⇒(ND)⇒(NL) holds.

Evidence for (1) and (3) (≠proof)

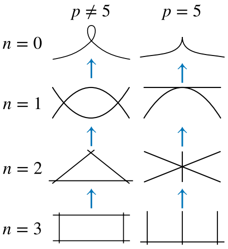

- (1): Members of $f_{1*}|-K_{W_1}|$ is defined by $(y^2 - z^2)(x + y) + t(x^2 - z^2)(y - x) = 0$ in $\mathbb{P}^2_{[x:y:z]}$ with $t \in F$.
  ⇒ Reduced irreducible singular members of $|-K_{W_1}|$correspond to the solutions of $t^2 + 11t - 1 = 0$, which has a double root only in $p = 5$.
- (3): In $p \neq 5$, C has a node.
  ⇒ The matrix of intersection numbers between irreducible components in $f_2^{-1}(C)$ differs if and only if $n > 2$. $(\mathrm{Dyn}(V)$ is its submatrix by definition.)

References

[1] P. Cascini, H. Tanaka, J. Witaszek, Compos. Math., 153(4):820–850 (2017)
[2] T. Kawakami, M. Nagaoka, ArXiv:2008.07700 (2020)
[3] J. Lacini, ArXiv:2005.14544 (2020)
[4] M. Nagaoka, ArXiv:2109.10558 (2021)

Acknowledgements

This work was supported by JSPS KAKENHI Grant Number 21K13768.

Zeros of random power series with finitely dependent Gaussian coefficients

Kohei Noda[1], **Tomoyuki Shirai**[2]
[1]Graduate School of Mathematics, Kyushu University, Japan. e-mail:noda.kohei.721@s.kyushu-u.ac.jp
[2]Institute of Mathematics for Industry, Kyushu University, Japan.

Faculty of Mathematics
Kyushu University
Institute of Mathematics for Industry
Kyushu University
マス・フォア・イノベーション
卓越大学院
Graduate Program of Mathematics for Innovation

1 Gaussian analytic function and our objective

- $D \subset \mathbb{C}$ is a smooth boundary domain and $\forall n \in \mathbb{N}, z_1, \dots, z_n \in D$.
- $K_f(z_j, z_k) = \mathbf{E}[f(z_j)\overline{f(z_k)}]$ and $\Sigma = (K_f(z_j, z_k))_{j,k=1}^n$.
- $f(z)$ is a Gaussian analytic function (GAF) on D
  $\overset{\text{def}}{\Longleftrightarrow}$ $(f(z_1), \dots, f(z_n)) \overset{d}{\sim} \mathcal{N}_{\mathbb{C}^n}(0, \Sigma)$, which is n-dimensional complex Gaussian distribution with mean 0 and covariance matrix Σ.

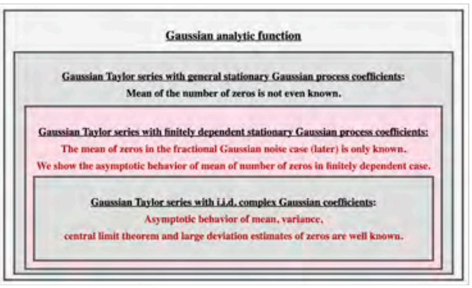

Gaussian analytic function

Gaussian Taylor series with general stationary Gaussian process coefficients:
Mean of the number of zeros is not even known.

Gaussian Taylor series with finitely dependent stationary Gaussian process coefficients:
The mean of zeros in the fractional Gaussian noise case (later) is only known.
We show the asymptotic behavior of mean of number of zeros in finitely dependent case.

Gaussian Taylor series with i.i.d. complex Gaussian coefficients:
Asymptotic behavior of mean, variance,
central limit theorem and large deviation estimates of zeros are well known.

Figure 1: Outline

2 Gaussian random power series : Peres-Virág GAF, other GAFs and known results

Theorem 1 (Peres-Virág, 2005 [3]). $f_{\mathrm{PV}}(z) = \sum_{k=0}^{\infty} \zeta_k z^k$, *where* $\{\zeta_k\}_{k=0}^{\infty}$ *are i.i.d. standard complex Gaussian random variables. Then, the zeros process* $\mathcal{Z}_{f_{\mathrm{PV}}}$ *is the determinantal point process (DPP) associated with* $K_{\mathrm{Berg}}(z, w) = (1 - z\overline{w})^{-2}$.

Remark 1. • $\mathbf{E}[f_{\mathrm{PV}}(z)\overline{f_{\mathrm{PV}}(w)}] = (1 - z\overline{w})^{-1}$ *(Szegő kernel).*
• $\mathbf{E}\binom{N_{f_{\mathrm{PV}}}(r)}{k} = \frac{r^{k(k+1)}}{(1-r^2)(1-r^4)\cdots(1-r^{2k})}$. *Hence,* $\mathbf{E}N_{f_{\mathrm{PV}}}(r) = \frac{r^2}{1-r^2}$.

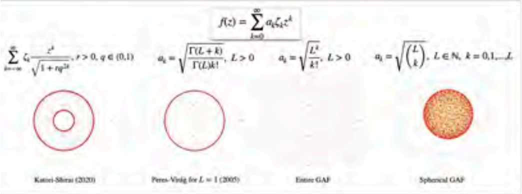

Katori-Shirai (2020)
Peres-Virág for $L = 1$ (2005)
Entire GAF
Spherical GAF

Figure 2: Gaussian analytic functions : Examples.

Question. i.i.d. complex Gaussian coefficients.
$\Longrightarrow$ stationary complex Gaussian process coefficients. What will happen ?

Known results. Mukeru, Mulaudzi, Nazabanita and Mpanda (2021) :
For fractional Gaussian noise $\Xi^{(H)} = \{\xi_k^{(H)}\}_{k=0}^{\infty}$ for $0 \le H < 1$ and $f_H(z) = \sum_{k=0}^{\infty} \xi_k^{(H)} z^k$,

$$\frac{r^2}{1-r^2} - C_{1,H}\left(\frac{1}{2\sqrt{1-r^2}} - \frac{1}{2}\right) \le \mathbf{E}[N_{f_H}(r)] \le \frac{r^2}{1-r^2} - C_{2,H}\left(\frac{1}{2\sqrt{1-r^2}} - \frac{1}{2}\right),$$

where $C_{1,H}, C_{2,H} \ge 0$ and $\mathbf{E}[\xi_k^{(H)}\overline{\xi_{k+n}^{(H)}}] = \frac{1}{2}|n+1|^{2H} + \frac{1}{2}|n-1|^{2H} - |n|^{2H}$.

Observation. A negative term of slower growth appears.

3 Main results [1]

Our setting. $\Xi = \{\xi_k\}_{k\in\mathbb{Z}}$: finitely dependent stationary complex Gaussian process with mean 0, variance 1 and $\gamma(k) = \mathbf{E}[\xi_n\overline{\xi_{n+k}}]$.
$\Longrightarrow f(z) = \sum_{k=0}^{\infty} \xi_k z^k$.

Our methods. $\mathcal{J}(r) = \frac{r}{2\pi i}\oint_{\partial\mathbb{D}} \frac{G'(rz)}{\Theta(r,z)} dz$, where $\Theta(r, z) = \sum_{k\in\mathbb{Z}} \gamma(k) r^{|k|} z^k$ and $G(z) = \sum_{n=1}^{\infty} \overline{\gamma(n)} z^n$ from the Edelman-Kostlan formula.
$\Longrightarrow$ The zeros of the spectral function $\Theta(1, r)$ play essential roles.

Theorem 2 ([1]). $\mathbf{E}[N_f(D)] \le \mathbf{E}[N_{f_{\mathrm{PV}}}(D)]$.

2-dependent model. $\gamma_{a,b}(k) = 1\delta_{k,0} + a\delta_{k,\pm1} + b\delta_{k,\pm2}$.
$\Theta(r, z) = 1 + ar(z + z^{-1}) + br^2(z^2 + z^{-2})$.

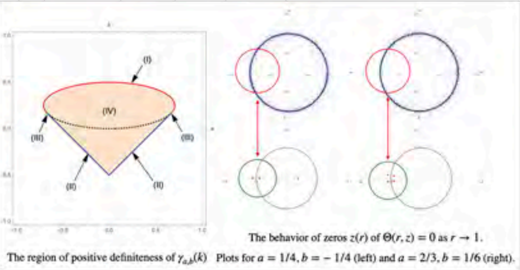

The behavior of zeros $z(r)$ of $\Theta(r,z) = 0$ as $r \to 1$.

The region of positive definiteness of $\gamma_{a,b}(k)$ Plots for $a = 1/4, b = -1/4$ (left) and $a = 2/3, b = 1/6$ (right).

Figure 3: Random zeros are affected by the multiplicity of zeros of $\Theta(1, z)$.

Theorem 3 ([1]).
(i) $\mathbf{E}N_{f_{a,b}}(r) = \frac{r^2}{1-r^2} - \sqrt{\frac{2b}{6b-1}}\frac{1}{(1-r^2)^{1/2}} + O(1)$ *as* $r \to 1$.
(ii) $\mathbf{E}N_{f_{a,b}}(r) = \frac{r^2}{1-r^2} - \frac{1}{2}\sqrt{\frac{1-2b}{1-6b}}\frac{1}{(1-r^2)^{1/2}} + O(1)$ *as* $r \to 1$.
(iii) $\mathbf{E}N_{f_{a,b}}(r) = \frac{r^2}{1-r^2} - \frac{1}{2^{5/4}}\frac{1}{(1-r^2)^{3/4}} + O\left(\frac{1}{(1-r^2)^{1/4}}\right)$ *as* $r \to 1$.
(iv) $\mathbf{E}N_{f_{a,b}}(r) = \frac{r^2}{1-r^2} - C(a,b) + O\left(1 - r^2\right)$ *as* $r \to 1$, *where* $C(a, b) \ge 0$.

n-dependent model. $\gamma_n(k) = \binom{2n}{n+k}\binom{2n}{n}^{-1}$ $(|k| = 0, 1, 2, \dots, n)$ and 0 (else).
$\Theta(1, z) = \sum_{k=-n}^{n} \gamma_n(k) z^k = \binom{2n}{n}^{-1} z^{-n}(z+1)^{2n}$.

Remark. We can not use the Implicit Function Theorem.

Theorem 4 ([1]).
$\mathbf{E}N_f(r) = \frac{r^2}{1-r^2} - D_n(1 - r^2)^{-\frac{2n-1}{2n}} + O\left((1 - r^2)^{-\frac{2n-3}{2n}}\right)$ *as* $r \to 1$,
where $D_n = \frac{1}{2n\sin\frac{\pi}{2n}}\left\{\binom{2(n-1)}{n-1}\right\}^{\frac{1}{2n}}$.

Theorem 5 ([1]). $\Xi = \{\xi_k\}_{k\in\mathbb{Z}}$ *is the stationary, centered, finitely dependent, complex Gaussian process.* $\Theta(1, z)$ *of* Ξ *has zeros* θ_j *of multiplicity* $2k_j$ *for* $j = 1, 2, \dots, p$. $\alpha = (2k-1)/(2k)$ *with* $k = \max_{1\le j\le p} k_j$; $\alpha = 0$ *otherwise. Then,* $\mathbf{E}N_f(r) = \frac{r^2}{1-r^2} - C_{\Xi}(1 - r^2)^{-\alpha} + o((1 - r^2)^{-\alpha})$ *as* $r \to 1$, *where* $C_{\Xi} > 0$.

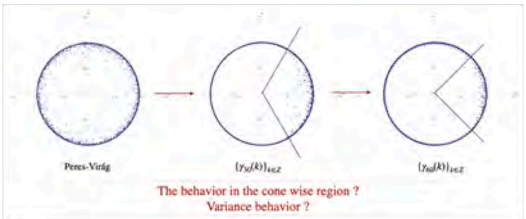

Peres-Virág
$\{\gamma_{30}(k)\}_{k\in\mathbb{Z}}$
$\{\gamma_{60}(k)\}_{k\in\mathbb{Z}}$

The behavior in the cone wise region ?
Variance behavior ?

Figure 4: Different pictures for $n = 0, 30, 60$.

4 Conclusion

- We obtained the asymptotic behavior of the mean of the number of zeros in the finitely dependent case. We would like to compute the the asymptotic behavior of the variance $\mathbf{Var}N_f(r)$ as $r \to 1$ in the future work.
- As Figure 4, we would like to see the asymptotic behavior of number of zeros in corner wise regions.
- We need to consider cases of more general stationary complex Gaussian process Ξ including the fractional Gaussian noise.

References:
[1] Kohei, N., Shirai, T.: Expected number of zeros of random power series with finitely dependent Gaussian coefficients. arXiv:2106.02860[math.PR] (2021).
[2] Mukeru, S., Mulaudzi, M. P., Nzabanita, J., Mpanda, M. M.: Zeros of Gaussian power series with dependent random variables. Illinois J. Math. **64**, no. 4 (2020), 569–582.
[3] Peres, Y., Virág, B.:Zeros of the i.i.d. gaussian power series: a conformally invariant determinantal process. Acta Math. **194**, no. 1 (2005), 1–35.

Acknowledgments:
This work was supported by Japan Society for the Promotion of Science (JSPS) KAKENHI [JP18H01124] and partially supported by KAKENHI [JP16H06338, JP20H00119, JP20K20884 to T.S.]; and K.N. was also supported by the WISE program (JSPS).

ALM FOR PIECEWISE LINEAR-QUADRATIC COMPOSITE OPTIMIZATION PROBLEMS

Nguyen Thi Van Hang – Institute of Mathematics & VIASM

PROBLEM FORMULATION

Consider the convex piecewise linear-quadratic composite optimization problem

$$\text{minimize} \quad \varphi(x) + g\big(\Phi(x)\big) \quad \text{subject to} \quad x \in \Theta, \tag{P}$$

where

- $\varphi : \mathbb{R}^n \to \mathbb{R}$ and $\Phi : \mathbb{R}^n \to \mathbb{R}^m$ are $\mathcal{C}^2$-smooth around the point of interest;
- $\Theta \subset \mathbb{R}^n$ is a simple polyhedral convex set;
- $g : \mathbb{R}^m \to \overline{\mathbb{R}}$ is a convex piecewise linear-quadratic (CPLQ) function:

$$g(z) = \begin{cases} \frac{1}{2}\langle A_i z, z\rangle + \langle a_i, z\rangle + \alpha_i & \text{for} \quad z \in C_i,\ i = 1, \ldots, s, \\ \infty & \text{otherwise,} \end{cases}$$

where A_i are $m \times m$ symmetric matrices, $a_i \in \mathbb{R}^m$, $\alpha_i \in \mathbb{R}$, and $C_i \subset \mathbb{R}^m$ are polyhedral convex sets, for $i = 1, \ldots, s$.

NOTATIONS

- *Lagrangian*: $L(x, \lambda) := \varphi(x) + \langle \lambda, \Phi(x)\rangle$
- *critical cone* to Θ at $\bar{x}$ for $\bar{v} \in N_\Theta(\bar{x})$:

$$K_\Theta(\bar{x}, \bar{v}) := T_\Theta(\bar{x}) \cap \{\bar{v}\}^\perp$$

- *critical cone* of g at $\bar{z}$ for $\bar{\lambda} \in \partial g(\bar{z})$:

$$K_g(\bar{z}, \bar{\lambda}) := \big\{v \in \mathbb{R}^m \big|\ \langle \bar{\lambda}, v\rangle = \mathrm{d}g(\bar{z})(v)\big\}$$

EXAMPLES

- classical NLPs
- unconstrained and constrained minimax problems
- ℓ_1−norm regularized least squares problems (Lasso regression)
- extended NLPs

OBJECTIVES

Study the local convergence of the Augmented Lagrangian method (ALM) seeking for an $\bar{x}$ satisfying

- First-order necessary optimality condition: $(\bar{x}, \bar{\lambda})$ satisfies the *KKT system*:

$$0 \in \nabla_x L(x, \lambda) + N_\Theta(x), \quad \lambda \in \partial g(\Phi(x));$$

- Second-order sufficient optimality condition (SOSC):

$$\langle \nabla^2_{xx} L(\bar{x}, \bar{\lambda})w, w\rangle + \mathrm{d}^2 g(\Phi(\bar{x}), \bar{\lambda})(\nabla\Phi(\bar{x})w) > 0,$$

for all $0 \neq w \in \mathscr{D} := K_\Theta\big(\bar{x}, -\nabla_x L(\bar{x}, \bar{\lambda})\big) \cap \big\{w \in \mathbb{R}^n \big|\ \nabla\Phi(\bar{x})w \in K_g\big(\Phi(\bar{x}), \bar{\lambda}\big)\big\}$.

Augmented Lagrangian for composite optimization problem (P): $\mathscr{L} : \mathbb{R}^n \times \mathbb{R}^m \times (0, \infty) \to \mathbb{R}$ defined by

$$\mathscr{L}(x, \lambda, \rho) := \varphi(x) + e_{1/\rho} g\Big(\Phi(x) + \tfrac{\lambda}{\rho}\Big) - \tfrac{\|\lambda\|^2}{2\rho}.$$

KEY REFERENCES

[1] Nguyen T. V. Hang and M. Ebrahim Sarabi, *Local convergence analysis of augmented Lagrangian methods for piecewise linear-quadratic composite optimization problems*, SIAM J. Optim. 31 (2021), 2665–2694.

[2] R. T. Rockafellar and R. J-B Wets, *Variational Analysis*, Grundlehren Series (Fundamental Principles of Mathematical Sciences), Vol. 317, Springer, Berlin, 2006.

VARIATIONAL PROPERTIES OF AUGMENTED LAGRANGIAN

PROPAGATION OF STATIONARY CONDITIONS: Let $(\bar{x}, \bar{\lambda})$ be a KKT point of (P). Then for all $\rho > 0$, $\bar{x}$ is a *stationary point* of the augmented problem

$$\text{minimize} \quad \mathscr{L}(x, \bar{\lambda}, \rho) \quad \text{subject to} \quad x \in \Theta.$$

TWICE EPI-DIFFERENTIABILITY: The function $x \mapsto \mathscr{L}(x, \lambda, \rho)$ is *twice epi-differentiable* at $\bar{x}$ for $\bar{v} := \nabla_x \mathscr{L}(\bar{x}, \lambda, \rho)$ and its *second-order epi-derivative* is calculated by

$$\mathrm{d}^2_x \mathscr{L}\big((\bar{x}, \lambda, \rho), \bar{v}\big)(w) = \big\langle \nabla^2_{xx} L(\bar{x}, \mu)w, w\big\rangle + e_{1/2\rho}\big(\mathrm{d}^2 g\big(\Phi(\bar{x}) + \tfrac{\lambda-\mu}{\rho}, \mu\big)\big)\big(\nabla\Phi(\bar{x})w\big),$$

where $\mu = \nabla_x\big(e_{1/\rho} g\big)\big(\Phi(\bar{x}) + \frac{\lambda}{\rho}\big)$.

PROPAGATION OF SOSC: Let $(\bar{x}, \bar{\lambda})$ be a KKT point and $\bar{v} := \nabla_x L(\bar{x}, \bar{\lambda})$. Then the following assertions are equivalent:

(i) The SOSC holds at $(\bar{x}, \bar{\lambda})$.

(ii) There exists $\bar{\rho} > 0$ such that for all $\rho \geq \bar{\rho}$, the *second-order condition* holds:

$$\mathrm{d}^2_x \mathscr{L}\big((\bar{x}, \bar{\lambda}, \rho), \bar{v}\big)(w) > 0 \quad \text{for all} \quad w \in K_\Theta(\bar{x}, -\bar{v}) \setminus \{0\}.$$

(iii) There exist $\bar{\rho} > 0, \gamma > 0$, and $\ell > 0$ such that for all $\rho \geq \bar{\rho}$, the *quadratic growth condition* holds:

$$\mathscr{L}(x, \bar{\lambda}, \rho) \geq \varphi(\bar{x}) + g\big(\Phi(\bar{x})\big) + \ell\|x - \bar{x}\|^2 \quad \text{for all} \quad x \in \mathbb{B}_\gamma(\bar{x}) \cap \Theta.$$

(iv) There exist $\bar{\rho} > 0, \gamma > 0, \varepsilon > 0$, and $\ell > 0$ such that for all $\lambda \in \Lambda(\bar{x}) \cap \mathbb{B}_\varepsilon(\bar{\lambda})$ and all $\rho \geq \bar{\rho}$, the *uniform quadratic growth condition* is satisfied:

$$\mathscr{L}(x, \lambda, \rho) \geq \varphi(\bar{x}) + g(\Phi(\bar{x})) + \ell\|x - \bar{x}\|^2 \quad \text{for all} \quad x \in \mathbb{B}_\gamma(\bar{x}) \cap \Theta.$$

LOCAL CONVERGENCE OF ALM

ASSUMPTIONS: Let $(\bar{x}, \bar{\lambda})$ be a KKT point satisfying the SOSC.

ALM: Choose $(x^0, \lambda^0) \in \Theta \times \mathbb{R}^m$ and $\bar{\rho} > 0$. Pick $\varepsilon_k \downarrow 0$ and $\{\rho_k\}$ with $\rho_k \geq \bar{\rho}$. Set $k := 0$.

Step 1 If (x^k, λ^k) satisfies a suitable termination criterion: STOP.

Step 2 Find an x^{k+1} satisfying

$$\mathrm{dist}\big(-\nabla_x \mathscr{L}(x^{k+1}, \lambda^k, \rho_k); N_\Theta(x^{k+1})\big) \leq \varepsilon_k.$$

Step 3 Update multiplier

$$\lambda^{k+1} := \nabla e_{1/\rho_k} g\big(\Phi(x^{k+1}) + \rho_k^{-1}\lambda^k\big).$$

Step 4 Set $k \leftarrow k + 1$ and go to **Step 1**.

SOLVABILITY OF SUBPROBLEMS: There exist $\tau > 0$ and $0 < \widehat{\gamma} \leq \gamma$ such that for all $\rho \geq \bar{\rho}$, the optimal solution mapping

$$S_\rho(\lambda) := \operatorname*{arg\,min}_{x \in \Theta \cap \mathbb{B}_{\widehat{\gamma}}(\bar{x})} \mathscr{L}(x, \lambda, \rho), \quad \lambda \in \mathbb{R}^m,$$

enjoys the *uniform isolated calmness* property $S_\rho(\lambda) \subset \{\bar{x}\} + \tau\|\lambda - \bar{\lambda}\|\mathbb{B}$ and satisfies $\emptyset \neq S_\rho(\lambda) \subset \operatorname{int} \mathbb{B}_{\widehat{\gamma}}(\bar{x})$ for all $\lambda \in \mathbb{B}_{\widehat{\gamma}/2\tau}(\bar{\lambda})$.

PRIMAL-DUAL CONVERGENCE: There exist $\bar{\gamma} > 0$, $\bar{\tau} > 0$, and $\bar{\varrho} > 0$ such that for all $(x^0, \lambda^0) \in \mathbb{B}_{\bar{\gamma}}(\bar{x}, \bar{\lambda}) \cap \big(\Theta \times \mathbb{R}^m\big)$ there is a primal-dual sequence $\{(x^k, \lambda^k)\}_{k \geq 0}$, generated by ALM with $\rho_k \geq \bar{\varrho}$ and $\varepsilon_k = \sigma(x^k, \lambda^k)$ for all k, *converges to* $(\bar{x}, \widehat{\lambda})$ for some Lagrange multiplier $\widehat{\lambda}$, and its *rate of convergence is linear*.

FUTURE PROJECTS

- Practical implementation of ALM for solving CPLQ composite models arising in machine learning and data science.

Optimal control problem in linear elasticity

Quang Huy Nguyen & Thi Thanh Mai Ta
Hanoi University of Science and Technology, School of Applied Mathematics and Informatics

Contact Information:
School of Applied Mathematics and Informatics
Hanoi University of Science and Technology
No1 Dai Co Viet Street, Hai Ba Trung District, Hanoi,
Vietnam

Email: `mai.tathithanh@hust.edu.vn`,
`huy.nq185454@sis.hust.edu.vn`

Abstract

In this work, we consider the linear elastic optimal control problems with small deformations. We study the first-order necessary optimality conditions of the solution and propose a new numerical method, based on a combination of variational principle and line-search method. We implement this strategy in two and three space dimensions for a model of linear elasticity and consider the quadratic cost functional with distributed load control.

Introduction

The advancement of high-performance computing in modelling and simulation makes it possible for us to measure fulfilled displacement fields of an elastic solid. In this work, we shall apply the theory of optimal control to the problems of linear elasticity. The model of a mixed boundary value problem with a load applied in the domain Ω is considered. We analyse the existence of optimal controls and the first-order necessary optimality conditions and consider the numerical approximations of control problems. The main goal is to propose a new numerical scheme to solve an inverse problem in linear elasticity, based on an interior-point filter line-search method. The proposed numerical scheme can be extended to solve optimal control problems in the context of other physical problems.

Problem Setting

The problem we consider is to minimize a cost functional:

$$\inf J(\boldsymbol{u},\boldsymbol{f}) = \frac{1}{2}\|\boldsymbol{u}-\boldsymbol{u}_\Omega\|^2_{\boldsymbol{L}^2(\Omega)} + \frac{\lambda}{2}\|\boldsymbol{f}\|^2_{\boldsymbol{L}^2(\Omega)}, \qquad (1)$$

subject to the constraints $\boldsymbol{f} \in \boldsymbol{F}_{ad}$ and $\boldsymbol{u}_\Omega$ is a desired displacement. Here, the vector field $\boldsymbol{u}$ is the solution to the equilibrium linear elasticity problem (see [1]):

$$\begin{cases} -\operatorname{div}(\boldsymbol{\sigma}(\boldsymbol{u})) = \boldsymbol{f} & \text{in } \Omega, \\ \boldsymbol{u} = \boldsymbol{0} & \text{on } \Gamma_D, \\ \boldsymbol{\sigma}(\boldsymbol{u})\cdot\boldsymbol{n} = \boldsymbol{0} & \text{on } \Gamma_N, \end{cases} \qquad (2)$$

where the stress tensor $\boldsymbol{\sigma}(\boldsymbol{u})$ is related to the strain rate tensor $\boldsymbol{\varepsilon}(\boldsymbol{u})$ by Hooke's law $\boldsymbol{\sigma}(\boldsymbol{u}) = \kappa\,\mathrm{tr}(\boldsymbol{\varepsilon}(\boldsymbol{u}))\boldsymbol{I} + 2\mu\boldsymbol{\varepsilon}(\boldsymbol{u})$. The Lamé coefficients κ, μ are determined through the Young modulus E and the Poisson coefficient ν by formulas: $E = \mu\frac{3\kappa+2\mu}{\kappa+\mu}$ and $\nu = \frac{1}{2}\frac{\kappa}{2\kappa+\mu}$. Because of the thermodynamic stability, the Lamé coefficients are such that $\mu > 0,\ \gamma = \kappa + \frac{2}{3}\mu > 0$. The bulk modulus γ describes the compressibility of the material. An almost incompressible material corresponds to a very large value of μ, which a Poisson coefficient very close to $\frac{1}{2}$.

Numerical Method

We consider the control–to–state operator $G\colon \boldsymbol{L}^2(\Omega) \mapsto \boldsymbol{H}^1_{\Gamma_D}(\Omega)$ to construct the operator: $S = E_U G\colon \boldsymbol{L}^2(\Omega) \to \boldsymbol{L}^2(\Omega),\ \boldsymbol{f} \mapsto \boldsymbol{u}(\boldsymbol{f})$, where E_U is the embedding operator from $\boldsymbol{H}^1_{\Gamma_D}(\Omega)$ to $\boldsymbol{L}^2(\Omega)$. Using this operator, the problem (1) is reduced to the quadratic optimization problem of cost functional J in the Hilbert space $\boldsymbol{L}^2(\Omega)$:

$$J(\boldsymbol{f}) = \frac{1}{2}\|S\boldsymbol{f}-\boldsymbol{u}_\Omega\|^2_{\boldsymbol{L}^2(\Omega)} + \frac{\lambda}{2}\|\boldsymbol{f}\|^2_{\boldsymbol{L}^2(\Omega)}.$$

As in [2], we can show that there exists a unique optimal solution $\overline{\boldsymbol{f}}$ of this problem satisfy the following inequality:

$$J'(\overline{\boldsymbol{f}})(\boldsymbol{f}-\overline{\boldsymbol{f}}) = \int_\Omega (\lambda\overline{\boldsymbol{f}}+\overline{\boldsymbol{p}})(\boldsymbol{f}-\overline{\boldsymbol{f}}) \geq 0, \quad \forall \boldsymbol{f} \in \boldsymbol{F}_{ad}. \qquad (3)$$

The adjoint state $\overline{\boldsymbol{p}}$ is the solution to the adjoint system:

$$\begin{cases} -\operatorname{div}(\boldsymbol{\sigma}(\boldsymbol{p})) = \overline{\boldsymbol{u}}-\boldsymbol{u}_\Omega & \text{in } \Omega, \\ \boldsymbol{p} = \boldsymbol{0} & \text{on } \Gamma_D, \\ \boldsymbol{\sigma}(\boldsymbol{p})\cdot\boldsymbol{n} = \boldsymbol{0} & \text{on } \Gamma_N, \end{cases} \qquad (4)$$

where $\overline{\boldsymbol{u}} = S\overline{\boldsymbol{f}}$. From (3) we obtain the reduced gradient $J'(\boldsymbol{f}) = \boldsymbol{p}+\lambda\boldsymbol{f}$, where $\boldsymbol{p}$ solves the associated adjoint equation:

$$\begin{cases} -\operatorname{div}(\boldsymbol{\sigma}(\boldsymbol{p})) = \boldsymbol{u}(\boldsymbol{f})-\boldsymbol{u}_\Omega & \text{in } \Omega, \\ \boldsymbol{p} = \boldsymbol{0} & \text{on } \Gamma_D, \\ \boldsymbol{\sigma}(\boldsymbol{p})\cdot\boldsymbol{n} = \boldsymbol{0} & \text{on } \Gamma_N. \end{cases} \qquad (5)$$

We approximate the optimal control problem by considering a family of triangulations $(T_h)_{h>0}$ of $\overline{\Omega}$. The control is discretized by piecewise constant functions. The admissible set of step functions is $\boldsymbol{F}^{ad}_h = \boldsymbol{F}_h \cap \boldsymbol{F}_{ad}$, where:

$$\boldsymbol{F}_h = \left\{\boldsymbol{f} \in \boldsymbol{L}^\infty(\Omega) \mid \boldsymbol{f} \text{ is constant on all } \hat{T} \in \hat{T}_h\right\}.$$

The linear finite elements are used to approximate the state and the adjoint solution:

$$\boldsymbol{V}_h = \left\{\boldsymbol{u}_h \in \boldsymbol{C}(\overline{\Omega}) \mid \boldsymbol{u}_h \in \boldsymbol{P}_1\ \forall T \in T_h \text{ and } \boldsymbol{u}_h = \boldsymbol{0} \text{ on } \overline{\Omega}\setminus\Omega_h\right\}.$$

The discrete state $\boldsymbol{u}_h(\boldsymbol{f}_h) \in \boldsymbol{V}_h$ is the unique solution that satisfies:

$$a(\boldsymbol{u}_h(\boldsymbol{f}_h), \boldsymbol{v}_h) = \int_\Omega \boldsymbol{f}_h\boldsymbol{v}_h, \quad \forall \boldsymbol{v}_h \in \boldsymbol{V}_h, \qquad (6)$$

where $a\colon \boldsymbol{V}_h \times \boldsymbol{V}_h \to \mathbb{R}$ is the bilinear form defined by:

$$a(\boldsymbol{u}_h, \boldsymbol{v}_h) = \int_\Omega \lambda\nabla\cdot\boldsymbol{u}_h\,\nabla\cdot\boldsymbol{v}_h + 2\mu\boldsymbol{\varepsilon}(\boldsymbol{u}_h):\boldsymbol{\varepsilon}(\boldsymbol{v}_h). \qquad (7)$$

The adjoint equation is discretized in the same way:

$$a(\boldsymbol{p}_h, \boldsymbol{v}_h) = \int_\Omega (\boldsymbol{u}_h-\boldsymbol{u}_\Omega)\boldsymbol{v}_h, \quad \forall \boldsymbol{v}_h \in \boldsymbol{V}_h. \qquad (8)$$

We propose a numerical scheme for the optimal control problem, based on a combination of variational principle and line–search method [3].

Algorithm 1 The optimal control algorithm

```
Initialization: $n = 0$, initial $f^0$ and computation domain $T_h$.
repeat
    Solve linear elasticity problem (6) to get the solution $u_h^n$.
    Calculate the discretized cost functional $J_h(f_h^n)$.
    Solve adjoint problem (8) for $p_h^n$.
    Update the reduced gradient $J'_h(f_h^n)$.
    Find $f_h^{n+1}$ by the Interior point filter line–search algorithm.
    $n = n + 1$.
until Convergence.
return: $f_h^{n+1}$.
```

Numerical Experiments

This strategy is implemented in FreeFEM++. The optimization problem is solved by using IPOPT software.

Tests	E	ν
Bar elevating in 2D	21×10^5	0.3
Bar bending in 2D	10×10^5	0.3
Beam deformation in 3D	21×10^5	0.3

Table 1: The parameters

The first test case is an elevation of a bar, where the undeformed body is $\Omega = [0,2] \times [0,0.1]$. The goal is to find an optimal load that transforms this material into the desired shape in which the right quarter part is elevated to the height $h = 0.2$.

Figure 1: The desired shape of a bar

Figure 2: The deformed shape achieved by an optimal control

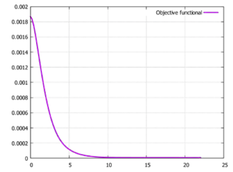

Figure 3: The convergence history of the functional J

In the second test, given a rectangular bar $\Omega = [0,20] \times [0,1]$ with two boundaries $x = 0$ and $x = 20$ are clamped. Suppose that we apply a bending force to get the desired displacement $\boldsymbol{u}_\Omega$.

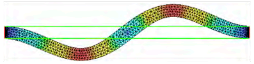

Figure 4: The desired deformation of the bar

Figure 5: The desired shape (orange) and the optimal shape (green)

In the last test, we consider a beam with the undeformed box shape $\Omega = [0,0.2] \times [0,0.2] \times [0,2]$. Suppose that the clamped part is the below surface and a distributed load is imposed in the domain.

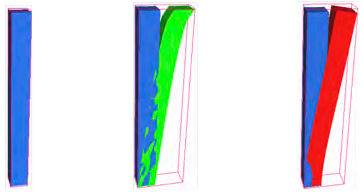

Figure 6: Beam deformation 3D test: The reference configuration (blue), the desired deformed shape (green) and the optimal deformed shape (red)

Conclusions

- We have proposed a numerical algorithm for optimal control problems in linearly elastic structures. Numerical examples in 2D and 3D for linear elasticity issues with the distributed load control are used to evaluate the efficiency and dependability of the current work.
- This algorithm can be extended to deal with general stationary elliptic equations and general objective functions.
- In Continuum Mechanics and Industry, this approach can be used to the material design and shape design problems.

Forthcoming Research

We plan to investigate the significance of λ in the algorithm's convergence, extend the method to semilinear and quasilinear elliptic equations, and develop a shape design application for the proposed methods in more complex physical situations in the future.

References

[1] Alexandre Ern and Jean-Luc Guermond. *Theory and Practice of Finite Elements*, volume 159 of *Applied Mathematical Sciences*. Springer, New York, 2004.

[2] Fredi Tröltzsch. *Optimal control of partial differential equations*. Graduate Studies in Mathematics 112. American Mathematical Society, 2010.

[3] Andreas Wachter and Lorenz Biegler. On the implementation of an interior-point filter line-search algorithm for large-scale nonlinear programming. *Mathematical programming*, 106:25–57, Mar 2006.

Acknowledgements

The authors wish to express our gratitude to the Vietnam Institute for Advanced Study in Mathematics (VIASM) for giving us the precious opportunity to present our research.

New methods of life expectancy estimation

Phuc Dang HO[1]*, **Thanh Nga NGUYEN**[2,1]
[1]Institute of Mathematics - VAST, [2]Banking Academy - Ha Noi

Contact Information:
Faculty of Mathematics
Banking Academy
12 Chua boc, Dong Da, Ha Noi

Email: `ngant@hvnh.edu.vn`

Abstract

Two novel methods of life expectancy estimation, applied to various annual reported demographic datasets, are proposed. First, for datasets that fully recorded birth date and death date of all dead individuals, we rely on the well-known Kaplan-Meier estimation method to provide an accurate estimation framework of life expectancy. The second new created method, called as local parametric method, based on the theoretical background of survival process with local parametric Weibull distributions, estimates life expectancy using abridged survival data. Experiments on real longitudinal datasets show the new method provides very exact life expectancy estimations for 10 among 15 one-year datasets, whilst the method of Chiang often yields overestimations.

Introduction

Life expectancy, usually understood as human average life time, has been used as a measure of the health status of the population of England and Wales since the 1840's. For example, in 1841 life expectancy for men in Surrey was 44 years, compared to 25 years for men in Liverpool (see HMSO). At the same time, length of life was used by William Farr to assess the health of populations and to make international comparisons between countries health. Life expectancy, nowadays obtained using modern mathematical tools of statistics, is selected by researchers as an indicator to examine geographic and socio-demographic inequalities in mortality (see [5], for instance).

Estimation of life expectancy requires to construct a life table to record the proportion alive at each age. The true average lifespan would need to follow up for over 100 years and such cohort specific life tables would be impractical for routine purposes. However, with a current demographic life table, we can define life expectancy at birth as the average life length of a newborn child, if current age specific mortality rates are or will be applied in the future. Chiang ([1], [2]) proposed a new method (*Chiang method*) of current life tables creation based on survival theory, which is quite simple and can be widely applicable. In that, Chiang method provides abridged life tables aggregating deaths and population data into age groups under 1, 1-4, 5-9 ... 80-84, 85 and over. However, there are biases in Chiang's current life tables related to the estimations of age specific mortality rates M_x and of the conditional probabilities of dying q_x in age intervals $[x; x+n)$ (see [5], [7]). Besides, as it is discussed in many studies (see [4], [8]), the Chiang method of life expectancy estimation has quite low performance in small areas' considerations.

Given the above, this article aims to develop novel estimation methods to address the mentioned lacks in the Chiang method.

Main Objectives

1. Presents a method of life expectancy estimation based on the ordinary Kaplan - Meier estimation method, that can be applied to fully observed longitudinal data.
2. We propose a novel method of life expectancy estimation based on theoretical background of survival process with local parametric Weibull distributions, called "Local parametric method" (LPM), can be applied to abridged datasets instead of the Chiang method.
3. We experiment the life expectancy estimation on a longitudinal survival dataset of FilaBavi using the Kaplan - Meier estimation method, the Chiang method, and our proposed LPM method. We then compare the obtained results.

Kaplan-Meier method of life expectancy

We split the population into age groups of people having age in the one year intervals $[0;1)$, $[1;2)$, ..., $[L;L+1)$, where L is the highest integer age in the data. In each age interval $[j;j+1)$, $j=0,1,...,L$, let $t^j_1 < t^j_2 < ... < t^j_{I_j}$ be the ordered age times of deaths occurred insides the interval. we have an estimation of life expectancy

$$\mathrm{KMLE} = \sum_{j=1}^{L-1}\Big\{\sum_{x=1}^{I_j-1} t^j_x \cdot [\hat{S}(t^j_x) - \hat{S}(t^j_{x+1})] + t^j_{I_j}\cdot[\hat{S}(t^j_{I_j}) - \hat{S}(t^{j+1}_1)]\Big\}$$

$$, \qquad +\Big\{\sum_{x=1}^{I_L-1} t^L_x \cdot [\hat{S}(t^L_x) - \hat{S}(t^L_{x+1})]\Big\} + t^L_{I_j}\cdot \hat{S}(t^L_{I_j})\,. \tag{1}$$

This can be called as the *Kaplan - Meier estimation of life expectancy* for semi-cohort data.

Local parametric method of life expectancy estimation

In this method, the probability of death q_x and the average time at death in each age interval are estimated by a survival model based on Weibull distribution with local parameterization (scale parameters λ_x, shape parameters k_x) in each age band of $[0;1)$, $[1;5)$, $[5;10)$, ..., $[80;85)$, and $[85;\infty)$.

Specifically, we fix the appropriate values less than 1 for k_0, k_1, k_5 and other values greater than or equal to 1 for k_x, $x = 10, 15, ..., 85$, before the use of data to estimate parameters λ_x for all age groups. We refer to data for estimating parameters λ_x as end-year abridged data. The shape parameter k_x is estimated as the slop coefficient of linear regression model by using 15 one-year semi-cohort data from

$$\ln[-\ln S_x(t)] = k_x \ln \lambda_x + k_x \ln t\,. \tag{2}$$

. The sequence of the local shape parameters k_x is given in the following sequence:

$$\{k_x\} = \{0.1; 0.2; 0.9; 1.0; 1.0; ...; 1.0\}\,, \tag{3}$$

where all local shape parameters equal 1.0, except of those for the first three age bands $[0;1)$; $[1;5)$ and $[5;10)$.

Life expectancy is estimated by summing all total remaining lifetimes of age bands, then dividing by the total number $N_0 = 100000$ of persons in the hypothetical population

$$\mathrm{LE} = \frac{\mathrm{TRL}_0 + \mathrm{TRL}_1 + \mathrm{TRL}_5 + ... + \mathrm{TRL}_{80} + \mathrm{TRL}_{85}}{100000}\,. \tag{4}$$

Results

To evaluate the accuracy of life expectancy estimation methods, we use 15 one-year semi-cohort data sets which is a longitudinal survival data set created by FilaBavi [3] to get Kaplan-Meier method gold standards of life expectancy "KMLE". After that, it is used to verify the validity of the above mentioned local parametric method of life expectancy estimation, comparing to Chiang method. . In Table 1, the estimation results are recorded in the column "K-M Est", "Chiang Est", "LMP Est".

Table 1 *Life expectancy estimations and residuals*

Year	K-M Est	Chiang Est	Chiang Res	LPM Est	LPM Res
2000	**76.02**	76.33	0.31	75.56	-0.47
2001	**76.03**	**76.30**	0.28	75.54	-0.49
2002	**75.65**	76.09	0.44	75.15	-0.50
2003	**77.43**	**77.47**	0.04	76.54	-0.89
2004	**76.58**	77.26	0.68	**76.57**	-0.01
2005	**75.69**	76.08	0.39	**75.73**	0.03
2006	**76.44**	77.30	0.86	**76.61**	0.17
2007	**77.98**	78.74	0.76	**78.27**	0.30
2008	**76.20**	76.96	0.75	**76.47**	0.27
2009	**76.88**	**77.15**	0.27	**76.86**	-0.01
2010	**77.05**	77.61	0.56	77.43	0.38
2011	**76.86**	**76.79**	-0.06	**76.89**	0.03
2012	**77.26**	**77.32**	0.07	**77.21**	-0.05
2013	**78.94**	79.52	0.58	**79.10**	0.16
2014	**80.05**	**80.09**	0.04	**80.30**	0.25
Average	**77.00**	77.40	**0.40**	76.95	**-0.06**

Discussion and conclusion

The study proposed two novel methods of life expectancy estimation that are applicable to various annual reported demographic datasets.

- The first one, named as Kaplan - Meier estimation method, extracting complete information from data fully recorded birth date and death date of all death individuals, provided the most accurate estimation of life expectancy.
- The second method called as local parametric method, can be applied to abridged datasets containing only a pair of number of deaths and number of persons in each age group. The validation by using the gold standard of Kaplan - Meier estimation method showed that the local parametric method can provide very exact life expectancy estimations for 10 among 15 one-year semi-cohort datasets. Simultaneously, the validation also pointed out that the ordinary method of Chiang is an overestimation method.
- However, some theoretical details should be clarified to strengthen the advantages of the local parametric estimation method. The first point is related to the series of local shape parameters' values that were chosen somewhat heuristically. It would be interesting to verify if the parameters can be used as universal shape parameters applied in the proposed method to estimate life expectancy for all other abridged datasets.
- Another open problem is to determine the variance of the life expectancy estimated by the local parametric estimation method. Usually, the variance is taken to create the confidence interval of the estimate, that is necessary to use in comparison between different life expectancy values.

References

[1] Chin Long Chiang. On constructing current life tables. *Journal of the American Statistical Association*, 67(339):538–541, 1972.

[2] Chin Long Chiang. Life table and its applications. In *Life table and its applications*, pages 316–316. 1984.

[3] Nguyen Thi Kim Chuc and Vinod K Diwan. Filabavi, a demographic surveillance site, an epidemiological field laboratory in vietnam, 2003.

[4] Daniel Eayres and ES Williams. Evaluation of methodologies for small area life expectancy estimation. *Journal of Epidemiology & Community Health*, 58(3):243–249, 2004.

[5] Clare Griffiths and Justine Fitzpatrick. Geographic inequalities in life expectancy in the united kingdom, 1995-97. *Health Statistics Quarterly*, (9):16–28, 2001.

[6] John J Hsieh. A general theory of life table construction and a precise abridged life table method. *Biometrical journal*, 33(2):143–162, 1991.

[7] Edward L Kaplan and Paul Meier. Nonparametric estimation from incomplete observations. *Journal of the American statistical association*, 53(282):457–481, 1958.

[8] John H Pollard. On the derivation of a full life table from mortality data recorded in five-year age groups. *Mathematical Population Studies*, 2(1):1–14, 1989.

[9] PBS Silcocks. Improving estimation of the variance of expectation of life for small populations. *Journal of Epidemiology & Community Health*, 58(7):611–612, 2004.

Acknowledgements

The analysis of this study has been realized by using the longitudinal dataset of FilaBavi - Ba Vi Epidemiological Field Laboratory. Thanks are due to Prof. Dr. Nguyen Thi Kim Chuc, the main coordinator of FilaBavi, and to other scientists and workers who participated in conducting many years surveys and processing to produce the dataset, that plays a critical role for this study.

SVM Classifications for Insurance Data Processing

Irfan Nurhidayat[1], Pawnwipa Meeklueb[2] and Busayamas Pimpunchat[3]

Center of Business Analytics and Synthetic Intelligence Strategy (BASIS), Department of Mathematics,
School of Science, King Mongkut's Institute of Technology Ladkrabang, Bangkok 10520, Thailand
Email: (64605130[1], 62605013[2], busayamas.pi[3])@kmitl.ac.th

Motivation

Considering that SVM is the best indicator of its overall statistical data processing and also is a classifier with a strong generalization ability.

Contribution

Informing SVM as a new innovation that is more accurate in data classification in the industrial sector in Thailand.

Objective

- Offers a new system for classifying data in industrial sectors.
- Replacing traditional methods with new methods of statistical data processing.
- Another alternative that is more accurate in data analysis.
- Answering doubts in insurance companies on determining which areas pay more and less.

Introduction

The Healthcare industry has witnessed major advancements and innovation over the years. However, there still exist diseases that are difficult to diagnose and require specialized care that can often destroy one's finances. Treatments like major organ transplants, surgery, etc, are such treatments that cost huge amounts of money where hospitalization is required multiple times and prolonged duration. For such situations, one should increase the cover through a combination of base cover and health insurance cover for added financial protection available at affordable cost. With the rising cost of healthcare in Thailand, a medical emergency could quickly deplete your savings. The primary purpose of health insurance is to provide financial coverage in case if you suffer from a medical condition so that you can keep your savings protected. Talking about income, inequality for each person becomes problematic in every region in Thailand. Based on this fact, we tried to reclassify by taking sum insured data from every province in Thailand. We assume for Bangkok to be a privileged area because the income of people in the capital city is relatively high.

Mathematical Models

The flowchart will express all of the building steps of mathematical models as following

Figure 1: Model constructing ideas.

The principal formula of the SVM

$$f(\mathbf{x}) = \mathbf{w}^T \cdot \mathbf{x} + b$$

where $\mathbf{w}$ as a parameter for a weight vector and b be a bias.

Hard margin SVM optimization

$$\min_{\mathbf{w},b}\left(\frac{1}{2}\|\mathbf{w}\|^2\right),$$
$$\text{s.t. } y_i(\mathbf{w}^T \cdot x_i + b) \geq 1, \ (i = 1, 2, \dots, N).$$

Soft margin SVM optimization problem

$$\min_{\mathbf{w},b,\xi}\left(\frac{1}{2}\|\mathbf{w}\|^2 + C\sum_{i=1}^{N}\xi_i\right),$$
$$\text{s.t. } y_i(\mathbf{x}^T x_i + b) \geq 1 - \xi_i,$$
$$\xi_i \geq 0, \ (i = 1, \dots, N).$$

Dual soft margin SVM problems

$$\min_{\alpha}\left(\frac{1}{2}\sum_{i=1}^{N}\sum_{j=1}^{N}\alpha_i\alpha_j y_i t_j x_i^T \cdot x_j - \sum_{i=1}^{N}\alpha_i\right),$$
$$\text{s.t. } \sum_{i=1}^{N}\alpha_i y_i = 0 \text{ and } 0 \leq \alpha_i \leq C, \ (i = 1, \dots, N).$$

Gaussian kernel form

$$\kappa(x_i, x_j) = \exp\left(-\frac{\|x_i - x_j\|^2}{2\sigma^2}\right)$$

with $\sigma > 0$ being a parameter.

Lagrangian form

$$L(\alpha) = \sum_{i=1}^{N}\alpha_i - \frac{1}{2}\sum_{i=1}^{N}\sum_{j=1}^{N}\alpha_i\alpha_j y_i t_j \kappa(x_i, x_j).$$

Methods

Simulations are performed by establishing databases in Microsoft Excel are then exported to R programming for SVM classifications. All numerical experiments are supported by Intel Core i5-5200U OS, 4GB RAM, 64 bit.

Simulations

Tune the best of C value in each region of Thailand as shown below

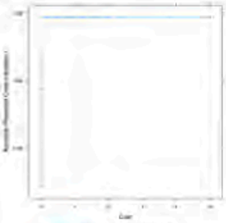

Figure 2: North provinces.

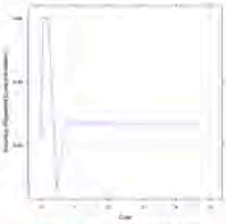

Figure 3: Northeast provinces.

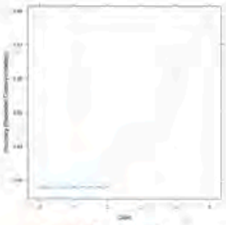

Figure 4: Central provinces.

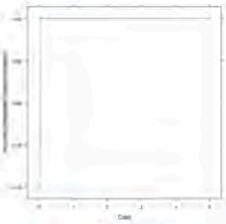

Figure 5: South provinces.

Conclusion

The results of R programming simulations in each of the regions in Thailand can be displayed on table as follows

Table 1: Accuracy and P-Value based on regions.

Regions	Accuracy		P-Value	
	Before Tune	After Tune	Before Tune	After Tune
North	0.8	0.8	0.7373	0.7373
Northeast	1	0.8333	0.3349	0.7368
Central	0.8571	0.8571	0.3605	0.3605
South	1	1	0.3164	0.3164

References

[1] Meeklueb P., Forecasting a distance of cycling for health using the hybrid GA-SVR approach. Master's Thesis. King Mongkut's Institute of Technology Ladkrabang. 2021.

[2] James, G., ed. (2013). An introduction to statistical learning with applications in R. New York: Springer.

[3] Steinwart, I. and Christmann, A. (2008). Support vector machines, New York: Springer.

Future Works

- Study for prescribing a relation of the premium and sum insured.
- Answering the question of our expectations for the premium in each province.

Acknowledgement

We are grateful to thank King Mongkut's Institute of Technology Ladkrabang for research funding and the Office of Insurance Commission (OIC) in Thailand for data availability.

Forum "Math for Industry" 2021: Mathematics for Digital Economy, December 13-16, 2021, VIASM, Hanoi, Vietnam

Asymptotic limit of fast rotation for the incompressible Navier-Stokes equations in a 3D layer

Hiroki Ohyama(1), Ryo Takada(2)

(1) Graduate School of Mathematics, Kyushu University, Fukuoka, Japan.
e-mail: oyama.hiroki.310@s.kyushu-u.ac.jp
(2) Faculty of Mathematics, Kyushu University, Fukuoka, Japan.

Introduction

Let us consider the Navier-Stokes equation with Coriolis force:

$$\begin{cases} \partial_t u - \Delta u + \Omega e_3 \times u + (u\cdot\nabla)u + \nabla p = 0 & (t,x) \in (0,\infty)\times\mathbb{D}, \\ \operatorname{div} u = 0 & (t,x)\in[0,\infty)\times\mathbb{D}, \\ u(0,x) = u_0(x) & x \in \mathbb{D}. \end{cases} \quad \text{(NSC)}$$

- $\mathbb{D} := \mathbb{R}^2 \times \mathbb{T}$: the 3D layer,
  $x = (x_h, x_3) \in \mathbb{D} \Leftrightarrow x_h = (x_1, x_2) \in \mathbb{R}^2$, $x_3 \in \mathbb{T} = \mathbb{R}/\mathbb{Z} \simeq [0,1]$
- $u = u(t,x) = (u_1(t,x), u_2(t,x), u_3(t,x))$: unknown velocity field
- $p = p(t,x)$: unknown pressure
- $u_0 = u_0(x) = (u_{0,1}(x), u_{0,2}(x), u_{0,3}(x))$: given initial velocity field
- $\Omega \in \mathbb{R}$: the Coriolis parameter and $e_3 = (0,0,1)$

Aim

- Global well-posedness of (NSC) in the scaling critical space
- Asymptotic limits of u as $|\Omega| \to \infty$

Preliminaries

Scaling Invariant Spaces

Let $u^\lambda(t,x) := \lambda u(\lambda^2 t, \lambda x)$, $p^\lambda(t,x) := \lambda^2 p(\lambda^2 t, \lambda x)$, $\Omega^\lambda := \lambda^2\Omega$, $\lambda > 0$.
(u,p): the sol. of (NSC) with $\Omega \Leftrightarrow (u^\lambda, p^\lambda)$: the sol. of (NSC) with Ω^λ.
Then, the Banach Space $X = X(\mathbb{R}^n)$ is called *scaling invariant* if $\|u(0,\cdot)\|_X = \|u^\lambda(0,\cdot)\|_X$ for any $\lambda > 0$.
(Example: Sobolev spaces $\dot{H}^{\frac{n}{2}-1}(\mathbb{R}^n)$ $n \in \mathbb{N}$, $L^2(\mathbb{R}^2)$, $\dot{H}^{1/2}(\mathbb{R}^3)$)

Decomposition

$u_0 = u_0(x)$ can be decomposed as $u_0 = \bar{u}_0 + \tilde{u}_0$, where

$$\bar{u}_0(x_h) = Qu_0(x_h) = \int_{\mathbb{T}} u_0(x_h, x_3)\,dx_3, \quad \tilde{u}_0(x) = u_0(x) - \bar{u}_0(x_h).$$

Known Results (Fast rotation limits in $\mathbb{R}^3$)

Theorem 1 [2,3]

Given $u_0 = v_0 + w_0 \in L^2(\mathbb{R}^2)^3 + \dot{H}^{1/2}(\mathbb{R}^3)^3$. Then,

- $\exists \Omega_0 = \Omega_0(u_0) > 0$ such that $\forall \Omega \in \mathbb{R}$ with $|\Omega| \geqslant \Omega_0$, the equation (NSC) in $\mathbb{R}^3$ has a global unique solution u.
- $u \to u^\infty$ in $L^2_{\mathrm{loc}}(0,\infty; L^q(\mathbb{R}^3))$ as $|\Omega| \to \infty$ for $2 < q < 6$.

Here, the limit equation is given as follows:

$$\begin{cases} \partial_t u^\infty - \Delta_h u^\infty + (u_h^\infty \cdot \nabla_h) u^\infty + (\nabla_h p, 0) = 0 & (t,x_h) \in (0,\infty)\times\mathbb{R}^2, \\ \nabla_h \cdot u_h^\infty = 0 & (t,x_h)\in[0,\infty)\times\mathbb{R}^2, \\ u^\infty(0,x_h) = v_0(x_h) & x_h \in \mathbb{R}^2, \end{cases} \quad \text{(Lim)}$$

where $\Delta_h = \partial_1^2 + \partial_2^2$, $\nabla_h = (\partial_1, \partial_2)$ and $u_h^\infty = (u_1^\infty, u_2^\infty)$.

References

[1] H. Ohyama and R. Takada, J. Evol. Equ. **21** (2021), 2591–2629.
[2] J.-Y. Chemin, B. Desjardins, I. Gallagher, and E. Grenier, Stud. Math. Appl., vol. 31, North-Holland, Amsterdam, 2002, pp. 171-192.
[3] ———, *Mathematical geophysics*, Oxford Lecture Series in Mathematics and its Applications, vol. 32, The Clarendon Press, Oxford University Press, Oxford, 2006.
[4] T. Gallay and V. Roussier-Michon, J. Math. Anal. Appl. **360** (2009), 14–34.

Acknowledgements

This work was supported by JSPS KAKENHI Grant Numbers JP19K03584, JP18KK0072, JP17H02851 and JP20H01814.

Known Results (The 3D layer $\mathbb{D}$)

Let us decompose $u = \bar{u} + \tilde{u}$, where $\bar{u} = Qu$ and $\tilde{u} = (1-Q)u$.
The equation for $\bar{u}$ on $\mathbb{R}^2$ is written as follows:

$$\begin{cases} \partial_t \bar{u} - \Delta_h \bar{u} + \mathbb{P}[(\bar{u}_h \cdot \nabla_h)\bar{u} + Q(\tilde{u}\cdot\nabla)\tilde{u}] = 0, \quad \nabla_h \cdot \bar{u}_h = 0, \\ \bar{u}(0,x_h) = \bar{u}_0(x_h). \end{cases}$$

The equation for $\tilde{u}$ on $\mathbb{D}$ is written as follows:

$$\begin{cases} \partial_t \tilde{u} - \Delta\tilde{u} + \Omega\mathbb{P}(e_3 \times \mathbb{P}\tilde{u}) + \mathbb{P}[(1-Q)(\tilde{u}\cdot\nabla)\tilde{u} + (\bar{u}\cdot\nabla)\tilde{u} + (\tilde{u}\cdot\nabla)\bar{u}] = 0, \\ \nabla \cdot \tilde{u} = 0, \\ \tilde{u}(0,x) = \tilde{u}_0(x). \end{cases}$$

Here, $\mathbb{P} : L^2(\mathbb{D})^3 \to \{v \in L^2(\mathbb{D})^3 | \nabla \cdot v = 0\}$ denotes the Helmholtz projection.

Theorem 2 [4]

Let $u_0 \in H^1_{\mathrm{loc}}(\mathbb{D})^3$ with $\tilde{u}_0 \in (1-Q)H^1(\mathbb{D})^3$, $\bar{u}_{0,3} \in H^1(\mathbb{R}^2)$, and $(\nabla \times \bar{u}_0)_3 \in (L^1 \cap L^2)(\mathbb{R}^2)$. Then,

- $\exists \Omega_0 = \Omega_0(u_0) > 0$ such that $\forall \Omega \in \mathbb{R}$ with $|\Omega| \geqslant \Omega_0$, the equation (NSC) has a global unique solution $u = \bar{u} + \tilde{u}$.
- $u \to$ 2D Lamb-Oseen vortex in $L^1(\mathbb{R}^2)$ as $t \to \infty$.

Main Results

Theorem 3 [1]

Let $u_0 = \bar{u}_0 + \tilde{u}_0 \in L^2(\mathbb{R}^2)^3 + (1-Q)\dot{H}^{\frac{1}{2}}(\mathbb{D})^3$ satisfy $\nabla_h \cdot (\bar{u}_0)_h = \nabla \cdot \tilde{u}_0 = 0$. Then, $\exists \Omega_0 = \Omega_0(\bar{u}_0, \tilde{u}_0) > 0$ such that $\forall \Omega \in \mathbb{R}$ with $|\Omega| \geqslant \Omega_0$, the equation (NSC) has a unique global solution $u = \bar{u} + \tilde{u}$ satisfying

$$\bar{u} \in C([0,\infty); L^2(\mathbb{R}^2))^3 \cap L^2(0,\infty; \dot{H}^1(\mathbb{R}^2))^3,$$
$$\tilde{u} \in C([0,\infty); (1-Q)\dot{H}^{\frac{1}{2}}(\mathbb{D}))^3 \cap L^2(0,\infty; (1-Q)\dot{H}^{\frac{3}{2}}(\mathbb{D}))^3.$$

Moreover, for $2 < p, q < \infty$ with $2/p + 2/q = 1$,

$$\lim_{|\Omega|\to\infty} \|u - u^\infty\|_{L^p(0,\infty;L^q(\mathbb{D}))} = 0.$$

Here, u^∞ is the global solution of (Lim) with the initial data $\bar{u}_0$ in the class

$$u^\infty \in C([0,\infty); L^2(\mathbb{R}^2))^3 \cap L^2(0,\infty; \dot{H}^1(\mathbb{R}^2))^3.$$

Remark 1. Let $2 < p, q < \infty$ satisfy $2/p + 2/q = 1$. Then, by the Sobolev embedding $\dot{H}^{1-2/q}(\mathbb{R}^2) \hookrightarrow L^q(\mathbb{R}^2)$ and the interpolation inequality, it holds

$$L^\infty(0,\infty; L^2(\mathbb{R}^2)) \cap L^2(0,\infty; \dot{H}^1(\mathbb{R}^2)) \hookrightarrow L^p(0,\infty; L^q(\mathbb{R}^2)).$$

Moreover, it follows from the Sobolev embedding $H^{\frac{3}{2}(1-2/q)}(\mathbb{D}) \hookrightarrow L^q(\mathbb{D})$, the interpolation inequality and the Poincaré inequality that

$$L^\infty(0,\infty; (1-Q)\dot{H}^{\frac{1}{2}}(\mathbb{D})) \cap L^2(0,\infty; \dot{H}^{\frac{3}{2}}(\mathbb{D})) \hookrightarrow L^p(0,\infty; (1-Q)L^q(\mathbb{D})).$$

Remark 2.

[2,3]	[1]
$2 < q < 6,$	$2 < p, q < \infty$ with $2/p + 2/q = 1,$
$\lim_{\lvert\Omega\rvert\to\infty} \|u - u^\infty\|_{L^2_{\mathrm{loc}}(0,\infty;L^q(\mathbb{R}^3))} = 0$	$\lim_{\lvert\Omega\rvert\to\infty} \|u - u^\infty\|_{L^p(0,\infty;L^q(\mathbb{D}))} = 0$

Key Estimate

Lemma 1 [1,4]

Let $R > 0$, $1 \leqslant p \leqslant \infty$ and $2 \leqslant q \leqslant \infty$. Then, $\exists C = C(R,p,q) > 0$ s.t. $\Omega \in \mathbb{R}$ and $\tilde{u}_0 \in (1-Q)L^2(\mathbb{D})^3$ with $\nabla \cdot \tilde{u}_0 = 0$ and $\operatorname{supp}\widehat{\tilde{u}_0} \subset \{\xi \in \mathbb{R}^2 \times 2\pi\mathbb{Z} \mid |\xi| < R\}$,

$$\|e^{t(\Delta - \Omega\mathbb{P}e_3\times\mathbb{P})}\tilde{u}_0\|_{L^p(0,\infty;L^q(\mathbb{D}))} \leqslant C\langle\Omega\rangle^{-\frac{\beta}{4}}\|\tilde{u}_0\|_{L^2(\mathbb{D})}.$$

Here, $\langle\cdot\rangle = (1 + |\cdot|^2)^{\frac{1}{2}}$, $\beta = \min\left\{\frac{1}{p}, 1 - \frac{2}{q}\right\}$.

Asymptotic behavior of the Hurwitz-Lerch multiple zeta function at non-positive integer points

Tomokazu Onozuka (Institute of Mathematics for Industry, Kyushu University)
email : t-onozuka@imi.kyushu-u.ac.jp
This is a joint work with Hideki Murahara (The University of Kitakyushu).

Previous Works (The Riemann zeta function)

The Riemann zeta function is defined by

$$\zeta(s) := \sum_{n=1}^{\infty} \frac{1}{n^s} \qquad (\Re(s) > 1).$$

This function can be continued meromorphically to $\mathbb{C}$.
This is one of the most important functions in number theory, and its importance comes from its relation to the distribution of primes.
For a non-positive integer $-n$, we have

$$\zeta(-n) = (-1)^n \frac{B_{n+1}}{n+1}$$

where B_n is the n-th Bernoulli number.

$$\zeta(0) = -\frac{1}{2}, \quad \zeta(-1) = -\frac{1}{12}, \quad \zeta(-2) = 0, \quad \zeta(-3) = \frac{1}{120}, \quad \zeta(-4) = 0,$$
$$\zeta(-5) = -\frac{1}{252}, \quad \zeta(-6) = 0, \quad \zeta(-7) = \frac{1}{240}, \quad \zeta(-8) = 0, \quad \zeta(-9) = -\frac{1}{132}.$$

Previous Works (The Hurwitz-Lerch zeta function)

Let $a, z \in \mathbb{C}$ be parameters with $\Re(a) > 0$, $|z| \leq 1$, and $z \neq 0$.
For $s \in \mathbb{C}$, The Hurwitz-Lerch zeta function is defined by

$$\zeta(s; a; z) = \sum_{0 \leq m} \frac{z^m}{(m+a)^s} \qquad (\Re(s) > 1).$$

This function also can be continued meromorphically to $\mathbb{C}$.
When $|z| = 1$, Apostol [1] showed

$$\zeta(-n; a; z) = -\frac{B_{n+1}(a; z)}{n+1}$$

for a non-positive integer $-n$, where $B_{n+1}(a; z)$ is the Apostol-Bernoulli polynomial defined by the generating function

$$\frac{xe^{ax}}{ze^x - 1} = \sum_{n \geq 0} B_n(a; z) \frac{x^n}{n!}.$$

Note that $B_n(a; 1) = B_n(a)$ is the Bernoulli polynomial and $(-1)^n B_n(1, 1) = B_n$ is the Bernoulli number.

$$\zeta(0; a; z) = \begin{cases} -\dfrac{1}{z-1} & \text{if } z \neq 1, \\ -a + \dfrac{1}{2} & \text{if } z = 1, \end{cases}$$

$$\zeta(-1; a; z) = \begin{cases} -\dfrac{a}{z-1} + \dfrac{z}{(z-1)^2} & \text{if } z \neq 1, \\ -\dfrac{1}{2}\left(a^2 - a + \dfrac{1}{6}\right) & \text{if } z = 1. \end{cases}$$

Problem

The Hurwitz-Lerch multiple zeta functions are defined by

$$\zeta(s_1, \ldots, s_r; a_1, \ldots, a_r; z_1, \ldots, z_r) := \sum_{0 \leq m_1, \ldots, m_r} \frac{z_1^{m_1} \cdots z_r^{m_r}}{(m_1 + a_1)^{s_1} \cdots (m_1 + \cdots + m_r + a_1 + \cdots + a_r)^{s_r}}.$$

This is a generalization of multiple zeta values and the Hurwitz-Lerch zeta function.
Almost all of non-positive integer points $(-n_1, \ldots, -n_r) \in (\mathbb{Z}_{\leq 0})^r$ are poles, so we can not give special values. However, we can give limit values, e.g.

$$\lim_{\epsilon \to 0} \zeta(\epsilon, \epsilon; 1, 1; 1, 1) = \frac{3}{8},$$

$$\lim_{\epsilon_1 \to 0} \lim_{\epsilon_2 \to 0} \zeta(\epsilon_1, \epsilon_2; 1, 1; 1, 1) = \frac{1}{3}.$$

Hence, we can consider asymptotic behavior at non-positive integer points.

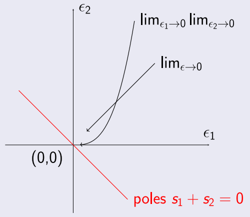

Main Result ([2])

Under certain conditions, we gave asymptotic behavior of $\zeta(-n_1 + \epsilon_1, \ldots, -n_r + \epsilon_r; a_1, \ldots, a_r; z_1, \ldots, z_r)$ with small $|\epsilon_1|, \ldots, |\epsilon_r|$.
For details, see [2].
For example, when $(-n_1, -n_2) = (0, 0)$, we have

$$\begin{aligned}\zeta(\epsilon_1, \epsilon_2; a_1, a_2; z_1, z_2) &= B_1(a_1; z_1)B_1(a_2; z_2) + \frac{1}{2}B_2(a_1; z_1)B_0(a_2; z_2) + \frac{1}{2}B_0(a_1; z_1)B_2(a_2; z_2)\frac{\epsilon_2}{\epsilon_1 + \epsilon_2} \\ &\quad + \sum_{j=1}^{2} O(|\epsilon_j|).\end{aligned}$$

More precisely:

$$\zeta(\epsilon_1, \epsilon_2; a_1, a_2; z_1, z_2)$$
$$= \begin{cases} (z_1 - 1)^{-1}(z_2 - 1)^{-1} + \displaystyle\sum_{j=1}^{2} O(|\epsilon_j|) & (z_1, z_2 \neq 1), \\ \left(a_1 - \dfrac{1}{2}\right)\dfrac{1}{z_2 - 1} + \left(\dfrac{1}{z_2 - 1}a_2 - \dfrac{z_2}{(z_2 - 1)^2}\right)\dfrac{\epsilon_2}{\epsilon_1 + \epsilon_2} + \displaystyle\sum_{j=1}^{2} O(|\epsilon_j|) & \\ & (z_1 = 1, z_2 \neq 1), \\ \dfrac{1}{z_1 - 1}\left(a_1 + a_2 - \dfrac{3}{2}\right) - \dfrac{1}{(z_1 - 1)^2} + \displaystyle\sum_{j=1}^{2} O(|\epsilon_j|) & (z_1 \neq 1, z_2 = 1), \\ \left(a_1 - \dfrac{1}{2}\right)\left(a_2 - \dfrac{1}{2}\right) + \dfrac{1}{2}\left(a_1^2 - a_1 + \dfrac{1}{6}\right) + \dfrac{1}{2}\left(a_2^2 - a_2 + \dfrac{1}{6}\right)\dfrac{\epsilon_2}{\epsilon_1 + \epsilon_2} & \\ + \displaystyle\sum_{j=1}^{2} O(|\epsilon_j|) & (z_1 = z_2 = 1). \end{cases}$$

Other Examples

Put $\boldsymbol{a} = (a_1, \ldots, a_r)$, $\boldsymbol{z} = (z_1, \ldots, z_r)$, and

$$B_{(n_1, \ldots, n_r)}(\boldsymbol{a}; \boldsymbol{z}) := \prod_{j=1}^{r} B_{n_j}(a_j; z_j)$$

for simplicity. When $r = 2$, we have

$$\zeta(-1 + \epsilon_1, \epsilon_2; a_1, a_2; z_1, z_2)$$
$$= \frac{1}{2}B_{(2,1)}(\boldsymbol{a}; \boldsymbol{z}) + \frac{1}{3}B_{(3,0)}(\boldsymbol{a}; \boldsymbol{z}) - \frac{1}{6}B_{(0,3)}(\boldsymbol{a}; \boldsymbol{z})\frac{\epsilon_2}{\epsilon_1 + \epsilon_2} + \sum_{j=1}^{2} O(|\epsilon_j|),$$

$$\zeta(\epsilon_1, -1 + \epsilon_2; a_1, a_2; z_1, z_2)$$
$$= \frac{1}{2}B_{(2,1)}(\boldsymbol{a}; \boldsymbol{z}) + \frac{1}{2}B_{(1,2)}(\boldsymbol{a}; \boldsymbol{z}) + \frac{1}{6}B_{(3,0)}(\boldsymbol{a}; \boldsymbol{z}) + \frac{1}{6}B_{(0,3)}(\boldsymbol{a}; \boldsymbol{z})\frac{\epsilon_2}{\epsilon_1 + \epsilon_2} + \sum_{j=1}^{2} O(|\epsilon_j|),$$

$$\zeta(-1 + \epsilon_1, -1 + \epsilon_2; a_1, a_2; z_1, z_2)$$
$$= \frac{1}{4}B_{(2,2)}(\boldsymbol{a}; \boldsymbol{z}) + \frac{1}{3}B_{(3,1)}(\boldsymbol{a}; \boldsymbol{z}) + \frac{1}{8}B_{(4,0)}(\boldsymbol{a}; \boldsymbol{z}) - \frac{1}{24}B_{(0,4)}(\boldsymbol{a}; \boldsymbol{z})\frac{\epsilon_2}{\epsilon_1 + \epsilon_2} + \sum_{j=1}^{2} O(|\epsilon_j|).$$

When $r = 3$, we have

$$\begin{aligned}\zeta(\epsilon_1, \epsilon_2, \epsilon_3; a_1, a_2, a_3; z_1, z_2, z_3) &= -B_{(1,1,1)}(\boldsymbol{a}; \boldsymbol{z}) - \frac{1}{2}B_{(2,0,1)}(\boldsymbol{a}; \boldsymbol{z}) - \frac{1}{2}B_{(2,1,0)}(\boldsymbol{a}; \boldsymbol{z}) \\ &\quad - \frac{1}{2}B_{(1,2,0)}(\boldsymbol{a}; \boldsymbol{z}) - \frac{1}{6}B_{(3,0,0)}(\boldsymbol{a}; \boldsymbol{z}) - \frac{1}{2}B_{(1,0,2)}(\boldsymbol{a}; \boldsymbol{z})\frac{\epsilon_3}{\epsilon_2 + \epsilon_3} \\ &\quad - \left(\frac{1}{2}B_{(0,2,1)}(\boldsymbol{a}; \boldsymbol{z}) + \frac{1}{6}B_{(0,3,0)}(\boldsymbol{a}; \boldsymbol{z})\right)\frac{\epsilon_2 + \epsilon_3}{\epsilon_1 + \epsilon_2 + \epsilon_3} \\ &\quad - \left(\frac{1}{2}B_{(0,1,2)}(\boldsymbol{a}; \boldsymbol{z}) + \frac{1}{6}B_{(0,0,3)}(\boldsymbol{a}; \boldsymbol{z})\right)\frac{\epsilon_3}{\epsilon_1 + \epsilon_2 + \epsilon_3} + \sum_{j=1}^{3} O(|\epsilon_j|).\end{aligned}$$

Reference

[1] T. M. Apostol, ‘On the Lerch zeta function’, Pacific J. Math. **1** (1951), 161–167.
[2] H. Murahara and T. Onozuka, ‘Asymptotic behavior of the Hurwitz-Lerch multiple zeta function at non-positive integer points’, arXiv:2111.06072.

Acknowledgements

This work was supported by JSPS KAKENHI Grant Number JP19K14511.

Modeling the duration of reaching the risk tipping point in the Covid-19 outbreak: A survival analysis approach.

Thi Huong Phan

Faculty of Applied Science, Ho Chi Minh City University of Technology - VNUHCM, Vietnam

Objectives

- What is the predicted duration for a country/territory to reach the risk tipping threshold (250 daily new cases per million) once it is designated as an orange region (accelerated spread)?
- How does the key factors affect the risk of reaching the red tipping point?

Introduction

The Covid-19 pandemic is still ongoing, with serious consequences for global health and the economy. Recent publications used country-level analysis only model the COVID-19 death counts, caseloads, or number of recoveries. In epidemic studies, however, patterns in the time to showing the event are just as important as the count of the event. As an example, the duration of outbreaks until the confirmed new cases reach an a specific threshold is also of interest. In July 2020, a criteria of outbreak classification based on the number of new cases was published by a group of researchers convened by Harvard's Global Health Institute and the Edmond J. Safra Center for Ethics[1].

Figure 1:The COVID-19 Risk Level dashboard

Motivated by the Covid Risk Level dashboard, we aim to discover a previously unreported question: how long does it take for a country or territory to reach the red level after being classified as an orange region? With the best of our knowledge we believe that there is no publication of modeling the duration of COVID-19 outbreak.

Study design

- From 222 countries and teritories extracted from Our World In Data [2], we collected a subgroup of 130 countries/territories that have daily new-case levels excess 100 cases per million (orange and red regions).
- The variable **Event** indicates whether this country/territory has reached the red tipping threshold (250 daily new cases per million) or not.
- The variable **Duration** is the number of days to reach the red tipping threshold or to end the follow-up period (11/10/2021) without showing the event.

Methods

- A key factor metric is defined to cover four categories: vaccination, policy response, demographic characteristics, and economics.
- The vaccination rate and stringency index are recorded as the highest values at each of four time intervals: 0-15 days, 15-42 days, 42-193 days, and after 193 days.
- A stratified Cox model is used to model the hazard function with time-dependent covariates and time-dependent effects. [3].

Results

- The risk of transforming to red regions among countries in orange regions is higher in older populations (HR = 1.06 and pvalue = 0.01).
- In comparison to Authoritarian countries/territories, Hybrid regime countries/territories and Flawed democracy countries/territories are at much higher risk (HR = 6.45, HR = 4.17).
- When compared to low and lower income countries/territories, upper-middle and high-income countries/territories experience faster outbreaks. (HR = 1.88, and HR = 2.79).
- After 193 days since the first date that countries/territories were classified as an orange region, the share of the population who received at least one dose of vaccination is showing its effectiveness (HR = 0.95), while there is no evidence about the effect of the stringency index.

The estimated hazard ratios.

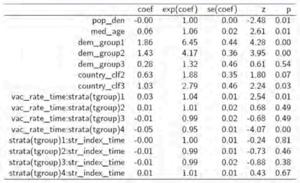

	coef	exp(coef)	se(coef)	z	p
pop_den	-0.00	1.00	0.00	-2.48	0.01
med_age	0.06	1.06	0.02	2.61	0.01
dem_group1	1.86	6.45	0.44	4.28	0.00
dem_group2	1.43	4.17	0.36	3.95	0.00
dem_group3	0.28	1.32	0.46	0.61	0.54
country_clf2	0.63	1.88	0.35	1.80	0.07
country_clf3	1.03	2.79	0.46	2.24	0.03
vac_rate_time:strata(tgroup)1	0.03	1.04	0.01	2.54	0.01
vac_rate_time:strata(tgroup)2	0.01	1.01	0.02	0.68	0.49
vac_rate_time:strata(tgroup)3	-0.01	0.99	0.02	-0.68	0.49
vac_rate_time:strata(tgroup)4	-0.05	0.95	0.01	-4.07	0.00
strata(tgroup)1:str_index_time	-0.00	1.00	0.01	-0.24	0.81
strata(tgroup)2:str_index_time	-0.01	0.99	0.01	-0.73	0.46
strata(tgroup)3:str_index_time	-0.01	0.99	0.02	-0.88	0.38
strata(tgroup)4:str_index_time	0.01	1.01	0.01	0.43	0.67

Figure 2:Results from fitting the stratified Cox model.

Estimated survival curves

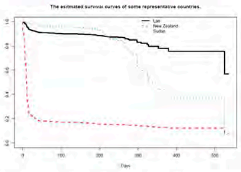

Figure 3:Estimated survival curves for 3 representative countries that haven't yet reached the orange threshold.

Data visualization

Figure 4:The map of worldwide orange regions where the red and blue circles indicate respectively countries and territories that have or haven't yet been classified as red regions. The sizes of circles are proportional to the countries/territories duration.

Extension

A dataset containing COVID-19 variants is currently being modeled.

References

[1] Harvard Global Health Institute.
Key metrics for covid suppression: a framework for policy makers and the public, 2020.

[2] Lucas Rodés-Guirao Cameron Appel Charlie Giattino Esteban Ortiz-Ospina Joe Hasell Bobbie Macdonald Diana Beltekian Hannah Ritchie, Edouard Mathieu and Max Roser.
Coronavirus pandemic (covid-19).
Our World in Data, 2020.
https://ourworldindata.org/coronavirus.

[3] Terry Therneau, Cindy Crowson, and Elizabeth Atkinson.
Using time dependent covariates and time dependent coefficients in the cox model.
Survival Vignettes, 2:3, 2017.

Contact Information

- Email: huongphan@hcmut.edu.vn

Harmonic analysis of quantum Laplacian on quantum Riemannian space

Masafumi Shimada*
*Graduated School of Mathematics, Kyushu University.
E-mail: Shimada.Masahumi.055@s.kyushu-u.ac.jp

1. Motivation

- Quantum groups, considered as Hopf algebras with certain features (such as classical limit), form a large class of noncommutative geometry.

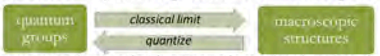

- Quantum group theory is deeply connected not only to branches of mathematics but also to branches of physics:
  - Math.: Lie group, Lie algebra and their representations, q-analysis, combinatorics, etc.
  - Phy.: particle physics, condensed matter physics, quantum gravity, etc.
- In our research, *we would like to relate various fields surrounding quantum group theory by focusing on quantum heat equations with harmonic analysis of quantized Laplacian*. Specifically, in previous researches, quantum Peter-Weyl theorem (in quantum harmonic analysis) is an example of modular functor conjecture (in quantum cluster algebra).

Keywords: harmonic analysis; Riemannian geometry; representation theory; quantum group

2. Purpose

- *Main goal*:
  recover quantum symmetric pairs and representations of quantum groups by means of harmonic analysis of symmetric spaces.
- *Other objective*:
  declare relations among quantum harmonic analysis, q-difference, q-special-function and quantum cluster algebra.

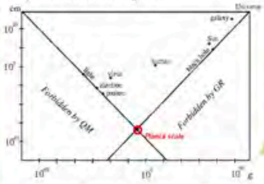

Figure1. Log-log plot of things. The left (resp. right) slope is a border determined by Quantum Mechanics (QM) (resp. General Relativity (GR)). Planck scale is the point where these two slopes intersect. (cf. [MAJ])

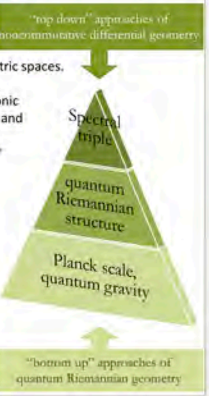

"top down" approaches of noncommutative differential geometry

Spectral triple

quantum Riemannian structure

Planck scale, quantum gravity

"bottom up" approaches of quantum Riemannian geometry

3. Method

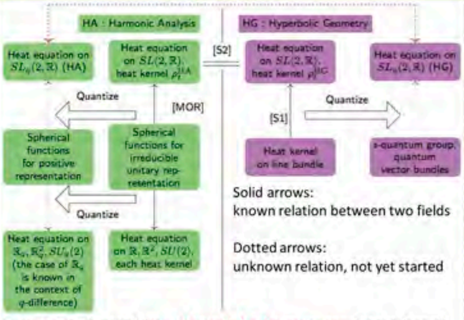

HA : Harmonic Analysis

HG : Hyperbolic Geometry

Heat equation on $SL_q(2,\mathbb{R})$ (HA)

Heat equation on $SL(2,\mathbb{R})$, heat kernel ρ_t^{HA}

[S2]

Heat equation on $SL(2,\mathbb{R})$, heat kernel ρ_t^{HG}

Heat equation on $SL_q(2,\mathbb{R})$ (HG)

Quantize

[MOR]

[S1]

Quantize

Spherical functions for positive representation

Spherical functions for irreducible unitary representation

Heat kernel on line bundle

s-quantum group, quantum vector bundles

Quantize

Heat equation on $\mathbb{R}_q, \mathbb{R}_q^2, SU_q(2)$ (the case of $\mathbb{R}_q$ is known in the context of q-difference)

Heat equation on $\mathbb{R}, \mathbb{R}^2, SU(2)$, each heat kernel

Solid arrows:
known relation between two fields

Dotted arrows:
unknown relation, not yet started

- Want to understand the red dotted left-right-arrow: equal or not, how HA and HG on quantum groups differ from HA and HG on classical cases.
- Formulate two forms of fundamental solutions of quantized heat equations: one by harmonic analysis, the other by hyperbolic geometry.

4. Results

Let $G := SL(2,\mathbb{R}), K := SO(2,\mathbb{R})$. Then,

Main theorem (S.)

$$\int_{\hat{G}(\tau_n)} e^{t\lambda^U_{\tau_n}}\Phi^U_{\tau_n}(g^{-1})d\mu(U) = e^{-(\frac{n}{2})^2 t - i\frac{n}{2}\theta(g)}\rho_{t,n}(x(g)+y(g)i).\ (n \in \mathbb{Z})$$

Theorem (Mori)

$$\rho_t^{HA}(g) = \sum_{n\in\mathbb{Z}}\int_{\hat{G}(\tau_n)} e^{t\lambda^U_{\tau_n}}\Phi^U_{\tau_n}(g^{-1})d\mu(U).$$

- $\tau_n : K \to \mathbb{C}^\times$, character of K corresponding to $\mathbb{C}^\times \ni z \mapsto z^n \in \mathbb{C}^\times$.
- $\hat{G}(\tau_n)$: the set of irreducible unitary representations on G such that their multiplicity for τ_n is nonzero.
- $\Phi^U_{\tau_n}$: the spherical function for τ_n and $U \in \hat{G}(\tau_n)$.
- $\lambda^U_{\tau_n} < 0$: eigenvalue of $\Phi^U_{\tau_n}$ with Laplacian (= Casimir operator + (extra)).

$=$

Theorem (S.)

$$\rho_t^{HG}(g) = \sum_{n\in\mathbb{Z}} e^{-(\frac{n}{2})^2 t - i\frac{n}{2}\theta(g)}\rho_{t,n}(x(g)+y(g)i).$$

- $x(g) \in \mathbb{R}, y(g) > 0, e^{i\theta(g)} \in \mathbb{C}^\times$ are uniquely determined by $g \in G$ (Iwasawa decomposition).
- $\rho_{t,n}$: heat kernel associated to Maass-Laplacian of wight $\frac{n}{2}$.

In the $n = 0$ case above, we regain the heat kernel of Poincaré upper-half plane $\mathbb{H}^2(\simeq G/K)$, one of well-known examples on non-Euclidean spaces (P_λ: Legendre function of the first kind):

$$\frac{1}{2\pi}\int_0^\infty e^{-(\frac{1}{4}+\nu^2)t}P_{i\nu-\frac{1}{2}}(\cosh r)\nu\tanh(\pi\nu)d\nu = \frac{\sqrt{2}}{(4\pi t)^{3/2}}\int_r^\infty e^{-\frac{t}{4}}\frac{\xi e^{-\frac{\xi^2}{4t}}}{\sqrt{\cosh\xi - \cosh r}}d\xi.$$

5. Discussion

- We obtain nice evaluations of $\rho_{t,n}$ with regard to Helgason-Fourier transformation.
- We achieve a simple presentation ρ_t^{HG}. This expression ρ_t^{HG} gives a hint to solve open problems in [MOR].
- A computation of the heat kernel on upper-half plane is a specialization of the main theorem ($n = 0$).
- In mathematical physics, expect to apply analysis of Harper operator H_ϕ with magnetic flux ϕ.

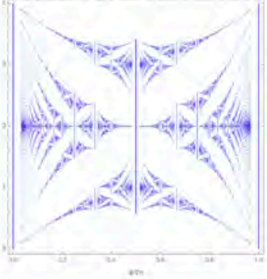

Figure2. The Hofstadter's Butterfly. The vertical axis expresses the range of spectrum of H_ϕ. The horizontal axis expresses the value of $\phi/2\pi$ corresponding to the strength of magnetic field or the magnetic flux. (cf. [DGHS])

6. Conclusions

Summary:
- Considering heat equations of quantum groups, in a framework of quantum Riemannian geometry, we find connections with quantum harmonic analysis, q-difference equation, q-special-function and quantum cluster algebra.
- Calculate the heat kernel of 2×2 real special linear group with two general techniques: harmonic analysis and hyperbolic geometry.
- We obtain a relationship between ρ_t^{HA} and ρ_t^{HG} by comparison of their K-isotypic components.

Future work:
1. Explain the reason why $\rho_{t,n}$, heat kernels of weighted Maass Laplacians, appear in the decomposition of ρ_t^{HG}.
2. Applications of the studies related with Harper operator H_ϕ to harmonic analysis on quantum Riemannian spaces.

References

- [DGHS] Z. Duan, J. Gu, Y. Hatsuda, T. Sulejmanpasic, *Instontons in the Hofstadter butterfly: difference equation, resurgence and quantum mirror curves*, Journal of High Energy Physics (2019).
- [MAJ] S. Majid, *Meaning of Noncommutative Geometry and the Planck-Scale Quantum Group*, Lecture Notes in Physics, (2000), 541, 227-276.
- [MOR] S.Mori, *The heat kernel on SL(2, R)*, arXiv:1909.03670.
- [S1] M. Shimada, *Weighted hyperbolic Laplacian approach for heat kernel on SL(2, R)* (in progress).
- [S2] M.Shimada, *Generalized integral formulae of the Legendre functions of the first kind and applications to harmonic analysis on hyperbolic spaces* (in progress).
- E.J. Beggs, S. Majid, Quantum Riemannian geometry, Grundlehren der mathematischen Wissenschaften,Vol. 355, Springer, Cham, 2020.
- R. Floreanini, L. Vinet, Symmetries of the q-difference heat equation. Lett Math Phys 32, 37-44 (1994).
- I. Ip, Parabolic positive representations of Uq(g(R)), arXiv:2008.08589, (2020).
- A. Klimyk & K. Schmüdgen: Quantum groups and their representation. Springer (New York) 1997.
- G. Letzter, Symmetric pairs for quantized enveloping algebras, J. Algebra 220 (1999), no. 2, 729-767.
- D. Levi, J. Negro and M. A. del Olmo, Discrete q-derivatives and Symmetries of q-difference Equations, J. Phys. A: Math. Gen., 37 (2004).

RISK SCORE OF THE COVID-19 OUTBREAK IN HANOI: AN EVALUATION AT CELL AND COMMUNE LEVELS

Huong Thi TRINH[1,2*], Hoang Long NGO [3], Binh Thi Thanh DAO[4], Quang Minh NGUYEN[3]

[1]Thuongmai University, Hanoi, [2]Vietnam Institute for Advanced Studies in Mathematics
[3]Hanoi National University of Education, [4]Hanoi University
*trinhthihuong@tmu.edu.vn

A. INTRODUCTION

- The fourth wave of COVID-19 pandemic in Vietnam.
- In Hanoi, government authorities need to focus on the pandemic areas as well as protect "green areas".
- It is then needed a risk model to evaluate DAILY the COVID-19 situation: includes the special characteristics of the confirmed cases, their social contact pattern contacting, and their community.
- Rapid evaluation at cell (300m x 300m) and commune levels.

Main contribution

- A risk score model for a confirmed case.
- Generate a cell risk model for each commune-level administrative unit, based on the number of confirmed cases in the previous days and the commune density population.
- Generate a cell risk model for a smaller spatial scale and include the degrees of contacts traced for each positive case.

B.METHOD

Model 1: Risk score of F0

F0Risk = ƒ (RT-PCR test, Time, Job, Community-case)

Model 2: Risk score of a commune

ComRisk = ƒ (Number of F0, density, sum RiskF0)

Model 3: Risk score of a cell.

CellRisk = ƒ (Number of F0, Population density, F0Risk, trace contacting (random walk)).

- Stratified by the most dangerous clusters.
- A comparison of three consecutive days.

REQUIRE: Need rapid assessment in emergency response for COVID-19

- Prior knowledge; expert knowledge.
- Rapid assessment; Visualization; Daily Update.
- Software: Excel, Algorithms in R.

C. DATASET

- Daily new infection counts separately for the confirmed cases, provided by the Hanoi's Center for Disease Control.
- Social media data are used to trace the confirmed cases – considered as a random walk in the model

E. DISCUSSION

- The risk score in Hanoi at cells and communes has changed every day.
- The trace contacting has created many red cells among Hanoi city, especially of the "Thanh Nga Mart COVID-19 clusters" in the beginning of August.
- During the conduct of the research, from June to September 2021, it can be seen that the most dangerous/rickiest COVID-19 ward in Hanoi was Thanh Xuan Trung, a ward in Thanh Xuan district, which had the highest risk score for many days.
- The risk score models have provided scientific results for policymakers and play the roles as an aid to the Decision Making Process to combat the COVID-19 pandemic in Hanoi.

H. ACKNOWLEDGEMENTS

We thank the Rapid Response Team of the Vietnam Steering Committee against COVID-19.

K. REFERENCES

1. Ge et al. (2021). The impact of social distancing, contact tracing, and case isolation interventions to suppress the COVID-19 epidemic: A modeling study. Epidemics, 36, 100483.
2. Ha et al. (2020). Combating the COVID-19 epidemic: experiences from Vietnam. International journal of environmental research and public health, 17(9), 3125.
3. Hoang et al. (2020). Describing the pattern of the COVID-19 epidemic in Vietnam. Global health action, 13(1), 1776526.
4. Gaudou et al. 2020. Comokit: A modeling kit to understand, analyze, and compare the impacts of mitigation policies against the covid-19 epidemic at the scale of a city. Frontiers in public health, 8.

D. RESULTS

Figure: Risk score; A comparison of a three-day

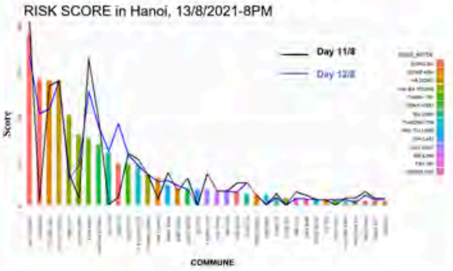

Figure: Risk score by commune and cluster

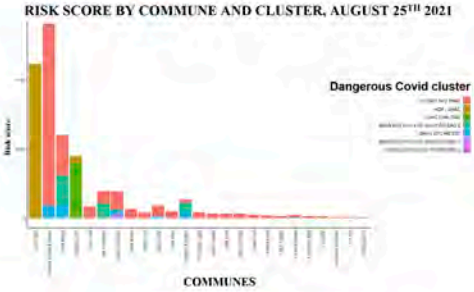

Figure: Total differences, composition and structure effects

FMFI, VIASM - HANOI 2021 FORUM "MATH-FOR-INDUSTRY" 2021 -MATHEMATICS FOR DIGITAL ECONOMY DECEMBER 13-16, 2021

EVALUATION OF HANOI POLICIES DURING COVID-19 LOCKDOWN 2021

Binh Thi Thanh DAO[1*], Hoang Long NGO [3], Huong Thi TRINH[4,2], Huyen Thi Ngoc NGUYEN[4]

[1]Hanoi University, [2]Vietnam Institute for Advanced Studies in Mathematics
[3]Hanoi National University of Education, [4]Thuongmai University, Hanoi
[*] binhdtt@hanu.edu.vn

A. HANOI POLICIES DURING COVID-19

- July 24: Hanoi authorities imposed 15 days of social distancing measures under the strict Directive 16. Extension August 6 and August 23.
- September 21: Hanoi authorities eased restrictions allowing several non-essential businesses to resume.
- Test PCR Covid-19, July 1st - July 23rd: related cases; July 24th - Aug 20th: larger scales; Aug 20th: massive test.

Main contribution

Highlight the effectiveness of:

- Policy on massive Covid-19 testing.
- Lockdown in Traditional Behavior of New Moon & Full Moon (15August Lunar Year).
- Heat map for Cough Medicine Declaration.

B.METHOD

- Step 1: Risk score of F0, commune, district
  Model 1: Risk score of F0
  Model 2: Risk score of a commune
  Model 3: Risk score of a cell.
- Step 2: Regression model.
  Dummy variables represented for the event to test for the significant effects.

REQUIRE: Need rapid assessment in emergency response for COVID-19

- Prior knowledge; expert knowledge.
- Rapid assessment.
- Visualization.
- Software: Excel, Algorithms in R.
- Daily Update.

C. DATASET

- Daily new infection counts separately for the confirmed cases, provided by the Hanoi CDC.
- Social media data are used to trace the confirmed cases – considered as a random walk in the model.
- Heat map for Cough Medicine Declaration from TKSK, HSHN.

E. DISCUSSION

- The mass testing would increase the number of confirmed case persons for the first week, that helps for control and isolation actions and helps to reduce the number of infections in later weeks.
- The lockdown policy is eased due to the ancestor Vietnamese culture of the Mid-autumn festival, people need to go out to buy fresh food, flowers and fruits. Especially the Full Moon of July under "Vu lan" name and Full Moon of August under " Trung Thu".
- The request for declaration to buy cough and fever medications and to put this information as the heat map, seem to be effective to isolate areas where the color of the heat is high.

H. ACKNOWLEDGEMENTS

We thank the Rapid Response Team of the Vietnam Steering Committee against COVID-19.

K. REFERENCES

1. Ge et al. (2021). The impact of social distancing, contact tracing, and case isolation interventions to suppress the COVID-19 epidemic: A modeling study. Epidemics, 36, 100483.
2. Ha et al. (2020). Combating the COVID-19 epidemic: experiences from Vietnam. International journal of environmental research and public health, 17(9), 3125.

D. RESULTS

Figure: Risk score: A comparison of a three-day 20/8 to 23/8

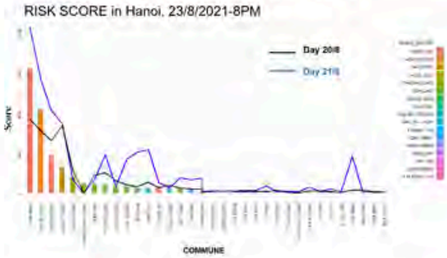

Figure: Risk score: A comparison of a three-day full moon 21/8 to 24/8

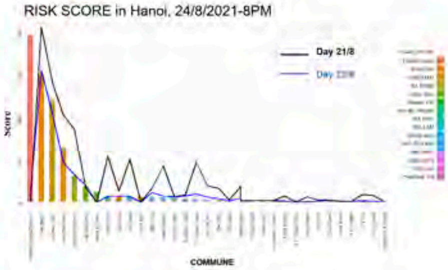

Figure: Massive test COVID-19

District	blockade areas	high-risk areas	high-risk cases	Total
THANH TRI	14,250	74,800	10,950	100,000
HOANG MAI	3,800	49,500	6,700	60,000
BAC TU LIEM	12,150	34,350	11,400	57,900
HAI BA TRUNG	1,000	32,500	24,000	57,500
BA DINH	5,500	34,500	10,000	50,000
DONG DA	5,000	40,000	5,000	50,000
DONG ANH	13,000	20,000	7,000	40,000
HOAI DUC	0	10,000	25,000	35,000
THACH THAT	0	17,500	16,500	34,000
THANH XUAN	0	0	0	32,000
HOAN KIEM	7,000	12,000	11,700	30,700
NAM TU LIEM	0	15,000	15,000	30,000

Figure: Patient with symptoms of COVID-19 August 26

ID	District	Latitude	Longitude	RiskScore
TKSK-015917371	CAU GIAY	21.0507579	105.8075708	0.1
TKSK-032330148	HOANG MAI	20.9836985	105.8508339	0.1
TKSK-032330034	LONG BIEN	21.0469744	105.8771173	0.1
TKSK-032329946	HOAN KIEM	21.0282271	105.8416552	0.1
TKSK-015916436	DONG DA	21.0108448	105.822425	0.1
TKSK-032328954	DONG DA	21.0204881	105.8273377	0.1
TKSK-015912853	CAU GIAY	21.0356998	105.7863297	0.1
TKSK-032325681	HOANG MAI	20.9669852	105.833383	0.1
TKSK-032324638	DONG DA	21.0299684	105.8345999	0.1
TKSK-015908592	HOANG MAI	20.9631778	105.8274311	0.1
TKSK-032322506	DONG DA	21.0183203	105.8168468	0.1
TKSK-032321806	HOANG MAI	20.9713643	105.8280009	0.1

Optimal Feed Intake of Pre-weaning Dorper Lamb

Nurzahirah Mohd Yussof[1], Nurul Syaza Abdul Latif[1], Nor Dini Rusli[2]
[1]Faculty of Computer and Mathematical Sciences, Universiti Teknologi MARA, Shah Alam Campus, Selangor, Malaysia
[2]Faculty of Agro Based Industry, Universiti Malaysia Kelantan, Jeli Campus, Kelantan, Malaysia

UNIVERSITI TEKNOLOGI MARA

Premier Digital Tech University™

Background of Study

In sheep development, there are three vital stages which are the lactation stage, followed by pre-weaning and post-weaning stages. Pre-weaning is one of the crucial stages in all domestic production systems that focused on meat production. Pre-weaning is defined as the stage of lamb that will be separated from its mother slowly and usually at the age of 3 to 4 months. At this stage, it is important for the lamb to get a sufficient and healthy feed intake along with desirable body weight before it enters the post-weaning stage, where the final stage before the sheep can be marketed. Thus, the research related to the pre-weaning stage of lamb is still lacking and need to be more emphasized especially in Malaysia. In Malaysia, Dorper sheep had been introduced because it is well suited to the Malaysian climate due to its hardiness and adaptability and this breed was introduced to increase local meat production. Hence, this study aims to determine the daily feed intake for the pre-weaning Dorper lamb that will achieve desirable body weight before they enter the next stage using the optimal control problem. This study was expected to provide new insights into the livestock industry, especially for the ranchers. It is also expected that can contribute to academic knowledge.

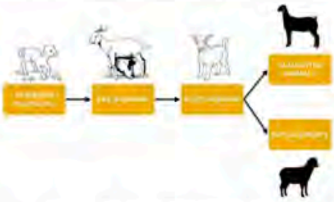

Figure 1: The Stage Development of Sheep

Modelling of Optimal Feed Intake

By fitting the dataset of body weight of pre-weaning Dorper lamb in the least square method, the expected feasible model of the growth rate is its either logistic function or the Gompertz growth model. The closer the value of the coefficient of determination to one, the more significant the fit model. Then, the necessary condition will be derived in the optimal control problem to determine the daily feed intake for pre-weaning lamb using the functional response of Holling Types. There are three types of Holling Types that depend on the graph curve which Holling Types I, Holling Types II or known as Michaelis–Menten equation, and Holling Types III or known as Hill function. In this study, Holling Types II was chosen based on the curve graph as shown in Figure 3 that was fitted using the dataset of daily feed.

Age (days)	**Daily feed (kg)**
Birth weight	0.11
7	0.21
14	0.34
28	0.48
42	0.62
56	0.69
70	0.77
84	0.83

Table 2: Dataset of Daily Feed

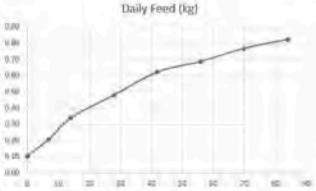

Figure 3: Graph of Holling Type II Based on Dataset of Daily Feed

Objective

The main goal of this study is to determine the daily feed intake along with the targeted bodyweight for the pre-weaning Dorper lamb. To be precise, the objective of this study are;

i) to determine a feasible model of the growth rate of pre-weaning Dorper lamb

ii) to derive the necessary condition in the optimal control for daily feed intake

iii) to propose strategies of the daily feeding for pre-weaning Dorper lamb based on the optimal solution of the proposed model

Parameter Estimation - Least Square Method

The least-squares method is a standard approach to provide an estimated model that best fits the sample data. Therefore, to find the best set of values for the parameters, the data will be fitted in the models. This procedure uses MATLAB's curve fitting tool to approximate the unknown parameters. There are four different functional forms as shown in Figure 2 and the dataset of body weight (Table 1) of pre-weaning Dorper lamb was used to get the paramater estimation.

$x(t) = x_0 + rt$ (linear function)

$x(t) = x_0 \cdot e^{rt}$ (exponential function)

$x(t) = \dfrac{x_0 K}{x_0 + (K - x_0)e^{-rt}}$ (logistic growth model)

$x(t) = Ke^{\ln\left(\frac{x_0}{K}\right)e^{-rt}}$ (Gompertz growth model)

Figure 2: Four Different Functional Forms in the Least Square Method

Age (d)	Weight (kg)
Birth weight	3.00
7	3.97
14	8.70
28	13.76
42	17.31
56	19.48
70	22.00
84	23.58

Table 1: The Dataset of Body Weight of Pre-weaning Dorper Lamb

All of these data have to do some simulation and the model simulation will compare the experimental data to find the sum of squares of error (SSE).

$$SSE = \sum_{i=1}^{N}\left[y_i - f(x_{1i}, \ldots, x_{mi}; \beta_1, \ldots, \beta_p)\right]^2$$

where x_i is the independent variable, y_i is the dependent variable (experimental data), and β_i are the unknown paramaters.

Then objective functional will be minimized as:

$$J(u) = \int_{t_0}^{t_1} g[t, x(t), u(t)]\, dt$$

subject to

$$\frac{d}{dt}x(t) = f(t, x(t), u(t))$$

$$x(t_0) = x_0$$

$$x(t_1) = x_1$$

where $u(t)$ is the daily feed intake at time t and $x(t)$ is the growth rate of the desired bodyweight of the pre-weaning Dorper lamb at time t. At the boundary condition $x(0) = 3.00$ kg and $x(84) = 23.58$ kg. This proposed optimal feed intake for the pre-weaning Dorper lamb will be used the Pontryagin Maximum Principle to derive the necessary condition for the optimal value of $u(t)$.

Conclusion

The expected result of the growth rate of bodyweight for the pre-weaning Dorper lamb is the logistic functions based on the coefficient of determination and the result of the optimal daily food intake variable is expected in the range of feed intake as shown in Table 2. In conclusion, the generic approach is expected to calculate the daily amount of feed required for Dorper lamb along with the desired weight. Furthermore, the model proposed in this study is expected to produce useful results that could potentially improve livestock quality and produce higher economic output for the Malaysian food production industry.

MI レクチャーノートシリーズ刊行にあたり

本レクチャーノートシリーズは、文部科学省 21 世紀 COE プログラム「機能数理学の構築と展開」（H.15-19 年度）において作成した COE Lecture Notes の続刊であり、文部科学省大学院教育改革支援プログラム「産業界が求める数学博士と新修士養成」（H19-21 年度）および、同グローバル COE プログラム「マス・フォア・インダストリ教育研究拠点」（H.20-24 年度）において行われた講義の講義録として出版されてきた。平成 23 年 4 月のマス・フォア・インダストリ研究所（IMI）設立と平成 25 年 4 月の IMI の文部科学省共同利用・共同研究拠点として「産業数学の先進的・基礎的共同研究拠点」の認定を受け、今後、レクチャーノートは、マス・フォア・インダストリに関わる国内外の研究者による講義の講義録、会議録等として出版し、マス・フォア・インダストリの本格的な展開に資するものとする。

平成 30 年 10 月
マス・フォア・インダストリ研究所
所長　佐伯修

Proceedings of Forum “Math-for-Industry” 2021
-Mathematics for Digital Economy-

発　行　2022年３月28日
編　集　Osamu Saeki, Ho Tu Bao, Shizuo Kaji, Kenji Kajiwara, Nguyen Ha Nam, Ta Hai Tung, Melanie Roberts, Masato Wakayama, Le Minh Ha, Philip Broadbridge
発　行　九州大学マス・フォア・インダストリ研究所
九州大学大学院数理学府
〒819-0395 福岡市西区元岡744
九州大学数理・IMI 事務室
TEL 092-802-4402　FAX 092-802-4405
URL https://www.imi.kyushu-u.ac.jp/

印　刷　城島印刷株式会社
〒810-0012 福岡市中央区白金２丁目９番６号
TEL 092-531-7102　FAX 092-524-4411

シリーズ既刊

Issue	Author／Editor	Title	Published
COE Lecture Note	Mitsuhiro T. NAKAO Kazuhiro YOKOYAMA	Computer Assisted Proofs - Numeric and Symbolic Approaches - 199pages	August 22, 2006
COE Lecture Note	M.J.Shai HARAN	Arithmetical Investigations - Representation theory, Orthogonal polynomials and Quantum interpolations- 174pages	August 22, 2006
COE Lecture Note Vol.3	Michal BENES Masato KIMURA Tatsuyuki NAKAKI	Proceedings of Czech-Japanese Seminar in Applied Mathematics 2005 155pages	October 13, 2006
COE Lecture Note Vol.4	宮田　健治	辺要素有限要素法による磁界解析 - 機能数理学特別講義 21pages	May 15, 2007
COE Lecture Note Vol.5	Francois APERY	Univariate Elimination Subresultants - Bezout formula, Laurent series and vanishing conditions - 89pages	September 25, 2007
COE Lecture Note Vol.6	Michal BENES Masato KIMURA Tatsuyuki NAKAKI	Proceedings of Czech-Japanese Seminar in Applied Mathematics 2006 209pages	October 12, 2007
COE Lecture Note Vol.7	若山　正人 中尾　充宏	九州大学産業技術数理研究センター キックオフミーティング 138pages	October 15, 2007
COE Lecture Note Vol.8	Alberto PARMEGGIANI	Introduction to the Spectral Theory of Non-Commutative Harmonic Oscillators 233pages	January 31, 2008
COE Lecture Note Vol.9	Michael I.TRIBELSKY	Introduction to Mathematical modeling 23pages	February 15, 2008
COE Lecture Note Vol.10	Jacques FARAUT	Infinite Dimensional Spherical Analysis 74pages	March 14, 2008
COE Lecture Note Vol.11	Gerrit van DIJK	Gelfand Pairs And Beyond 60pages	August 25, 2008
COE Lecture Note Vol.12	Faculty of Mathematics, Kyushu University	Consortium “MATH for INDUSTRY” First Forum 87pages	September 16, 2008
COE Lecture Note Vol.13	九州大学大学院 数理学研究院	プロシーディング「損保数理に現れる確率モデル」 — 日新火災・九州大学 共同研究2008年11月 研究会 — 82pages	February 6, 2009

シリーズ既刊

Issue	Author／Editor	Title	Published
COE Lecture Note Vol.14	Michal Beneš, Tohru Tsujikawa Shigetoshi Yazaki	Proceedings of Czech-Japanese Seminar in Applied Mathematics 2008 77pages	February 12, 2009
COE Lecture Note Vol.15	Faculty of Mathematics, Kyushu University	International Workshop on Verified Computations and Related Topics 129pages	February 23, 2009
COE Lecture Note Vol.16	Alexander Samokhin	Volume Integral Equation Method in Problems of Mathematical Physics 50pages	February 24, 2009
COE Lecture Note Vol.17	矢嶋　徹 及川　正行 梶原　健司 辻　英一 福本　康秀	非線形波動の数理と物理 66pages	February 27, 2009
COE Lecture Note Vol.18	Tim Hoffmann	Discrete Differential Geometry of Curves and Surfaces 75pages	April 21, 2009
COE Lecture Note Vol.19	Ichiro Suzuki	The Pattern Formation Problem for Autonomous Mobile Robots —Special Lecture in Functional Mathematics— 23pages	April 30, 2009
COE Lecture Note Vol.20	Yasuhide Fukumoto Yasunori Maekawa	Math-for-Industry Tutorial: Spectral theories of non-Hermitian operators and their application 184pages	June 19, 2009
COE Lecture Note Vol.21	Faculty of Mathematics, Kyushu University	Forum “Math-for-Industry” Casimir Force, Casimir Operators and the Riemann Hypothesis 95pages	November 9, 2009
COE Lecture Note Vol.22	Masakazu Suzuki Hoon Hong Hirokazu Anai Chee Yap Yousuke Sato Hiroshi Yoshida	The Joint Conference of ASCM 2009 and MACIS 2009: Asian Symposium on Computer Mathematics Mathematical Aspects of Computer and Information Sciences 436pages	December 14, 2009
COE Lecture Note Vol.23	荒川　恒男 金子　昌信	多重ゼータ値入門 111pages	February 15, 2010
COE Lecture Note Vol.24	Fulton B.Gonzalez	Notes on Integral Geometry and Harmonic Analysis 125pages	March 12, 2010
COE Lecture Note Vol.25	Wayne Rossman	Discrete Constant Mean Curvature Surfaces via Conserved Quantities 130pages	May 31, 2010
COE Lecture Note Vol.26	Mihai Ciucu	Perfect Matchings and Applications 66pages	July 2, 2010

シリーズ既刊

Issue	Author／Editor	Title	Published
COE Lecture Note Vol.27	九州大学大学院 数理学研究院	Forum “Math-for-Industry” and Study Group Workshop Information security, visualization, and inverse problems, on the basis of optimization techniques　100pages	October 21, 2010
COE Lecture Note Vol.28	ANDREAS LANGER	MODULAR FORMS, ELLIPTIC AND MODULAR CURVES LECTURES AT KYUSHU UNIVERSITY 2010　62pages	November 26, 2010
COE Lecture Note Vol.29	木田　雅成 原田　昌晃 横山　俊一	Magma で広がる数学の世界　157pages	December 27, 2010
COE Lecture Note Vol.30	原　　　隆 松井　　卓 廣島　文生	Mathematical Quantum Field Theory and Renormalization Theory 201pages	January 31, 2011
COE Lecture Note Vol.31	若山　正人 福本　康秀 高木　　剛 山本　昌宏	Study Group Workshop 2010 Lecture & Report　128pages	February 8, 2011
COE Lecture Note Vol.32	Institute of Mathematics for Industry, Kyushu University	Forum “Math-for-Industry” 2011 “TSUNAMI-Mathematical Modelling” Using Mathematics for Natural Disaster Prediction, Recovery and Provision for the Future　90pages	September 30, 2011
COE Lecture Note Vol.33	若山　正人 福本　康秀 高木　　剛 山本　昌宏	Study Group Workshop 2011 Lecture & Report　140pages	October 27, 2011
COE Lecture Note Vol.34	Adrian Muntean Vladimír Chalupecký	Homogenization Method and Multiscale Modeling　72pages	October 28, 2011
COE Lecture Note Vol.35	横山　俊一 夫　　紀恵 林　　卓也	計算機代数システムの進展　210pages	November 30, 2011
COE Lecture Note Vol.36	Michal Beneš Masato Kimura Shigetoshi Yazaki	Proceedings of Czech-Japanese Seminar in Applied Mathematics 2010 107pages	January 27, 2012
COE Lecture Note Vol.37	若山　正人 高木　　剛 Kirill Morozov 平岡　裕章 木村　正人 白井　朋之 西井　龍映 栄　伸一郎 穴井　宏和 福本　康秀	平成23年度 数学・数理科学と諸科学・産業との連携研究ワークショップ　拡がっていく数学　～期待される “見えない力” ～ 154pages	February 20, 2012

シリーズ既刊

Issue	Author／Editor	Title	Published
COE Lecture Note Vol.38	Fumio Hiroshima Itaru Sasaki Herbert Spohn Akito Suzuki	Enhanced Binding in Quantum Field Theory　204pages	March 12, 2012
COE Lecture Note Vol.39	Institute of Mathematics for Industry, Kyushu University	Multiscale Mathematics; Hierarchy of collective phenomena and interrelations between hierarchical structures　180pages	March 13, 2012
COE Lecture Note Vol.40	井ノ口順一 太田　泰広 筧　　三郎 梶原　健司 松浦　　望	離散可積分系・離散微分幾何チュートリアル2012　152pages	March 15, 2012
COE Lecture Note Vol.41	Institute of Mathematics for Industry, Kyushu University	Forum “Math-for-Industry” 2012 “Information Recovery and Discovery”　91pages	October 22, 2012
COE Lecture Note Vol.42	佐伯　　修 若山　正人 山本　昌宏	Study Group Workshop 2012 Abstract, Lecture & Report　178pages	November 19, 2012
COE Lecture Note Vol.43	Institute of Mathematics for Industry, Kyushu University	Combinatorics and Numerical Analysis Joint Workshop　103pages	December 27, 2012
COE Lecture Note Vol.44	萩原　　学	モダン符号理論からポストモダン符号理論への展望　107pages	January 30, 2013
COE Lecture Note Vol.45	金山　　寛	Joint Research Workshop of Institute of Mathematics for Industry (IMI), Kyushu University “Propagation of Ultra-large-scale Computation by the Domain-decomposition-method for Industrial Problems (PUCDIP 2012)” 121pages	February 19, 2013
COE Lecture Note Vol.46	西井　龍映 栄　伸一郎 岡田　勘三 落合　啓之 小磯　深幸 斎藤　新悟 白井　朋之	科学・技術の研究課題への数学アプローチ ―数学モデリングの基礎と展開―　325pages	February 28, 2013
COE Lecture Note Vol.47	SOO TECK LEE	BRANCHING RULES AND BRANCHING ALGEBRAS FOR THE COMPLEX CLASSICAL GROUPS　40pages	March 8, 2013
COE Lecture Note Vol.48	溝口　佳寛 脇　　隼人 平坂　　貢 谷口　哲至 島袋　　修	博多ワークショップ「組み合わせとその応用」　124pages	March 28, 2013

シリーズ既刊

Issue	Author／Editor	Title	Published
COE Lecture Note Vol.49	照井　　章 小原　功任 濱田　龍義 横山　俊一 穴井　宏和 横田　博史	マス・フォア・インダストリ研究所　共同利用研究集会 II 数式処理研究と産学連携の新たな発展　137pages	August 9, 2013
MI Lecture Note Vol.50	Ken Anjyo Hiroyuki Ochiai Yoshinori Dobashi Yoshihiro Mizoguchi Shizuo Kaji	Symposium MEIS2013: Mathematical Progress in Expressive Image Synthesis　154pages	October 21, 2013
MI Lecture Note Vol.51	Institute of Mathematics for Industry, Kyushu University	Forum “Math-for-Industry” 2013 “The Impact of Applications on Mathematics”　97pages	October 30, 2013
MI Lecture Note Vol.52	佐伯　　修 岡田　勘三 髙木　　剛 若山　正人 山本　昌宏	Study Group Workshop 2013 Abstract, Lecture ＆ Report 142pages	November 15, 2013
MI Lecture Note Vol.53	四方　義啓 櫻井　幸一 安田　貴徳 Xavier Dahan	平成25年度　九州大学マス・フォア・インダストリ研究所 共同利用研究集会　安全・安心社会基盤構築のための代数構造 ～サイバー社会の信頼性確保のための数理学～　158pages	December 26, 2013
MI Lecture Note Vol.54	Takashi Takiguchi Hiroshi Fujiwara	Inverse problems for practice, the present and the future　93pages	January 30, 2014
MI Lecture Note Vol.55	栄　伸一郎 溝口　佳寛 脇　　隼人 渋田　敬史	Study Group Workshop 2013 数学協働プログラム Lecture & Report 98pages	February 10, 2014
MI Lecture Note Vol.56	Yoshihiro Mizoguchi Hayato Waki Takafumi Shibuta Tetsuji Taniguchi Osamu Shimabukuro Makoto Tagami Hirotake Kurihara Shuya Chiba	Hakata Workshop 2014 ~ Discrete Mathematics and its Applications ~　141pages	March 28, 2014
MI Lecture Note Vol.57	Institute of Mathematics for Industry, Kyushu University	Forum “Math-for-Industry” 2014: “Applications + Practical Conceptualization + Mathematics = fruitful Innovation”　93pages	October 23, 2014
MI Lecture Note Vol.58	安生健一 落合啓之	Symposium MEIS2014: Mathematical Progress in Expressive Image Synthesis　135pages	November 12, 2014

シリーズ既刊

Issue	Author／Editor	Title	Published
MI Lecture Note Vol.59	西井　龍映 岡田　勘三 梶原　健司 髙木　　剛 若山　正人 脇　　隼人 山本　昌宏	Study Group Workshop 2014 数学協働プログラム Abstract, Lecture ＆ Report　196pages	November 14, 2014
MI Lecture Note Vol.60	西浦　　博	平成26年度九州大学 IMI 共同利用研究・研究集会（I）感染症数理モデルの実用化と産業及び政策での活用のための新たな展開　120pages	November 28, 2014
MI Lecture Note Vol.61	溝口　佳寛 Jacques Garrigue 萩原　　学 Reynald Affeldt	研究集会 高信頼な理論と実装のための定理証明および定理証明器 Theorem proving and provers for reliable theory and implementations (TPP2014)　138pages	February 26, 2015
MI Lecture Note Vol.62	白井　朋之	Workshop on “β-transformation and related topics”　59pages	March 10, 2015
MI Lecture Note Vol.63	白井　朋之	Workshop on “Probabilistic models with determinantal structure” 107pages	August 20, 2015
MI Lecture Note Vol.64	落合　啓之 土橋　宜典	Symposium MEIS2015: Mathematical Progress in Expressive Image Synthesis　124pages	September 18, 2015
MI Lecture Note Vol.65	Institute of Mathematics for Industry, Kyushu University	Forum “Math-for-Industry” 2015 “The Role and Importance of Mathematics in Innovation”　74pages	October 23, 2015
MI Lecture Note Vol.66	岡田　勘三 藤澤　克己 白井　朋之 若山　正人 脇　　隼人 Philip Broadbridge 山本　昌宏	Study Group Workshop 2015 Abstract, Lecture ＆ Report 156pages	November 5, 2015
MI Lecture Note Vol.67	Institute of Mathematics for Industry, Kyushu University	IMI-La Trobe Joint Conference “Mathematics for Materials Science and Processing” 66pages	February 5, 2016
MI Lecture Note Vol.68	古庄　英和 小谷　久寿 新甫　洋史	結び目と Grothendieck-Teichmüller 群 116pages	February 22, 2016
MI Lecture Note Vol.69	土橋　宜典 鍛治　静雄	Symposium MEIS2016: Mathematical Progress in Expressive Image Synthesis　82pages	October 24, 2016
MI Lecture Note Vol.70	Institute of Mathematics for Industry, Kyushu University	Forum “Math-for-Industry” 2016 “Agriculture as a metaphor for creativity in all human endeavors” 98pages	November 2, 2016
MI Lecture Note Vol.71	小磯　深幸 二宮　嘉行 山本　昌宏	Study Group Workshop 2016 Abstract, Lecture & Report　143pages	November 21, 2016

シリーズ既刊

Issue	Author／Editor	Title	Published
MI Lecture Note Vol.72	新井　朝雄 小嶋　　泉 廣島　文生	Mathematical quantum field theory and related topics　133pages	January 27, 2017
MI Lecture Note Vol.73	穴田　啓晃 Kirill Morozov 須賀　祐治 奥村　伸也 櫻井　幸一	Secret Sharing for Dependability, Usability and Security of Network Storage and Its Mathematical Modeling　211pages	March 15, 2017
MI Lecture Note Vol.74	QUISPEL, G. Reinout W. BADER, Philipp MCLAREN, David I. TAGAMI, Daisuke	IMI-La Trobe Joint Conference Geometric Numerical Integration and its Applications　71pages	March 31, 2017
MI Lecture Note Vol.75	手塚　　集 田上　大助 山本　昌宏	Study Group Workshop 2017 Abstract, Lecture & Report　118pages	October 20, 2017
MI Lecture Note Vol.76	宇田川誠一	Tzitzéica 方程式の有限間隙解に付随した極小曲面の構成理論 ―Tzitzéica 方程式の楕円関数解を出発点として―　68pages	August 4, 2017
MI Lecture Note Vol.77	松谷　茂樹 佐伯　　修 中川　淳一 田上　大助 上坂　正晃 Pierluigi Cesana 濵田　裕康	平成29年度　九州大学マス・フォア・インダストリ研究所 共同利用研究集会（I） 結晶の界面，転位，構造の数理　148pages	December 20, 2017
MI Lecture Note Vol.78	瀧澤　重志 小林　和博 佐藤憲一郎 斎藤　　努 清水　正明 間瀬　正啓 藤澤　克樹 神山　直之	平成29年度　九州大学マス・フォア・インダストリ研究所 プロジェクト研究　研究集会（I） 防災・避難計画の数理モデルの高度化と社会実装へ向けて 136pages	February 26, 2018
MI Lecture Note Vol.79	神山　直之 畔上　秀幸	平成29年度　AIMaP チュートリアル 最適化理論の基礎と応用　96pages	February 28, 2018
MI Lecture Note Vol.80	Kirill Morozov Hiroaki Anada Yuji Suga	IMI Workshop of the Joint Research Projects Cryptographic Technologies for Securing Network Storage and Their Mathematical Modeling　116pages	March 30, 2018
MI Lecture Note Vol.81	Tsuyoshi Takagi Masato Wakayama Keisuke Tanaka Noboru Kunihiro Kazufumi Kimoto Yasuhiko Ikematsu	IMI Workshop of the Joint Research Projects International Symposium on Mathematics, Quantum Theory, and Cryptography　246pages	September 25, 2019
MI Lecture Note Vol.82	池森　俊文	令和２年度　AIMaP チュートリアル 新型コロナウイルス感染症にかかわる諸問題の数理 145pages	March 22, 2021

シリーズ既刊

Issue	Author／Editor	Title	Published
MI Lecture Note Vol.83	早川健太郎 軸丸　芳揮 横須賀洋平 可香谷　隆 林　　和希 堺　　雄亮	シェル理論・膜理論への微分幾何学からのアプローチと その建築曲面設計への応用　49pages	July 28, 2021
MI Lecture Note Vol.84	Taketoshi Kawabe Yoshihiro Mizoguchi Junichi Kako Masakazu Mukai Yuji Yasui	SICE-JSAE-AIMaP Tutorial Advanced Automotive Control and Mathematics　110pages	December 27, 2021
MI Lecture Note Vol.85	Hiroaki Anada Yasuhiko Ikematsu Koji Nuida Satsuya Ohata Yuntao Wang	IMI Workshop of the Joint Usage Research Projects Exploring Mathematical and Practical Principles of Secure Computation and Secret Sharing　114pages	February 9, 2022
MI Lecture Note Vol.86	濱田　直希 穴井　宏和 梅田　裕平 千葉　一永 佐藤　寛之 能島　裕介 加葉田雄太朗 一木　俊助 早野　健太 佐伯　　修	2020年度採択分　九州大学マス・フォア・インダストリ研究所 共同利用研究集会 進化計算の数理　135pages	February 22, 2022

Institute of Mathematics for Industry
Kyushu University

九州大学マス・フォア・インダストリ研究所
九州大学大学院 数理学府

〒819-0395 福岡市西区元岡744　TEL 092-802-4402　FAX 092-802-4405
URL http://www.imi.kyushu-u.ac.jp/